

MIL-HDBK-241B
30 September 1983
SUPERSEDING
MIL-HDBK-241A
1 April 1981

MILITARY HANDBOOK
DESIGN GUIDE FOR ELECTROMAGNETIC INTERFERENCE
(EMI) REDUCTION IN POWER SUPPLIES



NO DELIVERABLE DATA REQUIRED BY THIS DOCUMENT

FSA EMCS

DEPARTMENT OF DEFENSE
WASHINGTON, DC 20363
30 September 1983

MIL-HDBK-241B
DESIGN GUIDE FOR ELECTROMAGNETIC INTERFERENCE REDUCTION IN POWER SUPPLIES
30 September 1983

1. This standardization handbook content and format revisions were developed by E. Kamm, Power Electronics Branch, Naval Ocean Systems Center, NOSC 5512 under the sponsorship of The Naval Electronic Systems Command in accordance with established procedures.
2. This publication was approved on 30 September 1983 for printing and inclusion in the military standardization handbook series.
3. This document provides basic and fundamental information on electromagnetic interference reduction in power supplies. It will provide valuable information and guidance to personnel concerned with the design of electronic, electrical, and electromechanical equipment.
4. This revision has been extensively revised in keeping with the renewed and increased emphasis of electromagnetic environmental effects (E^3) throughout the Navy. It reflects the latest information on the causes and control of unwanted electromagnetic energy as related to power supplies.
5. Beneficial comments (recommendations, additions, deletions) and any pertinent data which may be of use in improving this document should be addressed to: Commander, Naval Electronic Systems Command, Attention: ELEX-8111, Washington, DC 20363, by using the self-addressed Standardization Document Improvement Proposal (DD Form 1426) appearing at the end of this document or by letter.

FOREWORD

1. This design guide responds to a need common to many small businesses. They are often at a disadvantage in electromagnetic compatibility (EMC) design since budgetary restrictions preclude employing a full-time designated electromagnetic interference (EMI)/EMC engineer. This text is a compilation of EMI reduction design principles to assist those companies.

2. While experience indicates that power supplies are the source of most undesired conducted and radiated emissions, many of the basic suppression techniques are applicable to the entire unit.

3. In general, design is a compromise among various criteria imposed on the unit, (such as, weight, size, cost, power consumption, temperature extremes, humidity, reliability, maintainability, human engineering and performance) and EMC is merely one factor. Since EMI reflects lost or wasted power, it is an indication of inefficiency; and inefficiency, in turn, may result in unreliability through heat build-up.

4. The approach taken then is that with EMC, as an integral part of the conceptual design, less shielding and filtering will be necessary and the product will be lighter, smaller, more efficient, more reliable and cheaper.

5. NOTE TO CONTRACTORS. This guide has been provided not to supplant particular contract specifications and other contractual requirements but to assist where possible in meeting such specifications and requirements. Whether to employ any of the principles and techniques in this design guide is a decision solely for the contractor to make, and the Government makes no warranty, either express or implied, regarding the ultimate adequacy of these principles and techniques in any specific contractual application.

CONTENTS

SECTION		PAGE
1	INTRODUCTION	1
	1.1 Scope	1
	1.1.1 Switching-mode power supplies	1
	1.2 Designing to meet specific EMI requirements	1
	1.2.1 Differential versus common-mode interference	1
	1.2.1.1 Causes of common-mode interference	1
	1.2.2 Pertinent MIL-STD-461 requirements	1
2	REFERENCED DOCUMENTS	3
	2.1 Government documents	3
	2.1.1 Specifications, standards, and handbooks	3
	2.2 Other publication	3
3	POWER SUPPLIES	4
	3.1 Selection criteria	4
	3.1.1 AC or dc input power	4
	3.1.2 Continuity of power	4
	3.1.3 Power density	5
	3.1.4 System compatibility	5
	3.1.5 Life-cycle costs	5
	3.2 Power conversion approaches	7
	3.2.1 Dissipative regulators	7
	3.2.2 Ferroresonant regulators	7
	3.2.3 Phase control switching-mode regulators	7
	3.2.4 Off-line switching-mode regulators	11
	3.3 Off-line switching-mode power supplies	11
	3.3.1 Description	11
	3.3.2 Advantages	14
	3.3.3 Availability	14
	3.3.4 Potential problems	14
	3.3.4.1 Filter effects	17
	3.3.4.2 Constant input power characteristics	17
	3.3.4.2.1 Negative input resistance	20
	3.3.4.2.2 Low voltage and latch-up	20
	3.3.4.3 Stability difficulties	22
	3.3.4.3.1 Audio susceptibility	22
	3.3.4.3.2 Entrapment	22
	3.3.4.3.3 Right half-plane zero	25
	3.3.4.3.4 Duty cycles greater than 0.5	25
	3.3.4.4 Electromagnetic compatibility	25
	3.3.5 DC to dc converter topologies	25
	3.3.5.1 Basic topologies	27
	3.3.5.1.1 The bucks converter	27
	3.3.5.1.2 Boost converter	27
	3.3.5.1.3 Buck-boost converter	27
	3.3.5.1.4 Boost-buck (Cuk) converter	30
	3.3.5.2 Some transformer isolated derivatives	30
	3.3.5.2.1 Forward converter	30
	3.3.5.2.2 Reverse converter	32
	3.3.5.2.3 Flyback converter	32
	3.3.5.2.4 Isolated Cuk converter	32
	3.3.5.3 Multiple switch forms	32
	3.3.5.3.1 Push-pull buck-derived	34
	3.3.5.3.2 Half-bridge push-pull buck-derived	34
	3.3.5.3.3 Full-bridge push-pull buck-derived	34
	3.3.5.3.4 Shortcomings of basic push-pull designs	34
	3.3.5.3.5 Variations of the basic multi-switch approach	34

CONTENTS

SECTION		PAGE	
4	EMI CREATED BY AC TO DC RECTIFICATION	37	
	4.1	Introduction	37
	4.2	Basic rectifier action	37
	4.2.1	Pulse number	37
	4.2.2	Simplifying assumptions	37
	4.2.3	Single-phase half-wave rectifier	37
	4.2.3.1	Resistive load	37
	4.2.3.2	Inductive load or filter	38
	4.2.3.3	Capacitive load or filter	38
	4.2.4	Single-phase full-wave rectifiers	38
	4.2.4.1	Resistive load	38
	4.2.4.2	Inductive input filter (critical inductance)	42
	4.2.4.3	Capacitive input filter	42
	4.2.5	Three-phase rectifiers	42
	4.2.5.1	Inductive input filter (critical inductance)	42
	4.2.5.2	Capacitive input filter	42
	4.2.6	Resultant harmonic spectrums	46
	4.2.6.1	Two-pulse line current spectrums	46
	4.2.6.2	Six-pulse line current spectrums	46
	4.3	Other rectification EMI sources	46
	4.3.1	Rise/fall time effects	46
	4.3.2	Diode recover spike	46
	4.3.3	Phase controlled rectifiers	46
	4.4	Military specification requirements	51
	4.4.1	Problems from excessive harmonics	51
	4.4.1.1	Structure hull currents	51
	4.4.1.2	Power factor	51
	4.4.2	DoD-STD-1399, Section 300	52
	4.4.3	MIL-E-16400G, Amendment 1	52
	4.4.4	MIL-STD-461, CE01 requirement	52
	4.4.4.1	Surface ships and submarines	52
	4.4.4.2	Aircraft, spacecraft, and ground facilities	56
	4.5	Approaches to reduce rectifier harmonics	56
	4.5.1	Standard solutions	56
	4.5.1.1	Low pass filters	56
	4.5.1.2	Shunt filters	56
	4.5.1.3	Harmonic compensation or injection	56
	4.5.1.4	Ferroresonant transformers	56
	4.5.1.5	Multiphase rectification	57
	4.5.2	New approaches	57
	4.5.2.1	Simulation of a resistive load	57
	4.5.2.2	Switching-mode techniques	59
	4.5.2.3	AC to dc converter without large reactors	59
	4.5.2.4	Other related approaches	59
	4.6	Summary	60
5	EMI FROM SWITCHING-MODE CONVERSION	61	
	5.1	Introduction	61
	5.2	Powerline conducted differential-mode noise	61
	5.2.1	Basic waveform	64
	5.2.1.1	Fourier transform and basic waveform	64
	5.2.2	Turn-on spike	64
	5.2.2.1	Fourier transform and turn-on spike	64
	5.2.3	Resultant conducted noise spectrum (no filters)	64
	5.2.4	Input filters	64
	5.2.4.1	Recommended component types	68
	5.2.4.2	Potential instability problem	68
	5.2.5	Input noise current with two-stage filter	68
	5.2.6	Predicted noise current compared to Navy CE03 limits	68

CONTENTS

SECTION		PAGE
	5.3	Ripple on output leads 70
	5.4	Suppression of internally radiated noise 70
	5.4.1	Use of fast (soft) recovery diodes 70
	5.4.2	Control of transistor rise and fall times 71
	5.4.3	Mechanical suppression techniques and high frequency filtering 73
	5.4.4	EMI confinement techniques for transformers and inductors 77
	5.5	Future low-noise designs-two major developments 77
	5.6	Summary 77
6	COMPONENT AND CIRCUIT DESIGN CONSIDERATIONS	78
	6.1	Semiconductor switching devices 78
	6.1.1	Solid-state thyristors 78
	6.1.1.1	Types of thyristors 80
	6.1.1.2	Voltage (blocking voltage) and current ratings 80
	6.1.1.3	Turn-on and di/dt 81
	6.1.1.4	Recovery time (turn-on) 81
	6.1.2	Power bipolar transistors 81
	6.1.2.1	Pulse current and gain 81
	6.1.2.2	Delay and recovery 81
	6.1.2.3	Breakdown voltage versus forward voltage 82
	6.1.2.4	Life 82
	6.1.3	Power MOSFETS 82
	6.1.3.1	Types 83
	6.1.3.2	Drain resistance versus breakdown voltage 83
	6.1.3.3	Turn-on, turn-off and reliability 83
	6.1.4	Power diodes 83
	6.1.4.1	AC to dc rectifier diodes 83
	6.1.4.2	Commutating switching-frequency diodes 84
	6.2	Capacitors 84
	6.2.1	Input and output filter capacitors 84
	6.2.1.1	Electrolytic capacitors 86
	6.2.1.2	Plastic or ceramic input or output capacitors 86
	6.2.2	Capacitor type descriptions 86
	6.2.2.1	Aluminum versus tantalum electrolytics 88
	6.2.2.2	Controlled ESR and ESL 88
	6.2.2.3	Minimal ESR and ESL 89
	6.2.2.4	Mica and ceramic 89
	6.2.3	Capacitor paralleling and mounting 91
	6.2.4	Soft start 91
	6.3	Inductors 91
	6.3.1	Material (core) considerations 92
	6.3.2	Leakage and magnetic shielding 95
	6.3.3	Capacitive effects 95
	6.3.4	Optimally designed inductors 95
	6.3.5	Cross-noise in multiple-output converters 97
	6.4	Transformers 97
	6.4.1	Material (core) considerations 97
	6.4.2	Capacitive effects and electric field shielding 99
	6.4.3	Leakage and magnetic field shielding 103
	6.5	Ferrites and ferrite beads 106
	6.6	Conductors 108
	6.6.1	Planning minimal magnetic loop areas 108
	6.7	Resistors 110
	6.8	Mechanical contact protection 110
	6.9	Additional filter considerations 115
	6.9.1	Input and output impedances of filters 115
	6.9.2	Off-the-shelf type filters 117
	6.9.2.1	Installation of off-the-shelf power line filters 117

CONTENTS

SECTION		PAGE
6.9.3	DC versus ac filters	117
6.9.4	EMI filtering and MIL-STD-461B	118
6.10	Shielding	118
6.10.1	Shielding effectiveness	120
6.10.2	Magnetic material as a shield	122
6.10.3	Seams, joints, and holes	122
6.11	Reliability and EMI	122
6.11.1	EMI as a diagnostic tool to increase reliability	126
6.11.2	Effects from undesired signals	126

APPENDICES

APPENDIX

A	Modeling of switching-mode power supplies	127
B	Preventing input-filter oscillations in switching regulators	137
C	Filter and load characteristics computer program	149
D	Fourier transforms	161
E	References and bibliography	171

TABLES

TABLE

I	Output power density (P_D) requirements	6
II	Power conversion circuit selection parameters	9
III	Potential problems with switching-mode power supplies	15
IV	Harmonics in input current for ideal diode rectifiers	47
V	Military limits for harmonic line currents - 60 Hz power source	54
VI	Semiconductor switching devices	79
VII	Inductance and resistance of round conductors	109
VIII	Element values in the canonical model in FIGURE 91 for the buck, boost, and buck-boost converters	129

FIGURES

FIGURE

1	Equal thermal density volume versus efficiency	6
2	Power conversion circuits	8
3	Phase control switching-mode	10
4	Resonant converters	12
5	Duty cycle converter	13
6	Typical off-line switching-mode power supply-block diagram	13
7	Basic switching-mode power supply configurations	16
8	Overshoot	18

CONTENTS

FIGURE		PAGE
9	Switching-mode power supply input characteristics	18
10	General switching-mode regulator configuration	19
11	Middlebrook (1976) stability criterion	21
12	Attenuation (F) of line transients, lag compensation	23
13	Attenuation (F) of line transients, lead compensation	24
14	Duty cycle stability limit	26
15	The four basic dc-to-dc converter topologies	28
16	Implementation of the ideal switches in FIGURE 15 by bipolar transistor - diode networks (note $\rightarrow D' = 1-D$)	29
17	Transformer-isolated dc-to-dc converter topologies derived from the basic structure of FIGURE 16 ($D' = 1-D$)	31
18	Three key steps to evolving a dc-isolated version of the Cuk converter of FIGURE 17(d)	33
19	The basic two-transistor push-pull dc-to-dc converter (buck-derived)	35
20	Single ended a half-bridge version of the buck-derived push-pull converter	36
21	Full-bridge version of the buck-derived push-pull converter	36
22	Single-phase half-wave rectifier	39
23	Single-phase half-wave rectifier - R/L load	39
24	Single-phase half-wave rectifier - CR load	41
25	Two-pulse rectifier circuits	41
26	Effects of inductance on waveforms of two-pulse rectifier (voltage across inductance shown shaded)	43
27	Two-pulse rectifier circuit - RC load	44
28	Six-pulse rectifier circuit-IDEAL input filter (infinite inductance)	45
29	Harmonic line currents, two-pulse rectifier - RC load (computed using SPICE program)	48
30	Harmonic line currents, two-pulse rectifier - RC/L load (computed using SPICE program)	48
31	Harmonic line currents, six-pulse rectifier - IDEAL infinite inductance load	49
32	Harmonic line currents, six-pulse rectifier - RC/L load (computed using SPICE program)	49
33	Normalized conducted frequency spectrum of a full-wave bridge rectifier without transformer	50
34	Normalized conducted frequency spectrum of T-R power supply	50
35	Limit for CEO1 ac leads, MIL-STD-461B, part 5	53
36	Limit for CEO1 dc leads, MIL-STD-461B, part 5	55
37	Delco converter	58
38	Noise sources for dc-input switching regulators	62
39	Switching transistor and commutating diode currents for simplified buck switching regulator	63
40	Switching current basic waveform (without diode recovery spike)	65
41	Switching regulator basic waveform harmonic spectrum	65
42	An example of switching regulator spike "ringing" spectrum (from diode recovery)	66

CONTENTS

		PAGE
FIGURE		
43	Switching regulator input current spectrum (no filter)	66
44	Two-section optimum weight filter	67
45	Single-section optimum weight filter	67
46	Switching regulator input current without and with filter (two stages)	69
47	CE03 Navy limits for MIL-STD-461	69
48	Voltage and current snubbers	72
49	Examples of bad and good wiring layouts	74
50	Four high frequency lead filtering methods	75
51	Balun or neutralizing transformer	75
52	An easy way to wind a balun	76
53	Input/output lead, capacitor filter	76
54	Capacitor ac equivalent circuit	85
55	Compound capacitor	87
56	Capacitor response characteristics	90
57	Two features of ferromagnetic materials: high permeability μ (steep slope on a B-H curve) and saturation (slope is free space μ_0)	93
58	Double valued B-H loop characteristics of square (a) and linear (b) materials	93
59	Increase of airgap increases dc current capability of the inductor	94
60	Composite core with gapped and ungapped sections eliminates core saturation problems and keeps high inductance (L) at lower current (i)	94
61	Methods of winding toroid cores depicting only the first layer of winding	96
62	Soft inductor - composite core with variable inductance (L) and variable damping (Q)	96
63	Two-output forward converted (buck) with output inductor coupling	98
64	Transformer capacitive coupling transmits ground loop noise	100
65	Grounded electrostatic shield between transformer windings (Faraday shield) breaks capacitive coupling	100
66	Typical common-mode attenuation obtained with a single electrostatic shield grounded (connected) and ungrounded (disconnected) for a 115 Vac transformer	101
67	Common-mode attenuation obtained with two similar 115 Vac transformers, one unshielded and the other with an electro- static shield connected	101
68	Transformer with three electrostatic shields between windings	102
69	Common-mode attenuation obtained for a 115 Vac transformer with three electrostatic shields connected and disconnected	102
70	Power transformer after adding copper shading ring	105
71	Ferrites-inductance, reactance, resistance, impedance vs frequency	107
72	Insertion loss of ferrite core (or bead)	107
73	Conductors	109
74	Contact breakdown versus time with no protection	111
75	Available voltage across opening contact for inductive load	111

CONTENTS

FIGURE		PAGE
76	Comparison of available voltage and contact breakdown for inductive load	112
77	Contact protection circuits to minimize "inductive kick" (from inductive load) and minimize radiated and conducted noise	114
78	Contact protection circuits used across switch contacts	114
79	Filter input and output impedance	116
80	Power line impedance data: mean of measured values - good fit to curve A (parallel RL circuit with $R = 50 \Omega$ and $L = 30 \mu\text{H}$) Curves B and C are reasonable fits to standard deviations of measured values	116
81	Wave impedance for electric and magnetic fields	119
82	Shielding effectiveness (s) for metallic sheets in near and far fields	121
83	Appropriate shielding calculations for metallic sheets in near field ($A > 10 \text{ dB}$)	121
84	Magnetic material as a shield	123
85	Containing magnetic field with multilayer shield	123
86	Utilizing natural shielding	124
87	Seams, joints and holes	124
88	Hole formed into a waveguide ($d < t$)-magnetic shielding if operating frequency is \ll cutoff frequency	125
89	Round holes to provide ventilation	125
90	Canonical equivalent circuit that models the three essential functions of any dc-to-dc converter: control, basic dc conversion, and low-pass filtering (continuous conduction mode)	128
91	Canonical model representing any basic dc-dc converter	129
92	The basic dc-to-dc converter circuits for the (a) buck, (b) boost, and (c) buck-boost topologies	130
93	Basic Cuk switching-mode power supply configuration	132
94	Canonical circuit model of the Cuk converter for the continuous conduction mode ($D' = 1-D$ and $M(D) = D/D'$)	132
95	Push-pull transformer-coupled (quasi-square-wave) converter (buck-derived): (a) circuit; (b) Canonical model	133
96	Double-output single-ended transformer-coupled (forward) converter (buck-derived): (a) circuit; (b) Canonical model	133
97	Double-output single-ended transformer-coupled (flyback) converter (buck-boost-derived): (a) circuit (b) Canonical model	135
98	Asymptote shapes for the magnitudes of (a) the input impedance $ Z_{ei} $, (b) the transfer function $ H_e $, (c) the output impedance $ Z_{eo} $ of the effective low-pass filter in the Canonical model of FIGURE 91.	136

CONTENTS

FIGURE		PAGE
99	Model of the general switching-mode regulator with addition of a line input filter and incorporation of the Canonical model	138
100	Desired relative placement of the magnitude shapes of the input filter output impedance $ Z_S $ with respect to the open-loop input impedance $ Z_{ei}/M^2 $ and the open-loop short-circuit input impedance $(R_e + sL_e)/M^2$	138
101	Simplified circuit examples of open-loop input impedance	140
102	The basic single-section input filter, its two-pole transfer characteristics $[H_S(S)]$, and output impedance $ Z_S $ with $ Z_S _{max} = R_m$	142
103	Single-section input filter with extra series damping resistance R_c , its two-pole one-zero $ H_S(s) $, and $ Z_S $ with $ Z_S _{max}$ lower than R_m	142
104	Single-section input filter with parallel damping resistance R_p across the inductor, its two-pole one-zero $ H_S(s) $, and $ Z_S $ with $ Z_S _{max}$ lower than R_m	143
105	Single-section input filter with parallel damping resistance R_p across the capacitor, its two-pole $ H_S(s) $, and $ Z_S $ with $ Z_S _{max}$ lower than R_m	143
106	Double-section input filter and its four-pole one-zero $ H_S(s) $. Its $ Z_S $ has two maxima, shown in typical relation to the regulator open-loop input impedance $ \mu^2 Z_{ei} $	144
107	Q of an LC filter	146
108	Single-section low-pass LC filter with blocked shunt damping resistance	146
109	Circuit for computer program: Evaluation of input filter attenuation and its effect on stability of switching regulator	150
110	Symmetrical trapezoidal periodic pulse	162
111	Low frequency harmonic spectrum for $t_r + t_o = T/2$ trapezoidal pulse	162
112	Line current waveform for three-phase rectification	163
113	Low frequency harmonic comparison for rectangular and trapezoidal waveshapes	164
114	Low frequency harmonic spectrum for trapezoidal periodic pulse (narrow band)	165
115	Low frequency harmonic envelope for single-pulse (broad band)	165
116	Interference level for a 1-V, 1- μ s rectangular pulse	166
117	Interference level for a 1-V, 1- μ s trapezoidal pulse	166
118	Trapezoidal pulse interference	167
119	Interference levels for eight common pulses	167
120	Interference levels for various pulse shapes	169
121	Normalized frequency spectrum of damped sinewave pulse	169

SECTION 1. INTRODUCTION.

1.1 Scope. This handbook offers guidance to power supply designers in techniques which have been found effective in reducing conducted and radiated interference generated by power supplies. It is a compilation of information from library sources, pertinent military laboratory programs including contracts to universities and industry, and practical fixes derived from the experience of engineers.

1.1.1 Switching-mode power supplies. Switching-mode power supplies have characteristics such as high output power per unit volume and high efficiency, and as a result their use is increasing. If improperly designed, however, they create electromagnetic interference (EMI) that can degrade other systems. A major shortcoming of switching-regulator technology is that it is a complex technology that appears to be simpler than it actually is. Because of this apparent simplicity, misjudgments are prevalent in the design and application of switching-mode power supplies by the uninitiated engineer. In the past few years, the inherent advantages of switching-mode technology for power supplies have spurred advances in component design (to limit the noise sources) and design techniques (to curtail noise coupling to the outside world). The result is much less EMI.

Application of EMI reduction techniques cannot be done indiscriminately. Switching-mode power supplies are constant power devices and exhibit a negative input resistance. Improper design of filters can cause degradation of power supply parameters and even turn the whole power system into an oscillator. This handbook provides criteria for proper filter design in addition to providing pertinent EMI reduction techniques.

Unless otherwise specified herein, terms used in this handbook are as defined in MIL-STD-463.

1.2 Designing to meet specific EMI requirements. Electromagnetic interference (EMI) may be defined as electromagnetic energy which interrupts, obstructs, or otherwise degrades or limits the effective performance of electronic equipment. Electromagnetic compatibility (EMC) also implies susceptibility levels for equipment exposed to a particular EMI level that would enable the equipment not to suffer malfunction or reduced performance.

The emissions are generated either by conduction or radiation or both. Similarly the equipment may be susceptible to either conducted or radiated emissions or both.

1.2.1 Differential versus common-mode interference. Conducted emissions may interfere in either of the following modes:

- a. Differential-mode interference which causes the potential of one side of the transmission path to be changed relative to the other side.
- b. Common-mode interference which appears between both leads and a common reference plane (ground) and causes the potential of both sides of the transmission path to be changed simultaneously and by the same amount relative to the common reference plane (ground).

1.2.1.1 Causes of common-mode interference. Common-mode currents can be induced into electronic equipment in the following ways:

- a. Electromagnetic (radiated) energy impinging on cables induces common-mode currents into power or signal lines and returns. The effect on the system depends on the magnitude of the induced signals and the common-mode noise rejection of the system and grounding configuration. In a poorly designed system, the common-mode signal is converted to a differential-mode signal and acts as a valid differential signal -- resulting in problems. Interference problems may or may not occur depending on the system's balance, shielding, isolation, impedance, grounding, data rate, and signal threshold.
- b. Acting like common-mode noise currents are structure currents feeding into lines either capacitively or directly. The structure currents result from either ground voltage differences or electromagnetic energy induced into the structure. Ground voltage differences occur on ships despite the intentional ungrounding of the three-wire power lines. Stray capacitances are significant causes, but the main culprits are line-to-chassis capacitors in equipment EMI filters. Thus, varying alternating current (ac) voltage grounds are established from equipment to equipment. Hull currents then result, adversely affecting some equipments. These structure currents can also be brought directly into active circuitry by hard-wire connections. In Navy shipboard grounding practices, it is common to connect the signal ground to

chassis in each equipment. In fact, MIL-F-18870E makes this mandatory for fire-control systems. It is also mandatory to tie the chassis to the hull. When nonisolated line drivers and receivers are used - also a common practice -- structure current can be brought directly into the interface circuits being used to communicate information between equipments.

1.2.2 Pertinent MIL-STD-461 requirements. Power supplies are potential emitters and susceptors in the frequency range and of the EMI type specified in the following MIL-STD-461 requirements:

CE01	Conducted Emissions, Power and Interconnecting Leads, Low Frequency [up to 15 kilohertz (kHz)]
CE03	Conducted Emissions, Power and Interconnecting Leads, 0.015 to 50 megahertz (MHz)
CE07	Conducted Emissions, Power Leads, Spikes, Time Domain
CS01	Conducted Susceptibility, Power Leads, 30 hertz (Hz) to 50 kHz
CS02	Conducted Susceptibility, Power Leads, 0.05 to 400 MHz
CS06	Conducted Susceptibility, Spikes, Power Leads
RE01	Radiated Emissions, Magnetic Field, 0.03 to 50 kHz
RE02	Radiated Emissions, Electric Field, 14 kHz to 10 gigahertz (GHz)
RS01	Radiated Susceptibility, Magnetic Field, 0.03 to 50 kHz
RS02	Radiated Susceptibility, Magnetic Induction Field, Spikes and Power Frequencies
RS03	Radiated Susceptibility, Electric Field, 14 kHz to 40 GHz

All of the requirements may or may not be specified depending on the platform location of either the power supply or the equipment containing the power supply. Also limits for the requirements may be different for different platforms.

Both narrowband and broadband limits may be specified for some requirements. Although narrowband interference is discussed in this handbook, broadband interference may appear depending on both the bandwidth of the measuring equipment and also the super position of rectification emissions, switching-mode regulator emissions, and other nearby emissions.

SECTION 2. REFERENCED DOCUMENTS.

2.1 Government documents.

2.1.1 Specifications, standards, and handbooks. The following documents of the issue listed in the Department of Defense Index of Specifications and Standards (DoDISS) and its supplements, form a part of this document to the extent specified herein. The date of the applicable DoDISS and supplements thereto shall be as specified in the solicitation.

SPECIFICATIONS

MILITARY

MIL-T-27	Transformer And Inductor (Audio, Power, And High Power Pulse) General Specification For
MIL-E-16400	Electronic, Interior Communication And Navigation Equipment, Naval Ship And Shore: General Specification For
MIL-F-18870	Fire Control Equipment, Naval Ship And Shore, General Specification For
MIL-T-28800	Test Equipment For Use With Electrical And Electronic Equipment, General Specification For

STANDARDS

MILITARY

MIL-STD-461	Electromagnetic Emission And Susceptibility Requirements For The Control Of Electromagnetic Interference
MIL-STD-463	Definition And System Of Units, Electromagnetic Interference Technology
MIL-STD-785	Reliability Program For Systems And Equipment Development And Production
DoD-STD-1399, Section 300	Interface Standard For Shipboard Systems Section 300 Electric Power, Alternating Current (Metric)

(Copies of specifications and standards required by contractors in connection with specific procurement functions should be obtained from the procuring activity or as directed by the contracting officer.)

2.2 Other publication. The following document forms a part of this document to the extent specified herein. The issue of the document which is indicated as DoD adopted shall be the issue listed in the current DoDISS.

IEEE STD 519-1981	IEEE Guide For Harmonic Control And Reactive Compensation Of Static Power Converters
-------------------	--

(Application for copies should be addressed to the Institute of Electrical and Electronics Engineers, Inc. (IEEE) 345 East 47th Street, New York, NY 10017.)

SECTION 3. POWER SUPPLIES.

Military electronic systems use power processing circuits to convert and condition power from the electrical power provided by military platforms. These power processing circuits are called power supplies, a misnomer since they process rather than supply power. Both the requirements of the electronic system and the characteristics of the electrical power source place constraints on these power conversion circuits. In reference (1) of APPENDIX E these constraints are selected as criteria for evaluating the various approaches to power conversion and the conclusion is reached:

"Off-line¹ switching-mode power conversion technology is the only known technology that will meet present and projected requirements for shipboard electronic system power conversion." The same conclusion is likely to be reached for other military platforms. Much of the discussion through 3.3.4 is taken with some variations from a paper by J. Foutz (reference (1)).

3.1 Selection of criteria. Power source characteristics and electronic system requirements are selected as criteria for evaluating approaches to power conversion.

3.1.1 AC or dc input power. The power from military service generators can be either 60 Hz, or 400 Hz, or dc.

For example, on shipboard the power system is ac (60 Hz, three-phase) ungrounded, while the signal ground in electronic systems is typically grounded to the ship's hull. This requires the use of isolation transformers in the electronic systems power supplies.

Three-phase power is preferred over single-phase power for reasons not immediately obvious. Capacitors in power-line electromagnetic interference (EMI) filters form an ac ground. Unbalance between electronic system ac grounds causes currents to flow in the hull of the ship that can upset some ship systems. The ac ground formed by the EMI filters in electronic systems using single-phase power causes the greatest degree of unbalance. Since the use of three-phase power usually reduces the requirements for both filtering and energy storage in electronic system power supplies, the use of three-phase power is beneficial for both ship and electronic systems.

Voltage spikes are typically specified as characteristic of power provided by military platforms. The 2500 volt (V) spike specified for shipboard electric power is mostly absorbed in the power line filter and post rectifier input smoothing filter if inductive. It presents no special design problem if sufficient inductance is used with sufficient permeability to prevent saturation.

Electric power characteristics (such as those specified for ships by DoD-STD-1399, Section 300) usually include harmonic voltage limits. Limits, therefore must be imposed on the harmonic currents that an electronic system can draw from the power system. These harmonic currents are a major consideration in military power supplies. The problem is considered in Sections 4 and 5 herein.

One of the key selection criteria for evaluating an approach for power conversion for military electronic systems is the capability to operate from 60 Hz power, 400 Hz power, and dc power.

3.1.2 Continuity of power. Because of the importance of electrical power, military power systems are frequently highly redundant. Electrical power is usually restored to vital shipboard loads in from 50 microsecond (μ s) to several seconds after a malfunction in the electrical system (due to failure, battle damage, or other cause). However, this momentary interruption of power can have continuing adverse effects on the ship's capability to perform its mission. Time to achieve full equipment performance may require up to 20 hours.

A key selection criterion for evaluating an approach for power conversion for military electronic systems is the capability to withstand momentary power interruptions without degrading the performance of the electronic system.

¹ Off-line means that ac-power is directly rectified to direct current (dc) without using line frequency transformers. Power conversion is then accomplished by dc-to-dc or dc-to-ac converters. Isolation between input and output and voltage transformation is accomplished with high-frequency (typically 20 kHz) transformers. Since off-line switching-mode power supplies also operate from dc power, they are independent of power line frequency. The same power supply can be designed to operate from dc, 60 Hz, or 400 Hz power.

3.1.3 Power density. The output power density $D(o)$ of a power conversion circuit is its output power $P(o)$ divided by its volume. The electronic load that dissipates the converter's $P(o)$ has a thermal density $D(e)$ which is $P(o)$ divided by the electronic load's volume $V(e)$. Therefore,

$$\begin{aligned} D(o) &= P(o) / V(c), \\ D(e) &= P(o) / V(e), \\ \text{and } V(c) / V(e) &= D(e) / D(o). \end{aligned}$$

Thus the percentage volume of a system occupied by a power conversion circuit is a function of its $D(o)$ compared to the $D(e)$ of the electronic system it feeds.

The output power density in turn depends upon the efficiency and thermal density of the power conversion circuit. The impact of efficiency on the percentage system volume occupied by the power conversion subsystem is shown in FIGURE 1. The only assumption is that the power conversion subsystem operates at the same thermal density as the rest of the system. The efficiencies shown are not arbitrary but are the efficiencies for regulators supplying 5-V logic circuits that will operate from shipboard power. The efficiency is for the total subsystem between the ship service generators and the logic circuits and includes the power losses in motor generators as well as the electronic system power supplies. Twenty-two percent is the efficiency for submarine 400 Hz power and dissipative regulators, 27 percent for surface ship 400 Hz power and dissipative regulators, 35 percent for 60 Hz power and dissipative regulators, 65 percent for present 60 Hz or 400 Hz off-line switching-mode power supplies, and 80 percent for 60 Hz or 400 Hz off-line power supplies available by 1985. Equal thermal density constraints indicate that a 35 percent efficient dissipative regulator should occupy two-thirds of the volume of the system. This rarely happens because it is unacceptable to most system designers and program managers. The alternative is to operate the power supply hotter than the rest of the system, which degrades reliability; or to use special cooling techniques which increase the cost. Eighty-percent efficient power supplies would occupy only 20 percent of the system volume under similar equal density constraints.

Electronic system thermal densities are being increased and projected to increase even more in the future (this is shown in TABLE 1). Unless the output power densities likewise increase, the power conversion circuits will occupy most of the system volume.

A key criterion in selecting an approach for power conversion is the capability to provide output power densities of one watt (W) per cubic inch or more.

3.1.4 System compatibility. Power conversion approaches that cause problems to the rest of the system are undesirable. Compatibility problems that can be caused, aggravated, or ameliorated by the power conversion circuits include harmonic currents drawn from the power system, negative resistive loading of the power system, electromagnetic interference, and pulse loading of the power system.

A key criterion in selecting an approach for power conversion for electronic systems is compatibility, including compatibility with other systems and self-compatibility.

3.1.5 Life-cycle costs. Another key criterion in selecting an approach for power conversion is life-cycle costs, including acquisition and operating costs. Power conversion circuits can have substantial impact on energy consumption. Department of Defense policy now requires consideration, throughout the acquisition process, of utilization of energy during the project system life. This aspect of life-cycle costs is especially applicable to power conversion.

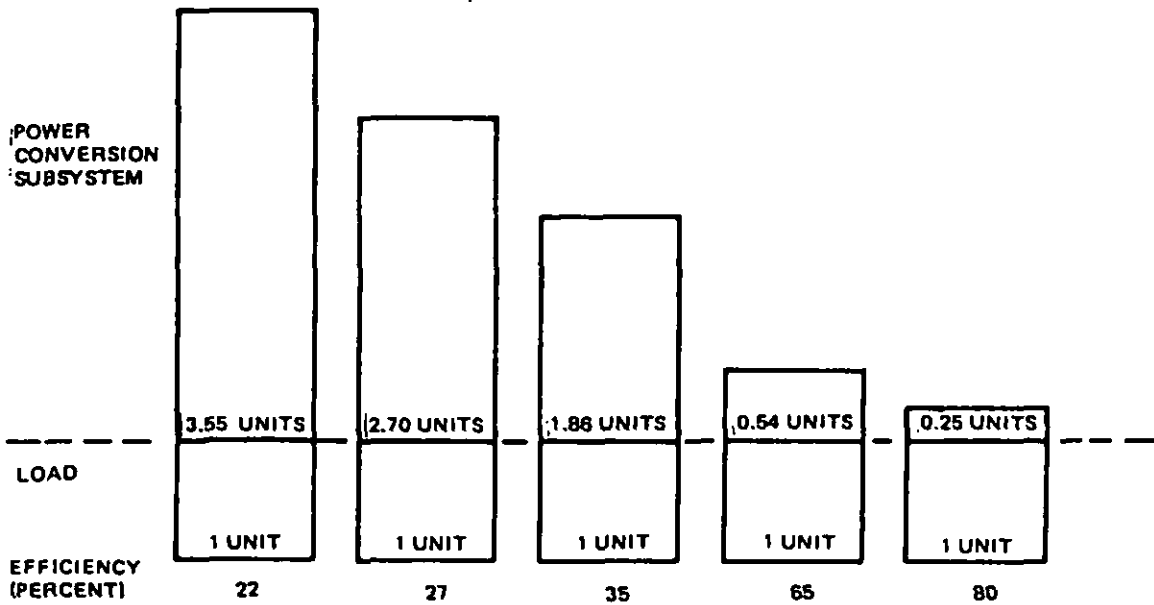


FIGURE 1. Equal thermal density volume versus efficiency.

TABLE I. Output power density (P_D) requirements.

Thermal Density, P_D/in^3	Efficiency (Percent)	Percentage System Volume of Power Supply Based Upon Efficiency (Percent)	Needed Power Output Density, P_O/in^3	Comment
1.7 W/in ³ Limit of SEM 1A unless special thermal analysis is made	35%	65%	0.9 W/in ³	Beyond 60-Hz dissipative technology. Just at 400-Hz dissipative technology
	65%	35%	3 W/in ³	Just at 1977-1978 switching-mode technology
6 W/in ³ Projected 1985 high-performance electronics	50%	50%	6 W/in ³	Just at projected 1985 switching-mode technology
	65%	35%	12 W/in ³	Major breakthrough needed for 1985 power supply to equal same percentage of system volume as 1978 power supply
	80%	20%	24 W/in ³	Another major breakthrough needed for P_O/in^3 to be compatible with efficiencies achievable in 1978

3.2 Power conversion approaches. Five types of power conversion circuits are shown in FIGURE 2. Some parameters for selecting the best circuit to a set of criteria are given in TABLE 11. The salient features of each circuit are discussed.

3.2.1 Dissipative regulators. Dissipative regulators draw much more power from the source than is required by the load. Regulation is accomplished by an electricity-to-heat conversion. The series pass element acts like a variable resistor (heat sink). Under worst case conditions of high input line voltage and low output dc voltage, the wattage across this series pass element becomes excessive. However, it also needs a nominal amount of control voltage under conditions of low line and high output voltage, and therefore voltage range specifications are important in determining the efficiency of this type supply. For example, the typical efficiency of 5-V regulators that operate with ship power (± 20 percent including transients) is 35 percent. This can be raised to slightly over 50 percent if the power supply does not have to operate through the ± 16 percent transient.

Simplicity and poor efficiency are their salient features. Isolation is achieved by bulky power-line transformers. A major cause of power supply failures and system malfunctions is found in attempts to improve the efficiency and output power density of dissipative regulators. Failure rates increase when size is reduced so that power supply components operate hotter than other system components. System malfunctions occur when the power supply is not designed to operate through negative transients.

3.2.2 Ferroresonant regulators. Ferroresonant regulators operate by resonating a capacitor in the secondary of the isolation transformer with a saturable reactor which is one leg of the transformer. Resonance increases the voltage and the nonlinear reactor clamps it at a stable voltage independent of the input voltage. The ferroresonant regulator is usually used as an ac regulator but the output can be rectified and filtered. The salient features include simplicity, inherent overload protection, poor power factor, and sensitivity to frequency changes. For example, the $+5.5$ percent frequency transient limit on shipboard power would typically cause a $+9.4$ percent voltage transient on the output. Also, when used for dc, the rectifier and filter are outside the regulation loop, resulting in poor static and dynamic load regulation. These poor characteristics can be compensated for, but the inherent circuit simplicity is then lost.

3.2.3 Phase control switching-mode regulators. The simplest phase control regulators operate by delaying the phase of the trigger circuit to a silicon controlled rectifier (SCR) so that it is off for the first part of an ac cycle and on for the remainder. They can be used as off-line switching-mode regulators unless isolation is required and then they must be used with a power line transformer. The simplest version, which produces the top waveform of FIGURE 3, has gained a reputation for degrading the quality of ac power lines severely. More sophisticated circuits are gentler on the ac power at some cost in simplicity. This is shown in the other waveforms of FIGURE 3. For each notch taken from the ac waveform, a power conversion parameter can be controlled. The bottom waveform has four notches and allows control of the dc component and any three harmonics; that is, the third, fifth, and seventh harmonics can be minimized. Other parameters can also be controlled, such as minimum total harmonic distortion or maximum power factor for any operating condition.

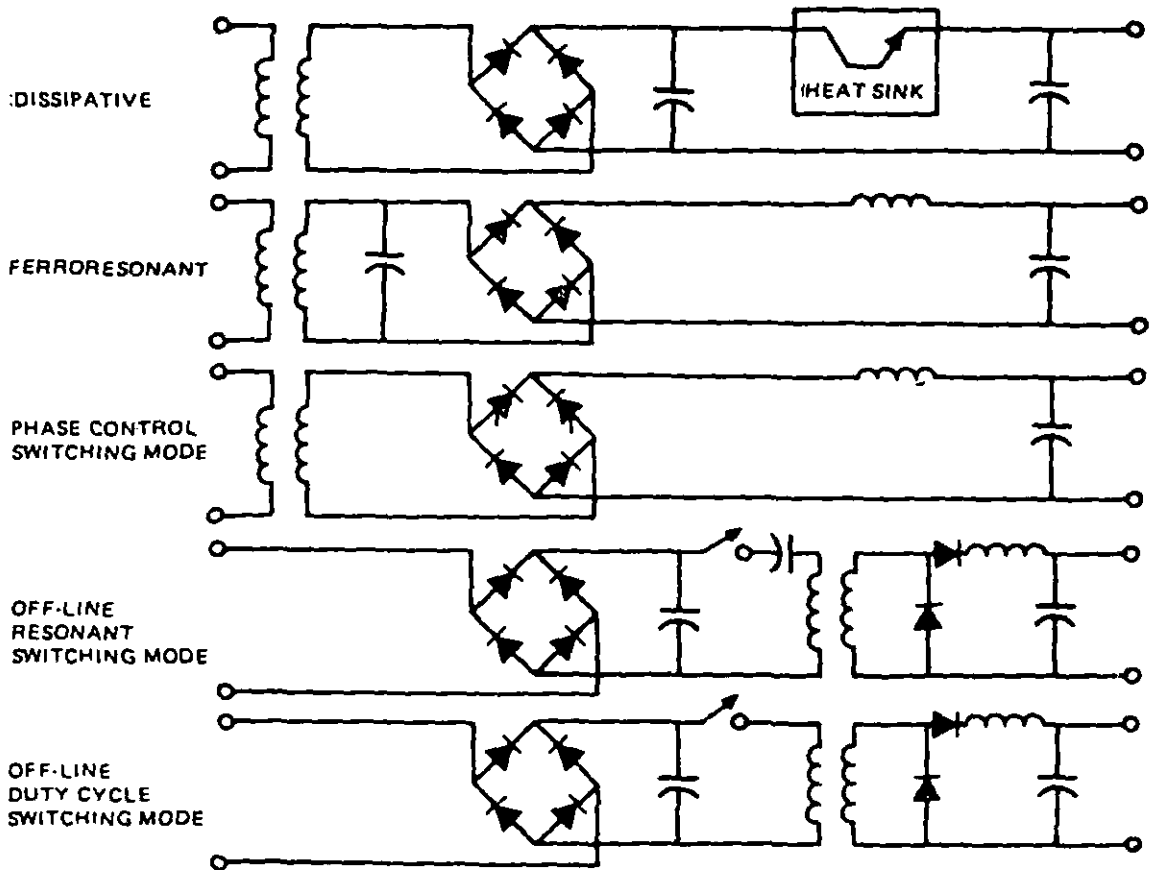


FIGURE 2. Power conversion circuits.

TABLE II. Power conversion circuit selection parameters.

Circuit Type	Complexity	Power Line Frequency	η , %	Efficiency Improvement Prospects	Power Density, W/in ³	Power Density Improvement Prospects	EMI
DISSIPATIVE							
60 Hz magnetics	simple	60/400 Hz	35	none	0.5	poor	little
400 Hz magnetics	simple	400 Hz only	35	none	1.0	poor	little
FERRO-RESONANT							
60 Hz resonant	simple	60 Hz only	65	poor	0.4	poor	little
400 Hz resonant	simple	400 Hz only	65	poor	0.9	poor	little
PHASE CONTROL SWITCHING MODE							
60 Hz	moderate	60 Hz only	65	poor	0.7	poor	high
400 Hz	moderate	400 Hz only	65	poor	1.2	poor	high
OFF-LINE SWITCHING MODE							
	moderate to complex	dc or any ac	65	good (80%)	2.0	good (6.0 W/in ³)	moderate

η = efficiency

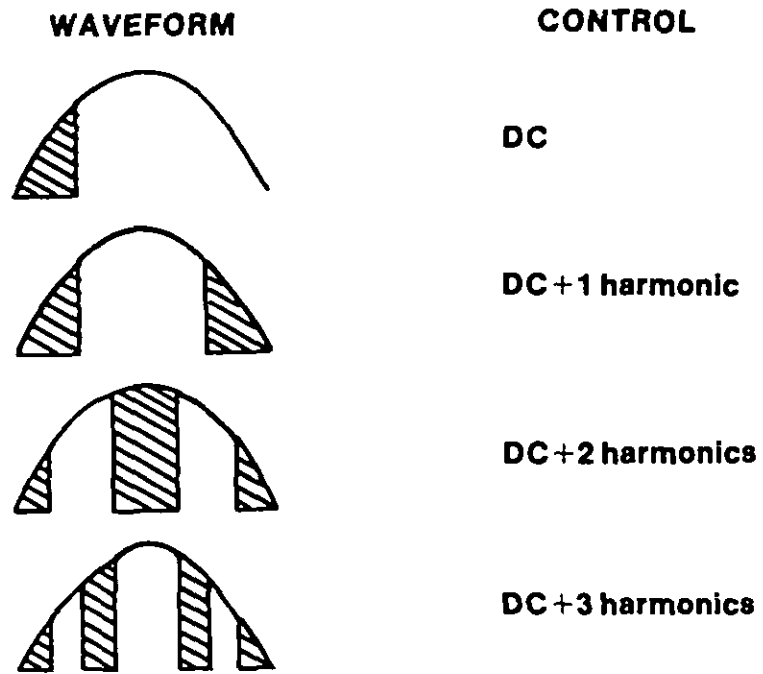


FIGURE 3. Phase control switching mode.

3.2.4 Off-line¹¹ switching-mode regulators. There are two general types of off-line switching-mode regulating power supplies--resonant converters and duty cycle converters. Both types immediately rectify ac power to dc power and perform power conversion at frequencies well above the line frequency. The typical switching frequency is 20 kHz but frequencies up to 200 kHz and even higher are increasingly being used. Power density is high because the size of the isolation transformer decreases inversely at the 3/4 power of the switching frequency. Also, the filter size decreases linearly with frequency. Power density and efficiency can be traded within limits. Where high efficiency is critical, higher efficiency can be obtained by lowering output power density. Salient features are high efficiency and high output power density, and they have the potential for increasing output power density significantly beyond what can be achieved today.

Two types of resonant converters are shown in FIGURE 4. One type operates by varying the pulse repetition rate, spacing or crowding the resonant pulses to achieve the desired average voltage. The other type operates by crowding the repetition rate so that the waveform approximates a continuous sinusoid. The outputs of two channels are then vectorially added in a transformer to produce the converter output. The magnitude of the output is controlled by shifting the relative phase between the two channels. The salient features of both types of resonant converters are minimal high-frequency EMI due to the filtering of the resonant circuit; and resonant commutation which facilitates the use of SCR's as the switch.

Duty cycle converters regulate by varying the ratio of switch on time to off time. A widely used version turns the switch on at fixed intervals (constant frequency) and varies the on-off time. FIGURE 5 shows this version used with a buck or voltage stepdown converter. The dc component of the rectangular wave output is recovered by a low-pass filter. Other versions of switching control vary the frequency which makes filtering less effective and, therefore less advantageous in reducing EMI. Duty cycle converters are better understood than resonant converters. This better understanding has resulted in some exceptional designs, including a configuration that behaves as a true dc transformer--with no pulsating voltages or currents on the input or output at the switching frequency. This configuration is specified in 3.3 wherein duty-cycle switching-mode power supplies are discussed in more detail. Unless otherwise stated, reference to switching-mode power supplies in this handbook implies the more common duty-cycle converters.

3.3 Off-line switching-mode power supplies. The following paragraphs discuss off-line switching-mode power supplies, their advantages, availability, future potential, and topologies, potential problems and solutions to these problems.

3.3.1 Description. FIGURE 6 is a block diagram of a typical off-line switching-mode power supply. The only component in the power supply that is affected by the power line frequency (dc, 60 Hz, or 400 Hz) is the circuit breaker, which for this particular supply is a 400 Hz circuit breaker. Except for this component, the power supply will operate from a dc or 60 Hz source as well as a 400 Hz source. The power transformer that provides isolation between signal and power ground is a relatively small part of the power supply, the power switches require little heat sinking, and the three-phase bridge rectifier is quite small.

The switching regulator shown in FIGURE 6 performs the voltage regulation function by means of a switching transistor [or field effect transistors (FET) or SCR or combinations of several devices]. The transistor chops the unregulated input voltage in such a manner as to maintain the average output voltage level constant. The regulator output is a series of rectangular pulses which are then smoothed by a low pass filter to a relatively constant dc level. Usually, voltage regulation is used but current-mode regulation is also starting to be used because it has several advantages. With voltage regulation, a portion of the output voltage is compared to a reference voltage; an error voltage is generated; and the error voltage is fed back to an oscillator controlling the drive circuit for the switching device. Voltage regulation is achieved by a pulse-duration modulation process.

¹¹ Line-transformer-isolated switching-mode power supplies are sometimes needed. For example, if the power supply is connected directly to shipboard 440 V three-phase, then the resultant dc voltage may be too high for today's transistorized switches (except for two recently announced power darlington's rated at 20 amps, 750 V or 850 V, and capable of blocking 1000 V or 1200 V). Also, to achieve low line harmonics one solution is to use multiphase rectification requiring the use of a line transformer (see Section 5). Although line transformers make switching-mode power supplies bulkier and heavier, they still have the efficiency advantage and other advantages.

Pulse repetition rate



Vector summation

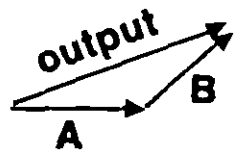
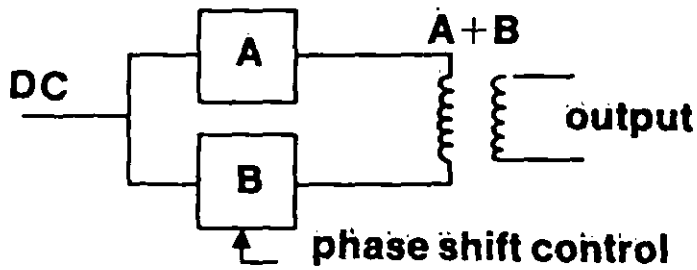


FIGURE 4. Resonant converters.

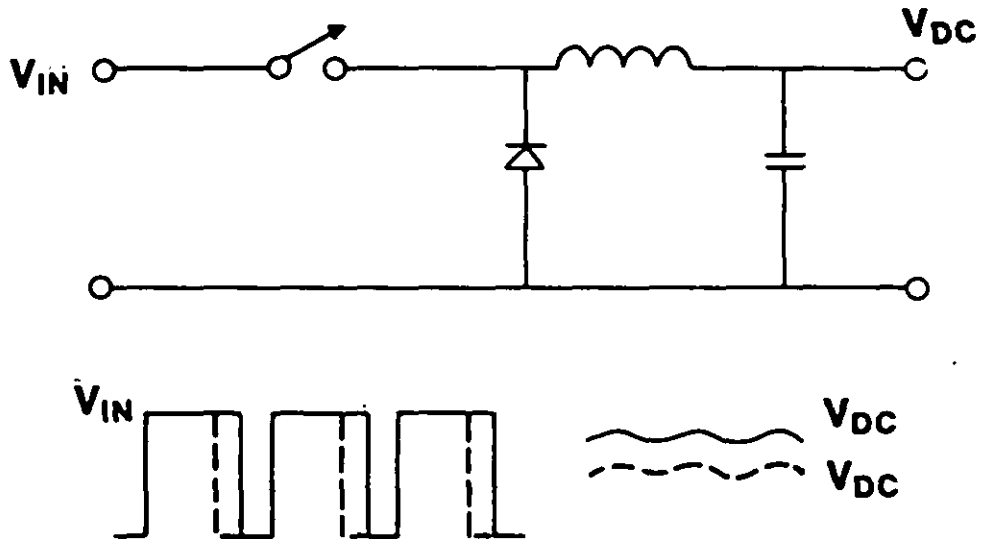


FIGURE 5. Duty cycle converter.

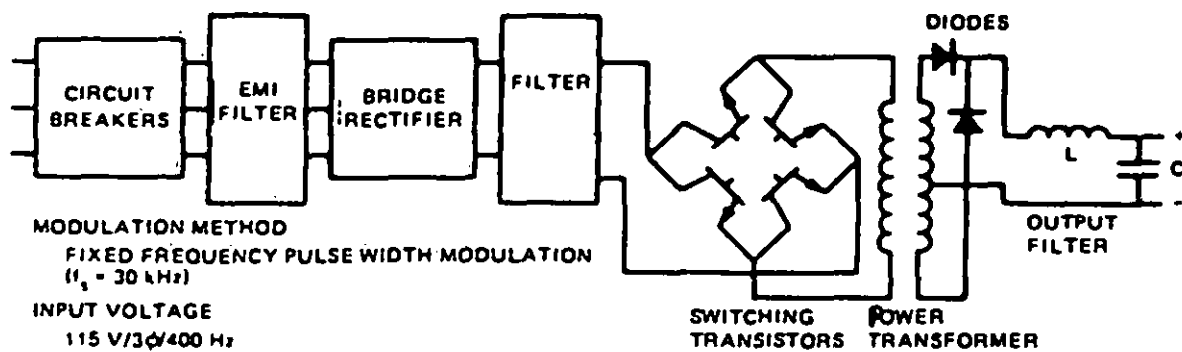


FIGURE 6. Typical off-line switching-mode power supply - block diagram.

3.3.2 Advantages. Compared to their 60-Hz dissipative counterparts, off-line switching-mode power supplies are two to six times smaller and three to six times lighter, accept all input frequencies (dc, 60 Hz, 400 Hz), and have high efficiency (65 percent to 95 percent), even with wide input voltage variations (up to 3:1, or ± 50 percent). This high efficiency means reduced power from the source and reduced cooling requirements. In addition, their initial costs are decreasing so they usually cost less except for low power levels where costs are equal, and their operating energy costs are very much less.

Off-line switching-mode power supplies have more inherent energy storage than conventional dissipative regulators that use a power line transformer to transform down the input voltage. Thus more stored energy is available to operate through a momentary interruption of power. The improvement occurs because the energy is stored at a higher voltage for off-line switchers-- and energy storage increases as the square of the voltage rating increases while capacitance decreases linearly as the voltage rating increases for a given size capacitor ($CV = \text{constant}$ for aluminum electrolytic and tantalum foil capacitors).

Off-line switching-mode power supplies are also compatible with many system loads. The use of digital processing incorporating memory elements is increasing as minicomputers, microcomputers, and microprocessors are embedded into electronic system design. These digital processing circuits are susceptible to transient loss of power. However, these systems can tolerate higher noise levels. Therefore, off-line switchers match these new loads in that their capability to operate over a wide variation in input voltage minimizes transient loss of power and their higher output ripple is tolerated by digital loads.

3.3.3 Availability. Switching-mode power supplies are now available in the low-voltage product line of most power supply manufacturers. There is an economic advantage for the DoD to be compatible with the main stream of commercial development since nonrecurring costs are minimized if slightly modified militarized versions of commercial designs can be used.

The trend toward more complex and miniaturized electronic products is leading to the need for optimized and more efficient power conditioning methods. Switching-mode technology is still emerging and new topologies are being explored by specialists in the field of power electronics. The advent of very large scale integration (VLSI) electronics presents a challenge, not only to those involved with their fabrication, test, and application, but also to power conditioning subsystem designers.

3.3.4 Potential problems. Switching-mode power supplies have characteristics different from those of dissipative power supplies. To be unaware of these differing characteristics is to invite design and application problems. The potential problems listed in TABLE III are discussed, and solutions for each problem are presented (except for solutions for electromagnetic compatibility which are discussed in detail in Sections 5 and 6).

a. **Modeling.** A model of a switching-mode power supply is useful in discussing characteristics. The state-space-averaged linear model developed at California Institute of Technology by R.D. Middlebrook and S. Cuk is used here (reference 2). The top line of FIGURE 7 shows the basic circuits of the three common duty cycle switching-mode power supplies--buck, boost, and the buck-boost. All three of these circuits can operate in two modes. In one mode there is continuous current through the inductor and in the other mode the current through the inductor is discontinuous (light load).

The continuous mode is modeled in the center line of FIGURE 7 for each circuit by two states representing the circuit--one state with the transistor switch closed and one with it open. These circuits can be averaged by topological manipulation into a single canonical model as shown in the lower left section of FIGURE 7. The canonical model consists of an ideal dc and ac transformer, a low-pass filter, and a voltage and a current generator that represent the duty ratio control of the output. The component values are shown in FIGURE 7. The component values are a function of the ratio of time spent in each state during a complete switching cycle (the duty ratio, D). The model is a linear model linearized about the duty cycle chosen and is valid to about one-half the switching frequency. More detailed information about the model and models of extended converter configurations are given in APPENDIX A. The model is used to explain several of the potential problems.

To model the discontinuous mode requires a third circuit state (with the switch open and no current in the inductor) for each topology. This is not depicted here but rather it is recommended to avoid the discontinuous mode because it causes--increased EMI. It can be avoided either by preloading the outputs with dummy loads or in a less lossy but more complex method using bidirectional current switching.

TABLE III. Potential problems with switching-mode power supplies.

Potential Problem	Areas Affected
Filter effects	Output ripple Load transient effects Line transient effects
Constant input power characteristics	Negative input resistance Low-voltage component stress Turn-on latch-up
Electromagnetic compatibility	Line frequency harmonic currents Noise spectrum Misuse of EMI filters Audio susceptibility
Stability difficulties	Entrainment or synchronization High-order system Right half plane zeros Nonlinear and discrete time High EMI environment

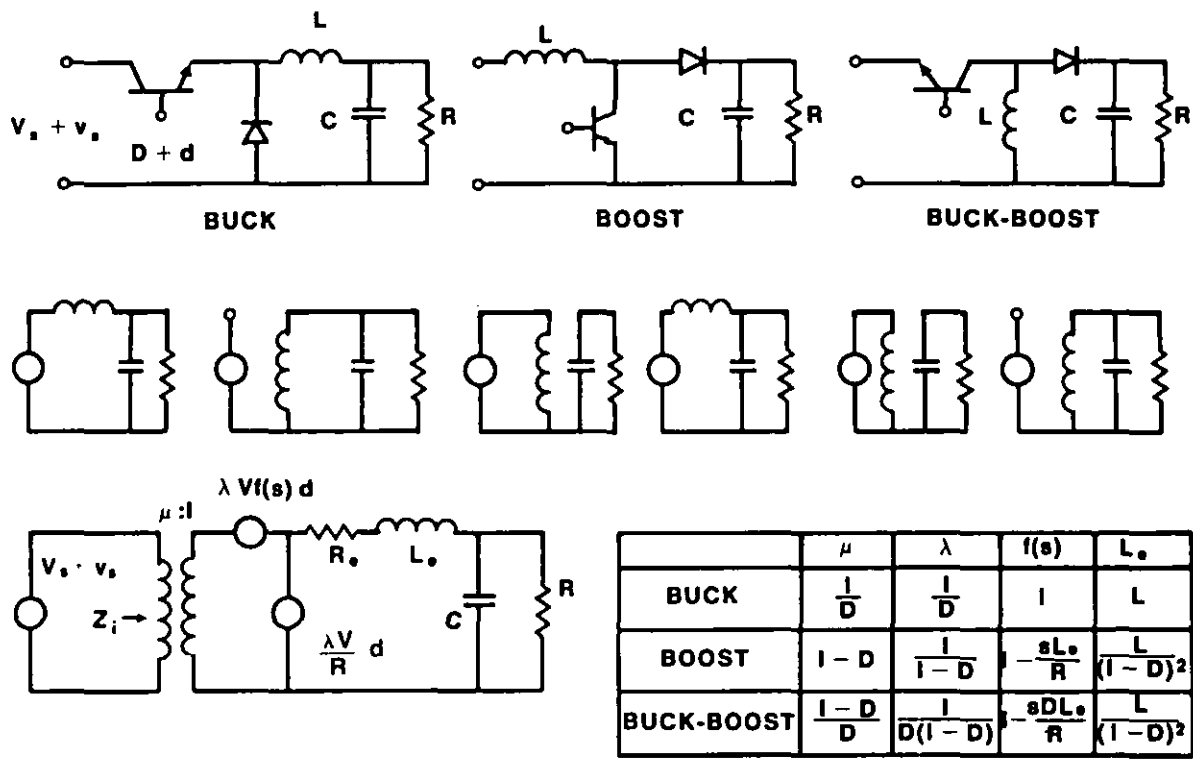


FIGURE 7. Basic switching-mode power supply configurations.

3.3.4.1 Filter effects. Following are some filter effects:

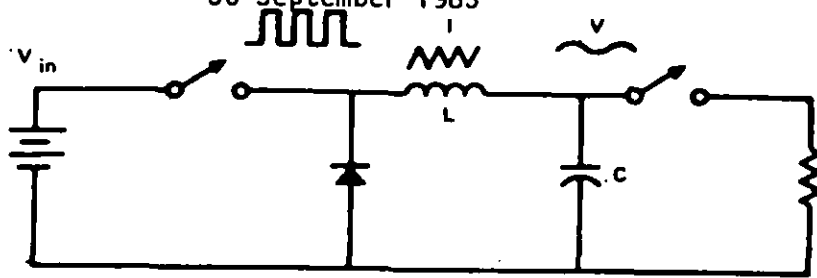
a. Output ripple: One inherent characteristic of switching-mode power supplies is the presence of output ripple at the switching frequency. The ripple can be made arbitrarily small by increasing the filtering but it is always present. Typically it is 1 percent of the nominal output voltage or 50 microvolt (μV) peak-to-peak, whichever is greater. If excessive for some circuit applications, a point-of-use dissipative regulator can be used to reduce it there.

b. Low voltage component stress: As shown in FIGURE 7, the canonical model for the continuous current mode always contains a second-order filter. This affects the load transient response. For example, if the power supply in FIGURE 8 is operating at full load and the load is suddenly removed, the maximum response of the control loop is to open the switch and keep it open. The energy stored in the inductor eventually is added to the output capacitor and an overshoot occurs. The magnitude of the overshoot is a vector addition of (1) the load current change times the characteristic impedance of the LC filter and (2) the original capacitor (output) voltage. Some designs give as much as a 15 V peak on a 5 V dc supply. By increasing C and decreasing L, overshoot on 5 Vdc power supplies can be limited to 1 V for a change from full to no load. This is compatible with TTL logic. A step increase in load has a similar transient effect. As soon as the output voltage drops, the feedback loop saturates in the direction to close the switch. The transient response is the open-loop filter response until the output rings up to the output voltage and the control loop regains control. Again, large C and small L minimize the transient effect.

A more subtle effect occurs for a step change in input voltage. A feedback loop sensing the input voltage can be used to change the duty cycle so that the volt-seconds into the filter is a constant. While this would appear to cancel input variation effects, an oscillatory migration of the minor hysteresis loop can still appear in the magnetic material of the output inductor. This somewhat obscure filter effect is more fully described in reference 3 along with the solution--an added feedback loop.

3.3.4.2 Constant input power characteristics. A dc and low frequency model of a switching-mode converter is simply a dc-to-dc transformer with a turns ratio, μ , (see FIGURE 7). To the extent that the converter is 100 percent efficient, ideal transformer ratios apply so that μ is the ratio of output to input voltage, and in an inverse manner, μ is the ratio of input to output current. However, the input resistance is the load resistance multiplied by negative μ^2 instead of positive μ^2 as in the conventional transformer. This is due to the constant input power characteristic of switching-mode converters. The derivation of the negative input resistance characteristic is shown in FIGURE 9. For a given load resistance R, the feedback action of the regulator adjusts the conversion ratio μ to maintain constant output voltage, and hence constant output power, even if the input voltage V_s varies. It follows that if V_s increases, I_s must decrease since the input power also remains constant. This is the low-frequency value of the regulator input impedance Z_i indicated in FIGURE 10. FIGURE 10 contains essential elements of a switching-mode regulator with input filter. The block diagram is general and a single-section LC input filter and a buck converter are shown as typical realizations.

30 September 1983



PRIOR TO SWITCH OPENING:

- ENERGY IN INDUCTOR = $\frac{I^2 L}{2}$
- ENERGY IN CAPACITOR = $\frac{V^2 C}{2}$

AFTER SWITCH OPENING (FINAL VALUE):

- ALL ENERGY STORED IN CAPACITOR

$$V_f = \frac{2E}{C}$$

$$= \left(V_i^2 + \frac{I^2 L}{C} \right)^{1/2}$$

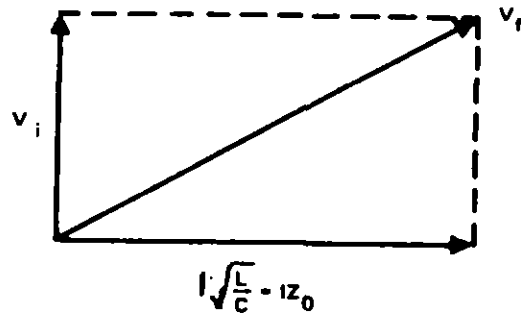


FIGURE 8. Overshoot.

$$R_i = \frac{dV_s}{dI_s} = \frac{d}{dI_s} \left(\frac{P}{I_s} \right) = -\frac{P}{I_s^2} = -\frac{V_s}{I_s} = -\mu^2 \frac{V}{I} = -\mu^2 R$$

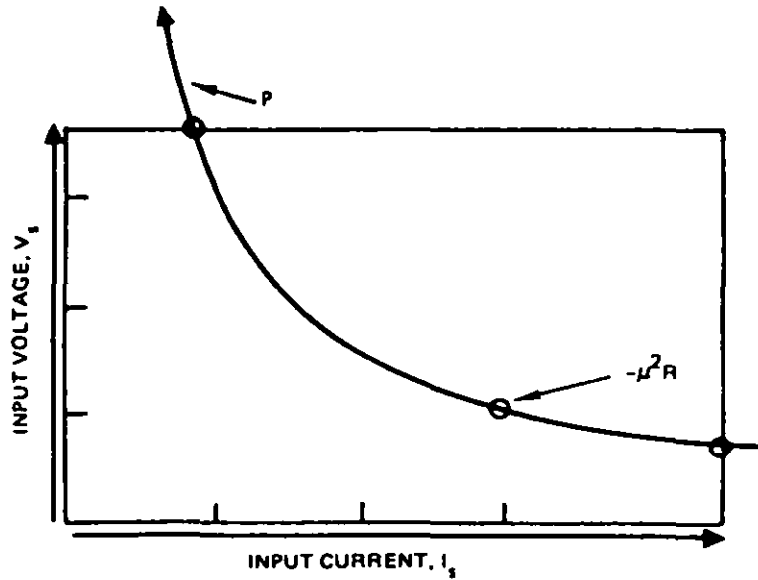


FIGURE 9. Switching-mode power supply input characteristics.

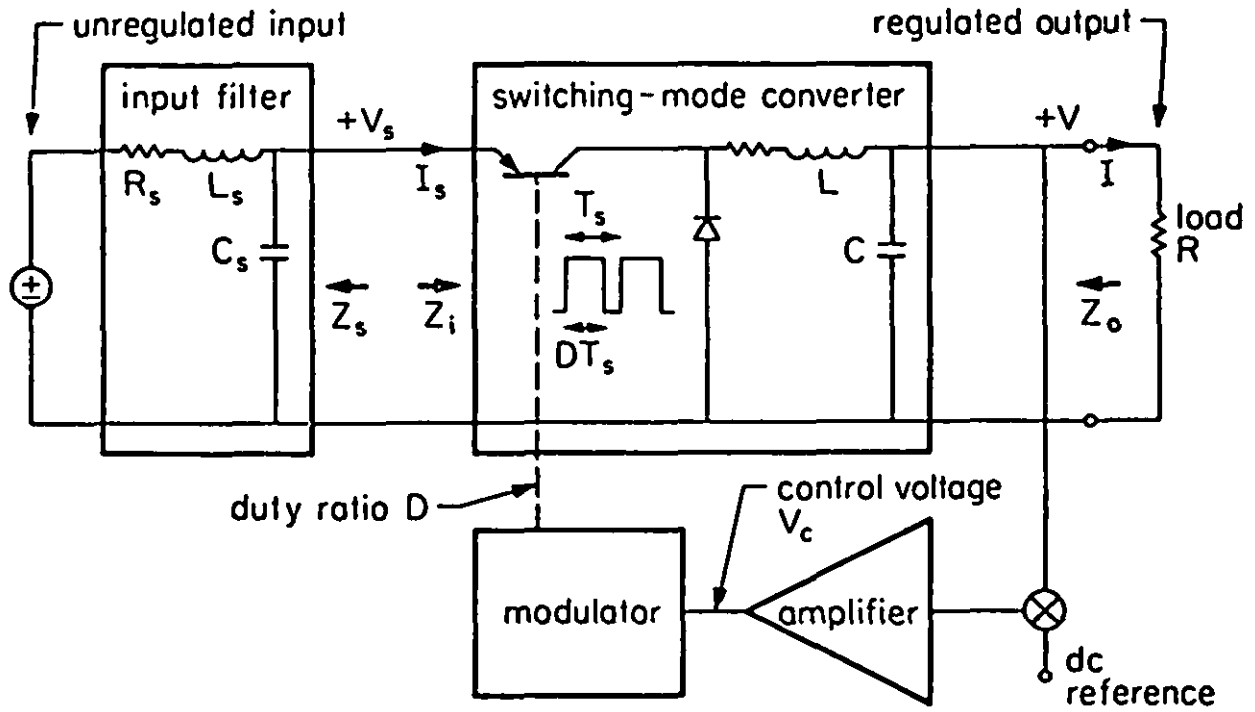


FIGURE 10. General switching-mode regulator configuration.

3.3.4.2.1 Negative input resistance. This negative input resistance in combination with the input filter (or EMI filter) between the source and switching-mode power supply can, under certain conditions, constitute a negative resistance oscillator, and is the origin of the system's potential instability. To prevent this instability, Middlebrook (reference 2, chapter 7) has developed a criterion requiring the output impedance of the input filter to be less than the open-loop input impedance of the switching-mode power supply. This is shown in FIGURE 11. The top curve represents the regulator open-loop input impedance, Z_i , which is the reflected impedance of the series-resonant loaded averaging (output) filter.

The lower solid curve represents the input filter's output impedance, Z_s , here shown for the single-section low-pass filter configuration. However, in the real world the output impedance configurations are more complex. A two section filter is described in 6.1.3 and shown to be smaller and lighter than a single-section filter with the same peaking, power loss, and attenuation at the switching frequency. Also, the power system including the generator and distribution network is part of the impedance configuration. The Middlebrook criterion applies to dc systems and to ac systems in which the rectifying diodes are in continuous conduction. However, since discontinuous line current results in increased rectification harmonics, it is recommended to avoid this by using inductive rather than capacitive input filters (see Section 4).

The addition of the input filter always impairs the performance feature of the regulator, that is, a nonzero Z_s (see FIGURE 10) always lowers the loop gain, raises the line transmission function factor (opens a frequency window to pass input noise to load), and raises the regulator's output impedance (the lower the output impedance the better the regulation). The loop gain and line transmission are essentially unaffected if the criterion for stability discussed above is met-- the output impedance of the input filter is very much less than the input impedance of the regulator. However, for the regulator's output impedance to be essentially unaffected it is necessary that the input filter's output impedance be well below the dotted line in FIGURE 11 (see APPENDIX B).

To meet either the stability criterion or more stringent criterion, two design recommendations follow:

- a. Keep the resonant frequency or frequencies (if multisectioned) of the input filter far away from the effective resonant frequency of the regulator's output filter; preferably using a lower resonance for the input filter thereby simultaneously decreasing the EMI conducted to the input power lines.
- b. Lower the Q of either or both input and output filters preferably by lossless damping (discussed in 6.1.4.3 and APPENDIX B).

APPENDIX B gives example of how to apply the Middlebrook criterion.

3.3.4.2.2 Low voltage and latch-up. The constant input power characteristic of switching-mode power supplies dictates that they draw more current at low input voltage than at nominal or high input voltage. Low input voltages can increase the input current to the extent that the power supply is damaged or destroyed. Some configurations are inherently protected from this failure mode. Other configurations require the addition of protection circuits to prevent operation, and hence destruction, at low input voltages.

When switching-mode power supplies are powered from a current-limited source, they may latch-up into an undesired mode upon turn-on. The turn-on current is high when the voltage is low, and the turn-on trajectory in FIGURE 9 is from right to left on the constant power curve. If the source is current limited, the circled point is a stable but undesired operating point and the regulator never reaches the desired operating point circled on the horizontal line. The solution is to keep the turn-on trajectory to the left of the current limit line. The low-voltage protection circuit can be designed to accomplish this.

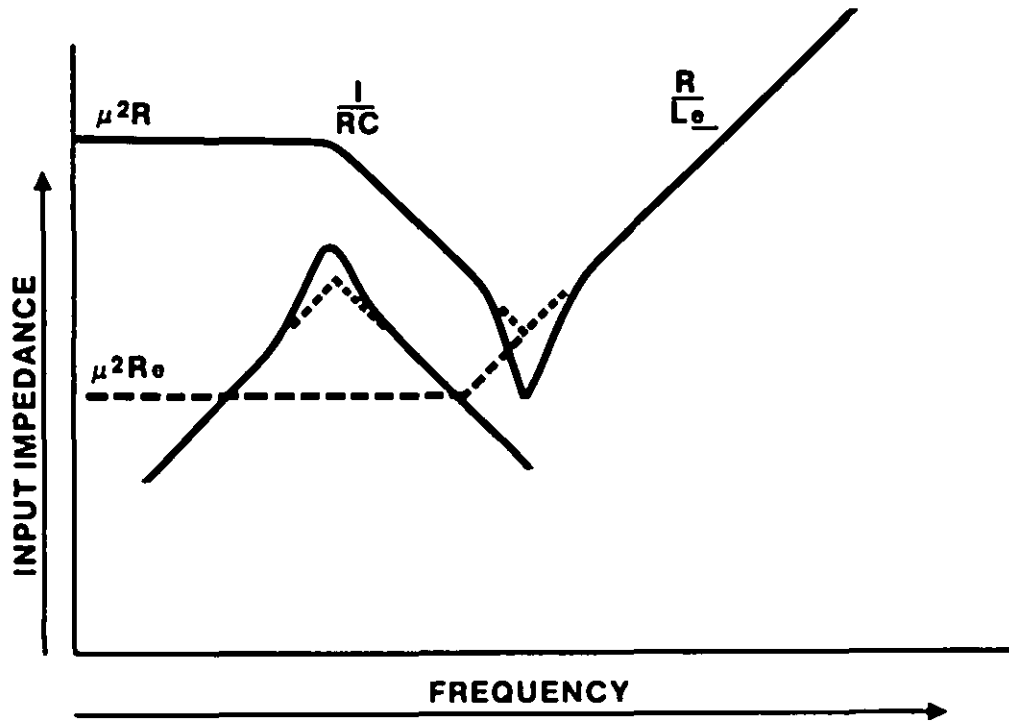


FIGURE 11. Middlebrook (1976) stability criterion.

3.3.4.3 Stability difficulties. Stability difficulties in switching-mode power supplies arise from a variety of linear and nonlinear phenomena.

3.3.4.3.1 Audio susceptibility. Some stabilizing techniques can cause an audio susceptibility problem (poor attenuation of modulations on the input power).

As mentioned previously, the canonical model often contains a second-order under-damped filter. If a single control loop is used for feedback, this filter must attenuate both the output ripple at the switching frequency and any extraneous input power frequencies beyond the zero decibels (dB) crossover of the loop gain. One way to stabilize such a switching-mode power supply is to use lag compensation in the feedback loop to roll off the gain so that adequate phase margin exists at the zero dB crossover frequency. This requires the amplifier gain to be less than zero dB at frequencies lower than the cutoff frequency of the output filter. A window is thereby opened in the closed loop attenuation, F . This window allows input line modulations between the amplifier crossover frequency and the output filter cutoff frequency to pass through the regulator with no attenuation. These relationships are shown in FIGURE 12. This is a surprisingly common design defect in switching-mode power supplies, a defect often revealed by failure to pass the CS01 audio susceptibility test of MIL-STD-461.

One method to close the attenuation window is to shape the frequency response of the feedback amplifier with lead-lag compensation as shown in FIGURE 13. A desired zero-dB crossover frequency is selected beyond the cutoff frequency of the output filter. The amplitude gain is set to compensate for the output filter attenuation at this frequency. A lead in the amplifier gain is also included at this frequency to obtain adequate phase margin since the output filter has contributed almost 180 degrees at this frequency. Higher frequencies are rolled off to control bandwidth for noise immunity, and the amplifier frequency gain is shaped at lower frequencies to give good dc regulation. The resultant closed-loop attenuation, F , closes the attenuation window as shown in FIGURE 13, but not without penalty. This is a conditionally stable system that can go unstable if the loop gain decreases. Saturation of the amplifier circuits usually reduces the gain and causes instability in conditionally stable systems. Saturation often occurs when the feedback loop compensates for a large change in line or load or the internal noise or EMI gets high enough. The latter can be insidious in digital systems. The EMI and noise internal to the power supply are a function of dynamic loading, which is often under software control. A particular software sequence, by producing more internal noise, can cause a momentary instability of the power supply with a resultant unexplained change in digital system logic states. The instability is never detected under static conditions that do not produce enough noise to saturate the amplifiers.

The solution is to avoid conditionally stable systems or to thoroughly test them for noise immunity. There are many circuit configurations and multiloop techniques for closing the attenuation window while retaining absolute stability.

3.3.4.3.2 Entrainment. Another particularly insidious characteristic of some switching frequency power supplies in digital systems is the effect of entrainment or synchronization of the switching frequency on periodic load or line transients. It has been observed in switching-mode power supplies whose switching frequency changes as a function of load or line conditions that a periodic line or load transient can pull the switching frequency to the nearest harmonic or subharmonic of the periodic transient. This usually results in an increase in output ripple. The increase is sometimes dramatic; for example, several volts peak-to-peak ripple on a five-volt power supply which typically possesses 50 millivolts peak-to-peak (mV p-p) ripple. Here again, the periodic transients can be under software control in digital systems so that a software programming change can cause component failures or random and unexplained system malfunctions in previously satisfactory systems.

The solution is to use fixed frequency switching-mode power supplies which are difficult to entrain, and to test for entrainment in all switching-mode power supplies, variable or fixed frequency.

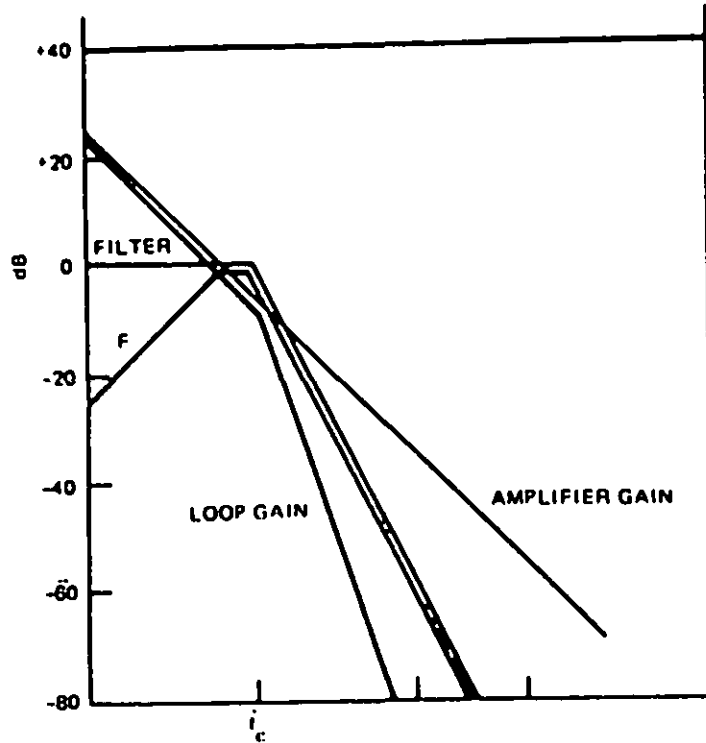


FIGURE 12. Attenuation (F) of line transients, lag compensation.

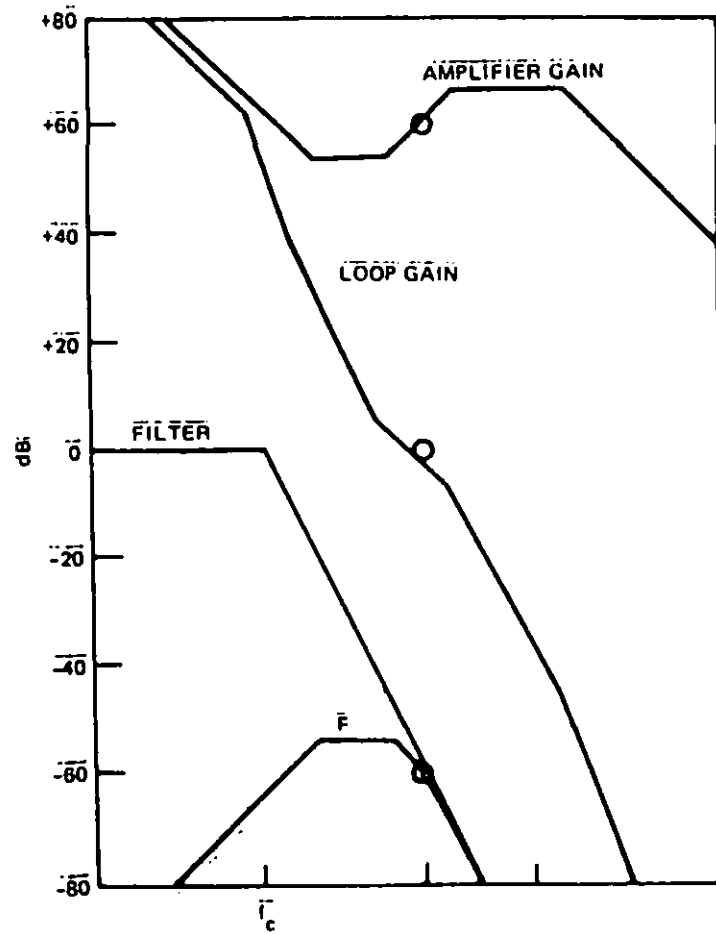


FIGURE 13. Attenuation (F) of line transients, lead compensation.

3.3.4.3.3 Right half-plane zero. Examination of the table in FIGURE 7 indicates that the voltage generator in the canonical model has a frequency-dependent term, f_s , which is unity for the buck converter but appears as a right-half plane zero for the boost and buck-boost converters. (In general, both the current and voltage generators in the canonical model have frequency terms. The current generator term is needed when the power source and filter input impedances are added to the model.) The right-half plane zero makes the system into a nonminimum phase system. This means, when using Bode analysis, that the phase versus frequency curve cannot be inferred from the amplitude versus frequency curve. When phase measurements are not made but are inferred, the right-half plane zero appears as lead in the amplitude plot inferring a positive 90 degree phase shift contribution whereas in reality it contributes a negative 90 degree phase shift.

The existence of right-half zeros can be found by accurate open-loop gain and phase measurements, but such measurements are considered to be difficult in switching-mode power supplies and are often neglected, although excellent techniques for making the measurements exist (references 2 and 4). Designers of switching-mode power supplies are often unaware of the existence of right-half plane zeros and their effect, and therefore are unprepared to cope with the stability problems they introduce. As a result, dynamic response (bandwidth) is often unnecessarily sacrificed to gain stability.

The solution is to have accurate models, adequate measurement tools, and a knowledge of modern stabilizing techniques available in the design stage. This is absolutely necessary in new configurations such as the Cuk converter (see 3.3.5.1.4), which is a sixth-order system with real and complex zeros in the right-half plane. The canonical model, APPENDIX A, is useful for linearizing the switching stage around a duty cycle and investigating small signal perturbations by means of linear techniques. It predicts the existence of right-half plane zeros and other nonobvious phenomena. It will not uncover some nonlinear phenomena that have to be analyzed by other techniques.

3.3.4.3.4 Duty cycles greater than 0.5. One stability problem often encountered is the long-short duty cycle oscillations that occur when a fixed frequency pulswidth modulated power supply duty cycle is extended beyond 0.5. The problem is shown by graphical techniques in FIGURE 14. The power switch is turned on by an external source at the start of every period T . This resets the pulswidth modulator integrator. It integrates down until a threshold is reached which turns the switch off, thereby producing the pulswidth modulation. When the power switch is operating at less than 50 percent on-time, the system is stable, which can be shown mathematically or by following the decay of a small perturbation, e , in the amplitude of the modulator graphically as in the top of FIGURE 14. If the duty cycle is greater than 50 percent, as shown in the bottom of FIGURE 14, the small perturbation grows instead of decaying and long-short oscillations occur.

The solution that allows operation beyond a 50 percent duty cycle is given in reference 3, which is the source of FIGURE 14. (The instability with duty cycles larger than 50 percent occurs for constant-frequency clocks initiating the on time. If constant-frequency clocks initiate the off time, the instability is observed with duty cycles smaller than 50 percent.)

3.3.4.4 Electromagnetic compatibility. System electromagnetic compatibility problems with off-line switching-mode power supplies occur because of a. rectification harmonics and b. switching frequency and its harmonics, and the high-rate current and voltage waveforms inherent in the switching transitions. Since EMI is the main topic of this handbook these two EMI problems and solutions are discussed in detail in Sections 5 and 6.

3.3.5 DC to dc converter topologies. In switched-mode power conversion, the controlling device is an ideal switch, which is either closed or open. The power flow to the load is efficiently controlled by controlling the ratio of the time intervals spent in the closed and open positions (often defined as the duty ratio). The need to generate dc output voltage introduces ideally lossless storage components, inductors and capacitors, whose role is to smooth out the inherent pulsating behavior originating from the switching action. The addition of a transformer provides an often very important practical requirement, dc isolation between input and output grounds.

The buck, boost, and buck-boost topologies and their first order derivatives constitute most of the power conversion approaches in use today. The boost-buck (Cuk) and its derivatives are new approaches with several performance advantages, particularly low EMI. This section is limited to a discussion of these basic topologies as well as some multiple switch and some transformer-isolated derivatives of these basic structures.

Much of the discussion and the figures in the following sections on topologies are taken (with permission) with some modifications from a paper by G. Bloom and R. Severns (reference 5).

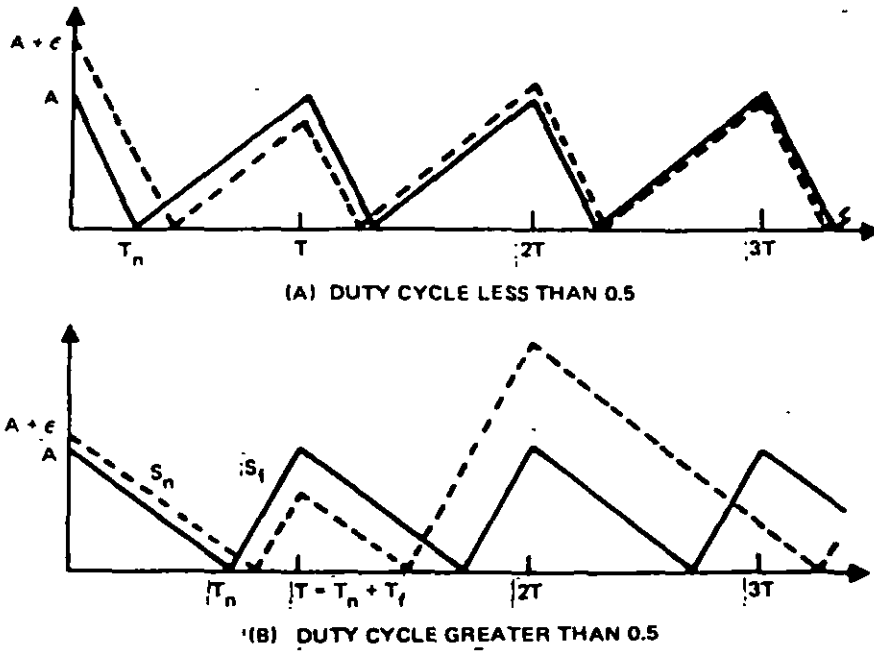


FIGURE 14. Duty cycle stability limit.

3.3.5.1 Basic topologies. A basic switching converter topology is defined here as one which comprises only a single switch and the reactive elements necessary for proper conversion action without isolation of input and output ports (no transformer). With these restrictions, there are only four possible basic topologies known, of which the fourth (the Cuk structure) is a recent addition. FIGURE 15 shows the four basic circuit structures.

These basic topologies are examined, assuming that conversion switches operate in the constant-frequency duty-ratio-controlled mode. The switch is in position A for time DT_s , with the duty ratio D corresponding to the fraction of the total switching period T_s , where $T_s = 1/f_s$, the reciprocal of the conversion frequency, f_s . For the remainder of the switching period, $D'T_s$ ($= T_s - DT_s$), the switch is in position B. Implied in these descriptions is the assumption that all converter inductor currents never fall to zero during the time $D'T_s$ (continuous conduction mode of operation).

FIGURE 16 shows a practical switch implementation by replacement with a bipolar transistor-diode arrangement in each of the four structures. Switch position A now represents the time DT_s when Q1 is on and diode D1 is not conducting in the forward direction. During the time $D'T_s$, Q1 is off and D1 does conduct.

3.3.5.1.1 The buck converter. The buck converter of either FIGURE 15 (a) or FIGURE 16 (a) is perhaps the most fundamental and well-known of all the basic structures. The input dc voltage is chopped by the switch and then averaged by an LC output filter. The ideal dc voltage gain from input to output will be

$$V_o/V = D, \quad (\text{buck})$$

where $0 < D < 1$. Referring to the port current waveforms of FIGURE 15 (a), the output current is non-pulsating (that is, continuous) because of the presence of inductor L. In contrast the input current of FIGURE 15 (a) is pulsating (that is, discontinuous), flowing only when the switch is in position A and abruptly interrupted when the switch is in position B. The pulsating current characteristic of the buck structure is one major undesirable feature of this conversion approach since it is a potential source of much greater line-conducted emission (EMI) than the non-pulsating input of the boost converter. A buck conversion approach, therefore, necessitates the inclusion of a highly attenuative low pass filter between the input voltage and the input port of the converter to reduce conducted EMI on source voltage lines (see Section 6).

3.3.5.1.2 Boost converter. The boost converters of FIGURES 15 (b) and 16 (b), as the term applies, will perform an ideal step-up voltage conversion given by

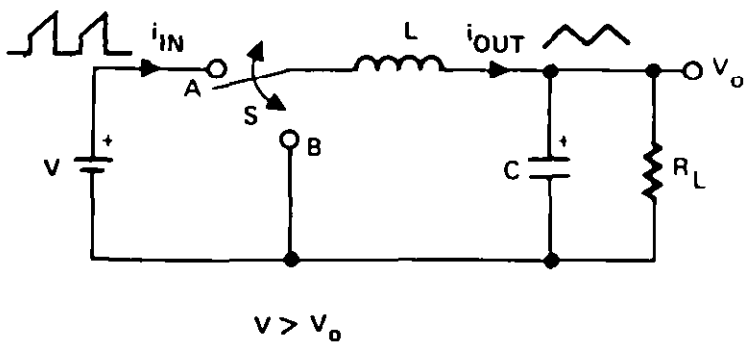
$$V_o/V = 1/D', \quad (\text{boost})$$

where $D' = 1-D$ as defined earlier. The switching action first stores energy in L during the transistor Q1 on time, DT_s , and then releases energy into capacitor C and the load R_L when the diode is conducting ($D'T_s$). The boost structure is the dual of the buck in that a step-up translation is attained rather than a step-down, and the input and output currents now reverse pulsating/non-pulsating roles. The pulsating output is a potential source of higher output ripple than the non-pulsating output of the buck approach. Therefore, if the output ripple needs to be low, more output filtering is required than would be required with non-pulsating output of the buck approach.

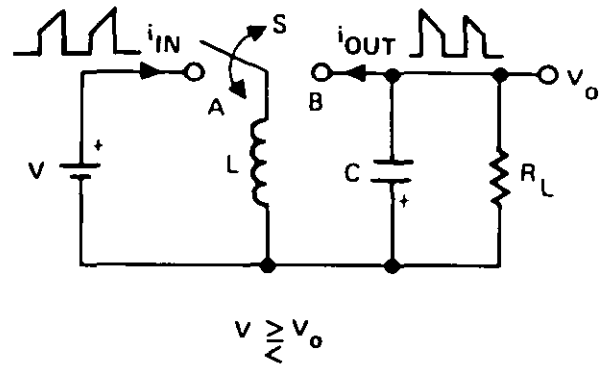
3.3.5.1.3 Buck-boost converter. The buck-boost converter is a voltage inverting structure with its conversion function a product of ideal buck and boost gains such that

$$V_o/V = -D/D', \quad (\text{buck-boost})$$

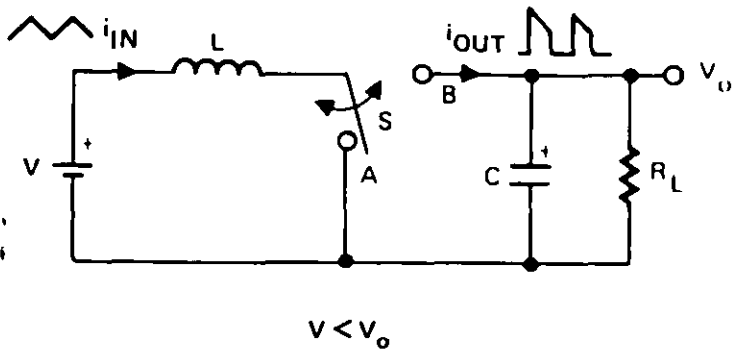
As shown in FIGURES 15 (c) and 16 (c), the switch action commutates the continuous inductor current alternately between input and output ports. Hence, both input and output currents are pulsating. Thus the buck-boost converter structure, from a low EMI point of view, is the worst structure.



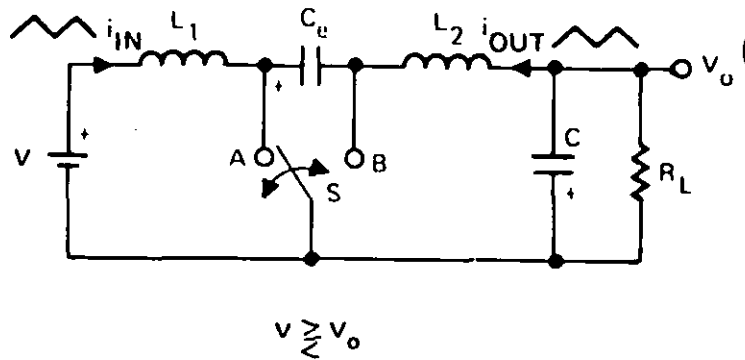
(a) Buck converter (see 3.3.5.1.1)



(c) Buck-boost converter (see 3.3.5.1.3)



(b) Boost converter (see 3.3.5.1.2)



(d) Cuk converter (boost buck)
(see 3.3.5.1.4)

FIGURE 15. The four basic dc-to-dc converter topologies.

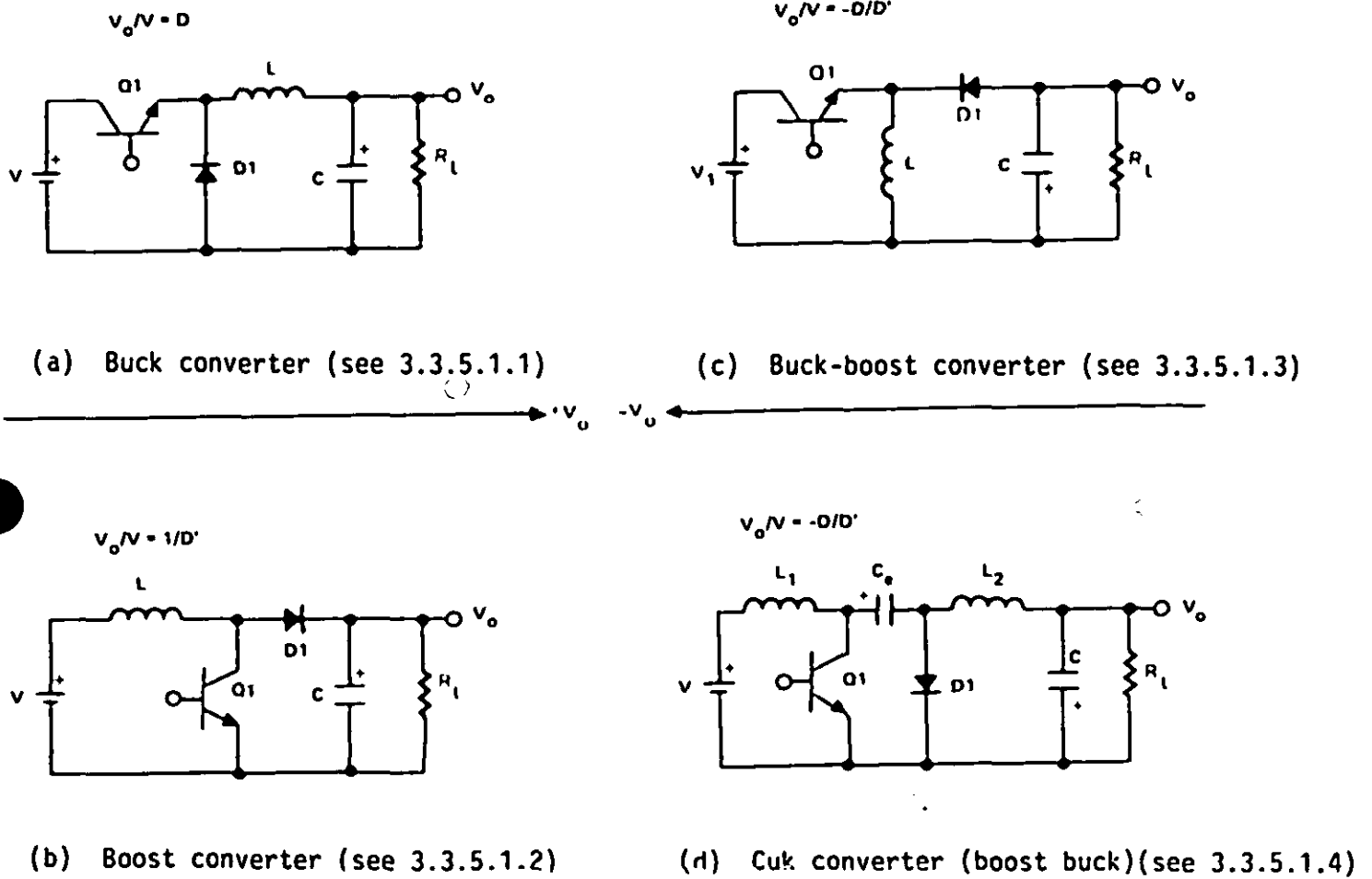


FIGURE 16. Implementation of the ideal switches in FIGURE 15 by bipolar transistor-diode networks (note $\rightarrow D' = 1-D$).

3.3.5.1.4 Boost-buck (Cuk) converter. The boost-buck converter was added to the basic family in 1977 by Dr. S. Cuk of the California Institute of Technology and is known as the Cuk converter. This new converter is the dual network of the buck-boost structure. FIGURES 15(d) and 16(d) are representative circuit diagrams of the new basic converter structure. The topology has the same inverting and dc voltage transfer function as its dual counterpart, the basic buck-boost network, shown in FIGURES 15(c) and 16(c), or

$$V_o/V = -D/D', \quad (\text{boost-buck, Cuk})$$

but, in other circuit performance areas, there are striking differences. One major and distinguishing difference is the non-pulsating characteristic of both input and output currents, whereas the buck-boost circuit has pulsating currents at both circuit ports.

Referring to FIGURE 16(d), when the transistor Q1 is off, the energy transfer capacitor C_e is charged by the input current through diode D1 and inductor L_1 . When Q1 is turned on during time DT_s , the voltage of the energy transfer capacitor reverse-biases the diode, turning it off, and the stored energy of C_e is released through Q1 to the output filter network and load. Thus, capacitive energy transfer in the Cuk converter is fundamental to its operation just as inductive energy is essential for operation of the other three basic converters in FIGURES 15 and 16.

Because all pulsating currents are contained within the inner triad of components and input/output ports isolated by instantaneous current-limiting inductances, the Cuk structure is ideally suited for low conducted EMI applications. As will be shown later, some extensions of this topology can lead to the realization of a switching conversion structure that closely approximates a true dc-to-dc transformer.

This new conversion approach shows promise of yielding maximum conversion performance with a minimum of power circuit components. It, therefore, has been termed optimum by many of its advocates (reference 2).

3.3.5.2 Some transformer isolated derivatives. The basic conversion approaches for FIGURES 15 and 16 are usually found in evolved forms for other performance reasons. For example, the basic structures do not electrically isolate the input and output grounds. For isolation, transformers must be added to each of the topologies as shown in FIGURE 17.

The presence of a transformer places the selection of the output return terminal at the option of the designer. Thus, the restriction of inherent inverting or non-inverting voltage gains is removed. Also, the transformer's turn ratio can be selected to either increase or reduce voltage conversion gain as noted by the ideal equations in FIGURE 17 where

$$n = \text{number of secondary turns} / \text{number of primary turns} = N_s / N_p$$

3.3.5.2.1 Forward converter. Adding an isolation transformer to the basic buck results in the forward converter of FIGURE 17(a). The input energy is pushed or fed-forward to the output and not stored as in the case of the flyback of FIGURE 17(c). When the transistor conducts, the output inductor current rises linearly, fed by the transformer secondary current via diode D_f , and flows into the output capacitor and load. During this time, energy is both transferred to the output and stored in the inductor L. When the transistor Q1 turns off, the energy is kept flowing into the load by the commutating diode, D1.

The transformer in FIGURE 17(a) has a third winding plus a series diode, D_m , for demagnetizing the core when the transistor is off. So as not to waste this magnetizing energy, it is returned to the input voltage source as shown. This third winding is necessary in practical designs to safely limit the peak collector-to-emitter voltage of Q1 when it is not conducting to no more than twice the input voltage value.

Forward converters have inherent lower output ripple than comparable flyback design because of the continuous nature of the output inductor current.

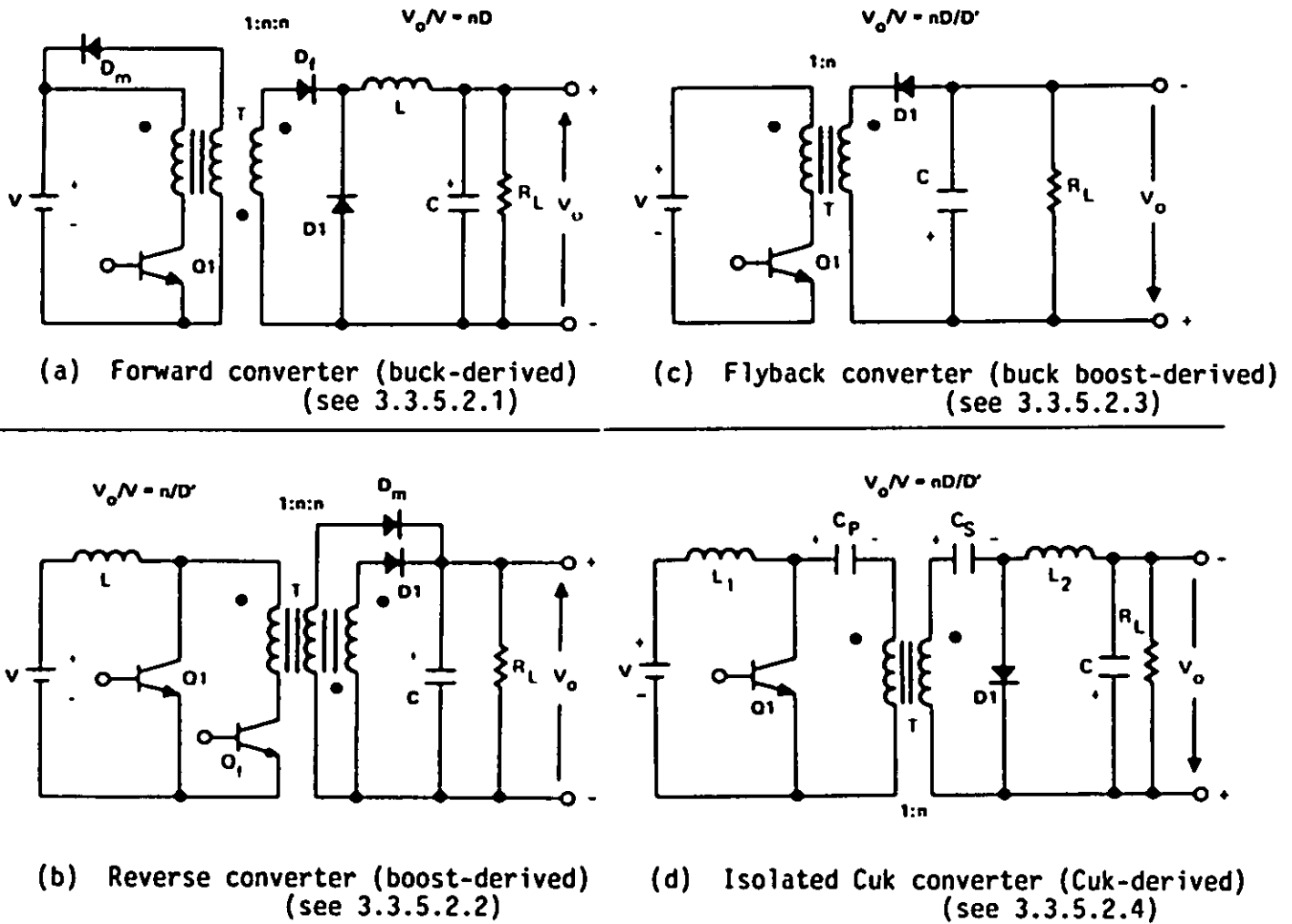


FIGURE 17. Transformer-isolated dc-to-dc converter topologies derived from the basic structure of FIGURE 16 ($D' = 1-D$).

3.3.5.2.2 Reverse converter. The boost derived converter of FIGURE 17(b) is an unusual structure rarely found in power supply designs today. Bloom and Severns (reference 5) have coined the term reverse converter to emphasize the dual nature of the structure compared to that of the forward converter shown in FIGURE 17(a).

As was the case for the basic non-isolated designs of FIGURES 15 and 16, the input current of the reverse converter of FIGURE 17(b) is non-pulsating, while that of the forward converter is pulsating. During the times transistor Q_1 is on, energy is supplied primarily by capacitor C. Transistor Q_f is always turned off while Q_1 is on and vice versa. When Q_f is turned on, the energy of inductance L is released to the output capacitor and load by transformer action through diode D1. As for the forward converter, a third winding of the transformer is used to remove magnetizing energy stored in the transformer while Q_f is off. But, in contrast to the forward converter of FIGURE 17(a), this energy is returned to the load instead of the source to help supply load power during those times Q_1 is on.

Interestingly enough, if the magnetizing inductance of the transformer and that of the input inductor are proportioned correctly, the output ripple current waveform can be made very small since both the capacitor C and the magnetizing inductance clamp-winding of the transformer will share the job of supplying load power while Q_1 is on and Q_f is off. Thus, the reverse structure of FIGURE 17(b) has the design potential of obtaining low conducted EMI on both input and output ports.

3.3.5.2.3 Flyback converter. In the buck-boost derived flyback converter of FIGURE 17(c), the transformer also serves as the inductive energy storage element. When the transistor Q_1 is on, energy is stored in the primary, and diode, D1 does not conduct. When Q_1 turns off, the diode turns on and the energy stored in the magnetic field of the transformer is released to the output capacitance and load via the secondary winding. Flybacks require considerable input and output EMI filtering since they have the same pulsating input and output currents as the basic buck-boost.

3.3.5.2.4 Isolated Cuk converter. In the case of the isolated Cuk converter shown in FIGURE 17(b), there are three key steps to adding the transformer to the basic non-isolated topology as diagrammed in FIGURE 18.

The first step is to separate the coupling capacitance C_e of the basic structure (see FIGURE 16(d)) into two series capacitors C_p and C_s , thus making the original symmetrical structure divisible into two halves, as shown in FIGURE 18(a), without affecting the operation of the converter. The second step is to recognize that the connection point between these two capacitances has an indeterminate dc (average) voltage, but that this dc voltage can be set at zero by connecting an inductance between this point and ground (see FIGURE 18(b)). If the inductance is large enough, it diverts a negligible current from that passing through the series capacitors, so that the converter's operation is unaffected. The third step is the separation of the extra inductance into two equal transformer windings, thus providing the dc isolation, resulting in the isolated version of the new converter shown in FIGURE 18(c).

The isolation transformer in this new converter has no dc current component in either winding which is a size and loss advantage over to the transformers required for the other isolated topologies (see FIGURES 17(a), (b), and (d)). The Cuk converter can use an ungapped toroid of square-loop material whereas the other isolated topologies require gapped cores. Therefore, the Cuk converter's transformer is smaller, less lossy, and can minimize leakage inductance (less EMI). Reference 3 (chapter 17) discusses these comparisons and also compares stress levels on circuit components.

3.3.5.3 Multiple switch forms. For most low and many medium power delivery applications, the quartet of basic single-switch dc-to-dc converters and their first order derivatives are usually preferred for simplicity and low component count. For higher power situations, multiple semiconductor switch forms are usually used. Basic push-pull and bridge topologies are usually buck-derived (although they could be derived from the other three single-switch basic converters). New variations of the basic multi-switch approaches show desirable features.

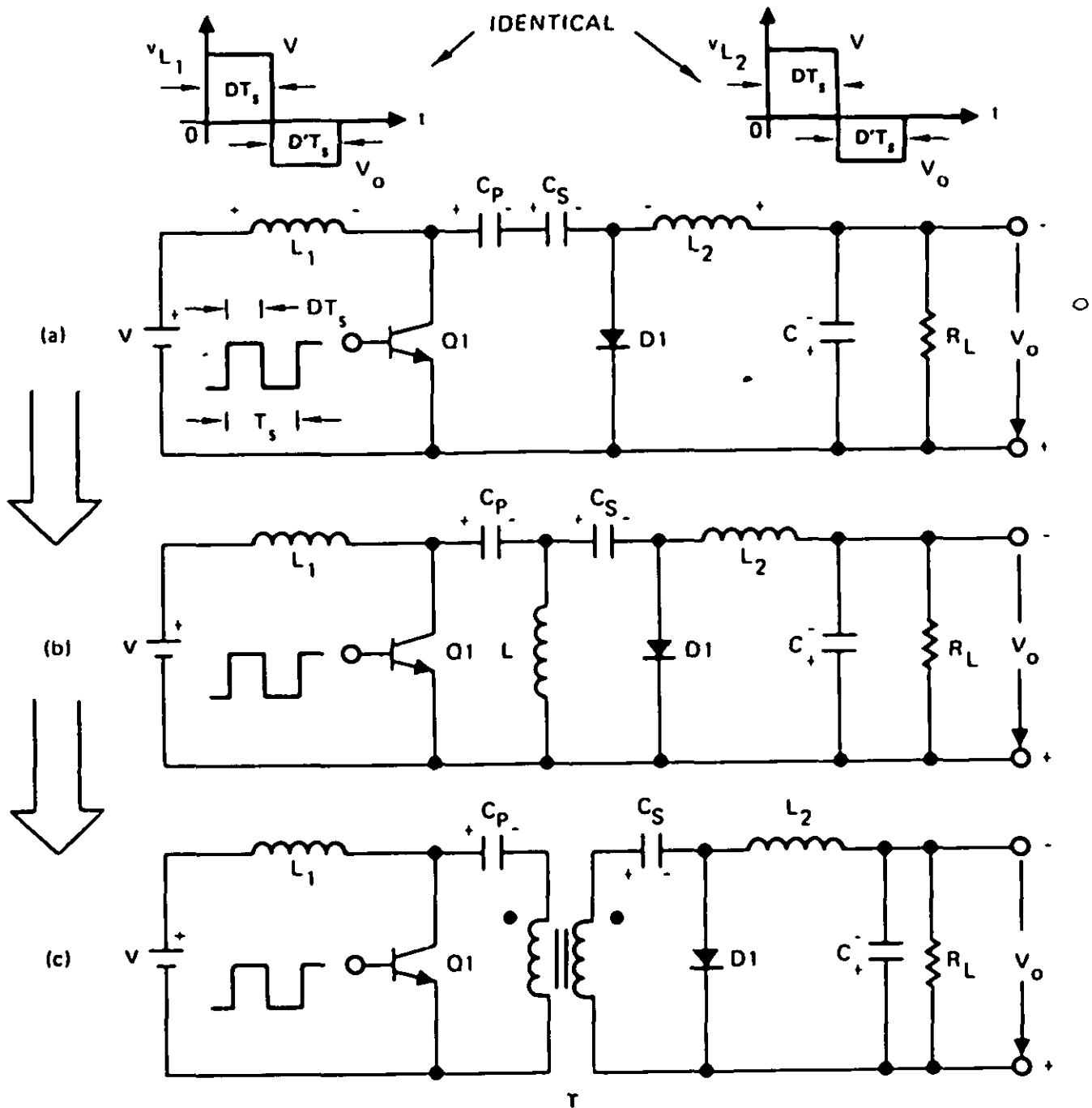


FIGURE 18. Three key steps to evolving a dc-isolated version of the Cuk converter of FIGURE 17(d).

3.3.5.3.1 Push-pull buck-derived. The most familiar of the two-transistor converter structures is the push-pull topology shown in FIGURE 19. As verified by the accompanying voltage waveform at the input to the L-C filter network, this push-pull converter is a member of the buck-derived family and has an ideal voltage gain identical to the forward converter of FIGURE 17a, or $V_o/V = nD$. The presence of two sets of alternating conversion switches (Q1 and D1, Q2 and D2) allows the average current levels in each set to be reduced by 50 percent from the single-switch basic approaches. When both transistors in FIGURE 19 are off, both secondary diodes work in parallel to commutate the output inductor current, allowing it to be continuous in form.

Each converter transistor in FIGURE 19 will ideally see no more than twice the value of the input voltage ($2V$) when in an off state. When the value of V is large, alternate primary switch arrangements are often used, such as the single-ended half-bridge version shown in FIGURE 20 or the full-bridge topology of FIGURE 21.

3.3.5.3.2 Half-bridge push-pull buck-derived. In the case of the half-bridge network, division of the input voltage is performed by capacitors C1 and C2 in FIGURE 20, where C1 equals C2 in value. The common connection point of these capacitors, therefore, must be at an average potential of $V/2$. Therefore, the peak off voltage seen by each of the transistors is V in contrast to $2V$ for the basic push-pull circuit of FIGURE 19. However, for the same secondary output power, the average primary current and, hence, transistor currents are twice those in the basic push-pull arrangement. Because the two division capacitors are asked to handle large rms currents, they are often large and expensive.

3.3.5.3.3 Full-bridge push-pull buck-derived. The full-bridge eliminates the need for the capacitors and, therefore, is a somewhat more economical and definitely more volume efficient approach. It is illustrated in FIGURE 21. Here, on alternate half-cycles, diagonally opposite transistors Q1 and Q2 or Q3 and Q4 are simultaneously turned on. Therefore, the voltage V across the primary of the transformer T1 will change polarity with every half-cycle of operation. Like the half-bridge circuit, no transistor ideally sees more than V when in an off state.

3.3.5.3.4 Shortcomings of basic push-pull designs. The push-pull converter and the two variations just described have some major shortcomings from a practical design viewpoint and, if not compensated for, can cause permanent damage to the major transistor switch networks. In FIGURE 19, transistors Q1 and Q2 can never be perfectly electrically-matched and differences in switching speed and voltage drop between them can produce imbalances in primary currents in the transformer. The imbalance can cause transformer saturation, ultimately destroying the transistors. In the half-bridge circuit of FIGURE 20, overlap in switching one transistor off and the other one on can effectively short the input voltage source, resulting in high-surge currents and possible transistor damage. The full-bridge converter of FIGURE 21 has the same potential imbalance and overlap problems as the other two variations.

To eliminate the possibility of primary transistor damage from overlapping conduction or component-induced imbalances, protective circuit measures are required. The protective circuits employed are frequently elaborate, inefficient and costly. Approaches potentially more cost-effective are discussed in 3.3.5.3.5.

3.3.5.3.5 Variations of the basic multi-switch approach. Two topologies are known which can inherently limit the flow of instantaneous primary current and still exhibit the desired voltage gain and power-sharing features of the basic structure of FIGURE 19. One is referred to as the Weinberg Converter and the other the Severns Converter. Both approaches show inherent advantages in their stress-reduction and current-limiting capabilities and are described in detail in reference 5.

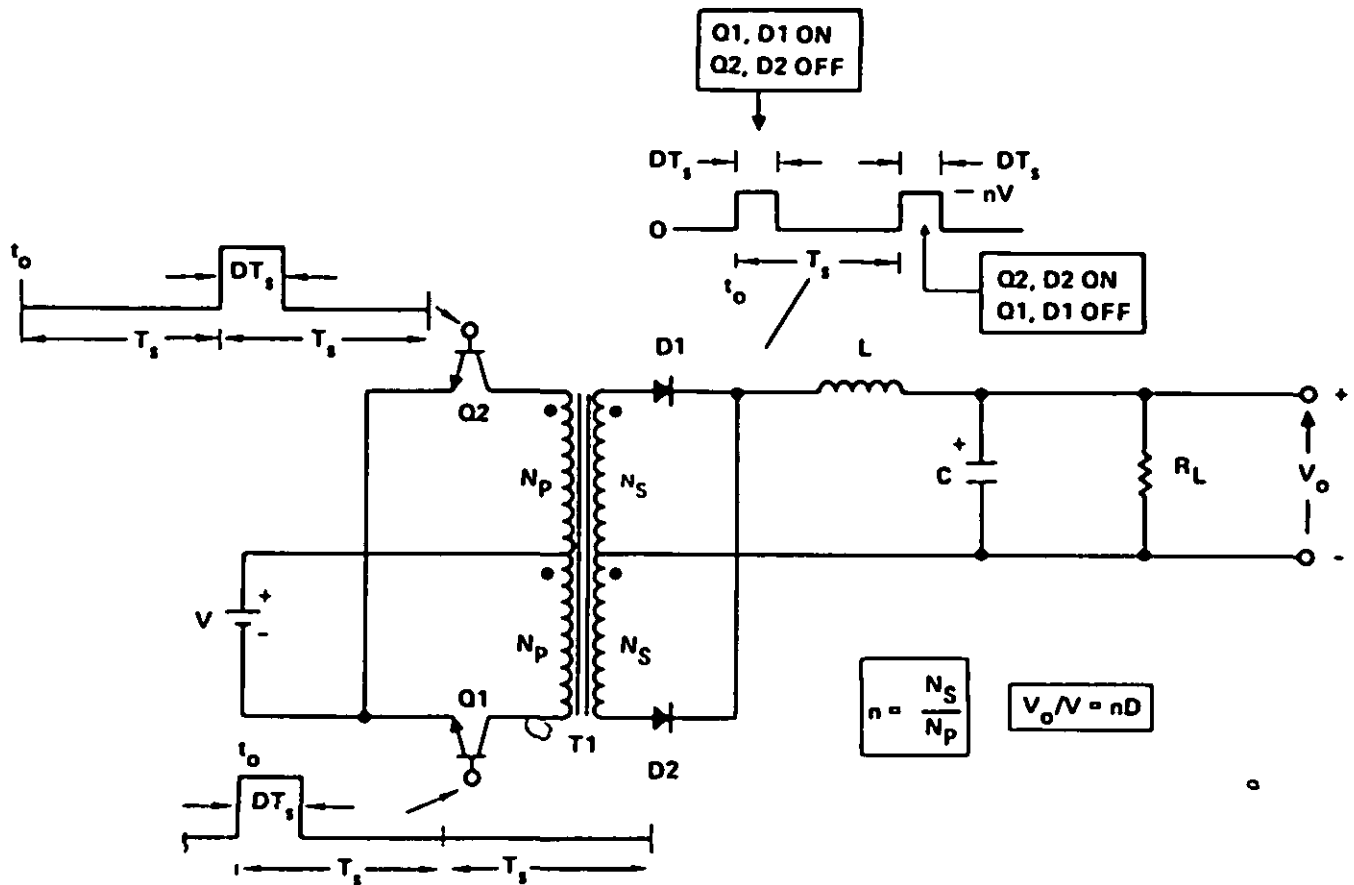


FIGURE 19. The basic two-transistor push-pull dc-to-dc converter (buck-derived).

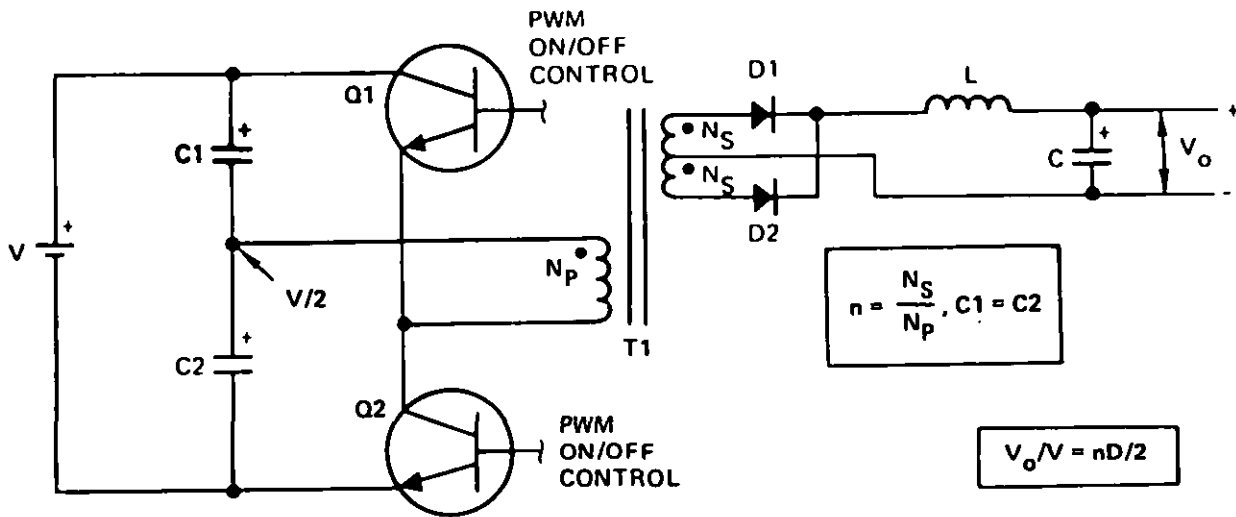


FIGURE 20. Single ended or half-bridge version of the buck-derived push-pull converter.

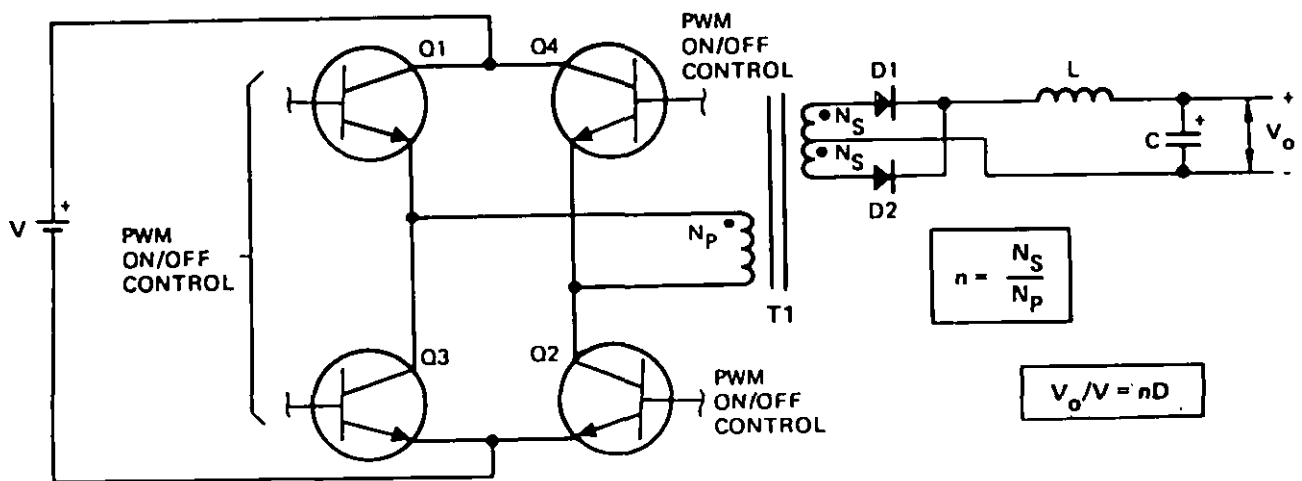


FIGURE 21. Full-bridge version of the buck-derived push-pull converter.

SECTION 4. EMI CREATED BY AC TO DC RECTIFICATION.

Rectification in power supplies causes the input ac line to set up harmonics which not only adversely affect sensitive loads on the same input line but also decrease the power factor. For these reasons several military specifications have been amended to lower the permissible emissions of these harmonics. These specifications are discussed in relation to the types and magnitudes of the emissions obtained with some common rectification architectures. Approaches used to reduce these emissions are evaluated. Also, this handbook specifies certain revisions of the specifications and standards, some of which have been changed.

4.1 Introduction. Harmonic currents of the ac frequency (for example, 60 Hz) are conducted on the input line of ac to dc power supplies due to the nonlinearity of the rectification process. Regardless of whether a dissipative or switching-mode regulator is used, conversion from ac to dc will generate harmonic currents due to rectification. To the extent that the more efficient regulators require less source power (maybe less than half), a switching-regulator will result in lower amplitude harmonic currents than a comparable less efficient dissipative type power supply. The magnitudes of individual harmonics depend upon the rectification architecture. Although some of the commonly used topologies generate less EMI than others, even the better designs emit harmonic emissions above the limits of several military specification requirements.

4.2 Basic rectifier action. The possible configurations for rectifier circuits are manifold. The most widely used, however, are bridge circuits either for single-phase or three-phase power supplies. Of importance to EMI are other variations in the rectification system, such as the following characteristics:

- a. Whether or not an input transformer is used (switching-mode power supplies frequency omit the input transformer)
- b. Whether or not phase-controlled rectification is used (a commonly used type of switching-mode regulation for high power applications)
- c. Whether the load is primarily inductive or capacitive (pure resistive loads require energy storage to remove undesired ripple)

4.2.1 Pulse number. The ripple voltage at the dc terminals is an important factor in influencing the choice and design of the rectifier. The smaller the magnitude and the higher the frequency, the cheaper it is to filter the ripple to specified tolerances.

The ratio of the fundamental frequency of the dc ripple to the ac supply frequency is commonly called the pulse number. Most single-phase rectifiers are two-pulse, and most three-phase rectifiers are six-pulse.

4.2.2 Simplifying assumptions. Initially, the analysis of a rectifier circuit usually assumes an idealized version of the circuit (reference 6). Practical deviations can then be added as needed. Design tables are almost always based on the assumptions listed below:

- a. Switches have no voltage drop or leakage current
- b. Instantaneous switching
- c. Sinusoidal voltage source
- d. Constant dc current over each cycle (an infinite inductive filter)

4.2.3 Single-phase half-wave rectifier. Although the half-wave diode rectifier is used only for some simple low power applications, it nevertheless permits a number of useful principles to be explained in their simplest terms (reference 7). Simplifying assumptions a, b, c of 4.2.2 are adopted but assumption d of 4.2.2 is not valid for this one-pulse circuit.

4.2.3.1 Resistive load. If the load is purely resistive, the output voltage waveform consists of half-cycles of a sine wave separated by half-cycles of zero output voltage. The current waveform is identical in shape to the voltage waveform and both are depicted in FIGURE 22.

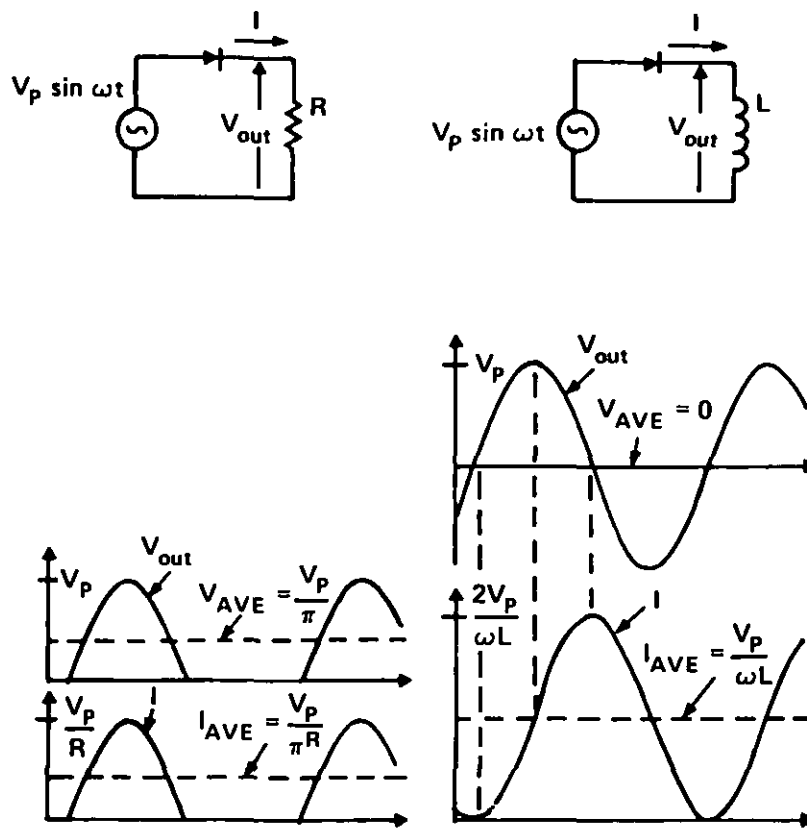


FIGURE 22. Single-phase half-wave rectifier.

4.2.3.2 Inductive load or filter. If the load is purely inductive, the waveforms change considerably (see FIGURE 22). During the first half cycle, the current builds up from zero to a peak value and energy has been transferred from the ac source to the inductor. The diode continues to conduct throughout the second half-cycle, during which the output voltage is negative and the total energy stored in the inductor is returned to the ac line. At the end of each full cycle the total net energy transfer is zero (for a lossless inductor). Since the diode conducts continuously, the load voltage is identical to the ac source voltage.

In practice, the inductor is not lossless but has at least some series resistance (FIGURE 23). At the end of the first half cycle, the current is less than for the pure inductor because of the voltage drop and consequent power loss in R. During the second half cycle, R continues to dissipate power as long as current flows. Since there is less total energy to return to the ac line, current always ceases before the second half cycle is completed.

As L/R increases, the delay in commutation increases and the current waveform approaches a sine wave (plus a dc component). However, since the peak current cannot exceed $2V_p/\omega L$, the inductance cannot be increased sufficiently to hold the current constant as required by simplifying assumption 4.2.2d.

If the intent of the rectifier is to get maximum power transfer into the load, the flow of power back into the ac line is undesirable. This reverse flow can be prevented by placing a freewheeling or by-pass diode across the output to conduct whenever the output voltage tries to go negative. The energy stored in L then discharges into R rather than being returned to the ac line. The freewheeling diode helps prevent the load current from ever going to zero, and thereby reduces the ripple.

4.2.3.3 Capacitive load or filter. If the load is purely capacitive, the load voltage charges up to the peak voltage and thereafter current ceases.

When a capacitor is connected in parallel with a resistive load, as shown in FIGURE 24, the capacitor tends to smooth the ripple in output voltage, but the current (in the diode) occurs in brief spikes. During the initial charging time the capacitor voltage, V, reaches a value equal to the maximum input voltage. When the supply voltage falls, the capacitor discharges through the load resistor. Current is, therefore, maintained in the load during the period when the input voltage is falling to zero and also during the negative half-cycle.

Because current is maintained through the resistor when the diode is not conducting, the average dc value is increased, and the ripple factor is decreased. The diode conducts only during the time when the input voltage is greater than the capacitor voltage. During this conduction time the diode must supply current to the load and also supply the capacitor with the charge necessary to maintain the increase in average current to the load. Thus the diode current, I, must be very high during its conduction period.

4.2.4 Single-phase full-wave rectifiers. The most common type of full-wave rectifier is the bridge-rectifier. As shown in FIGURE 25 it may be used without a transformer and this is a major advantage compared to the two-diode full-wave rectifier. However, this advantage is only practical for switching-mode power supplies where isolation is more cost-effectively achieved with a transformer at the higher switching frequency. Single-phase full-wave diode rectifiers are two-pulse circuits since the fundamental ripple frequency is twice the ac supply frequency.

4.2.4.1 Resistive load. If the load is purely resistive, the dc voltage consists of successive half-cycles of a sine wave, and the dc current has the same waveform as the voltage. The ac line current is the same as the dc current except that alternate half cycles are reversed in polarity. Thus the ac line current is purely sinusoidal with no harmonic content--no EMI. However, this current has limited practical value because of the large ripple in the dc output voltage. FIGURE 25 shows the circuits for both types of full-wave rectifiers and the waveforms which are the same for both circuits.

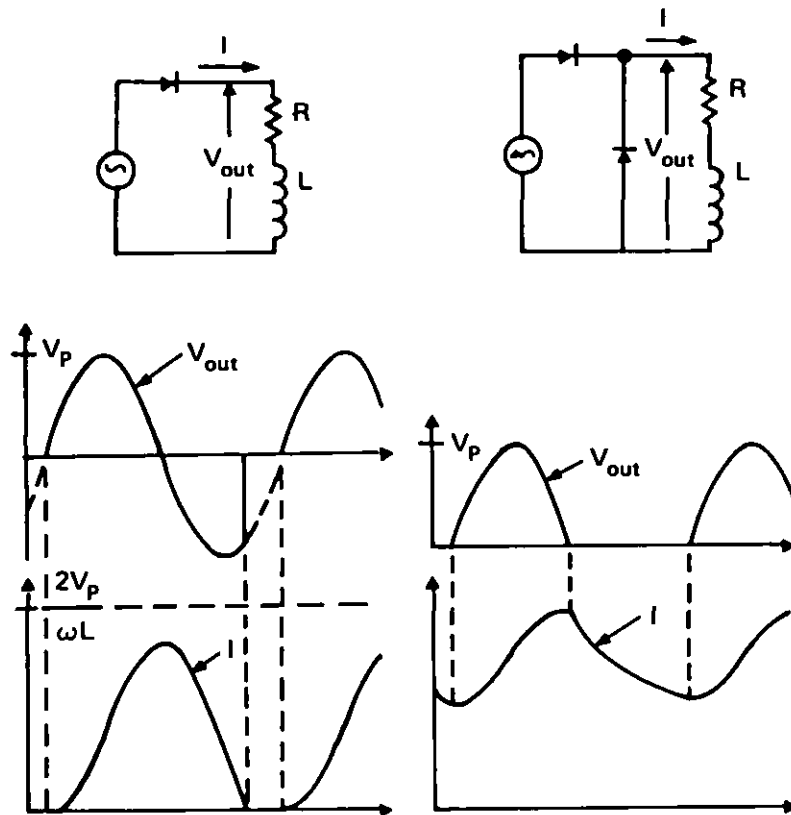


FIGURE 23. Single-phase half-wave rectifier - R/L load.

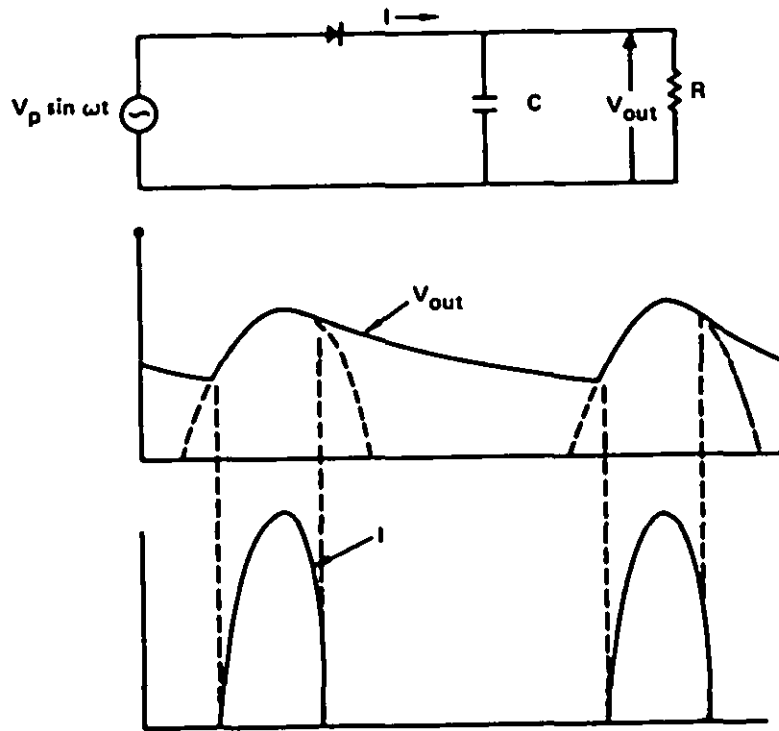


FIGURE 24. Single-phase half-wave rectifier - CR load.

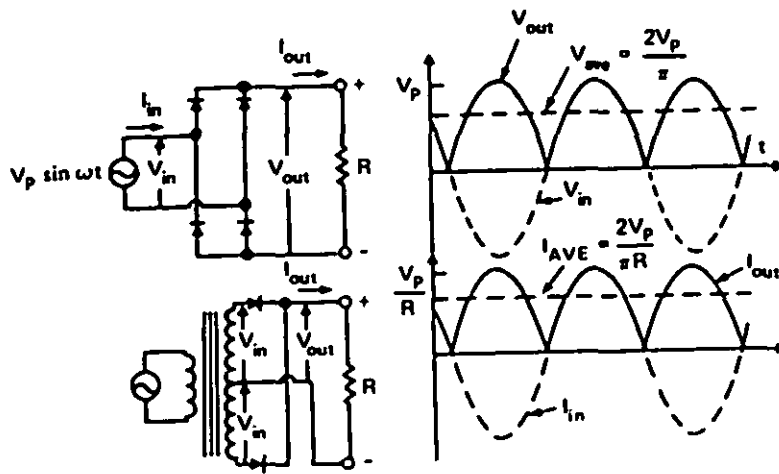


FIGURE 25. Two-pulse rectifier circuits.

4.2.4.2 Inductive input filter (critical inductance). FIGURE 26 shows the effects of inductance in series with the load in two cases. In the first case, the inductance is big enough to have an appreciable smoothing effect but small enough that the ripple is still significant. An approximate value for this inductance is R/ω (reference 7). The ac line current is no longer sinusoidal. The inductance has reduced the harmonic content of the load current by increasing the harmonic content of the ac source current. In the second case, the series inductance is increased until it is much larger than R/ω . The ripple across the load is now insignificant, and simplifying assumption 4.2.2d is valid. The inductance has totally removed the harmonic content of the load voltage and current, but the ac current waveform has become a square wave.

Unless otherwise stated, most rectifier analyses assume these idealized conditions.

These inductive input-filter conditions also apply when one or more LC sections are used as the input filter. As a minimum, a critical value of inductance exists that assures continuous current in the inductor. For a single LC filter two-pulse circuit, the inductance must be large enough so that $\omega L_c/R$ is greater than or equal to .35 (reference 8). L_c is called critical inductance and assures continuous current in the inductor.

4.2.4.3 Capacitive input filter. When a capacitor is connected in parallel with the load of a full-wave rectifier, as shown in FIGURE 27, the percent of ripple is decreased. Since the capacitor is charged to peak input voltage twice per cycle, the resultant average voltage across the load is higher than if a half-wave rectifier were used with the same RC load. Here as in the half-wave rectifier the line current is pulsating and high to supply sufficient charge to the capacitor.

4.2.5 Three-phase rectifiers. The pulse number of a single-phase rectifier cannot be increased beyond two. On the other hand, the pulse number of a polyphase rectifier may be made arbitrarily high by various interconnections of transformer windings. Half-wave, full-wave, bridge, and many other configurations are possible, but the most widely used are bridge circuits because they better utilize the transformer windings or eliminate the need for a transformer. The most common multiphase rectifiers are supplied from a three-phase source and use a three-phase bridge (6-pulse) circuit.

4.2.5.1 Inductive input filter (critical inductance). If bridge rectifiers are used for three-phase power sources, the transformer is optional for switching-mode regulators (see FIGURE 28). The three-phase bridge rectifier has a pulse number of 6 (less ripple to filter), and as will be shown in the next section less harmonic distortion of the input current. FIGURE 28 shows two possibilities for the line current waveforms depending on whether or not a transformer is used and on the type of transformer. Both three-phase waveforms contain identical harmonics (in number and amplitude) but the phases of the individual harmonics do not correspond, which explains the differences in the waveforms.

Here again, as for the single phase case, the idealized waveform is assumed when one or more sections of LC filters with sufficient filtering is used. The critical inductance for six-pulse circuits requires a minimum of .01 for $\omega L_c/R$ ---so that L_c can be much smaller (reference 8).

NOTE: The LC filter is preferred for switching-mode power supplies because it also does a better job of decreasing the switching frequency and its harmonics on the power line. In fact, a two-stage filter is even more advantageous. It is lighter in weight than a single-stage filter when both are optimally designed to meet identical peaking, attenuation and efficiency requirements (references 9 and 10). However, when using LC input filters (of one or more stages) with switching-mode regulators, care must be taken to prevent instability (see 3.3.4.2 and APPENDIX B). Input filter stability considerations also apply to single-phase, half-wave and other multi-phase rectifiers.

4.2.5.2 Capacitive input filter. As for single phase, a capacitive filter results in pulsating and high currents. Theoretically less capacitance is required to obtain a level of filtering comparable to the single-phase case. Frequently very large capacitors are used to keep the dc bus within the voltage regulation range of the control circuit. It is cheaper than using an inductive input filter. Also the capacitance of some electrolytics vary a great deal with temperature so large C's are used to provide sufficient capacitance even when hot. However, the larger the capacitor, the narrower and higher are the line current pulses.

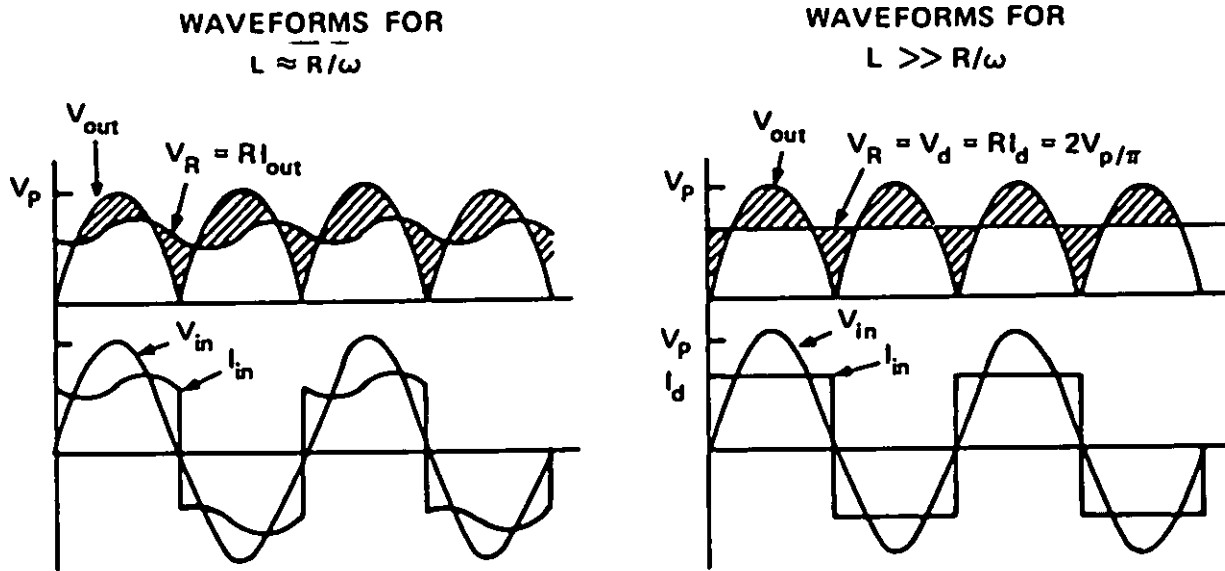


FIGURE 26. Effects on inductance on waveforms of two-pulse rectifier (voltage across inductance shown shaded).

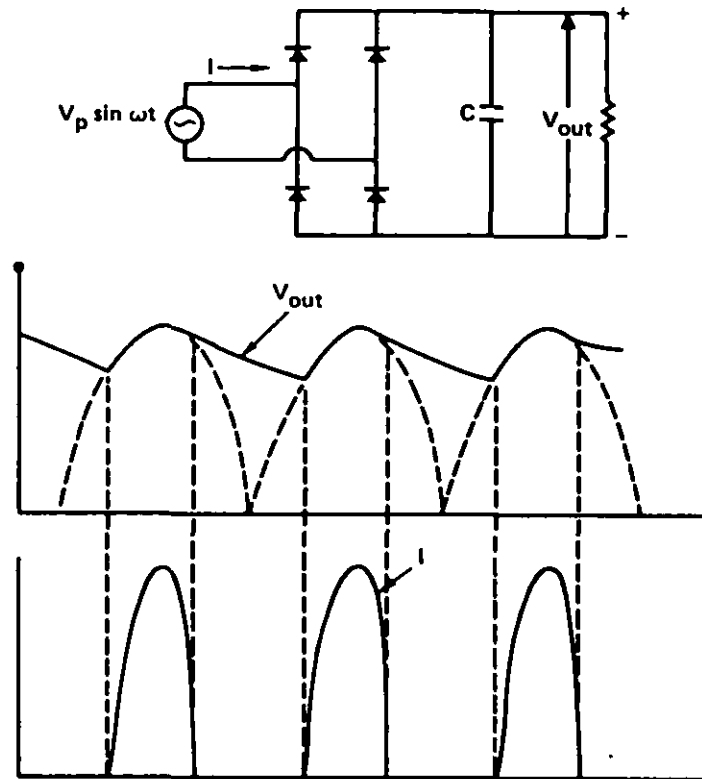


FIGURE 27. Two-pulse rectifier circuit - RC load.

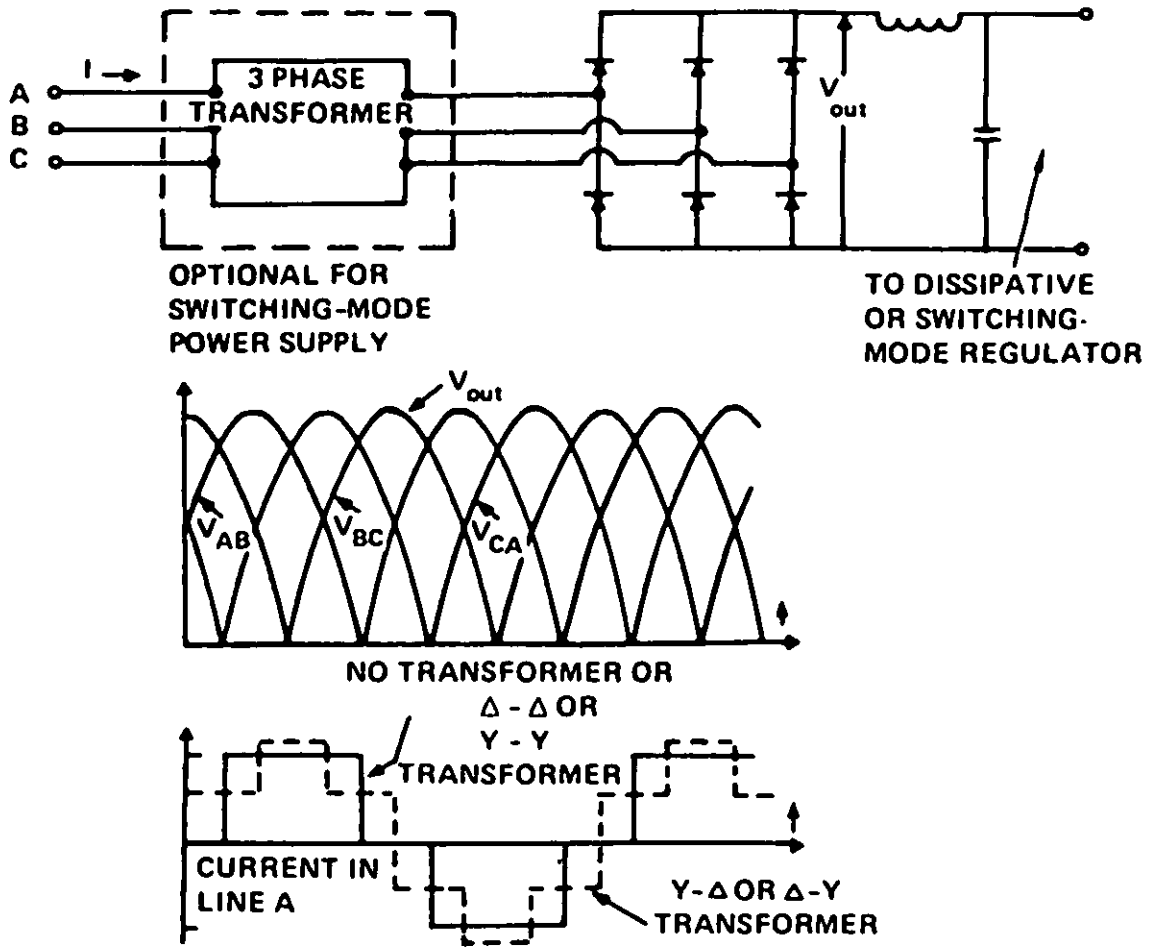


FIGURE 28. Six-pulse rectifier circuit - IDEAL input filter (infinite inductance).

4.2.6 Resultant harmonic spectrums. As the previous paragraphs have shown, rectifiers followed by either inductive or capacitive input filters cause the line current to be distorted. By applying Fourier analysis these non-sinusoidal line currents can be broken up into sinusoids, a fundamental and harmonics. It is the number and amplitudes of the harmonics that determine the non-sinusoidal waveshape (see APPENDIX D).

If p is the pulse number and f is the source frequency, the only harmonics present in the input current (in addition to f) occur at $(np \pm 1)f$, $n=1,2,3,\dots$. The amplitude of each harmonic current, relative to the fundamental current, is inversely proportional to its order (that is, to $np \pm 1$) for ideal diode rectifiers (reference 7). That is, the pulse number determines which harmonics of f are present but does not change the relative amplitude of a given harmonic if present (see TABLE IV).

However, for non-ideal capacitive loads higher amplitudes are present particularly for the lower order harmonics. Two-pulse and six-pulse spectrums will be examined (single-pulse spectrums are so high they should be limited to very low power devices if used at all).

4.2.6.1 Two-pulse line current spectrums. For the ideal infinite inductive filter, harmonic amplitudes can easily be predicted from the rule in 4.2.6. The waveform (see FIGURE 26) is a square wave containing only odd harmonics (33 percent third, 20 percent fifth, 14 percent seventh, and so forth). For capacitive and LC filters computations are more difficult. Therefore the CAD SPICE-2 computer program was used. The program only computes the first nine harmonics. FIGURE 29 shows the results for two values of capacitance with the same resistive load. The large C , 2650 microfarad (μF), produces 86 percent third harmonic. Also shown on the figure is the 3 percent maximum allowable specification limit (to be discussed in more detail later on).

FIGURE 30 shows the results of adding inductance to the large C . Considerable improvement is obtained and for $L = 13$ millihenry (mH) the results appear to be similar to the ideal filter (critical inductance calculates to be 9 mH, see 4.2.4.2).

4.2.6.2 Six-pulse line current spectrums. The ideal rectification spectrum is shown in FIGURE 31 for the six-pulse case. Triplen harmonics (multiples of three) no longer exist and so the lowest is the fifth (20 percent). Also shown are the specified 3 percent harmonic current limits. SPICE-2 computations were made using the same values of C (see FIGURE 32). For $C=2650 \mu F$, the fifth harmonic reached 90 percent. However, a 13 mH inductor brought the fifth down to 21 percent close to the ideal situation. A smaller inductor may still achieve close to the ideal harmonic values since CRITICAL inductance is now .3 mH (see 4.2.5.1). The inductance also includes any parasitic wiring and transformer leakage inductances.

4.3 Other rectification EMI sources. In the real world, components are not ideal. Even for large inductive filters the waveshape is, of course, not a zero rise time step but more like a trapezoid with some rounding of the corners. Spikes occur in the waveshape during diode recovery. A deliberate change in waveshape occurs if phase control regulation is used.

4.3.1 Rise/fall time effects. The typical current risetime is on the order of one or two microseconds (μs) without a transformer, and approximately 200 μs with a transformer (the leakage inductance slows down the rise (fall) times). A Fourier analysis of this trapezoidal waveshape compared to the rectangular waveshape indicates a more rapid diminishing of harmonics above a frequency, $1/t$, (where t is the rise time). A 40 dB per decade drop-off compared to a 20 dB per decade drop-off starting at a lower frequency for the slower rise time (see FIGURES 33 and 34 and APPENDIX D, Section 10).

4.3.2 Diode recovery spike. Whereas the rise/fall time effects decrease the higher frequency harmonics, the rectifier diode recovery spike increases them. Effectively the spike Fourier harmonics are superimposed on the basic Fourier spectrum. For bridge rectifiers the spike harmonics become noticeable usually between 50 kHz and 2 MHz. The current spikes are more pronounced with a transformer.

4.3.3 Phase controlled rectifiers. As discussed in 3.2.3, if phase controlled switching-mode regulators are used, they create additional line frequency harmonic distortion. As shown in FIGURE 3, circuit designs are available to decrease individual harmonics and total harmonic distortion.

TABLE IV. Harmonics in input current for ideal diode rectifiers.

HARMONICS OCCUR AT $(n P \pm 1) f$, $n=1, 2, 3, \dots$

$$\text{AMPLITUDES} = \frac{\text{FUND}}{nP \pm 1} \text{ WHERE } \left\{ \begin{array}{l} P = \text{PULSE NUMBER} \\ f = \text{SOURCE FREQUENCY} \\ \text{FUND} = \text{FUNDAMENTAL CURRENT} \end{array} \right.$$

FOR EXAMPLE: FOR $P = 6$

<u>HARMONIC #</u>	<u>AMPLITUDE</u>
5	$\frac{\text{FUND}}{5}$
7	$\frac{\text{FUND}}{7}$
11	$\frac{\text{FUND}}{11}$
etc.	etc.

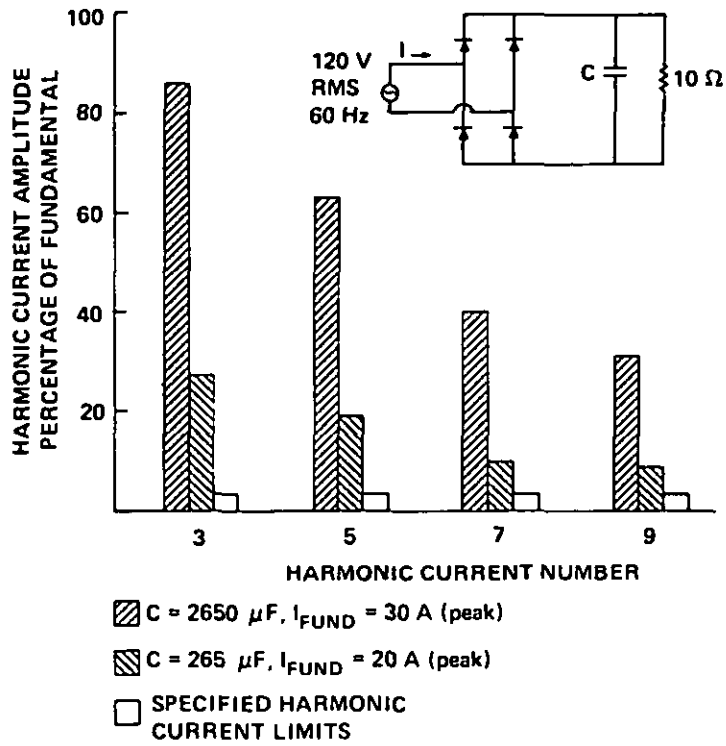


FIGURE 29. Harmonic line currents, two-pulse rectifier - RC load (computed using SPICE program).

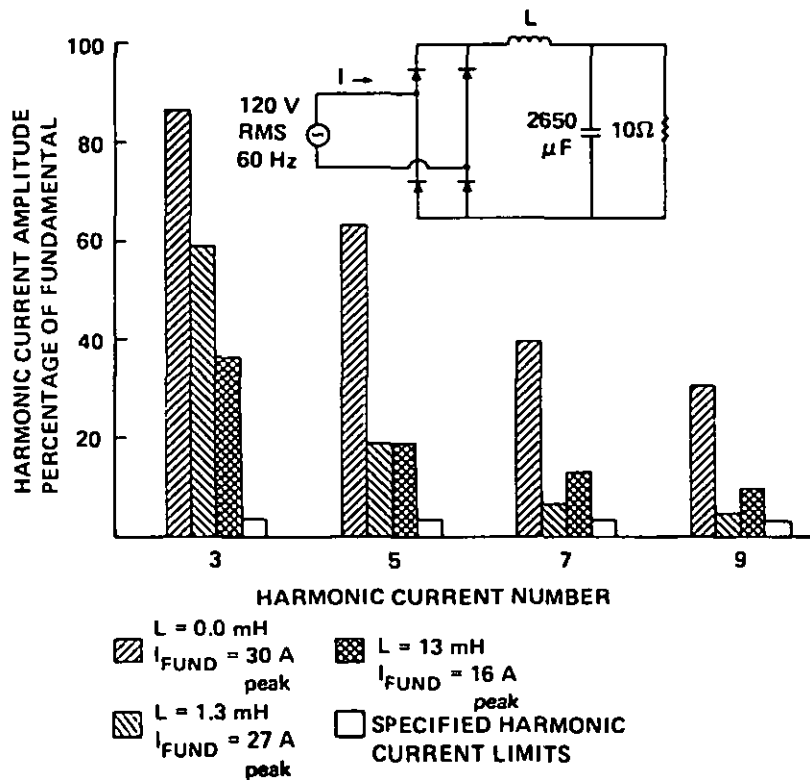


FIGURE 30. Harmonic line currents, two-pulse rectifier - RC/L load (computed using SPICE program).

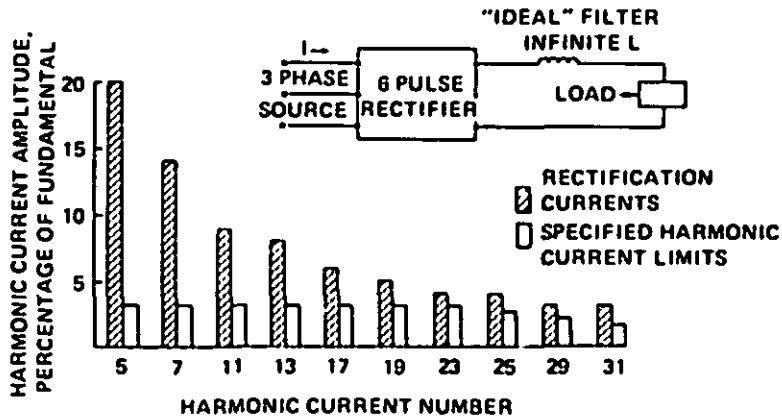


FIGURE 31. Harmonic line currents, six-pulse rectifier - IDEAL infinite inductance load.

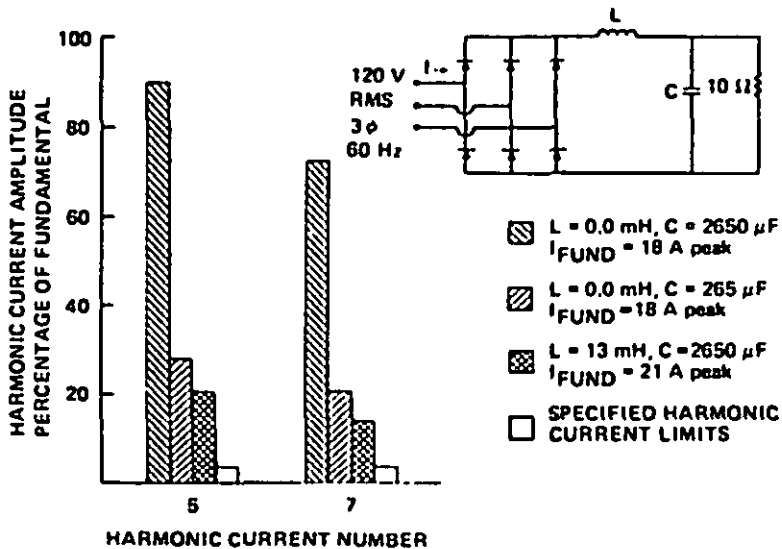


FIGURE 32. Harmonic line currents, six-pulse rectifier-RC/L load (computed using SPICE program).

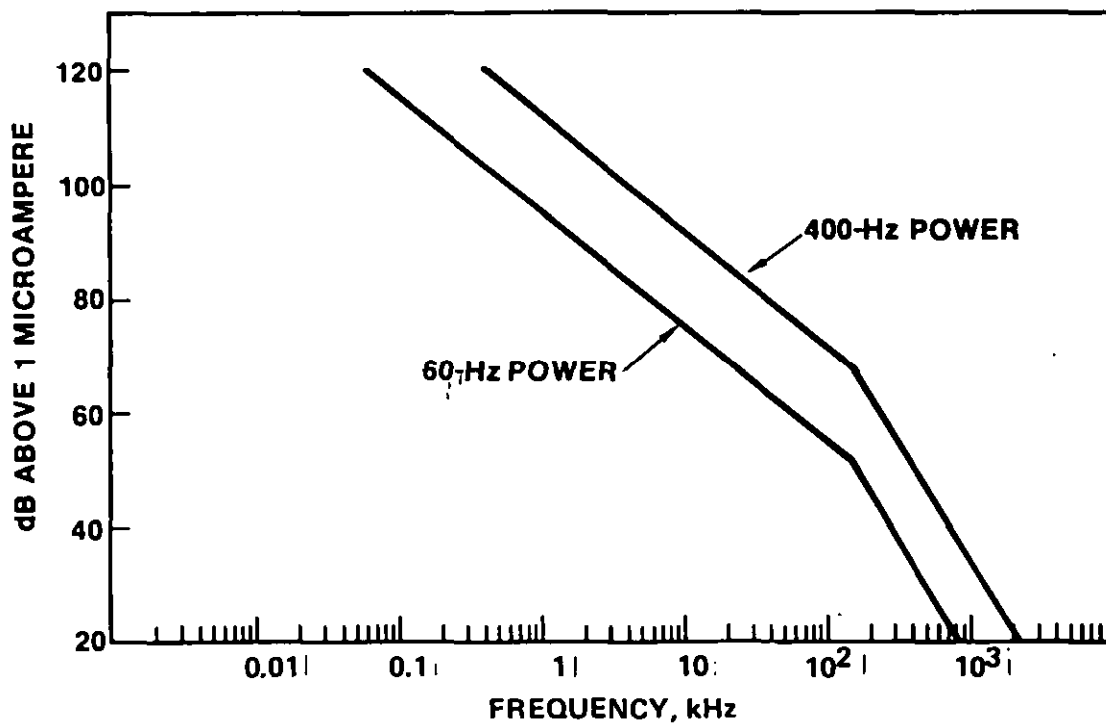


FIGURE 33. Normalized conducted frequency spectrum of a full-wave bridge rectifier without transformer.

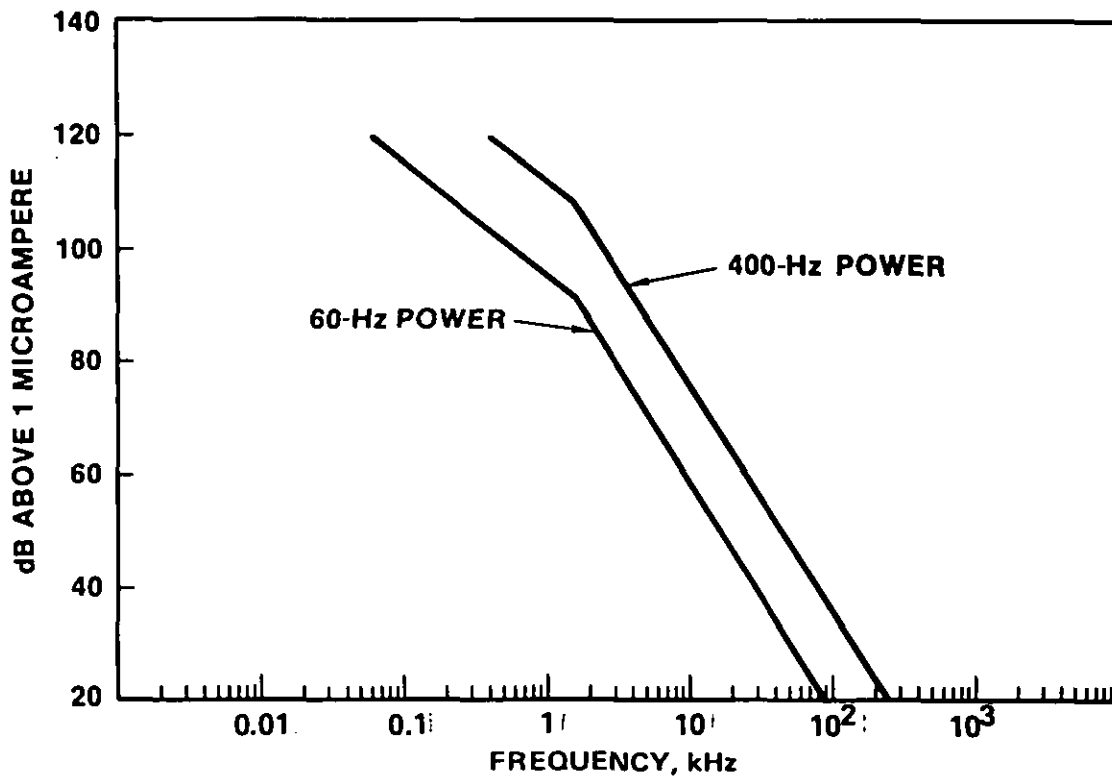


FIGURE 34. Normalized conducted frequency spectrum of T-R power supply.

4.4 Military specification requirements. Several military specifications place a 3 percent limit on the amplitude of any harmonic current for power supplies drawing power above one kilovolt amperes (kVA) for 60 Hz or above 0.2 kVA for 400 Hz (reference 12). Harmonic currents distort the ac voltage waveform through the source and distribution system impedance. Limiting harmonic currents to 3 percent amplitude (for the higher powered equipment), is based on keeping the total harmonic voltage distortion on the ship power system within 5 percent and the amplitude of any single harmonic within 3 percent. There are several undesirable effects of excessive harmonic voltage distortion.

4.4.1 Problems from excessive harmonics. The distorted voltage can cause problems in poorly designed electronic equipment, increased power losses in motors and other magnetic devices, reduced torque in high-efficiency induction motors, and excitation of undesirable vibration modes through electrical-mechanical couplings. Furthermore, a distorted waveform can act as a driving source for hull currents in ships. Similar problems can be created by low frequency harmonic line-currents generating magnetic fields which couple into other lines or equipment.

4.4.1.1 Structure (hull) currents. Structure currents in ships can create problems in sensitive equipment. Extensive investigations were conducted to identify, to determine the causes and to find solutions for this problem. The structure currents were found to be caused by large line-to-chassis EMI filters feeding harmonics to the structure. For example, tests on the USS GUITARRO 400 Hz power line showed that capacitive-input filter type power supplies were causing large structure currents through line-to-ground capacitors of approximately 135 μF per phase. The switching-frequency power supplies were major offenders but not primarily from their switching frequency harmonics. They were supplying excessive rectification harmonics because they used capacitive-input filters. (NOTE: In the past, it has been very common for switching-mode power supplies to be designed with capacitive-input filters. However, as discussed in 5.2.3 either one or two-stage L-C filters are recommended to sufficiently attenuate the conducted switching-frequency line current.) Although rectification harmonics appear to be the major source of structure currents, switching-frequency harmonics, if present, will also cause structure currents.

Some of the solutions recommended include: a. isolation transformers, b. line-to-line filters, c. multi-phase transformers to reduce harmonic levels, and d. limiting line to chassis capacity in EMI filters (MIL-STD-461 now specifies line-to-ground capacitance not to exceed 0.1 μF for 60 Hz equipments or 0.02 μF for 400 Hz equipments). New solutions to reduce rectification harmonics are being developed (see 4.5.2).

4.4.1.2 Power factor. Another disadvantage of harmonic currents is that they decrease the power factor of the system. Power factor is universally defined as the ratio of the average or real power in watts passing through the terminals to the apparent voltamperes, [root-means-square (rms) volts times rms amps] at the terminals. A maximum value of unity power factor is achieved when the instantaneous voltage and current at the circuit terminals are in time-phase at every instant of the cycle. When a sinusoidal voltage is applied to a nonlinear circuit the current is periodic but non-sinusoidal. Average power is transferred from the supply to the load only by the combination of sinusoidal supply voltage and fundamental harmonic of the current. Therefore, an expression for power factor can be conveniently split into two components (reference 11).

$$\text{PF} = \left[\cos a \right] \left[\frac{I_f}{I_t} \right]$$

(Displacement factor) (Distortion factor)

where PF = power factor for non-sinusoidal supply currents (assuming sinusoidal supply voltage)

a = displacement angle between supply voltage and fundamental current

I_f = rms value of fundamental supply current

I_t = rms value of total supply current (ammeter)

The non-sinusoidal I_t can be shown. Fourier analysis to be composed of a sinusoidal fundamental and sinusoidal harmonics; so that I_t is equivalent to the square root of the sum of the squares of the rms values of all the Fourier components.

Thus, the greater the number and amplitude of harmonics above the fundamental, the lower the power factor, requiring the source to supply more voltamperes--a costly requirement.

4.4.2 DoD-STD-1399, Section 300. This military standard, the Interface Standard for Shipboard Systems, AC Electric Power, was issued 1 August 1978 to supersede MIL-STD-1399, Section 103. Paragraph 6.2.7 of DoD-STD-1399, Section 300 reads as follows:

"Harmonic current. The operation of equipment shall be designed to have minimum harmonic distortion effect on the electrical system. The operation of such equipment with the following specified ratings shall not cause harmonic line currents to be generated that are greater than 3 percent of the unit's full load fundamental current between the 2nd and 32nd harmonic.

Frequency of power source (Hz)	Rating of unit
60	1 kVA or more
400	0.2 kVA or more on other than a single-phase, 115-volt source
400	2 amperes or more on a single-phase, 115-volt source

Additionally, currents with frequencies from the 32nd harmonic through 20-kHz shall not exceed 100/n percent of the unit's rated full load fundamental current, where n is the harmonic multiple number. Units with power ratings less than those specified above shall be current amplitude limited such that no individual harmonic line current from the 2nd harmonic through 20-kHz exceeds a magnitude of 100/n percent of the unit's full load fundamental current."

By no coincidence the 1/n fall-off rate corresponds to the fall-off rate of the ideal filter. Therefore, for the lower power units using a highly inductive input filter, no additional low frequency filtering should be necessary.

4.4.3 MIL-E-16400G, Amendment 1. This is the General Specification for Electronic, Interior Communication, and Navigation Equipment for Naval Ship and Shore. The amendment, dated 1 December 1976, specifies in paragraph 3.5.10 essentially the same requirement as for DoD-STD-1399. In addition, paragraph 4.8.5.11 specifies the following test conditions:

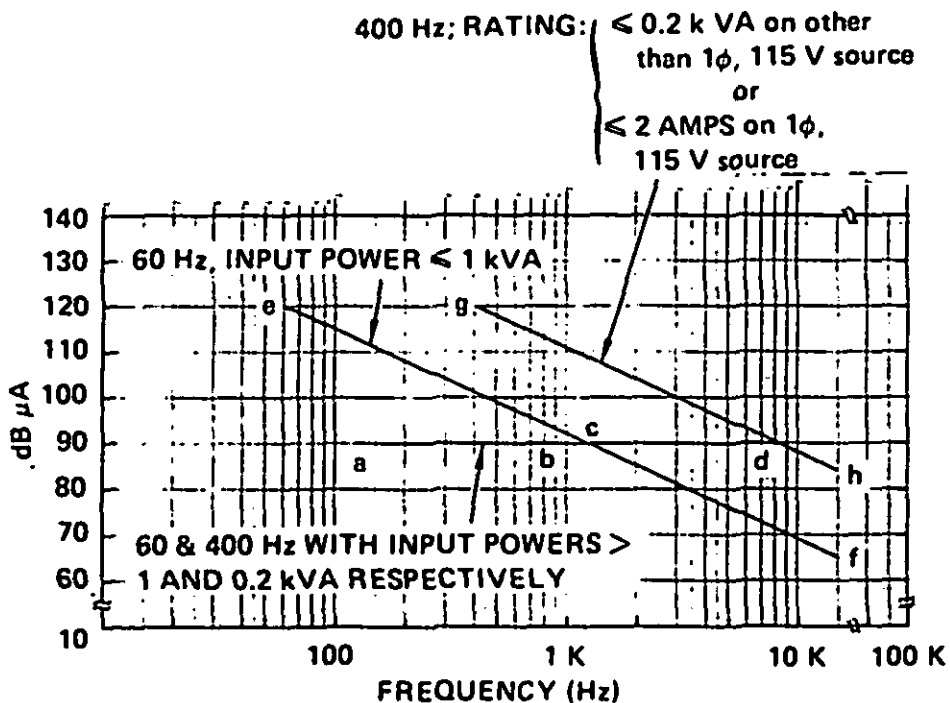
"Harmonic current. Equipment shall be tested to determine conformance with 3.5.10, when operating in the mode that generates the highest input current harmonics. The power source shall not have a harmonic voltage content in percent rms at any frequency which is greater than 25 percent of the allowable harmonic current at any frequency. The accuracy of measurement of harmonic currents shall be plus or minus 5 percent of the harmonic being measured."

NOTE: Two other specifications also were modified to include similar harmonic current limits; MIL-F-18870E(OS), dated 25 April 1975, and MIL-T-28800B, Amendment 1, dated 20 July 1977.

4.4.4 MIL-STD-461, CE01 requirement. This military standard specifies the Electromagnetic Emissions and Susceptibility Requirements for the Control of Electromagnetic Interference. CE01 is the Conducted Emissions Requirement for Power and Interconnecting Leads, Low Frequency (up to 15 kHz). Other requirements such as CE03 (.015 MHz to 50 MHz) and RE01 (magnetic radiation, .03 kHz to 50 kHz) are also affected by harmonic currents but these requirements are discussed in Section 5. MIL-STD-461B, dated 1 April 1980 is divided into nine categories of equipment and subsystem classes for limit requirements. A CE01 requirement is imposed on equipments installed in critical areas such as the platforms specified in 4.4.4.1 and 4.4.4.2.

4.4.4.1 Surface ships and submarines. For ac power leads, FIGURE 35 specifies the limits. The limits are very similar to those of DoD-STD-1399 with a few small variations. For the higher powered equipment, 90 dB microampere (μ A) corresponds to 3 percent when the dB relaxation equation is used (120 dB μ A is one amp). Likewise for the fall-off rates, except that 23 dB per decade is used instead of 20 dB per decade (the dB equivalent of 1/n). The maximum variation occurs at 15 kHz where for MIL-STD-461B, the limit is 7 dB tighter. TABLE V compares these ac limits to the similar limits imposed by DoD-STD-1399, Section 300 and MIL-E-16400.

For dc power and interconnecting leads (see FIGURE 36), the limits start at 30 Hz at 120 dB μ A remaining at this dB level until 400 Hz and then falling off at 42 dB per decade again with dB relaxation for currents over one amp. These limits correspond to the MIL-STD-461A, Notice 1 limits which, however, are not relaxed for currents over one amp. These limits (see FIGURE 36) are looser than the preceding ac 60 Hz limits (see FIGURE 35) until 4 kHz at which point they become tighter.



LIMIT SHALL BE DETERMINED AS FOLLOWS

1. For devices operating \leq the stated ratings, use the limit lines connecting point e, c and f and g, d and h for 60 and 400 Hz equipments and subsystems, respectively.
2. For devices operating $>$ stated ratings, the limits are:
 - a. For 60 Hz equipment: Use the limit line connecting points a, b, c and f.
 - b. For 400 Hz equipment: Use the limit line connecting points b, c, d and h.
3. For equipments and subsystems with load currents > 1 ampere, the limit shall be related as follows:
dB relaxation = $20 \log$ (load current)..

FIGURE 35. Limit for CE01 ac leads, MIL-STD-461B, part 5.

TABLE V. Military limits for harmonic line currents - 60 Hz power source.

N = HARMONIC NUMBER	FUND = AMPLITUDE OF FUNDAMENTAL CURRENT	
	< 1KVA	1KVA OR MORE
DOD-STD-1399 SECTION 300 AND MIL-E-16400 G AMENDMENT-1	<ul style="list-style-type: none"> • $< \frac{\text{FUND}}{N}$ UP TO 20 kHz (20 dB PER DECADE) 	<ul style="list-style-type: none"> • $< 3\% \text{ FUND}$ UP TO 1.92 kHz • $< \frac{\text{FUND}}{N}$ FROM 1.92 kHz TO 20 kHz
MIL-STD-461B, CE-01 SURFACE SHIPS, SUBMARINES, AND NAVY GROUND FACILITIES	<ul style="list-style-type: none"> • 23 dB PER DECADE UP TO 15 kHz 	<ul style="list-style-type: none"> • $< 90 \text{ dB}\mu\text{A}$ (CORRESPONDS TO 3% WITH dB RELAXATION) UP TO 1.2 kHz • 23 dB PER DECADE FROM 1.2 kHz TO 15 kHz

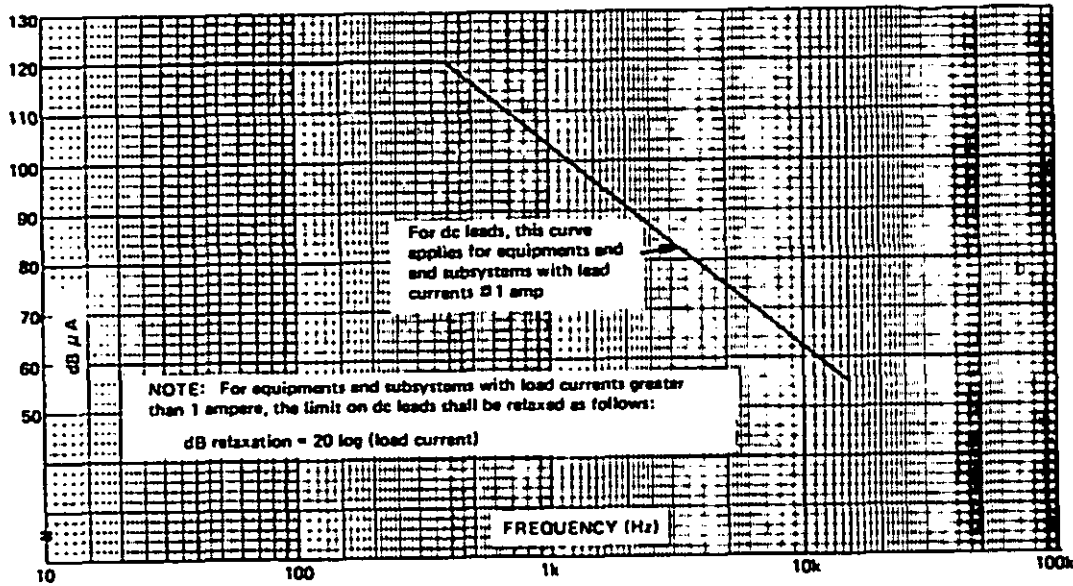


FIGURE 36. Limit for CE01 dc leads, MIL-STD-461B, part 5.

4.4.4.2 Aircraft, spacecraft and ground facilities. The CEOI requirement has only limited applicability for these classes of equipment and, except for Navy ground facilities, a looser limit is used starting at 130 dBμA (similar to MIL-STD-461A, Notice 3). Navy ground facility limits correspond to surface ship and submarine limits stated in 4.4.4.1.

4.5 Approaches to reduce rectifier harmonics. Two and six pulse power supplies drawing less than 1 kVA (if 60 Hz, or 0.2 kVA if 400 Hz) and using a highly inductive input filter (see FIGURE 31) will meet the $1/n$ fall-off limit of the three military specifications. However, equipment requiring higher power will not meet the 3 percent limit without additional bulky components or new approaches.

4.5.1 Standard solutions. The control of harmonic currents is not a new subject. It has been theoretically and experimentally investigated for more than fifty years. In 1974, after static power converters had been in use about ten years and promised to be increasingly used in industry and home, the IEEE formed a committee to develop a guide for harmonic control and reactive compensation of status power converters. This work was published in April 1981 as IEEE Std 519-1981, (reference 13).

Various approaches are being employed to reduce harmonic currents, including the use of 12, 18, and 24 pulse rectification, the use of harmonic traps, the use of large low-pass filters, and the use of active techniques that add or subtract power to the line to cancel harmonic currents (active filters). These approaches, in general, increase the size, weight, and complexity of the electronic equipment power supply and can cause other problems.

4.5.1.1 Low pass filters. Brute force low-pass filtering of the fifth harmonic in 60 Hz systems (300 Hz) to three percent can result in a filter larger than an off-line switching-mode power supply. In addition, as discussed in reference 14, the effect of power factor variations on filter gain at the line frequency, especially at higher line currents, is totally unacceptable. The interaction of the input filter with the switching-mode power supply output filter has to be carefully examined to prevent degradation of the output impedance of the power supply or the stability margin of the feedback loop (see APPENDIX B).

4.5.1.2 Shunt filters. Series-tuned shunt filters, sometimes called harmonic traps, are also large, complex for multifrequency inputs, not completely effective for variations in line frequency, and can cause system instabilities. Also, a contractor uses them at considerable risk to his field reliability. If another power user neglects to reduce his harmonics, they are absorbed by the harmonic trap of the contractor who uses this approach, over stressing and often destroying the filter components. There has been limited success in adding a shunt filter to a group of 400 Hz equipments to reduce the harmonic currents (reference 15). The problem is that the filter appears to have to be individually sized and designed, or at least extensively tested, in each application.

4.5.1.3 Harmonic compensation or injection. Harmonic injection techniques are discussed in reference 13 and also APPENDIX D of reference 16. These active filters can become very complex and heavy if all major harmonics are to be reduced over a large load range.

4.5.1.4 Ferroresonant transformers. Ferroresonant transformers have successfully been used to reduce the harmonics below three percent (reference 14). The disadvantages are those typical of the ferroresonant approach (see 3.2.2). That is, the transformer is larger than a conventional transformer and requires a fairly large resonant capacitor in addition. If the ferroresonant transformer is also used to regulate, the output voltage varies with frequency by a transfer ratio of about 1.7. This is a minor disadvantage when used on a major utility where frequency variations are rare but more of a consideration on ships where frequency variations can be expected. Also, power factor may be poor and regulation may be a strong function of power factor.

a conventional bridge to 1.43. A trade-off study indicates much better configurations are available (reference 7) such as the six phase center-tapped ring connected transformer which decreases the transformer VA to 1.03 rather than increasing it (reference 18).

If isolation is not required, then an auto-transformer configuration can be used with a considerable savings in size, reduced acoustic hum, and reduced stray magnetic field. An excellent discussion of the merits of this approach is in reference 19.

For ships, the best way to use the multi-pulse method is to exploit the characteristics of the ship electrical system combined with the combat system. The present state-of-the-art in off-line switching-mode power supplies strongly favors using 115V rather than 440V as the input power to the power supply. Since a transformer is needed some place in the system to make this transformation, it can be used with multi-pulse rectification to provide 155V dc to the off-line switching mode power supplies. These power supplies will operate from 115V ac or 155V dc equally well. If a transformer-rectifier scheme such as the six phase center-tapped ring connected transformer can be used, the three percent limit can be met with no size or weight penalty to the combined ship and combat system (reference 17).

4.5.2 New approaches. Several promising new techniques have been conceived and are in various stages of development.

4.5.2.1 Simulation of a resistive load. FIGURE 37 shows a solution developed by Delco Electronics which tries to make the switching-mode power supply appear as three single-phase resistive loads to the three-phase power source. To the extent that the input into the three individual converters can be made to appear resistive no harmonics are generated (see 4.2.4.1). Actually reactive components are required but they are designed to be low and to generate primarily triplen harmonics which are cancelled in the three-phase system (reference 20). A model was developed which resulted in a maximum individual harmonic distortion of 3.8 percent (7th harmonic) at the light load power level, 6kW, of a converter designed for 15kW where the distortion was less. Although resonant converters were used, duty cycle converters should be just as feasible.

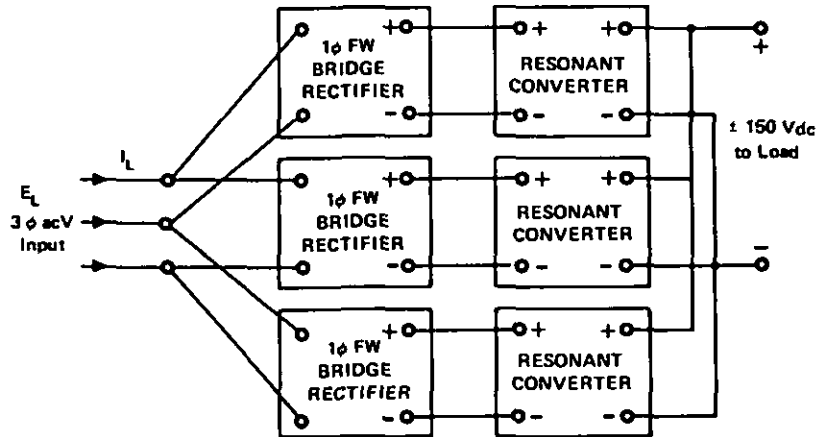


FIGURE 37. Delco converter.

4.5.2.2 Switching-mode techniques. Conceptually, for an applied sinusoidal voltage, a sinusoidal line current can be accurately approximated by applying high frequency switching techniques which regulate the current magnitude to be proportional to the applied voltage magnitude over the entire line frequency period. The high-frequency switching noise is much easier to suppress than low frequency harmonics. In addition, the electronic regulation of line current can be designed to control current surges.

In order to approximate a resistive load, the converter has to draw power at near zero input voltage which eliminates the buck configuration from consideration. When a boost configuration is used, the dc output voltage must be greater than the peak ac input voltage. When isolation is required, a buck-boost or boost-buck (Cuk) configuration must be used. The output voltage can then be adjusted as required by a combination of transformer turns ratio and duty cycle control.

A basic limitation of these approaches is the bandwidth of the control loop. In concept, a single buck-boost converter could provide line and load regulation as well as harmonic reduction by controlling both frequency and duty cycle of the switch. In practice, the control must be constant over one half the period of the line frequency in order to keep from introducing harmonics. This greatly degrades the response to load and line transients. As a result, a two stage configuration is often used with one converter controlling input harmonics and the other converter providing line and load regulation.

Several designs along these lines have been proposed. An example of such a technique is described in a Powercon 6 paper (reference 21) for an off-line duty-cycle converter with a capacitive input filter. For this, design power factor improved from about .6 to .95 and since this was due to the distortion factor (see 4.4.1), harmonics are thereby diminished. The system can become a complete ac to dc switching regulated power supply. Some degradation in performance resulted when compared with conventional switching power supply designs. Another example uses this concept to control the waveshape of a thyristor (SCR) phase-control converter (reference 22). A third example is given in reference 23 wherein the concept is applied to a battery charger.

Further development of this conceptual approach appears likely to result in new or improved performance designs or both.

4.5.2.3 AC to dc converter without large reactors. A new power conversion concept that would eliminate line low-frequency distortion was described in two papers by M. Venturini (references 24 and 25). These papers propose an ac to ac, three-phase to three-phase converter but the concept can be applied to ac to dc conversion.

This concept is based on theoretical work (reference 26) that predicts a class of converters that, given no pulsating input power (that is, three-phase input) and no pulsating output power (that is, dc power), power conversion and control can be accomplished by connecting the input lines to the output lines through switches with no energy storage devices in the circuit.

The circuit has unity power factor and no harmonics below the switching frequency which can be 20 kHz or higher. In concept, the total converter consists of six switches, control logic for the switches, and high frequency filters. Since switching techniques are used, the efficiency is high. This is an attractive topology even if it did not solve the harmonic problem.

The basic operating principle is to piece together an output voltage waveform with the wanted fundamental component (which can be dc) from selected segments of the input voltage waves. A generalized transformer results, capable of frequency, voltage, and power factor change. A sinusoidal input current waveform can be obtained with good input power factor.

More development work is needed. The major restrictions are that the output voltage is limited to one half the peak ac input voltage and there is no isolation between input and output since there are no transformers in the circuit. The lack of isolation is the only major drawback presently known to the approach restricting it from being an elegant solution to the Navy three percent harmonic limit problem.

4.5.2.4 Other related approaches. References 27 through 35 are papers relating to the new approaches discussed in the preceding sections. Most of them are by authors outside the U.S., indicating the universal interest in reducing rectifier harmonics.

4.6 Summary. Topics included in Section 4 are:

a. Power line low-frequency harmonics are limited by new military specifications. Particularly for Navy use, the limits require appropriate design of the input architecture of ac to dc converters.

b. For 60-Hz converters powering less than 1-kW the specifications are easy to meet but only if sufficiently large inductive input filters are used, and, at least single-phase full-wave rectification is used although three-phase is preferable.

c. For 60-Hz converters above 1-kW a tighter limit is specified, a 3 percent maximum limit for each individual harmonic between the 2nd and 32nd harmonic. To meet these limits bulky filters or large multiphase transformers are used but more cost-effective solutions are starting to be developed and used.

d. 400-Hz converters must meet the tighter three percent limit if they power 0.2 kVA or more on other than single-phase, 115 V or 2 amperes or more on a single-phase, 115 V source.

SECTION 5. EMI FROM SWITCHING-MODE CONVERSION.

Components and techniques are discussed to curtail or contain electromagnetic interference (EMI) in switching-mode converters. The frequency spectrums of the power line conducted switching-action noise are determined analytically. By using an optimally designed input filter these conducted emissions are shown to be less than CE03 limits for MIL-STD-461. Radiation from wiring and non-ideal components within the chassis can be suppressed by using recommended components, layouts, shielding, snubbers, baluns and high frequency filter designs. RE01 specifications for MIL-STD-461 can thereby be met.

5.1 Introduction. A major shortcoming of switching-regulator technology is that it is a complex technology that appears to be simpler than it actually is. Because of this apparent simplicity, misjudgements are prevalent in the design and application of switching-mode power supplies by the uninitiated engineer. Nowhere was this more evident than in the early days of switching-mode power supplies when designs were made without regard for noise prevention and reduction techniques.

In the past few years, however, the inherent advantages (especially high efficiency) of switching-mode technology for power supplies have spurred advances in component design (to limit the noise sources) and design techniques (to curtail noise coupling to the outside world). The result is much less EMI. Because the more efficient power supplies may require less than half as much source power, a well designed ac input switching-mode power supply can result in less EMI than a comparable less efficient ac input dissipative type power supply (since all 60 Hz or 400 Hz ac to dc rectifiers emit an EMI spectrum reaching beyond the commonly used 20 kHz switching-mode frequency).

There are two types of nondissipative switching-mode power supplies capable of being operated off-line. In both types, ac power is immediately rectified to dc and power conversion is performed at frequencies well above line frequency. The type referred to in this report as a switching regulator is a duty cycle converter that regulates by varying the ratio of switching ON time to OFF time. It is the one usually referred to as a switching-mode regulator.

Another type of off-line switching-mode regulator is called a resonant converter (see 3.2.4). A salient feature of resonant converters is minimal high-frequency EMI due to the filtering of the resonant circuit; and, therefore, only the EMI characteristics of the duty cycle converters are discussed here.

Switching regulators, due to the switching action, are potential generators of EMI noise at higher frequencies than the noise produced by rectification although there are overlapping frequencies. This section will limit its scope to the switching action noise. It can be manifested in the following ways:

- a. Differential-mode conducted noise on the power line which also in turn causes a radiated magnetic field
- b. Differential-mode conducted noise on the output leads (referred to as ripple voltage)
- c. Noise generated within the wiring and non-ideal components of the power supply and coupled to the outside world either inductively or capacitively--which, if coupled to the input or output leads, causes common-mode noise

5.2 Power line conducted differential-mode noise. The switching action generates a spectrum of the switching frequency and its harmonics on the power line. The magnitude of these emissions depends on the type of switching regulator and the amount of input filtering (internal and external). The main noise sources of switching frequency harmonics are the switching transistor (or thyristor) and commutating diode. FIGURE 38 shows a simplified buck switching regulator using a power transistor as the switching element. FIGURE 39 depicts the transistor current waveform for the buck switching regulator in the continuous mode. The buck waveform was selected because it represents the maximum conducted EMI compared to other types of switching regulators (the boost results in less EMI and the buck-boost results in the same EMI as the buck). Superimposed on the basic transistor waveform is a turn-on spike caused by the diode recovery current (also shown in FIGURE 39).

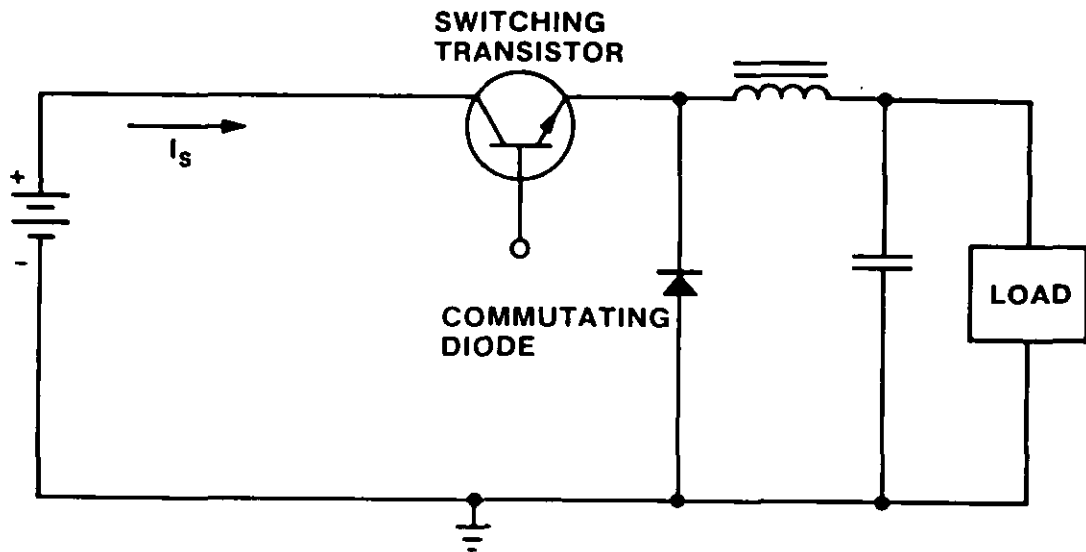
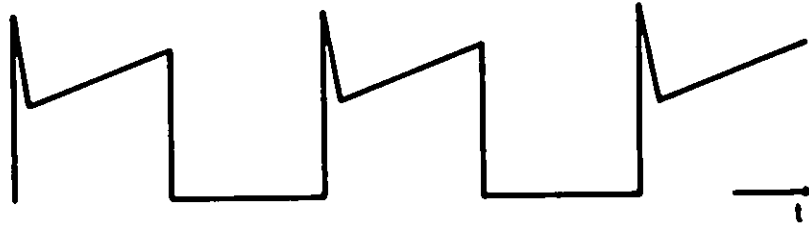


FIGURE 38. Noise sources for dc-input switching regulators.

TRANSISTOR
CURRENT



DIODE
CURRENT

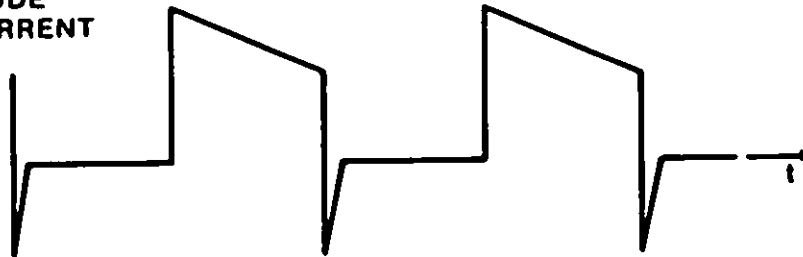


FIGURE 39. Switching transistor and commutating diode currents for simplified buck switching regulator.

5.2.1 Basic waveform. The basic switching waveform (without considering the diode action) is shown in FIGURE 40 where T is the period for one cycle (50 μ sec for 20 kHz). A rise time for the transistor, t_r , is also shown (for simplicity it was not shown in FIGURE 39). Rise times will vary with different transistors. A fast rise time will decrease heat losses (more efficient) but will result in more potential EMI. Typical rise/fall times associated with the switches are of the order of 100 nanoseconds (nsec). The waveform (see FIGURE 40) represents operation in the continuous mode for $d > 0$. Operation in the discontinuous mode would be represented by $d = 0$.

5.2.1.1 Fourier transform of basic waveform. For both continuous and discontinuous operation, the basic waveform can be modeled as a trapezoid to obtain the Fourier transform (see APPENDIX D). The low frequency interference levels are identical for any trapezoid pulse shape. Above a frequency of approximately one/pulsewidth, the frequency level is determined by the rise and fall times of the pulse.

FIGURE 41 is a plot of the loci of maximum frequency amplitudes (C_n) for a 20 kHz frequency switching regulator with a 30 nsec rise time. The first harmonic, 20 kHz sinusoid, will have an amplitude of $2A/\pi$ so that for a one ampere peak pulse the fundamental peak current is 0.64 amp or 4 dB down from the pulse peak. The amplitudes of the higher harmonics will be equal to or less than the spectrum in FIGURE 41. The actual spectrum, $(\sin x)/x$ function will result in low or zero amplitudes for some frequencies depending on the width of the pulse.

5.2.2 Turn-on spike. The spike (see FIGURE 39 and 5.4.1) caused by the diode recovery current can also be modeled as trapezoid. The usual waveshape, however, is a damped sinusoid as a result of circuit and parasitic resonances.

5.2.2.1 Fourier transform of turn-on spike. The Fourier transform of a ringing waveform peaks close to the ringing frequency and then decreases at 40 dB per decade (see APPENDIX D). The amplitude of the damped sinusoid will depend on the characteristics of the diode recovery. This effect can be limited by the use of a fast recovery diode. Typical ringing frequencies are in the vicinity of 3 MHz. FIGURE 42 is a plot of the loci of maximum frequencies for a one ampere ringing spike with a peak at 3 MHz, attenuation (α) of 1.153×10^5 nepers, and a pulse repetition rate (P.R.R.) of 20 kHz. The peak amplitude, 98 dB μ A, is close to 3 MHz and the individual frequencies start at the P.R.R., 20 kHz, with lower amplitudes.

5.2.3 Resultant conducted noise spectrum (no filters). FIGURE 43 is the noise spectrum plot combined from both the basic waveform and the turn-on spike. The resultant envelope is shown extended at the low frequency end to account for subharmonic frequencies caused by potential imbalances when multiple switching transistors are used in the regulator design (push-pull or bridge operation). This resultant noise spectrum assumes no filters.

5.2.4 Input filters. EMI input filters can be designed as a single-section low-pass filter or by cascading several single-section filters to obtain more attenuation. Yu et al (reference 36) demonstrates that a two-stage filter (see FIGURE 44) results in a lighter optimum weight than a single-stage (see FIGURE 45) filter when both are designed to meet identical peaking, attenuation, and efficiency requirements. Design details for both filters are given in APPENDIX B, paragraph 60. Methodologies and computer programs for optimum power processing circuits (such as these filters) used in switching regulator power supplies have been developed for the NASA Modeling and Analysis of Power Processing Systems (MAPPS) programs.

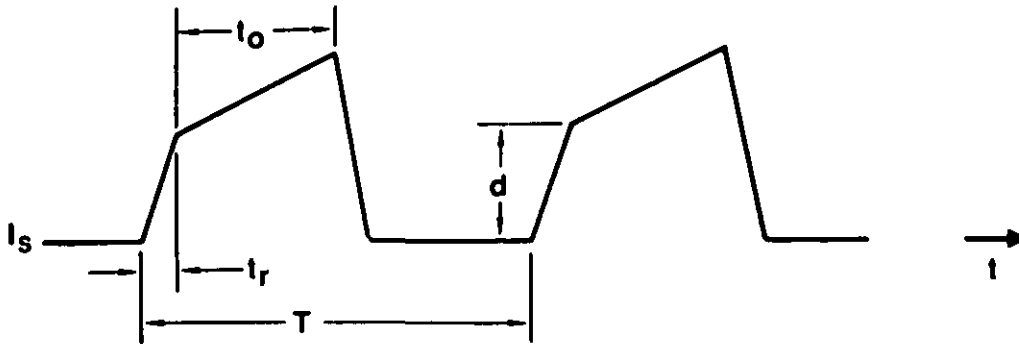


FIGURE 40. Switching current basic waveform (without diode recovery spike).

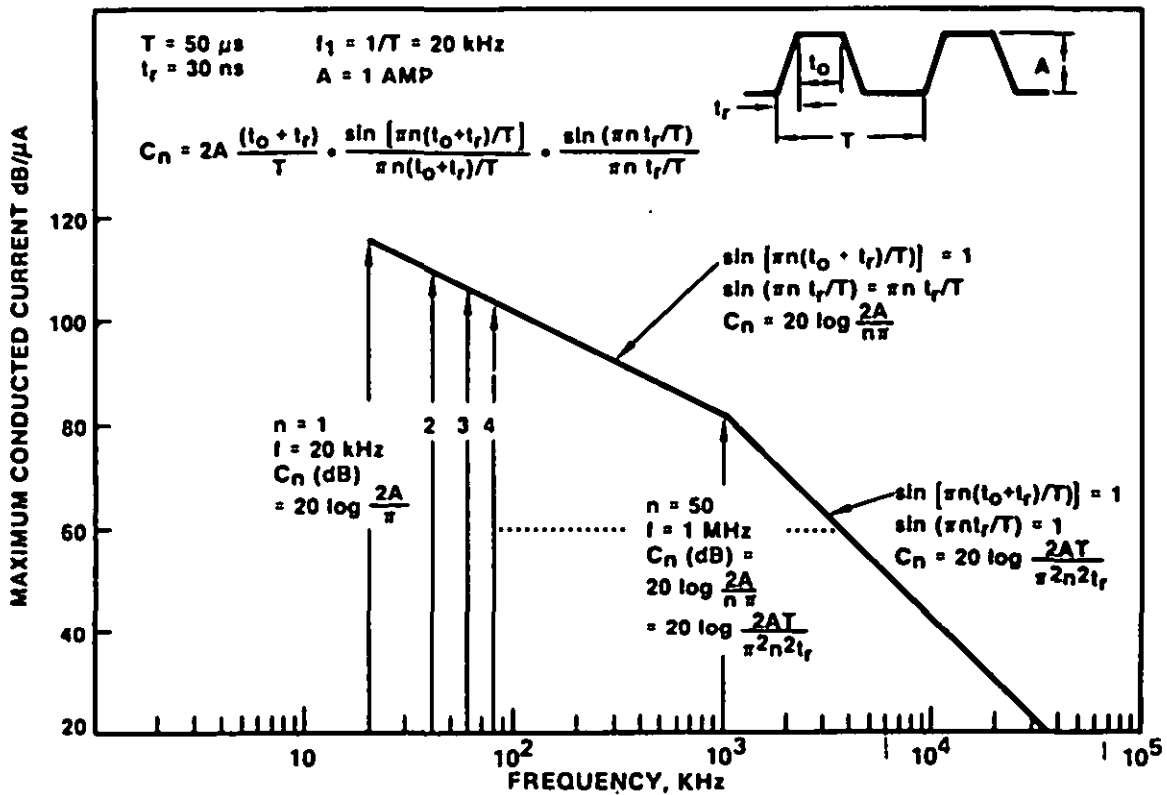


FIGURE 41. Switching regulator basic waveform harmonic spectrum.

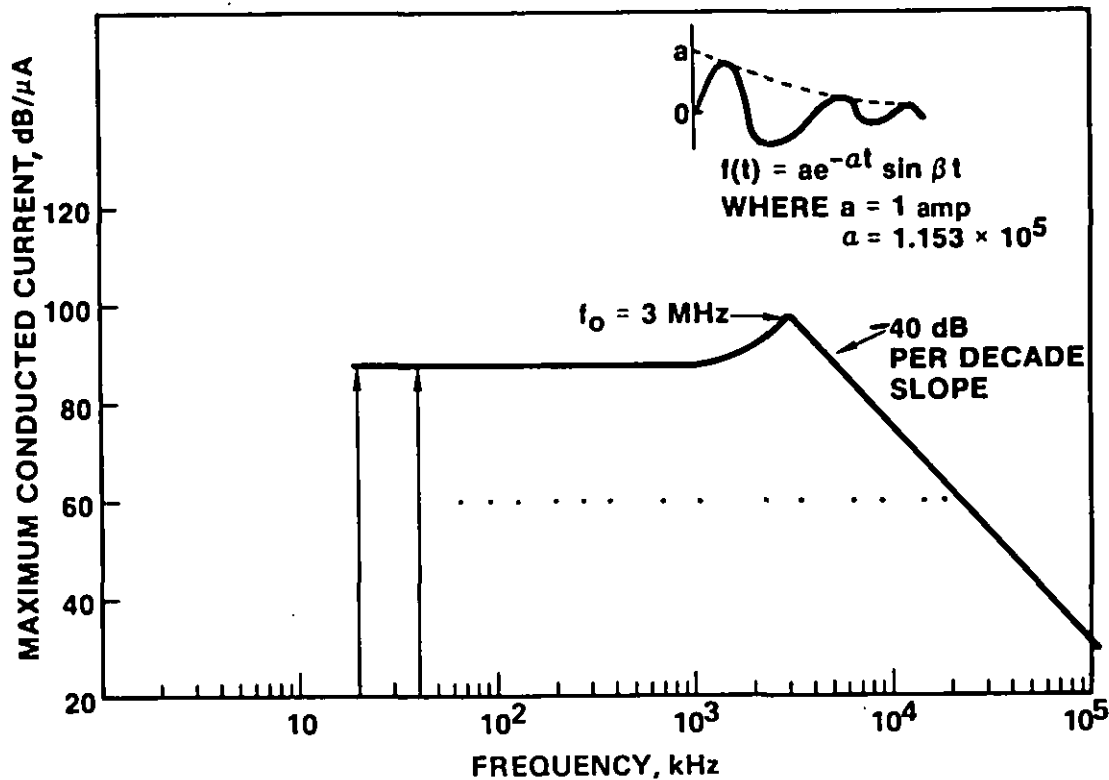


FIGURE 42. An example of switching regulator spike "ringing" spectrum (from diode recovery).

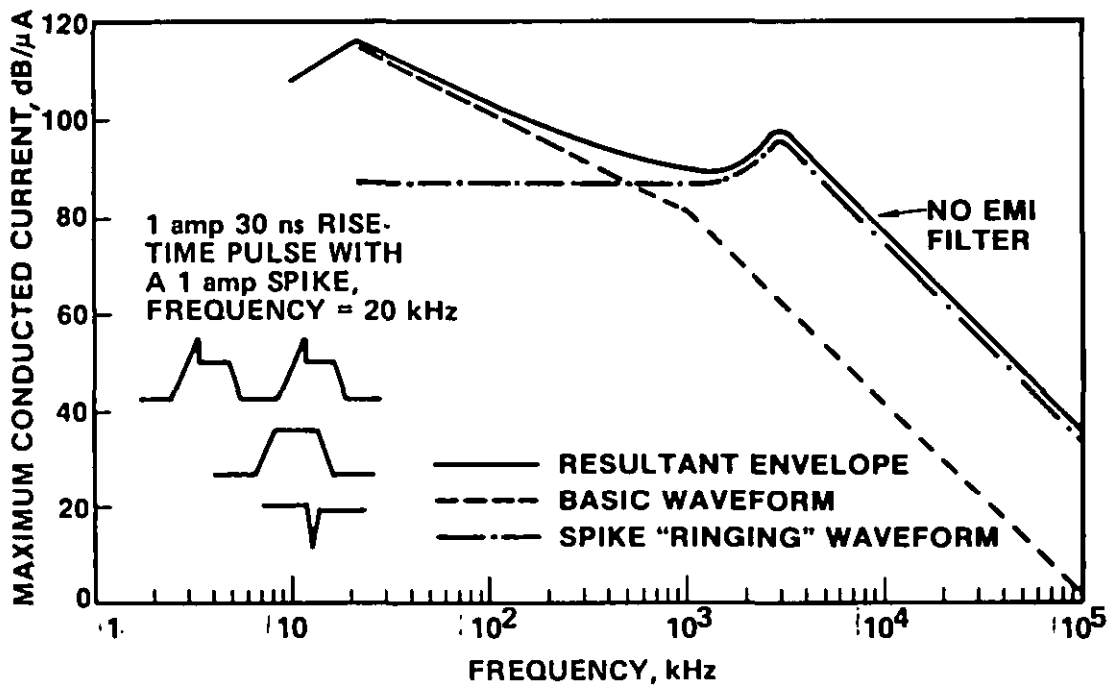


FIGURE 43. Switching regulator input current spectrum (no filter).

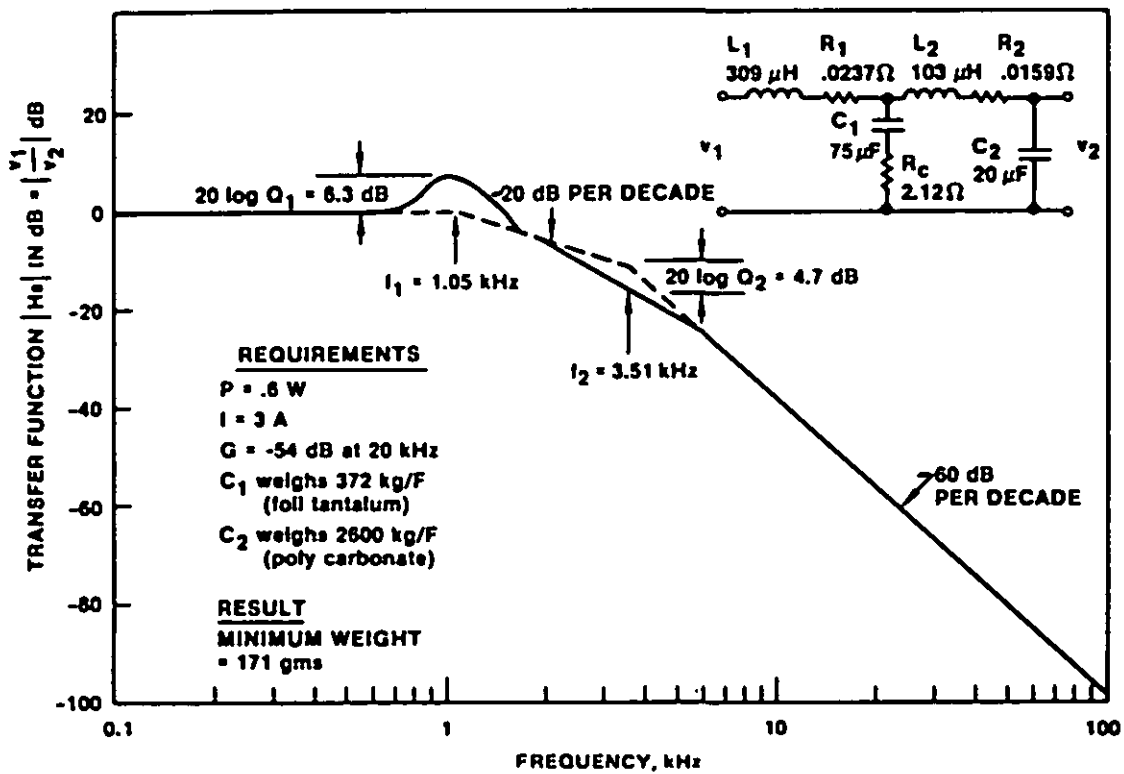


FIGURE 44. Two-section optimum weight filter.

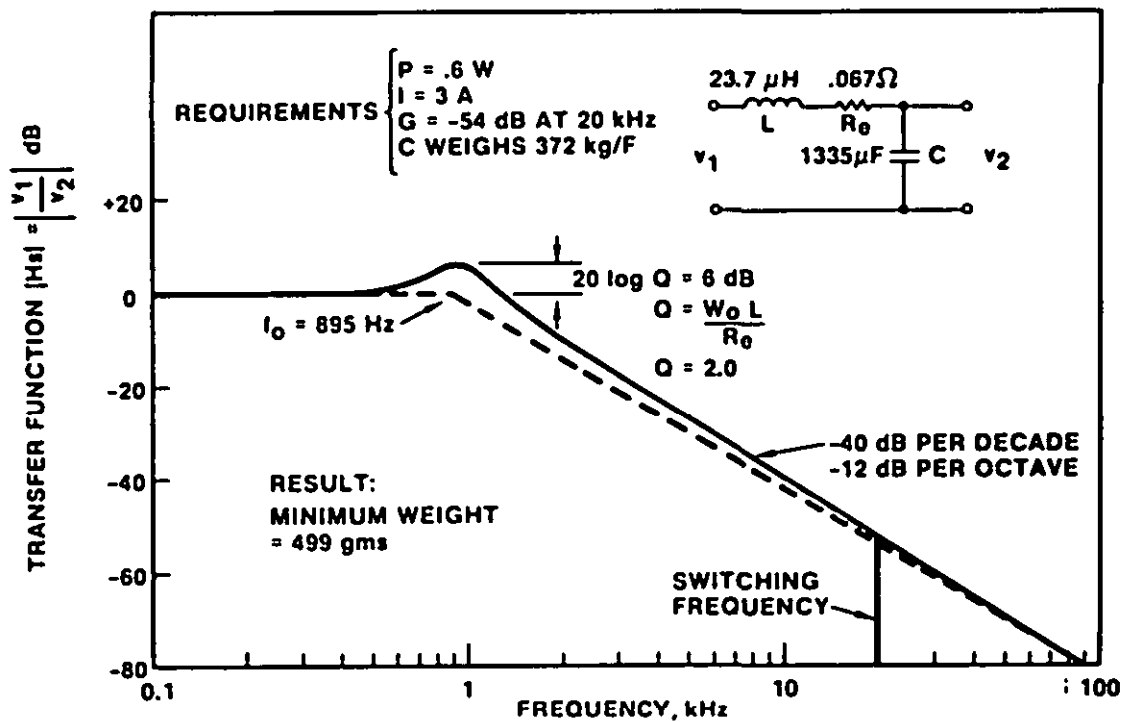


FIGURE 45. Single-section optimum weight filter.

5.2.4.1 Recommended component types. Referring to FIGURE 44, the resistor R_C is placed in series with C_1 to control resonant peaking because negligible current flows in C_1 and R_C except during line and load changes. The following guidelines are recommended in reference 10 for selecting components (also see Section 6):

- a. Since C_2 supplies most of the pulse current, use low-dissipative capacitors such as ceramic, mylar, and poly-carbonate.
- b. Powdered permalloy core for L_2 will achieve a small core loss.
- c. Inductor L_1 passes essentially a direct current, therefore, eddy current and hysteresis losses are negligible. High saturation flux core material, such as gapped silicon steel, can be used for size and weight savings (reserve flux capability is required to prevent saturation during input transients and audio susceptibility tests).
- d. For C_1 foil, or wet-slug tantalum capacitors are suitable as are low inductance aluminum electrolytics.

5.2.4.2 Potential instability problem. As discussed in 3.3.4.2, switching-mode regulators can become unstable by the addition of input filters. APPENDIX B gives design criteria (developed by Middlebrook) and recommendations to prevent instability including simplified models.

APPENDIX B also includes two-stage filter spectrums as analyzed by Middlebrook (references 2 and 37) who also prefers a two-section LC filter. Greater flexibility in achieving stability is achieved with a two-section filter.

5.2.5 Input noise current with two-stage filter. FIGURE 46 shows plots of the noise current without and with the FIGURE 44 two-stage input filter (designed for 54 dB attenuation at 20 kHz). The attenuation curves shown in FIGURE 46 assume ideal components (L, C and R) which are frequency-invariant. The dotted line shows the theoretical attenuation slope if the filter capacitance values were invariant with frequency and negligible ESR and ESL existed. For the frequency region shown, the unfiltered noise declines at a 20 dB per decade slope and the filtering at a 60 dB per decade slope so the maximum attainable slope is 80 dB per decade.

A more realistic curve is represented by a solid line which assumes: a. capacitors are chosen to have the specified values at the switching frequency but decrease with increasing frequency; b. ESR and ESL values are low, with ESL between 1 and 15 nH; and c. lead lengths cause about 10 dB less attenuation at 1 MHz. Macomber (reference 38) recommends particular capacitors (see 6.2) and gives experimental data which are noted in FIGURE 45.

5.2.6 Predicted noise current compared to Navy CEO3 limits. FIGURE 47 compares the predicted (realistic) noise current to Navy CEO3 limits for MIL-STD-461B. The predicted envelope (a worst-case prediction) is below the limits for load currents of one amp and below. For load currents greater than one amp and up to two MHz, the limits are relaxed in proportion to the increased current and, therefore, the predicted noise levels remain below the relaxed limits up to two MHz. Limits are exceeded above two MHz for load currents greater than 45 amps (153 dB μ A). However, high power loads often use a resonant-type switching converter which generates minimal high frequency EMI or sufficient high frequency filtering can be added to the basic two-stage filter to meet the specified limits.

Even lower noise levels throughout the spectrum can be achieved by using larger input filter components or increasing the switching frequency. For example, the input two-stage filter in FIGURE 44 was designed for -54 dB at 20 kHz. Another 10.6 dB of attenuation is attainable by shifting f_1 from 1.05 kHz to 700 Hz with larger filter components. Using the same filter but doubling the switching frequency increases the attenuation from -54 dB to -72 dB at the new switching frequency (40 kHz).

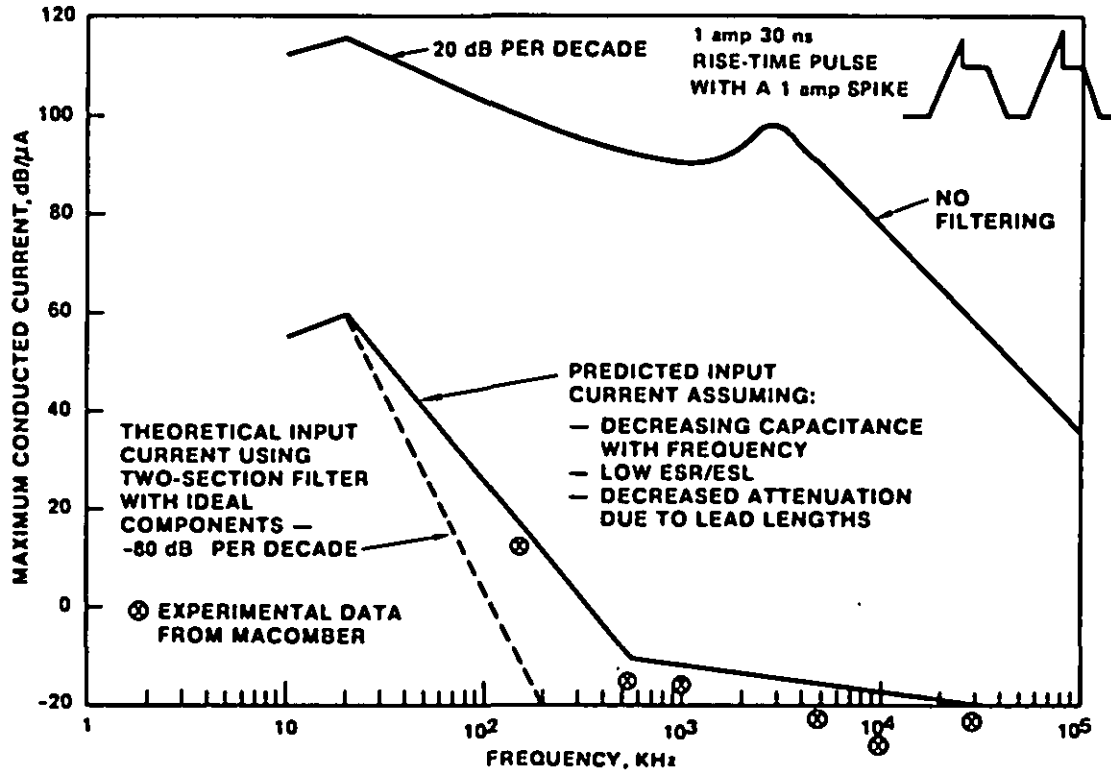


FIGURE 46. Switching regulator input current without and with filter (two stages).

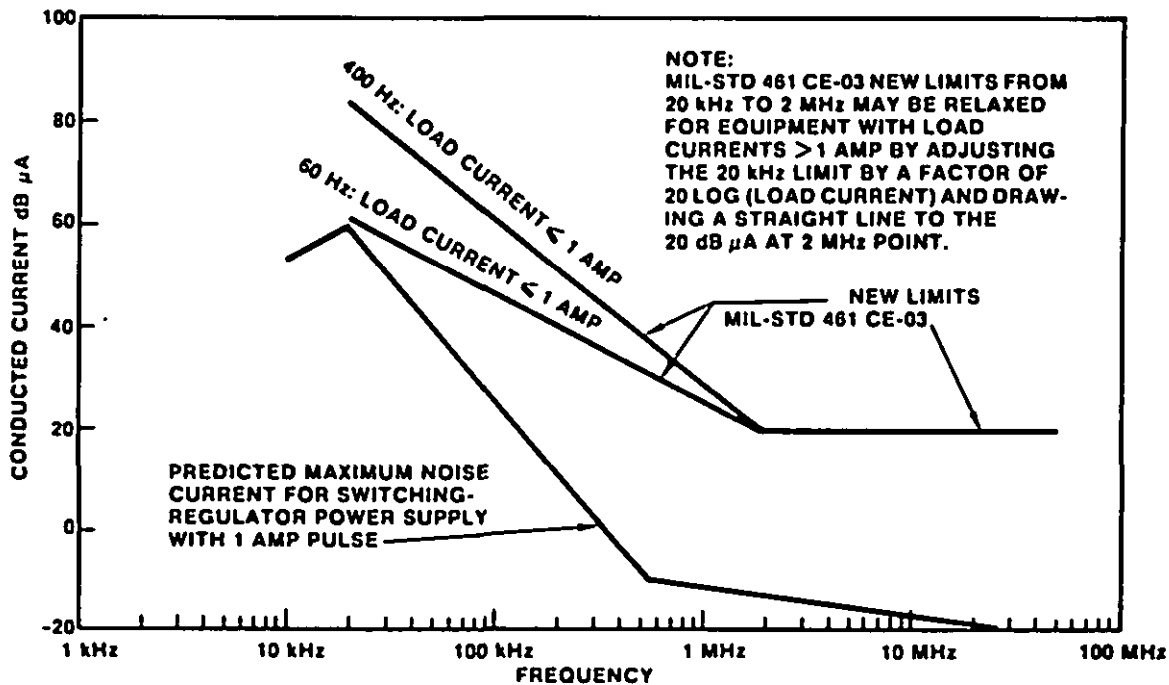


FIGURE 47. CE03 Navy limits for MIL-STD-461B.

5.3 Ripple on output leads. Output ripple is an inherent characteristic of switching-mode power supplies. There is always a residual component of the switching frequency conducted differentially on the output leads. FIGURE 38 shows a typical LC output filter. It can be designed for low output ripple (and even lower ripple values are achievable with multi-stage filters). Very low ripple designs, however, can be expensive in component cost, and are more difficult to stabilize. Fortunately, modern day digital logic circuits have excellent noise immunity and wide switching margins. It is poor economy to over-specify power source output noise.

The question remains--what is the most cost-effective way to deal with analog circuits that cannot tolerate such ripple? Often only one or two critical circuits require very low ripple. These sensitive circuits are best handled by adding a point-of-use series regulator. By locating the lossy regulator only at the noise sensitive circuit, losses are kept to a minimum. Other circuits fed by the power supply may not need very low-ripple voltages.

5.4 Suppression of internally radiated noise. EMI radiation from within the chassis no longer need be a major problem. Noise generated within the wiring and non-ideal components can be coupled either to the outside world or to the input and output leads, inductively or capacitively. This potential noise problem has been successfully solved in recent years. In the past, switching-mode power supply manufacturers avoided reference to EMI except for specifying output ripple. Today, however, many low EMI designs exist and many manufacturers do not hesitate to refer to low EMI in their catalogs, in some cases referencing MIL-STD-461 and other Governmental or industrial specifications.

Several texts have recently appeared in which noise reduction techniques are discussed. Gottlieb (reference 41) states that recent understanding of noise filtering and suppression techniques has enabled the designer to contain the spurious noise energy within the physical confines of the power supply. A book by Ott (reference 42) is devoted exclusively to noise reduction in electronic systems and much of the detailed theoretical and practical information therein is directly applicable to switching-mode power supply noise reduction.

5.4.1 Use of fast (soft) recovery diodes. Diodes are non-ideal and exhibit a phenomenon known as reverse recovery. A spike occurs at the end of a diode conduction cycle when reverse voltage is just applied by the transistor. A short pulse of reverse current through the diode is required to sweep out minority carriers and to establish the reverse biased junction. The transistor must supply this current in addition to the commutated inductor current. Therefore, there is a corresponding transistor current spike. This effect can be limited by the use of a fast recovery diode.

Where the Schottky diode is applicable, one can considerably diminish this source of noise. Schottky diodes have low forward voltage drops but their reverse leakage current increases with high reverse voltages and rising temperatures. At the present time Schottky rectifiers are obtainable (references 43 and 44) with acceptably low reverse current and reverse voltage capabilities up to 100 volts. A safety factor is recommended, however, limiting their use to lower voltages (50 volts or 60 volts). However, a Schottky diode has four to five times more junction capacitance than pn rectifiers. In a practical power supply, this capacitance together with transformer's leakage inductance forms an equivalent tuned series circuit. Energy in this inductance can force excess charge into the capacitance building to a breakdown voltage level (reverse-blocking state) unless a protective snubber circuit is provided. Resistance-capacitance (RC) snubber across the Schottky will protect it and also help minimize voltage spikes and thus reduce conducted and radiated interference.

For higher voltages other types of fast recovery diodes become increasingly competitive as forward voltage drop diminishes in importance. These fast recovery diodes, however, can generate radiated energy due to the steep di/dt . To control this radiation, use ferrite beads on transformer output leads feeding rectifier diodes and place lossy mylar capacitors across the diodes (reference 45). Reducing the need for beads and capacitors are new high speed rectifiers with soft recovery characteristics which reduce the di/dt on turn-off of the diodes.

5.4.2 Control of transistor rise and fall times. Fast rise/fall time transistors result in more efficient switching-mode power supplies. Unless controlled, however, they result in high frequency radiated or conducted emissions and also stress the transistor. The Fourier analysis of the basic switching waveform (see FIGURES 41 and 116 of APPENDIX D) shows a series of harmonic components extending into the megahertz region of the spectrum. The initial rate of roll-off with increasing frequency is only 20 dB per decade for the trapezoidal waveshape, and the 20 dB roll-off extends to higher frequencies as the switching speed increases. By rounding the switching waveshape, a roll-off of 60 dB to 80 dB per decade can be obtained (see FIGURES 118 and 119). The rounding can be accomplished by snubbing networks.

Two basic snubbing configurations are shown in FIGURE 48 and design equations are given for them for six types of switching regulator/converter circuits in reference 46. Snubbers use reactive elements to shape the load line. For the current snubber most of the power dissipated in the snubber would otherwise be dissipated in or radiated from the transistor. The voltage snubber can lead indirectly to improved efficiency by allowing for a lower average junction temperature. Recommendations are also made for component selection for the passive elements of the two snubbers considering the transient performance in addition to the normal voltage, current and power constraints. They state that more elegant techniques are available to those who are willing to trade simplicity for greater efficiency (reference 46).

For example, unique snubber networks are given in references 47 and 48. Switching spikes are considerably reduced. At high power levels most of the switching losses from the switching transistor are removed with either of two networks, each containing three components: an inductor or a capacitor, diode, and a resistor. With proper design they even somewhat improve the overall efficiency.

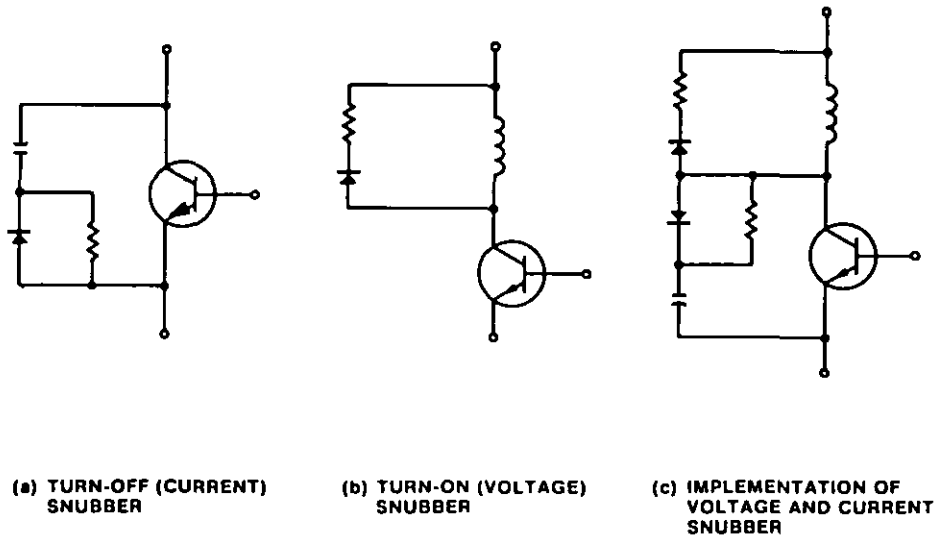


FIGURE 48. Voltage and current snubbers.

5.4.3 Mechanical suppression techniques and high frequency filtering. To minimize magnetic field radiation, all switched current leads, both ac and dc, should be kept short and the hot and return leads twisted, or where the wiring is a printed circuit, the hot and return leads should be run in mirror-image conductors. Inductive loops should be avoided wherever possible (see FIGURE 49) and the wiring layout should aim for capacitive isolation of high dV/dt points in the circuits (see 6.6.1).

Ideally, the transistor collector should be isolated from its grounded heat sink to prevent a ground loop of common-mode switching-frequency current. However, the capacitance between a TO-3 encapsulated transistor and its heat sink when a mica insulating washer is used is typically 100 pF. This may result in more conducted EMI than is permitted. One solution to this problem is to use transistors with better insulators such as beryllium. Another solution is to connect the heat sink to the transistor emitter or positive supply line. This ensures that the current in the collector-to-heat sink capacitance remains in the primary circuit and is prevented from flowing into the line via the ground connection. Another solution is to enclose the heat sink within a screen which is connected to the dc supply line. The optimum solution will depend on the electrical and mechanical details of the individual power supply. Also, isolated transistors are starting to be manufactured by some power transistor companies.

It will usually be necessary to enclose the power supply in an attenuating enclosure. For shielded enclosures to be effective, all leads entering or leaving the shield should be filtered to prevent them from conducting noise out of the shield. For lower frequencies, normal decoupling filters are adequate. At higher frequencies, however, special care must be taken to guarantee the effectiveness of the filter and the following filtering methods (see FIGURE 50) are recommended in reference 42:

- a. The use of feedthrough capacitors where the conductor passes through the shield: the mica or ceramic capacitor, with short leads, between the conductor and ground at the circuit end
- b. Shielding the conductor inside the enclosure to decrease the noise picked up by the conductor
- c. Obtain additional filtering with a π type filter using the feedthrough as one capacitor
- d. Further improve this π -filter by enclosing the choke in a separate shield inside the primary shield to prevent it from picking up noise.

In all the above filters the lead lengths on the capacitors and shield grounds must be kept short.

Although filtering of input and output leads is essential, packaging in a shielded enclosure may not always be necessary. Use of low EMI techniques may be sufficient to permit open-frame power supplies. Some newer techniques being used include the use of lossy ferrites in balun and other line inductors. A balun is a transformer used as a longitudinal choke (see FIGURES 51 and 52). It is also called a neutralizing transformer. A transformer connected in this manner presents a low impedance to the differential current and allows dc coupling. To any common-mode noise, however, the transformer is a high impedance. Thus the ground loop is broken without the use of an isolating transformer (see pages 71-76 of reference 42).

Another use for ferrites is as beads (see 6.5). Ferrite beads provide an inexpensive and convenient way to add high frequency resistive loss in a circuit without introducing power loss at dc and low frequencies. The beads are small and can be installed by slipping them over a component lead or conductor. They are most effective above one MHz and can provide high frequency decoupling, parasitic suppression and shielding. They are being used to damp out the high frequency oscillations generated by switching transients. If a single bead does not provide sufficient attenuation, two or three beads may be used. They are frequently used as part of an EMI LC filter. To reduce common-mode conducted emission, see FIGURE 53 where a mylar lossy capacitor is placed from each input and output lead to ground and the input and output leads are routed through ferrite beads (reference 45).

External EMI filters should be mounted close to the power supply. This will prevent external noise (for example computer noise) from entering the power supply.

To reduce EMI, some manufacturers physically divide the power supply into two parts - a high-power section and low power section - which are separated by shielding.

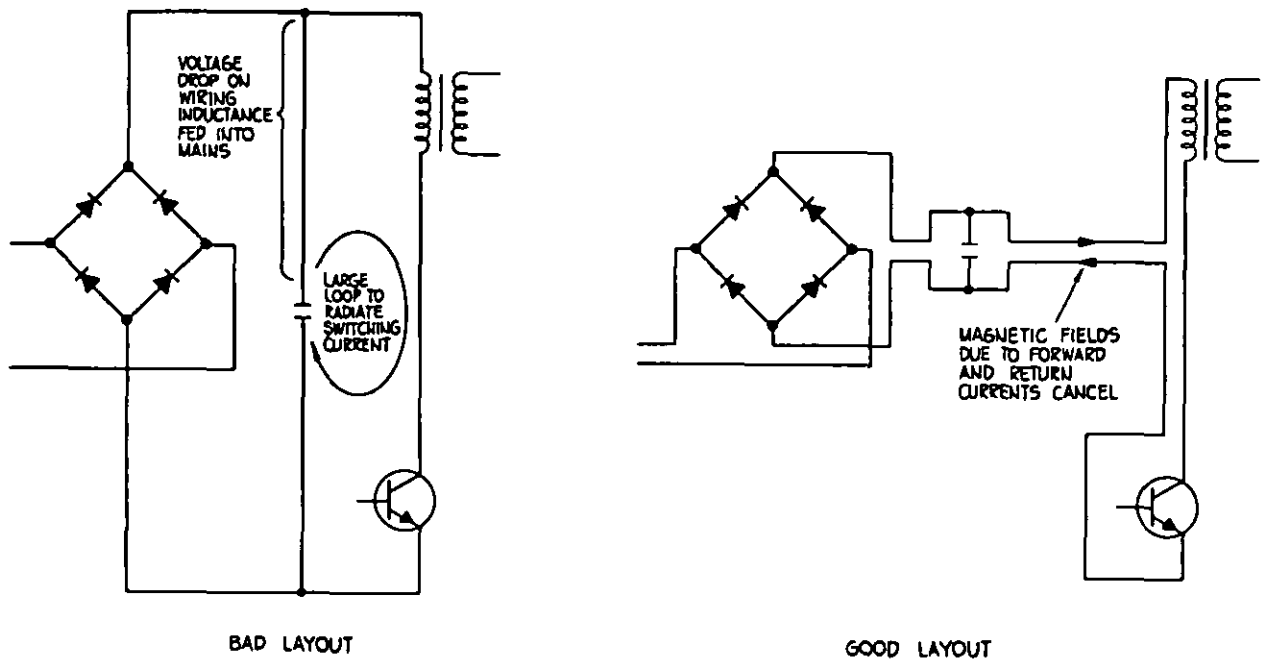


FIGURE 49. Examples of bad and good wiring layouts.

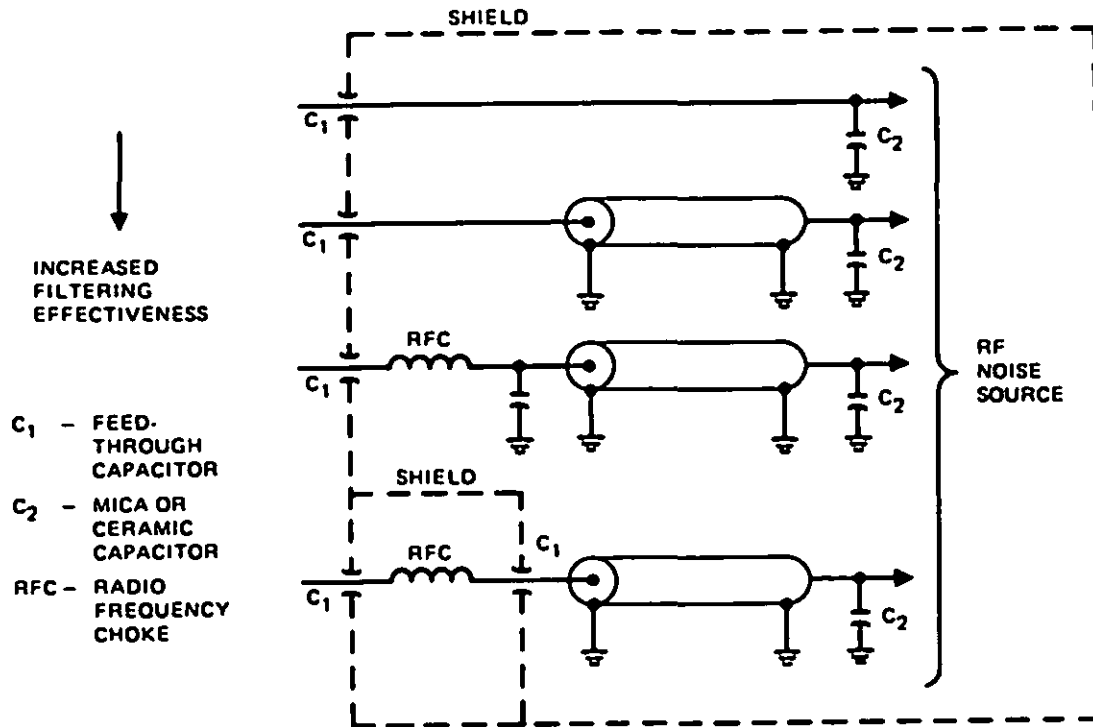


FIGURE 50. Four high frequency lead filtering methods.

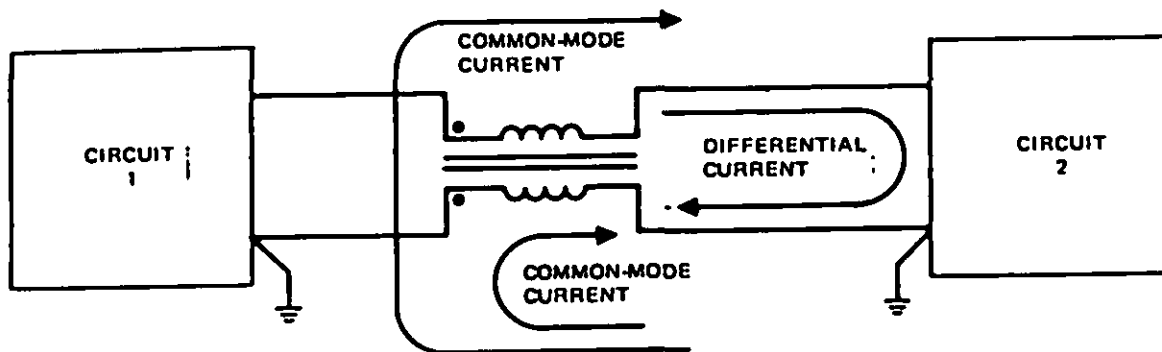


FIGURE 51. Balun or neutralizing transformer.

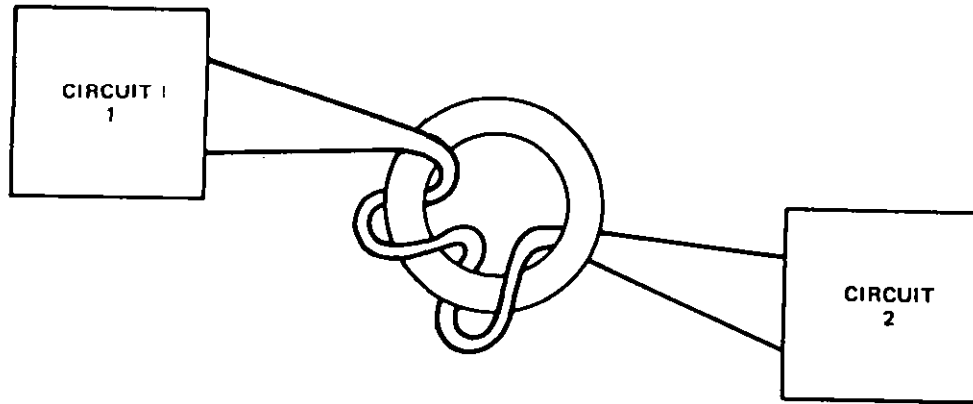


FIGURE 52. An easy way to wind a balun.

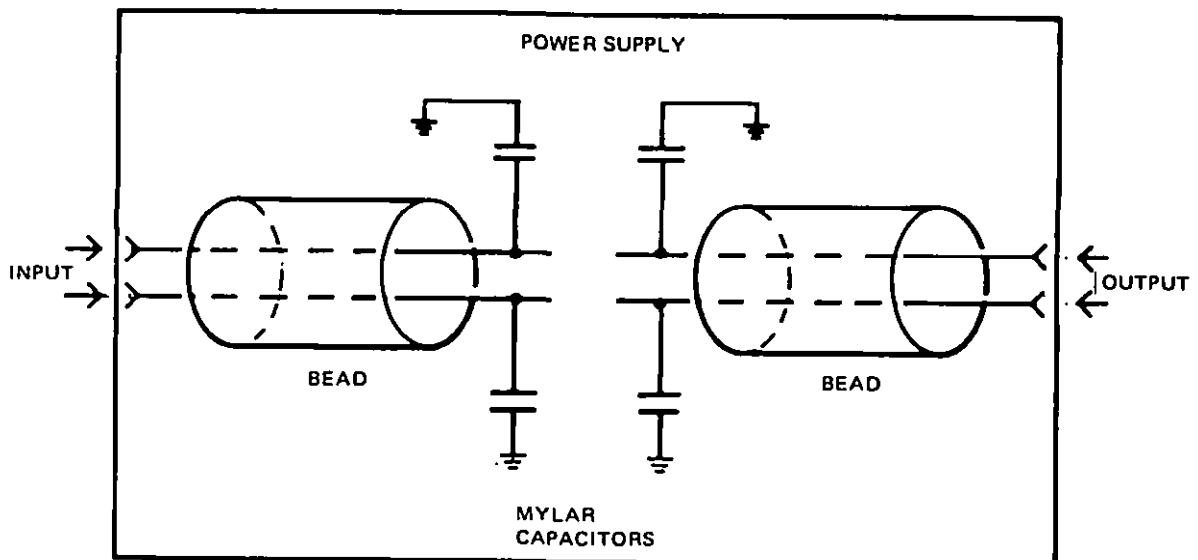


FIGURE 53. Input/output lead, capacitor filter.

5.4.4 EMI confinement techniques for transformers and inductors. Transformers, not being ideal, have capacitance between primary and secondary windings, and this allows noise coupling through the transformer. This coupling can be reduced by providing a properly grounded electrostatic, or Faraday, shield (a grounded conductor between the two windings). Inductors wound on closed magnetic cores (for example, toroidal) have less external magnetic field than open cores. If necessary, high-permeability magnetic shielding material can be used to confine the magnetic field from transformers and inductors. Magnetic coupling is minimized by the use of twisted leads. Reference 53 recommends quadrature placement of toroids in reference to adjacent toroids to minimize magnetic cross-coupling; and 90 degree orientation of high-level and low-level twisted pairs where they must cross.

5.5 Future low-noise designs--two major developments. A recently developed version of a cascaded optimum topology switching-mode power supply is a major breakthrough in reducing EMI (references 2 and 49). This novel converter has the same general conversion property (increase or decrease of the input dc voltage) as does the conventional buck-boost converter. However, its new optimum topology (maximum performance for minimum number of parts) results in reduced EMI, as well as higher efficiency, lower output voltage ripple, smaller size and weight, and excellent dynamic response. For example, as discussed in 3.3.5.2, in the Cuk converter the isolation transformer has no dc current component which makes it possible to minimize its size, loss and leakage inductance (less EMI). The converter, however is a sixth order system with real and complex zeros in the right-half plane; and therefore, requires skillful stabilizing procedures (see 3.3.4.3.3). The advent of MOS field effect transistors (FET) has made possible higher-switching-frequency (duty cycle) power supplies. Higher switching frequencies are easier to filter. Increasing the switching frequency can result in more attenuation for given size filter components (or smaller components for the same attenuation). The advantages of higher frequency operation are therefore as follows:

- a. Magnetics are simpler and should be less expensive to fabricate
- b. Ceramic and film (polycarbonate) capacitors replace electrolytics
- c. Decreased size and weight
- d. RFI filtering is simpler and one can now use commercial low pass EMI filters (usually ineffective at 20 kHz or 40 kHz) which begin to provide significant rejection as they approach 300 kHz.

The primary drawback--degraded efficiency due to increased switching losses--has been largely overcome by the application of MOSFET switching devices (reference 50). It is anticipated that as MOSFET technology matures, operation at 100 kHz and beyond will become much more commonplace (see 6.1.3).

5.6 Summary. Topics included in Section 5 are:

- a. Switching frequency fundamental and harmonics on the input power line can be sufficiently attenuated to be compatible with sensitive circuits.
- b. State-of-the-art switching-mode power supplies can be designed to meet the Navy CE03 limits for MIL-STD-461.
- c. Internally radiated noise is no longer a major problem. Noise reduction techniques must be used but they are being successfully used and information about them is available.
- d. Output ripple is an inherent characteristic of switching-mode power supplies. The most cost effective way to deal with intolerant sensitive analog circuits (usually only a few require very low ripple) is by adding a point-of-use regulator.
- e. A major breakthrough in reducing EMI is a recently developed optimum topology switching-mode power supply. Both the input and output current ripple at the switching frequency can be made essentially to vanish. Further development of resonant converters and MOSFET devices will also result in reduced EMI converters.

SECTION 6. COMPONENT AND CIRCUIT DESIGN CONSIDERATIONS.

Fundamental to power electronics is that lossless components must be used as circuit elements-- to do otherwise is too costly in terms of lost power. The lossless components are switches, inductors, capacitors, and transformers. The objective of power electronics design is to combine these four components in a topology and control the switches such that the system requirements are met (reference 55).

These lossless components all are subjected to either fast current changes or fast voltage changes, or both. As a result, they are potential generators of high frequency EMI (see APPENDIX D) unless consideration is given to preventing EMI from these lossless sources. The EMI may be generated as an external magnetic or electric field or may be coupled internally to other parts of the circuit via real or parasitic components. Information is presented here on the selection process for these lossless components to better understand how to prevent them from being a source of EMI.

6.1 Semiconductor switching devices. The switches in power conversion circuits today are solid-state semiconductors. Both current and voltage change rapidly and EMI can be induced during turn-on and turn-off. The power semiconductor marketplace is characterized by a growing variety of special components which offer to the user a high degree of flexibility in the design of electrical circuits and in the mechanical construction of equipment. All component manufacturers are trying to make their power devices faster and capable of handling more power. But a major emphasis is on packaging, to produce cheaper and more energy-efficient devices. This is especially true with industrial-power devices.

The switch is central to power electronics. Whatever can be achieved at any given time in power electronics is a strong function of the current state-of-the-art in switches. Solid-state thyristor switches with voltage ratings over 1 kV and current ratings over 1 kA are routine with ample margin to trade-off parameters to increase speed-of-operation or other parameters. This is a power maximum (Pmax) rating of over 1 megawatt in a single device. Transistors capable of switching up to the 100 kHz frequency band are routinely available in Pmax ratings of 10 kW to 20 kW. The Pmax figure-of-merit is defined as the ratio of output power to the peak-voltage and peak-current product of the amplifying device. It is a measure of how well a circuit utilizes the power handling capability of a device (reference 55).

Because of their different limiting capabilities, thyristors are generally used for the higher powered uses and transistors (both bipolar and MOSFETS) for the higher frequency requirements. However, thyristors are available for use up to 60 kHz and transistors, particularly MOSFETS, are increasing their power handling capability. Both monolithic and hybrid combinations are being manufactured to combine the advantages of individual types, often resulting in effective synergisms. These combinations include not only integrated Darlington (bipolar) connections but also MOSFET and bipolar transistors in a cascade configuration and a polyphase SCR topology with FET commutation (reference 54).

Much of the discussion that follows on thyristors and transistors (6.1.1 through 6.1.3) is taken from reference 55 and from a comprehensive report on the state-of-the-art of high power switching prepared by Texas Tech University (TTU) (reference 56).

TABLE VI lists the semiconductor switching devices discussed.

6.1.1 Solid-state thyristors. Various types of thyristors are discussed. Thyristor design involves a tradeoff between voltage rating, current rating and switching speed (both turn-on and turn-off). These tradeoffs are discussed in relation to the types of thyristors.

TABLE VI. Semiconductor switching devices.

- Thyristors — High power
- Bipolar transistors — High frequency
- MOSFETs — High frequency
- Bipolar Darlington
- Hybrid synergistic combinations
 - MOSFET & bipolar
 - SCR & FET
- Power diodes
 - Schottky — Low forward dissipation
 - Fast epitaxial — High reverse voltages
 - Diffused diodes — Various combinations of reverse voltage, forward voltage, & reverse recovery time

6.1.1.1 Types of thyristors. A thyristor, generally speaking, is a semiconductor whose switching action depends on regenerative feedback. It is a four-layer, three-terminal device, with connections to a cathode, an anode, and a control gate. A number of different types of thyristors have been reported: gate-triggered, light-triggered, laser triggered, non-reverse blocking, gate-assisted turn-off, gate turn-off, reverse-blocking diode, and field-controlled. (Field-controlled thyristors are not, strictly speaking, thyristors; they have no regenerative gain and do not latch on.)

The gate-triggered thyristor is the conventional silicon-controlled-rectifier (SCR) which is triggered on by an electrical pulse. Both forward and reverse blocking are obtained with this structure, but switching times are relatively long for large blocking voltages because of the amount of charge which must be injected into or extracted from the base regions during switching.

Light-triggered SCRs are similar to gate-triggered devices, but use a weak light pulse for triggering; light-triggering is useful for electrical isolation, but has no other obvious advantage over electrical triggering.

Laser triggering involves higher light energies; turn-on is probably obtained through a narrow region of very high carrier density (generated by the light pulse), which dissipates very low power, permitting high di/dt and high peak currents.

The non-reverse blocking thyristor (or reverse-conducting thyristor (RCT or ASCR) has an asymmetrical structure. One blocking junction has been eliminated, and voltage blocking takes place only in the forward direction. The charge-modulated volume is smaller than in the conventional SCR, so that faster switching is obtained.

A negative gate pulse is applied to assist turn-off in the gate-assisted turn-off thyristor (GATO) to help reduce switching times; however, anode current must be commutated.

The gate turn-off thyristor (GTO) does not require commutation; a reverse gate bias squeezes the conduction plasma into a high current filament which is pinched off.

The reverse blocking diode thyristor (RBDT) is essentially self-gated, using dv/dt switching.

Finally the field-controlled thyristor (FCT) is a modified vertical channel field-effect transistor containing a reverse blocking junction. In the on-state, the structure behaves like a p-i-n diode; when the gate is reverse-biased, the internal field distribution is such that the device is off.

6.1.1.2 Voltage (blocking voltage) and current ratings. The breakdown, and hence the blocking voltage, is controlled by the properties of the n-base, that is, by its doping and width, or by the character of the n-type surface near the center or the anode junctions. The blocking voltage itself is less than the breakdown voltage.

Most thyristors are designed around the bulk breakdown voltage of the n-region. The base width must be increased as the blocking voltage is increased. However, the dynamic properties of the thyristor (such as turn-off time) degrade with increasing base width, so that a compromise between blocking voltage and other thyristor characteristics is required.

The carrier concentration of the n-base is established by the resistivity of the thyristor starting material. Resistivity variations occur from wafer to wafer, and radially across individual wafers themselves. For large area high current devices, such variations must be compensated for by making the n-base wide. Such a worst-case design results in a large variation in breakdown voltage for a given base width, affecting yield, and degrading the dynamic performance of the thyristor at a given breakdown voltage. However, this problem has recently been circumvented by the introduction of the technique of neutron doping.

SCR forward current is usually limited by thermal constraints and is essentially limited by the product of current-squared and resistance until the current densities approach several hundred and several thousand amperes per square centimeter.

6.1.1.3 Turn-on and di/dt. The rate at which a device turns on depends on the amount of current which can safely flow through the small region where switching is initiated. In the center gated thyristors, only a small part of the device immediately adjacent to the gate electrode turns on. A considerable time may elapse before the entire cathode area turns on, and during this time, the entire anode current flows through only a small part of the total conducting area; at high values of di/dt, high power dissipation and localized heating can cause considerable damage to the device.

Laser triggered thyristors are a solution to slow turn on. The turn-on time can be many orders of magnitude greater than electrically turned on devices.

6.1.1.4 Recovery time (turn-off). A conventional SCR latches on, that is, remains on after the gate-trigger signal has been removed, and can be turned off only by interrupting the anode current (commutation). The turn-off time, that is, the time which must elapse before forward blocking capability is reestablished is usually long. The reapplication of a forward voltage while substantial charge still remains in the base regions will turn the device on again. Turn-off time is usually adjusted by introducing suitable impurities, such as gold, to reduce carrier lifetime; with gold-doping, turn-off times can be reduced to 10 μ s without seriously affecting other device parameters. However, if minority carrier lifetime is reduced excessively, forward voltage drops are increased, and leakage currents become large enough to affect leakage power dissipation.

Reverse conducting thyristors (RCT), or asymmetrical SCRs (ASCR), sacrifice reverse blocking capability to reduce the n-base width while maintaining forward blocking; forward voltage drop and turn-off time are thereby reduced. In developing the ASCR for high frequency applications, a basic SCR structure is gold doped for faster turn-off--which gives slower turn-on, greater forward drop, and decreased punch-through voltage. The n- region is then thinned--which speeds up turn-on, reduces forward drop, and reduces the blocking voltage. Then an additional n+ region is added--which increases the forward blocking voltage and reduces the reverse blocking voltage. In effect, the device has been speeded up keeping all other characteristics the same except reverse blocking voltage which is sacrificed.

6.1.2 Power bipolar transistors. A transistor is a semiconductor, opening and closing switch, whose switching action is controlled by the presence or absence of current flow through a p-n junction (the emitter-base junction). When the p-n junction is forward biased, and forward diode current flows, the switch is closed. The transistor is a three-layer three-terminal device, with connections to an emitter, a collector and a control base.

The principal design consideration for high power transistors is the standoff voltage, that is, the collector-base junction breakdown voltage. Starting resistivity, diffusion depths and base widths are all chosen with respect to the voltage requirements, and switching performance is affected by those choices. Fabrication processes are affected as well; device configurations must be consistent with high voltage operation.

6.1.2.1 Pulse current and gain. The current gain (the ratio of collector current to base current) of a transistor falls off considerably at high forward current densities. The net effect of high currents is a wider base width and gain fall-off at high currents.

Destructive effects at high currents are generally the result of high temperatures which follow the formation of current constructions. High forward current stability can be enhanced by interdigitation of the emitter and base contacts.

6.1.2.2 Delay and recovery. Delay and recovery effects in transistors are the result of junction depletion and charge storage capacitances. When a base signal is first applied, the emitter base depletion capacitance must be charged through the source output resistance and transistor input resistance before base current can flow. The charging time constant is the intrinsic delay time of the transistor, which, when added to the rise time of the collector current pulse, establishes the transistor switching delay time. As the base current increases, the transistor turns on, charge is stored in the base region as current flows. This stored charge represents an equivalent storage capacitance which must be charged up as the collector current increases, and which affects the rise time of the collector current pulse.

Switching delay time may be reduced by overdriving the base with base currents in excess of those required to sustain a given collector current, but such overdriving reduces the effective current gain and introduces excess charge to be stored in the base, increasing the collector current fall time, hence the recovery time.

Switching recovery time is determined by the storage capacitance, which must be completely discharged before the current pulse is off. The recovery time has two components: the storage time required to remove excess stored charge introduced into the base by base overdrive currents; and the pulse fall time, which corresponds to the removal of stored charge introduced by normal base drive.

The maximum value of di/dt is determined by the rise time of the collector current. The pulse rise time may be increased by base overdrive; however, inasmuch as the maximum pulse repetition rate depends on the recovery time, an increase in di/dt will be accompanied by a diminished maximum pulse repetition rate.

6.1.2.3 Breakdown voltage versus forward voltage. The introduction of a v-layer affects the output behavior of a transistor by increasing the breakdown voltage.

Although breakdown voltage is improved by introducing the v-region, the forward voltage in the on-state, typically several tenths of a volt, is also increased. Turn-on (delay) time is relatively high in quasi-saturation, so that power dissipation may be increased excessively during turn-on. It is possible, by increasing the base doping level, to reduce the final on-state voltage drop across the transistor and to reduce the delay time; but quasi-saturation effects are not eliminated, and turn-on times remain relatively high.

6.1.2.4 Life. The life of transistors is established generally by the same constraints which affect the life of thyristors. If a transistor is heat sunk well-enough, it is reasonable to expect a lifetime in the order of tens of years, providing that transient adiabatic heating is not so great as to cause catastrophic damage. Transistors, moreover, do not experience the pulsed thermal shocks which damage thyristors in which high currents are required to flow through small turned-on regions. A transistor with dimensions comparable to those typical for a thyristor inverter will turn-on in around 0.5 ns, the time required for the base signal to propagate across the base. Within the same period of time, approximately 0.001 percent of the total thyristor area will conduct. However, transistors can be driven into unstable operation relatively easily, particularly when switching inductive loads, and catastrophic failure can quickly result once a transistor has been driven into an unsafe power region.

This unstable operation is called secondary breakdown and is specified by at least four safe operating area (SOA) descriptions. Forward biased SOA is often exceeded during current overloads where the collector current goes beyond the product of the gain and base current product, or if a transformer saturates. Collector-base clamped SOA is a special case of forward biased SOA seen in ignition circuits and solenoid drivers. Unclamped reverse-biased SOA occurs when a device is forced into avalanche. Clamped reverse-biased SOA occurs in switching an inductive load with the collector current clamped to a voltage source.

Failure of the circuit to keep the transistor within the various SOA limits is one of the major failure modes of transistor switching circuits.

6.1.3 Power MOSFETs. The power MOSFET is a semiconductor opening and closing switch whose switching action is controlled by an electrical field applied across a semiconductor channel. It is a three terminal device with connections to the drain, source, and gate. Unlike thyristors and bipolar transistors, which are minority carrier devices, the power MOSFET is a majority carrier semiconductor device and has a fundamentally different construction and mode of operation. (The discussion of MOSFETs is mostly taken from reference 55).

The MOSFET is a voltage driven device as opposed to a bipolar transistor which is current driven. With no voltage applied between the gate and source electrodes, the impedance between the drain and source terminals is very high, and only a small leakage current, in the region of nanoamperes, flows in the drain.

The gate is isolated electrically from the body of the semiconductor by a layer of silicon oxide. When a voltage is applied between the gate and the source terminals, a field is formed in the p channel inverting it to an n channel and current flows from drain to source. The gate is still isolated from the source and no dc gate current flows.

6.1.3.1 Types. Power MOSFETs are of two basic construction types: surface groove MOS structures, with the trade names of V MOS and U MOS; and D MOS structures with the trade names of HEXFET, T MOS, Z MOS, SIPMOS and SUPERFET. High voltage, high current power MOSFETs are almost without exception D MOS structures. The major differences between surface groove and D MOS is the structure. The groove used in the surface structure makes it more susceptible to voltage breakdown above 100 V. Breakdown voltage is increased by rounding the bottom of the groove, hence the name U MOS. D MOS has a planar structure with no grooving, and consequently has a higher breakdown voltage--up to 1000 V.

6.1.3.2 Drain resistance versus breakdown voltage. The goal of all of the power MOSFET constructions is to parallel many channels to get low on-resistance. A single device may have a thousand parallel cells. The positive temperature coefficient allows successful paralleling of cells within the structure of individual devices. Unfortunately, the on-resistance is a strong function of breakdown voltage and increases exponentially (by a power of 2.3 to 2.7). The design issues for a power MOSFET is to make the shortest possible channel, to make the thinnest possible defect-free gate-insulator, to make the greatest possible channel-source periphery per unit area of chip, to minimize the gate input-capacitance consistent with a thin gate-insulator and large channel source periphery, and to minimize the series drain resistance consistent with the needed breakdown voltage.

6.1.3.3 Turn-on, turn-off and reliability. Power MOSFETs are fast for semiconductor devices. Devices with a 500 V, 10 A rating (P_{max} of 5 kW) have typical turn-on delays of 40 ns, rise times of 60 ns, turn-off delays of 200 ns, and fall times of 90 ns in standard test circuits. Special drive techniques can force faster times.

Devices appear to have excellent field reliability if: the gate is protected from overvoltage (the thin oxide insulator can be destroyed with any overvoltage, even spikes of nanosecond duration and minimal energy content), the drain to source voltage is not exceeded; and the heat sinking and application keeps the device out of a narrow region susceptible to thermal runaway. The device has no secondary breakdown problems. Designers observing the above precautions reported that they have yet to lose a MOSFET in development projects where they would expect to lose dozens of bipolar devices during the development stage. However, some MOSFETs do have finite energy capability requiring care if switching an inductive load.

Power MOSFETs have just begun to be widely used since they are more expensive at present than bipolar devices with similar P_{max} ratings. They have proven to be excellent drivers for high power bipolar and thyristor devices.

6.1.4 Power diodes. Power diodes are ac to dc rectifiers in power supplies, and if the power supply is a switching-mode type, then diodes are also used as commutating (free-wheeling or catch) diodes. At the present time, the following types are available:

- a. Schottky diodes with up to 60 V reverse voltage, low forward dissipation and extremely short switching time.
- b. Fast epitaxial diodes with reverse voltages up to 300 V.
- c. Diffused diodes in various combinations of reverse voltage and recovery time, and forward voltage.
- d. Diffused diodes with a specified recovery current waveform (soft recovery).

6.1.4.1 AC to dc rectifier diodes. In a low-voltage ac to dc rectifier, the forward voltage drop is important. So much so that a center-tapped transformer full-wave rectifier is often used instead of a full-wave bridge rectifier in order to eliminate one-half of the diode power losses. Of vital interest is the recovery characteristics of the diode, particularly when inductance is present in the source. Reactance of the input transformer, if one is used, can place a very high voltage-transient on the diode being commutated off if the diodes have snap-off recovery characteristic.

The Schottky diode, often used for rectification particularly in designs employing a full-wave diode, does have two severe limitations: a high leakage current above 100 degree centigrade junction temperature; and a low peak inverse voltage breakdown limit. The other types listed above are more applicable where higher reverse voltages are present.

6.1.4.2 Commutating switching frequency diodes. Selecting a rectifier diode for use in high frequency converter circuits involves a number of trade-offs and a number of circuit constraints must be considered. Many of these have been discussed by Fred Blatt (reference 57). In summary, the characteristics to be balanced include primarily: forward voltage (V_{FM}), reverse voltage (V_{RWM}), and reverse recovery time (t_{rr}). The Schottky barrier diode is generally regarded as the best choice for low voltage supplies (12 V or less) because of its extremely low forward voltage drop, which, coupled with its freedom from stored charge effects, yields a low loss rectifier circuit. However, presently available V_{RWM} is limited to about 60 V.

Recently, p-n junction devices (often made by a combination of ion-implantation and epitaxial technology) have been introduced which offer high speed and voltage ratings to 150 V, with forward drops somewhat lower than the ordinary fast recovery rectifier diodes. These diodes appear to warrant first consideration in supplies in the 10 V to 24 V range, particularly if voltage transients are a problem. The ordinary fast recovery device is often satisfactory in higher voltage supplies. Switching speed of any of these diodes is satisfactory from a rectifier efficiency point of view, if operation is not much over 20 kHz; but the slower the diode the higher the penalty, in terms of switching losses in the transistors, contrary to a demand for transistors with higher safe operating area.

6.2 Capacitors. The growth of switching-mode power supplies has spurred advances in capacitor development, particularly for the input and output filter capacitors.

In addition to its filtering function, the input capacitor for ac to dc power supplies must have sufficient capacitance to support the load during the period when the rectifier is non-conducting.

The output filter capacitor must also support the load during the non-conductive periods of the regulator and when substantial increases in the output current occur. However, since the discharge period is in microseconds rather than milliseconds, substantially smaller capacitance values are required. The capacitor must also be sufficiently large to absorb the energy transfer from the choke should the load decrease dramatically.

Because of advanced configurations (multitab, stack-foil, and four-wire) better foil-etching techniques, and new materials (such as nonaqueous electrolytes) aluminum and tantalum electrolytic capacitors now demonstrate lower equivalent-series inductances (ESL) and lower equivalent-series resistances (ESR) and pack higher CV products into a given case size.

Smaller capacitors (mica and ceramic) are also required for higher frequency filtering. Some of these take the form of feed-through construction.

6.2.1 Input and output filter capacitors. All capacitors have parasitic inductance and resistance. As shown in FIGURE 54, this forms a series-resonant circuit so that at frequencies below self-resonance, the capacitor is capacitive, and above self-resonance it is inductive. In general, larger valued capacitors have lower self-resonant frequencies. At 20 kHz an electrolytic capacitor is usually used for the output capacitor, with the size determined by the ESR needed for the ripple current. The result is that to obtain a low ESR the filter capacity may be much larger than is required for filtering. This large value of capacitance results in a very low self-resonant frequency.

The input capacitor is usually even a larger electrolytic (or bank of parallel electrolytics) again oversized--but for different reasons. One reason is to increase the hold up time should the input power be cut off. A second reason is oversized input capacitors are used is to compensate for a decrease of capacitance with increasing frequency. However, these large input capacitance values will cause high rectification harmonics to distort the input line unless sufficient inductance is part of the LC filter or unless one of the newer techniques are used, for example by switching-mode techniques to regulate the input current to follow the input sinusoidal voltage (see 4.5.2.2).

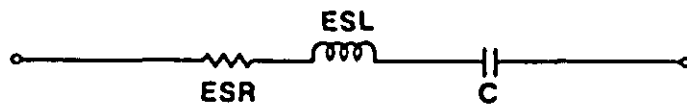


FIGURE 54. Capacitor ac equivalent circuit.

6.2.1.1 Electrolytic capacitors. Electrolytic capacitors are neither ideal nor frequency invariant. Typical low ESR/ESL aluminum electrolytic capacitors may lose about 15 percent to 50 percent capacitance from 120 Hz to 10 kHz, settling down to a high frequency value of less than 1 percent of the 120 Hz capacitance.

ESR also decreases with frequency but for low voltage capacitors increases again. (For example, a 6 V dc capacitor typically decreases with frequency about 40 percent from 120 Hz to a minimum near 1 MHz. The ESR then typically increases with frequency to within 25 percent of the 120 Hz value above 10 MHz).

ESL is relatively independent of frequency, but it depends enormously on the capacitor's construction (if designed for fast manufacturability, ESL typically runs more than 50 nH but low ESL aluminum electrolytic capacitors run between .5 nH and 15 nH). The net effect is to reduce the capacitor's attenuation ability at high frequencies. Above approximately 150 kHz the capacitor's ability to attenuate EMI depends almost entirely on ESL. A high voltage capacitor especially designed for low ESL (see 6.2.2.3) might be expected to provide two to six dB additional noise attenuation at 1 MHz and 18 dB at 150 kHz. Experimental results (in reference 38) using a 20 kHz power supply drawing 3 amperes and a low ESL input capacitor resulted in conducted EMI values of 12 dB μ A 150 kHz, -15 dB μ A at 50 kHz, -16 dB μ A at 1 MHz, -26 dB μ A at 5 MHz, -30 dB μ A at 10 MHz, and -26 dB μ A at 30 MHz (these points are plotted in FIGURE 46).

ESR and capacitance decrease with increased frequency for those capacitors generally suited to switching regulator input filter applications (aluminum electrolytic, tantalum foil, tantalum wet slug, and solid aluminum) (reference 40). For example, it is common to find the capacitance or ESR of tantalum wet slug capacitors at 50 kHz equal to 50 percent of their 120 Hz rated values. The lowered capacitance results in a higher ripple voltage across the capacitor in the time domain (at the switching frequency). Referring to FIGURE 45 for the one stage filter, the frequency domain curves would be less steep because attenuation, v_2/v_1 at any frequency is

inversely proportional to a capacitive function, $1/(1 + j\omega RC + \omega^2 LC)$.

6.2.1.2 Plastic or ceramic input or output capacitors. Where capacitance values less than 50 μ fd are adequate for system performance (which is sometimes true even at 20 kHz) plastic dielectric capacitors offer much lower ESR losses, and long term stability over a wide temperature range (see C_2 in FIGURE 44). Polycarbonate and other film capacitors are used extensively in high frequency switching power supply applications and applications where substantial ac currents must be tolerated by the capacitor--high frequency power filtering and series resonant power conversion circuits, for example. For switching-mode power supplies operating at very high frequencies (for example, 200 kHz) either plastic film or ceramic capacitors are used. The ESR of a good film capacitor may be two orders of magnitude less than the best electrolytic. At 200 kHz the smaller capacity for a given ESR is an asset in that it raises the self-resonant frequency. As the current capability of the capacitor increases however, the self-resonant frequency goes down, and in high power designs a point is reached where the high frequency impedance is unacceptable. One circuit trick to beat this problem is to parallel small, high self-resonant-frequency capacitors in a low inductance structure. Another scheme is two different parallel capacitors as shown in FIGURE 55. Keep in mind that the effective ESL of the capacitor includes the leads and mounting arrangement, so that a capacitor that stands up from a non-ground plane board may have a much lower resonant frequency than the same capacitor mounted close on a ground plane board with minimum lead lengths and the outer foil grounded to the ground plane board (reference 58).

6.2.2 Capacitor type descriptions. Aluminum and tantalum electrolytic capacitors are described, and their performance properties are compared particularly for power supply needs. Mica and ceramic capacitors are described including feed-through types.

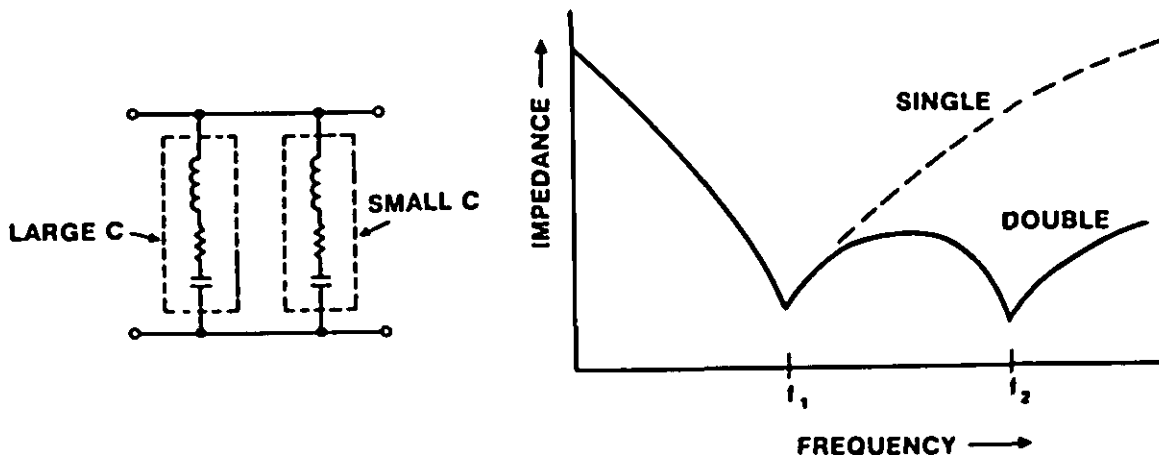


FIGURE 55. Compound capacitor.

6.2.2.1 Aluminum versus tantalum electrolytics. Aluminum electrolytic capacitors have finite lives, and present serious temperature limitations; their ESL and ESR, working-voltage, surge-voltage, ripple-current, and leakage-current capabilities all need improvement. Nevertheless, these capacitors provide by far the bulk of the ripple filtering in switching power supplies and dominate other switcher-capacitor needs because--so far--they cannot be beaten in providing a high capacitance per dollar along with a high CV product per unit volume.

Moreover, aluminum electrolytics can be very suitable for the switcher-filter market if they are designed with minimum impedance (see 6.2.2.3). A major drawback of electrolytic capacitors, particularly the aluminum types, is their finite (but predictable) operating and shelf lives. By contrast paper, mica, ceramic, and film capacitors--the electrostatic varieties--have indefinite lives, barring catastrophic problems. Tantalum types have substantially longer lives than equivalent aluminum types, but in either case, the working conditions--working and surge voltages, operating temperature, and ripple current--are the ultimate arbiters of electrolytic-capacitor life. The closer each of these factors gets to the capacitor's limits, the shorter its life. For a given set of working conditions and capacitor quality, the larger unit is likely to live the longest.

For more exacting needs, tantalum is one of the more expensive materials applied to electrolytics. But for its much higher cost, a tantalum-oxide dielectric offers a much higher dielectric constant than aluminum oxide; therefore, much smaller capacitors can be built with tantalum for a given CV product. The anode of a tantalum capacitor can be made of foil or sintered tantalum material. The electrolyte can consist of a dry solid-semiconductor material, such as manganese dioxide, instead of a gel (wet unit). But each new technique or ingredient exacts a price. Solid-tantalum capacitors have low internal inductance and resistance, and thus don't resonate until well beyond 1 MHz.

In fact, solid-tantalum electrolytics offer specifications that no single aluminum electrolytic can beat in every respect. However, individual tantalum specifications can be challenged by specific aluminum units. For instance, small size, always one of the primary tantalum advantages, is now characteristic of some aluminum units.

The dc-leakage, life, and ripple-current handling of aluminum units generally are not as good as those of tantalum units. Some larger aluminum units, however, can match the leakage, and still others can compete in ripple-current handling, but none can simultaneously offer a long life span (2000 hours at 85 degrees C for the tantalum 1000 h for the aluminum) and as small a size. In operating temperatures, some aluminums can beat the tantalytics--but the aluminum is larger, it leaks more, and loses more power.

Stability is one characteristic of tantalum devices that no aluminum can match, especially when the electrolytic tantalum capacitor has a solid anode. Reliability is also unmatched, but tantalum working-voltage ratings are limited--to 50 V. Aluminum-electrolytics easily attain higher working voltage.

Differences exist even between different tantalum capacitors. Wet-electrolytic units can be built smaller for a given CV product than solid-electrolytic units. Unfortunately, the tantalum wets are not quite as reliable as tantalum solids.

Where very high capacitance is necessary, as in the filter circuits of large power supplies, the designer does not have a choice between aluminum and tantalum; only aluminum capacitors are made with sufficient CV product. Considerable effort has been spent in improving the large aluminum electrolytics.

The result is that the good grades are quite good. ESR is amazingly low, as low as one milliohm near resonance for some types. Temperature range can reach -55°C and +105°C. Controlled values of both ESR and capacitance are possible.

6.2.2.2 Controlled ESR and ESL. The necessity for filtering the outputs of switched-mode power supplies has led to the requirement not only for very low ESR and ESL at frequencies between 10 kHz and 50 kHz, but for controlled values of these characteristics. The output filter is part of the control loop, so the loop designer needs to know with some degree of precision what the output impedance will be, else he will have difficulty designing a stable loop. It is now possible to control capacitance to within 20 percent and ESR within 30 percent.

6.2.2.3 Minimal ESR and ESL. There are several ways to minimize ESR and ESL. One is to bring out multiple tabs connecting to each electrode foil at several points in the roll (see FIGURE 56b). Connecting the tabs together yields a low-inductance, low-resistance link to the terminals.

The stacked-foil capacitor represents another approach (see FIGURE 56D). In aluminum stacked-foil capacitors, the result is achieved a little differently than in films. For example, several rolled capacitors are placed in parallel. Each roll is a flattened cylinder. The anode foil protrudes on the other side. All the anode-foil edges are welded together, as are all the cathode-foil edges. Each weld is connected to a broad strip conductor, terminating on the outside of the can. The profusion of parallel paths through the capacitor results in low ESR in the milliohms range and ESL to less than 2 nanohenrys.

Still another method of achieving low effective inductance and minimizing the ESR is the four-terminal capacitor, an axial unit with both an input and output at each end (see FIGURE 56C). Load current flows in at one end, through the length of the anode electrode and out the other end, thence through the load and back through the length of the cathode electrode in the reverse direction. Since the current paths in the two directions lie very close together through the capacitor, the magnetic fluxes due to the currents cancel quite well and the net inductance is small (less than 1 nanohenry is possible).

Stacked-foil and four-terminal capacitors exhibit impedance curves that are flat over a frequency range of two decades or more; in this range the inductive reactance is equal to or less than the ESR. More conventional electrolytics have an impedance minimum that covers about a decade (see FIGURE 56).

6.2.2.4 Mica and ceramic. Mica and ceramic capacitors of small values are useful for higher frequencies and up to about 200 MHz. A capacitor of flat construction, if the capacitor plates are round as in a ceramic disc capacitor, will remain effective to higher frequencies than one of the square or rectangular construction.

Other factors must be considered in selecting ceramic filter capacitors. A ceramic capacitor element is affected by operating voltage, current, frequency, age, and ambient temperature. The amount the capacity varies from its nominal value is determined by the composition of the ceramic dielectric. The dielectric composition can be adjusted to obtain a desired characteristic such as negative temperature or zero temperature coefficient, or minimum size. In obtaining one characteristic, other characteristics may become undesirable for certain applications. For example, when the dielectric composition is adjusted to produce minimum size capacitors, the voltage characteristic may become negative to the extent that 50 percent capacity exists at full operating voltage, and full ambient temperature may cause an additional sizeable reduction in capacity. Also, from the time of firing of the ceramic, the dielectric constant may decrease; after 1000 hours, the capacitance may be as low as 75 percent of the original value. The designer should make ceramic capacitor selection based on required capacity under the most adverse operating conditions, taking into account aging effects.

Capacitors of short-lead construction, and feed-through capacitors, are three-terminal capacitors designed to reduce inherent end lead inductances. Theoretical insertion loss of three-terminal capacitors is the same as for an ideal two-terminal capacitor. However, the insertion loss of a practical three-terminal capacitor follows the ideal curve much more closely than does a two-terminal capacitor. The useful frequency range of a feed-through capacitor is improved further by its case construction enabling a bulkhead or shield to isolate the input and output terminals from each other.

Capacitor selection for shunt capacitive filters, or any other filter application, is determined in part by the voltage, temperature, and frequency range in which the filter must operate. For 28 Vdc applications, capacitors rated at 100 working volts dc (WVdc) are adequate. Metallized mylar capacitors offer the most compact design and good reliability. Their dissipation factor is very low, and lead length can generally be kept short to improve high frequency performance. For high voltage dc applications, ceramic capacitors are available with capacitances as great as 16,000 pF at 6000 volts dc.

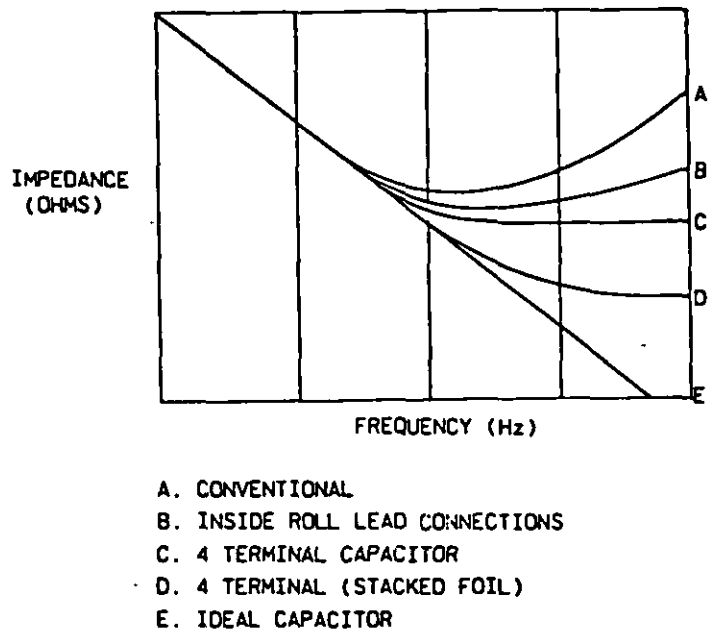


FIGURE 56. Capacitor response characteristics.

6.2.3 Capacitor paralleling and mounting. It often occurs that because of their large physical size, electrolytic capacitors may be located some distance from their associated working components (diodes, resistors, and so forth). This necessitates long interconnecting leads on printed circuit (PC) boards or between subassemblies, and these leads usually carry high circulating currents. In addition to the wiring loops (and H fields) thereby created, the effective ESL of the capacitor is increased from its inherent ESL (see FIGURE 54) and the resonant frequency is even further decreased. These effects can be reduced by placing a ceramic capacitor in parallel with the electrolytic capacitor, but physically located on the PC board near the associated components (see FIGURE 55).

However, not all ceramic dielectrics have low losses, particularly those with the highest K, so some care must be exercised in selecting ceramic capacitors (reference 58).

It is important when paralleling these capacitors to use very short leads for the high frequency capacitor so it is really capacitive, keeping f_2 in FIGURE 55 resonant at a high frequency. The following rules are therefore recommended:

a. Capacitor leads should be kept as short as possible. When mounted on a PC board, the PC tracks become, in effect, an extension of the capacitor leads increasing the ESL of the capacitor.

b. Paralleling two capacitors to cancel long lead length effects, keep the leads to the smaller high frequency capacitor as short as possible.

In addition, the following procedures are also recommended:

c. The outside foil of a capacitor may be indicated either by a negative sign, a wide band printed on the casing, or by a drop of solder on that particular lead. This lead should be directed towards the lowest ac impedance to circuit ground.

d. The ground return lead for chassis-mounted capacitors can be twisted with the hot lead, if the wires are insulated, to reduce magnetic field emissions.

e. A capacitor should be mounted at right angles axially, with respect to another capacitor or element, in order to reduce interaction effects.

6.2.4 Soft start. The input filter capacitor may create a potential problem--high inrush current. If it is intentionally chosen for high storage capacity and low ESR, it behaves like a nearly perfect short circuit when the power supply first turns on (unless considerable inductance is included in the input filter). The short-duration peak inrush current can destroy the input rectifiers and still lack sufficient energy to open protective fuses or circuit breakers.

To deal with this problem, many designs incorporate circuits that include either a thermistor or a series resistor that is effectively shorted out by a triac or SCR after the turn-on surge has subsided.

6.3 Inductors. To design an inductor one selects the size and type of core, the core material, the wire size and number of turns, and the optimum design permeability. Generally, the size and weight of the conductor is determined by the power capabilities desired of the inductor. The size and weight of the inductor core is determined by the peak energy storage requirements of the inductor. The size and weight vary as the square of the peak current times the inductance divided by the core permeability, provided there is space in the core window for the required number of turns with the wire size needed to keep the winding resistance within limits. Toroidal inductors have been optimally designed for either minimum weight or minimum loss. Leakage and magnetic shielding requirements depend on the core material and construction. Coupling of multiple output inductors affect regulation and other parameters of power supplies.

Many switching regulator topologies require one or more inductors for the output filter. Also, as discussed in Section 3, the input filter should include one, and preferably more, inductors. The choice of core material for these inductors is determined by design considerations such as power level, frequency, size, and loss. Tape wound bulk metals, powdered iron, ferrites, and the newer amorphous metal have different magnetic and loss characteristics and are used in various core shapes. Where skin effect becomes pronounced, at frequencies above 100 kHz (and

lower frequencies at high power), Litz, multifilar magnet, or copper ribbon provide lower ac resistance (Litz wire is essentially multifilar magnet wire that has been braided to further equalize the current distribution). Additional inductors may be used in balun configuration to diminish common-mode EMI, and ferrite beads may be used to diminish high frequency EMI.

If better methods are not used to eliminate rectification harmonics (power line frequency harmonics) it may be necessary to use large inductors as part of a filter to reduce one or more of these harmonics (see Section 3).

6.3.1 Material (core) considerations. (The discussion in this section is excerpted from a paper by S. Cuk, pages 292-309 of reference 2.) The magnetic field has associated with it two vector quantities. One, the field strength H , is directly related to the electric current which produced the magnetic field. The other, the flux density B , is directly related to the effects of the field (mechanical forces, electric voltages). The ratio of B divided by H is termed permeability, μ . Certain materials are able to augment the effects of the H field and result in higher B for a given H compared to free space. However, this rapid increase of flux density stops at a value of B called saturation flux density, B_{sat} . These materials are ferromagnetic and the B_{sat} has a direct bearing on the size and weight of the magnetic components. It may vary from 0.3 tesla for ferrite materials (mixture of $MnFeO_4$ with $ZnFeO_4$) to better than 2T for pure iron. The intermediate range is covered by alloys of iron and the other two materials, nickel and cobalt. FIGURE 57 illustrates the high permeability and saturation of ferromagnetic materials compared to the permeability of free space. Beyond the saturation point ferromagnetic effects no longer occur and the permeability returns to the free space value.

Ferromagnetic materials are frequently classified as either square-loop or linear and this is shown in FIGURE 58. In some materials such as silicon iron (3 percent Si, 97 percent Fe), Orthonol (50 percent Ni, 50 percent Fe), Permendur (50 percent Co, 50 percent Fe), even a very small field strength can cause saturation and usually the saturation flux density will be high. These are termed square-loop materials. In other materials such as ferrite (MnZn alloy) the flux density is gradual such that a distinct linear region is visible before saturation is reached and the saturation flux density will be lower. These materials are termed linear. These magnetization characteristics are further compounded by the fact that the $B-H$ characteristic is double-valued, exhibiting hysteresis loop behavior (see FIGURE 58). Furthermore the static losses are directly associated with the area of $B-H$ loop at a given frequency, while the dynamic losses include additional core loss at higher frequencies resulting in a widening of the $B-H$ loop.

An air gap is frequently part of the core design and it is important from an EMI point of view since depending on how it is constructed it may cause significant magnetic radiation. Air gaps permit higher peak inductor currents before core saturation is reached, but at the sacrifice of reducing inductance. FIGURE 59 shows this. The $B-H$ material properties with its μ slope can be scaled by geometric factors (cross-section, magnetic path length, and turns ratio) to obtain the coordinates shown in FIGURE 59 where the slope is now inductance L , the ordinate is now turns ratio N multiplied by flux ϕ , and the abscissa is the current i . Higher DC currents are now possible. Another example of a magnetic circuit with air gap is shown in FIGURE 60 which not only changes the slope but also changes the shape. One core configuration for achieving this magnetic characteristic is an EI core with only one outer leg gapped. The flux first follows the ungapped loop until this leg saturates. Then the flux chooses the alternative lower reluctance path through the gapped leg and, finally the gapped leg saturates as seen in the third slope. Thus high L is available for lower currents and saturation is extended to higher current values. (This is sometimes termed a Swinging Choke and can also be achieved with other configurations, for example, two inductors or cores with different permeabilities and saturation levels.) The composite core is useful for large dc load variations, and for prevention of transient saturation of transformers in switching regulators. Composite cores with different losses as well as different permeabilities are used to damp high frequency oscillations as explained in 6.3.3.

The introduction of the air gap into square-loop cores has the effect of linearizing the permeability μ . It is often referred to as a shearing over of the square-loop $B-H$ characteristic into the linear one, although the material properties are still unchanged. However, in some cases, powdered iron is mixed with some nonmagnetic material to introduce a distributed air gap, which produces an equivalent slope μ_{eff} usually referred to in manufacturer's data sheets.

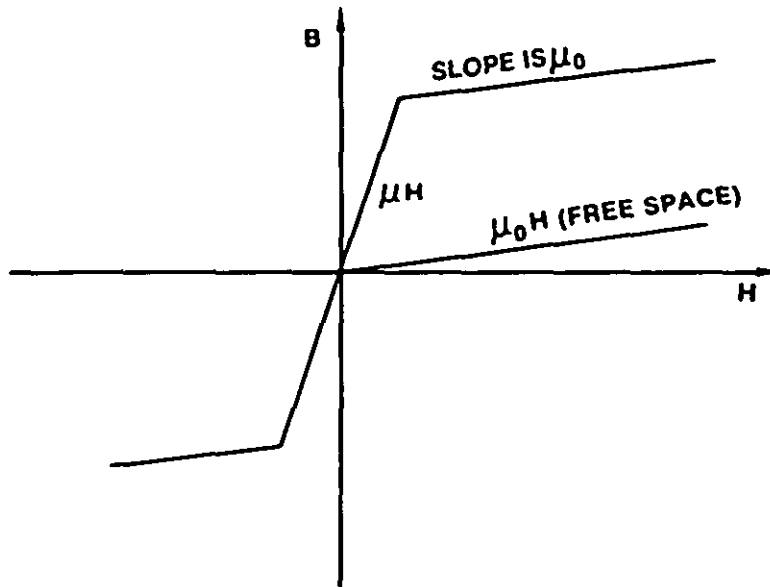


FIGURE 57. Two features of ferromagnetic materials: high permeability μ (steep slope on a B-H curve) and saturation (slope is free space μ_0).

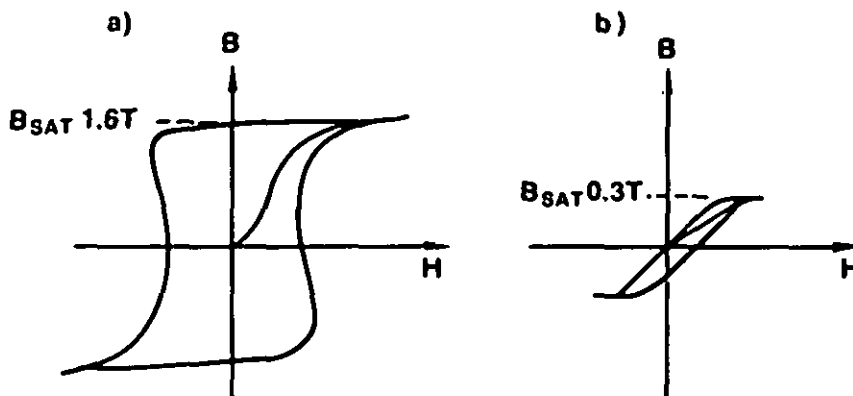


FIGURE 58. Double valued B-H loop characteristics of square (a) and linear (b) materials

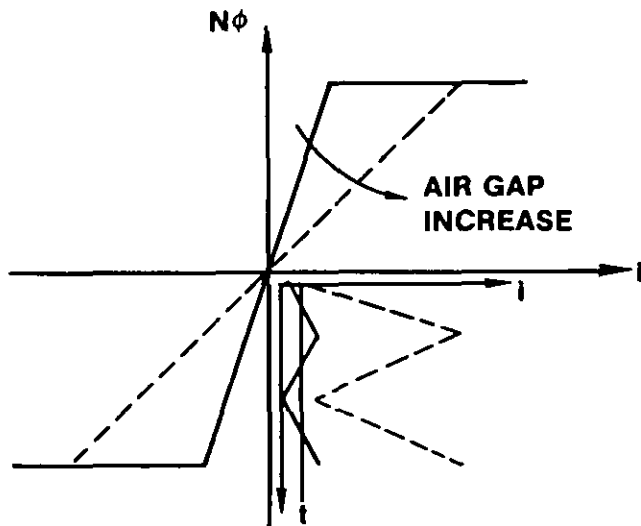


FIGURE 59. Increase of air gap increases dc current capability of the inductor.

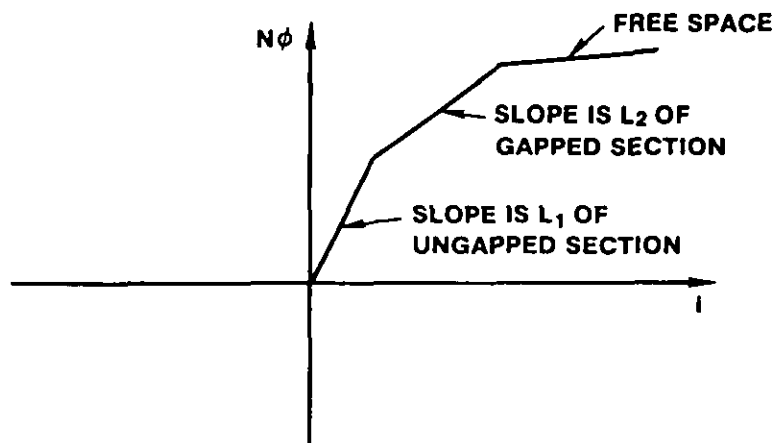


FIGURE 60. Composite core with gapped and ungapped sections eliminates core saturation problems and keeps high inductance (L) at lower current (i).

6.3.2 Leakage and magnetic shielding. As discussed in 6.3.1, air gaps in the form of open magnetic core inductors are likely to result in magnetic leakage and, therefore, may cause magnetic field interference. Closed magnetic cores including distributed air gaps have much reduced magnetic field since nearly all the flux remains in the core. To diminish the leakage the following configurations are recommended:

- a. Use toroidal cores with distributed air gaps or pot core construction. They will produce the minimum leakage. In pot cores the gap is well shielded by the core.
- b. Wherever possible windings should cover the entire core. Air gaps should be located inside the coil windings, and preferably at the center of the coil length.
- c. Gap the center leg if core has a center leg.
- d. Use the smallest gap possible. This has the added advantage of increasing L and using less core material.
- e. Orient the inductor so that the flux lines are farthest from the power supply cabinet.
- f. If necessary, shield the inductor, using one or more layers of magnetic shielding (see 6.10 on shielding). Magnetically shielding the inductor may make it unnecessary to magnetically shield the entire power supply and prevent the field from interfering with other parts of the power supply.

6.3.3 Capacitive effects. Inductors are not ideal and in addition to resistance they also exhibit capacitive effects between coil windings. There will, therefore, be a resonant frequency associated with each inductor giving rise to possible ringing. It is desirable to decrease this capacitance and thereby extend the resonant frequency and extend the inductive effect to as high a frequency as possible. There are a number of winding techniques that can be used to decrease this capacitance: single layer spaced turns, minimizing the winding to core capacity by wrapping the core with a low K dielectric, and bank winding. For example, for a toroid the following procedure will result in less C. The wire is wound back and forth building up layers over a 180 degree section of the coil until half of the turns have been wound. The coil is then turned over and the same routine is again used to wind the second half of the turns. The two half coils are tied together by the beginning leads and the terminals of the inductor are the end leads of the individual halves. FIGURE 61B depicts this for the first layer of winding. Smaller sections can be used. FIGURE 61C shows a first layer of winding for 90 degree sections. This construction results in lower voltage differences between layers. At very high switching frequencies (over 100 kHz) there is a limit to how high the self-resonant frequency can be pushed and it is usually necessary to use multisection filters.

The resonant frequency resulting from the parasitic capacitance can give rise to high frequency oscillations (ringing) particularly under discontinuous mode operation (low load). Reference 60 describes a composite core inductor which damps these resonant oscillations without the need for a damping circuit. This inductor is termed a soft inductor. Over most of its load operating range, the inductor operates much as any other inductor, but at low drive currents it presents a very low Q to ac signals with frequencies greater than the basic 10 kHz to 50 kHz switching rate (see FIGURE 62), thus damping out most low level ringing. Also, since the inductance swings quite high at low current levels, either discontinuous mode may be avoided or a lower ringout frequency will occur.

6.3.4 Optimally designed inductors. Three computer programs have been developed by TRW Defense and Space Systems Group, Redondo Beach, CA as part of the Modeling and Analysis of Power Processing Systems (MAPPS) project sponsored by NASA (references 36, 61, and 62). These optimally designed inductors are limited to toroidal cores. Toroidal cores, however, produce low EMI inductors. The programs' identification and brief description are as follows:

- a. INDOS1 - Optimum-Weight Inductor Design With Wire Size Predetermined
- b. INDOS2 - Optimum-Weight Inductor Design With a Given Loss Constraint
- c. INDOS3 - Optimum-Loss Inductor Design With a Given Weight Constraint

NOSC verified the derivation of the design equations based on Lagrange multipliers and also the usefulness of the programs. To verify that these programs are indeed useful NOSC designed inductors without and with the aid of the program. For each of the three optimum conditions, several inductors were first designed using procedures recommended in a commercial catalog (without using the programs). Then, for the same design requirements, the programs were used to design the inductors, and catalog cores were selected with dimensions close to the program values. For all nine inductors the results verified that the computer programs considerably shortened design time and produced better designs. The computer programs produced a lighter weight design (for INDOS1 and INDOS2) and a less lossy design (for INDOS3).

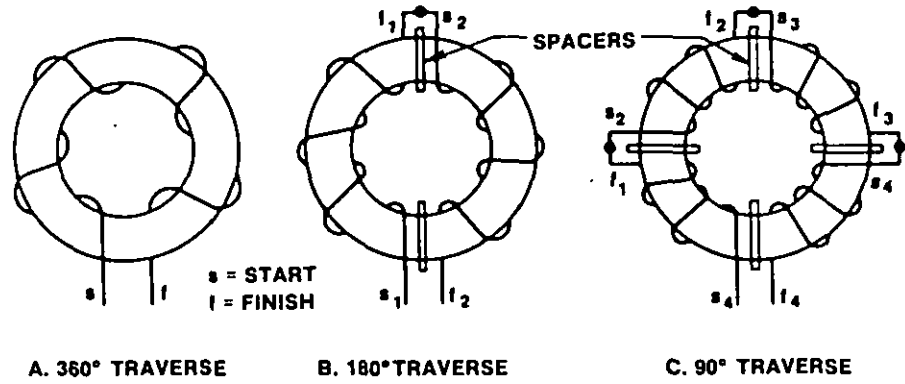


FIGURE 61. Methods of winding toroid cores depicting only the first layer of winding.

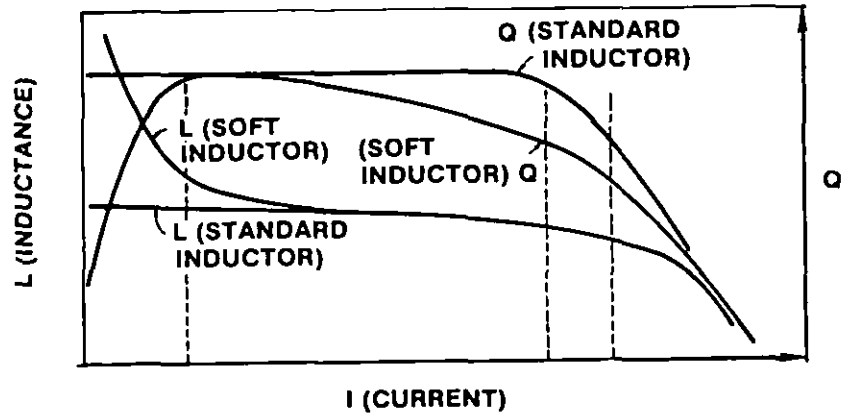


FIGURE 62. Soft inductor-composite core with variable inductance (L) and variable damping (Q).

6.3.5 Cross-noise in multi-output converters. In dc-to-dc converters with multi-output inductor coupling, noise generated in one of the multiple loads is transmitted to the other loads. Reference 63 calls it cross-noise and describes analytical and experimental work for a two-output buck-boost and a two-output forward (buck) converter.

In practical electronic systems, dc voltage sources of different voltage levels are frequently required. Multi-output power converters are an economical way to provide these different voltages but a noise problem appears. When a load such as a dc motor, a line printer or other noisy load is connected on one of the multiple outputs, the noise generated in this apparatus is transmitted to the other output terminals. The amount of cross-talk transmitted depends on how the multi-output converters are configured with respect to regulation. For multi-regulators (uncoupled) the cross-noise is low, but cross regulation types can produce considerable cross-noise.

For the buck converter, the cross regulation is performed by coupling the output inductors (see FIGURE 63). Experimental results (reference 63) showed that loose coupling of the output inductors suppressed the cross-noise by 55 dB to 65 dB from .1 MHz to 5 MHz compared to 35 dB to 45 dB suppression obtained with tight coupling over the same frequency range; and this was accomplished with only a little expense of the cross regulation characteristic. The output inductor was about 500 μ H and the leakage inductance was about 50 μ H. Loose coupling provided considerable suppression of the cross-noise without an additional noise filter.

6.4 Transformers. Designing transformers is similar to designing inductors with the added considerations of turns-ratio and the effects of leakage inductances and capacitances between primary and secondary windings. Transformers are used not only to change voltages but also to isolate segments of the power supply. Linear dissipative power supplies require transformers to be located in the 60 Hz or 400 Hz section of the power supply. These low frequency transformers are necessarily large and, therefore, high permeability cores are used to keep the size and weight as small as possible. Switching-mode power supplies can achieve isolation and voltage change at the switching frequency with smaller transformers, and the cores that perform best at these frequencies are lower in permeability but still considerably smaller and lighter than the 60 Hz or 400 Hz transformers.

6.4.1 Material (core) considerations. The discussion in 6.3.1 for inductors also applies here to transformers. Air gaps (either confined to one or more sections of the core or distributed through the core) are frequently used particularly if dc flows through the windings to increase dc current capability of the transformer (see FIGURE 59). It should be noted that one transformer-isolated basic topology (the Cuk-derived one) does not have dc flowing in the windings (as is true for the three other basic topologies) because the energy is transferred capacitively rather than magnetically (see FIGURE 17). Also for those topologies where the dc winding currents reverse permitting the core to be reset, air gaps may possibly be avoided (for example, bridge topologies, FIGURES 19, 20, and 21); although some gapping may be advisable due to not being able to perfectly match transistor properties resulting in imbalances causing transformer saturation (see 3.3.5.3d). The Cuk-derived converter has a true ac waveform (zero voltage average) and a core creep and eventual core saturation is avoided; permitting use of a smaller ungapped square-loop core with smaller leakage inductances (less potential EMI), and lower copper and core losses.

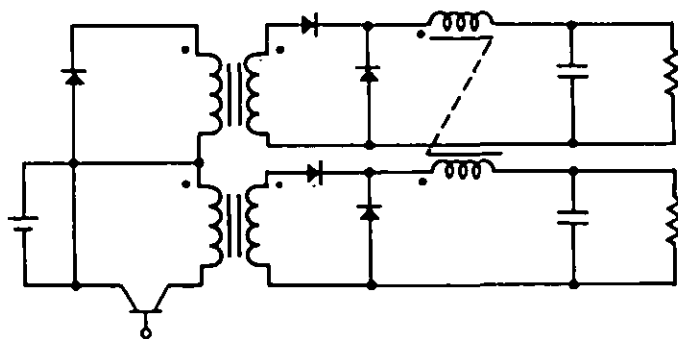


FIGURE 63. Two-output forward converter (buck) with output inductor coupling.

6.4.2 Capacitive effects and electric field shielding. Transformers, like inductors, have a primary self-winding capacitance and a secondary self-winding capacitance and the recommendations given in 6.3.3 to minimize these capacitances should be followed. In addition, transformers have capacitance between the primary and secondary windings, as shown in FIGURE 64, and this allows noise coupling through the transformer. Methods of minimizing primary to secondary capacitance are:

- a. Increase dielectric thickness
- b. Reduce winding width and thus reduce the area
- c. Increase number of layers
- d. Avoid large potential differences between winding sections, as the effect of capacitance is proportional to applied potential squared
- e. Use electrostatic (Faraday) shields

To decrease this capacitance by separating the primary and secondary windings is, of course, counter to the desirable coupling from the magnetic field, and thereby increases leakage inductance. In fact, leakage inductance and capacitance requirements may have to be compromised in practice since some corrective measures are opposites (see 6.4.3 on leakage inductance). A way that will have little effect on leakage inductance is to reduce the capacitive coupling by providing an electrostatic, or Faraday shield (a grounded conductor between the two windings), as shown in FIGURE 65. The single Faraday shield should be grounded at point B to prevent the noise from reaching the load since if the ground connection is made at point A the shield will be at the noise potential and can couple into the load through C2. Therefore, the transformer should be located near the load to simplify the connection between the shield and point B (reference 42).

Tests were performed on seven 115 V ac transformers to determine the effects of both single and triple electrostatic shields. The test procedures used were from MIL-T-27D, paragraph 4.8.11.11, for common-mode rejection, and paragraph 4.8.11.7 for differential-mode rejection. Results of the differential-mode test, from 100 Hz to 1 MHz, indicate the shield has little or no effect. The results of some of the common-mode tests are shown in FIGURES 66, 67, and 69. FIGURE 66 shows the common-mode rejection (typical) for a single shield transformer, with the shield grounded and disconnected--over 30 dB over the range 100 Hz to 1 MHz. FIGURE 67 shows the common-mode rejection for two similar transformers, one with a single shield and the other unshielded--over 25 dB over the range 100 Hz to 1 MHz. Even better common-mode rejection is obtainable when a three-shielded configuration (see FIGURE 68) is used; with the primary shield connected to the low side of the primary, the secondary shield connected to the low side of the secondary, and the central Faraday shield connected to the transformer outer case and to the safety ground. The results for this triple shield are shown in FIGURE 69 for the three shields connected and disconnected--with common-mode rejection so high it was well beyond the instrumentation range for frequencies up to 40 kHz and a minimum of over 30 dB at 1 MHz. At higher frequencies, the common-mode rejection is also dependent on the capacitance between the transformer terminals and the windings, and the terminals and ground.

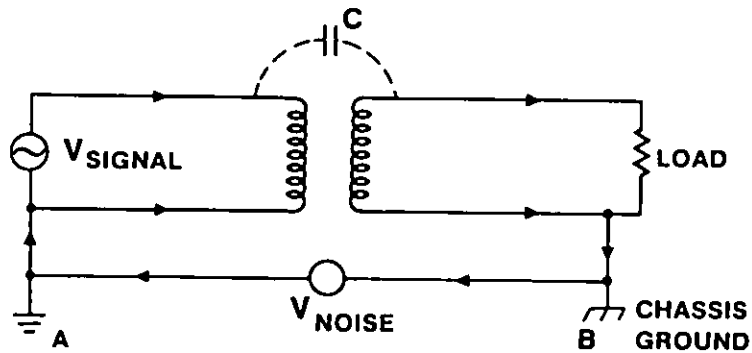


FIGURE 64. Transformer capacitive coupling transmits ground loop noise.

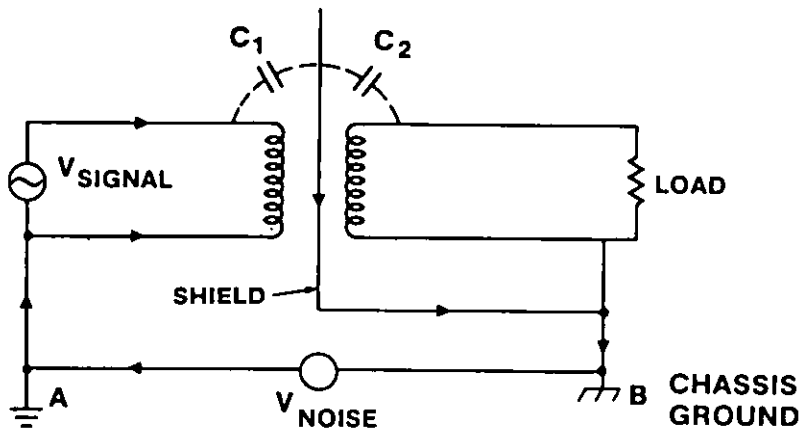


FIGURE 65. Grounded electrostatic shield between transformer windings (Faraday shield) breaks capacitive coupling.

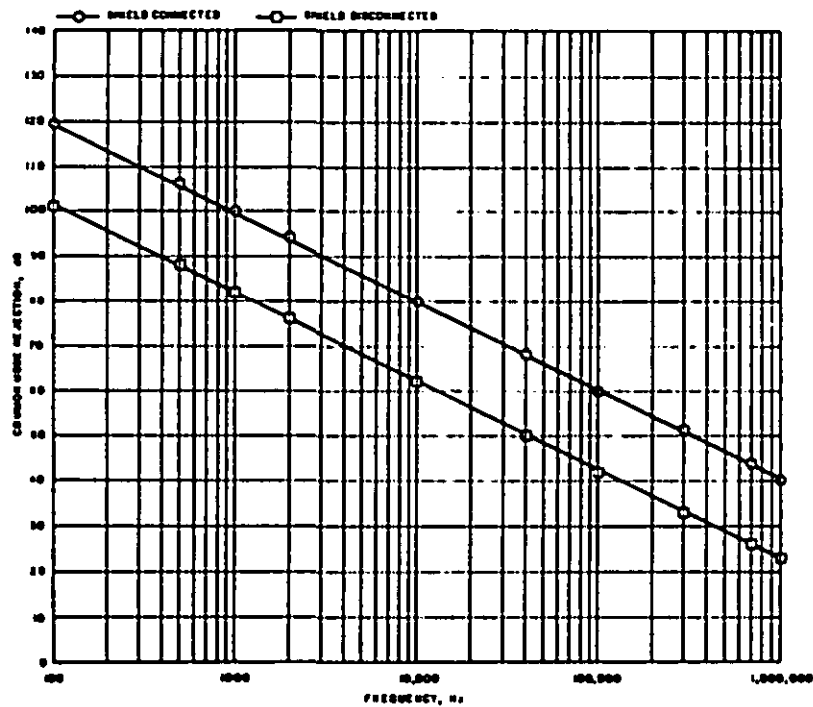


FIGURE 66. Typical common-mode attenuation obtained with a single electrostatic shield grounded (connected) and ungrounded (disconnected) for a 115 Vac transformer.

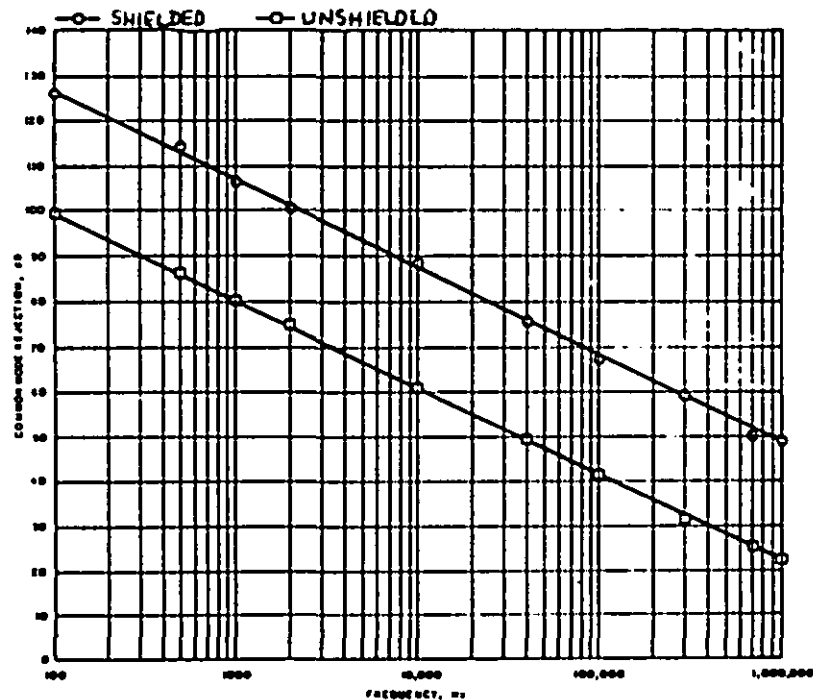


FIGURE 67. Common-mode attenuation obtained with two similar 115 Vac transformers, one unshielded and the other with an electrostatic shield connected.

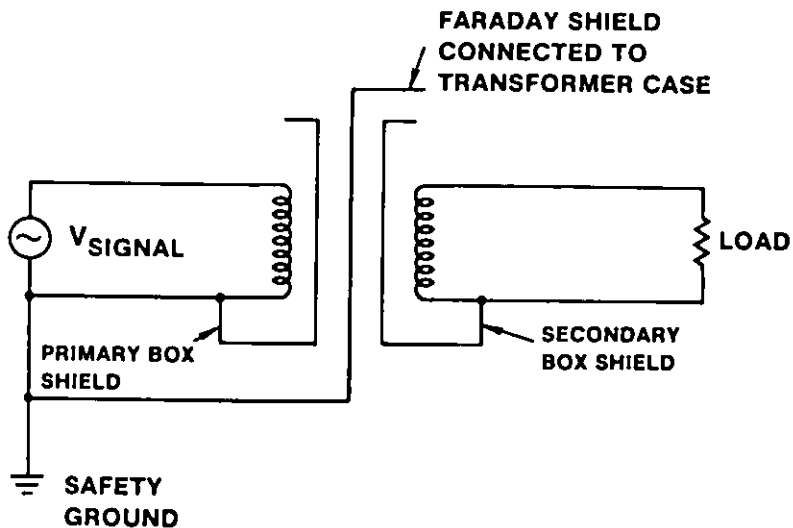


FIGURE 68. Transformer with three electrostatic shields between windings.

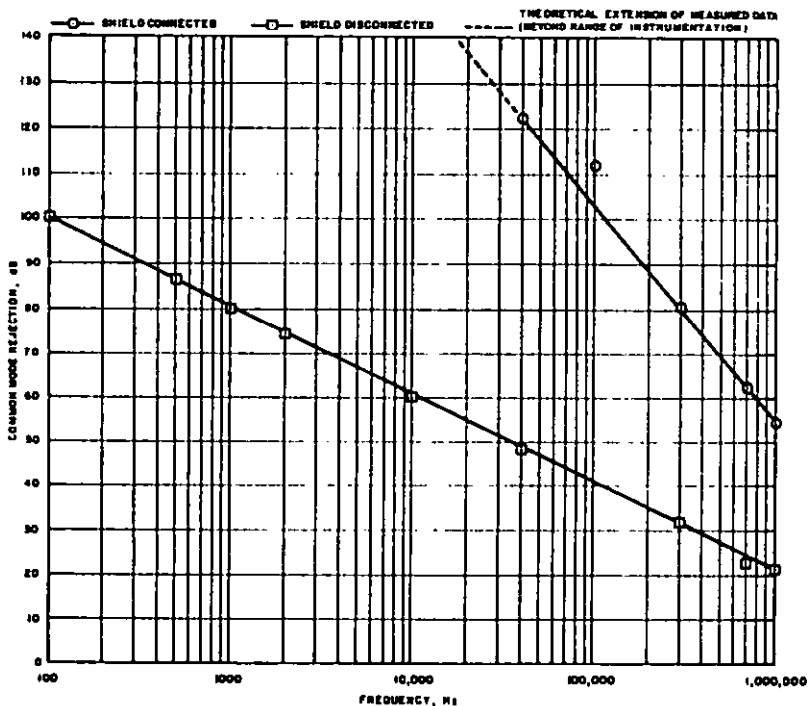


FIGURE 69. Common-mode attenuation obtained for a 115 Vac transformer with three electrostatic shields connected and disconnected.

6.4.3 Leakage and magnetic field shielding. In an ideal transformer all the energy entering the primary is transferred to the secondary. In a practical transformer, however, some of the energy is not coupled to the secondary. This uncoupled energy is proportional to the leakage inductance of the transformer (usually modelled as a primary leakage inductance and a separate secondary leakage inductance). In a switching regulator, large leakage inductances have the following disadvantages:

- a. Produces an unwanted radiated magnetic field at the switching frequency and its harmonics (a major cause of over limit REO emissions in MIL-STD-461)
- b. Induces voltage spikes which produce voltage stress on the switching components--requiring special snubber circuits
- c. Reduces the efficiency of the power supply
- d. Impairs cross regulation between multiple outputs

Leakage inductance cannot be completely eliminated but it can be reduced to a low value. Patel in reference 64 derives the leakage inductance for a pot core where the leakage inductance is directly proportional to the cross-section of the uncoupled area and inversely proportional to the width of the winding. Also it is a square function of the number of turns of the primary. Pertaining to gapped cores both reference 64 and section 13 of reference 2 experimentally demonstrate the somewhat surprising result that the leakage inductances are essentially independent of the air gap length. However, coupling coefficient decreases with increasing air gap length, and both self inductances decrease with increasing air-gap. So the practical design effect is an effectively leakier transformer to achieve the ungapped higher (primary and secondary) inductance values even with increasing air-gaps. Section 13 of reference 2 predicts and experimentally confirms that the leakage inductance of one winding of a three-winding transformer is increased by closer coupling between the other two windings. Methods of minimizing leakage inductance are:

- a. Minimize turns by using a core material with the highest possible permeability
- b. Reduce build of coil
- c. Increase winding width
- d. Minimize spacing between windings, insulation thickness should be as small as possible
- e. If possible, use bifilar windings
- f. For high voltage primary to secondary, use parallel or interleaving winding techniques
- g. Use smallest possible wire diameter

If leakage inductance is not sufficiently reduced, it may be necessary to use magnetic shielding. At low frequency, magnetic materials are required for magnetic shielding and even then shielding is difficult, frequently requiring thick shields for effective magnetic shielding. Better results are achieved with layers of materials with different permeabilities and saturation levels (6.10 discusses this and other shielding considerations in more detail).

For line frequency transformers (60 Hz or 400 Hz), a non-magnetic metallic shield in the form of an encircling band has been demonstrated by measurements to be effective out to 5 kHz. This highly conductive band of metal encircling the transformer is commonly called a shading ring. In principle, the coil of a transformer having an alternating magnetic field induces a large current flow in the shading ring, setting up a magnetic field opposing the original magnetic field and, theoretically, reducing it. In practice, this can be easily done by placing a copper band about .063 centimeters (cm) (.025 inches) thick around the core and windings, centered on the windings, and then shorting the ends with solder (see FIGURE 70). The ratio of the width of the shading ring to the width of the windings should be about 1:2 (for example, a 5.08 cm (two inch) wide winding would have about a 2.54 cm (one inch) shading ring). Using a wider shading ring (larger ring to winding ratio) or completely enclosing the windings does not seem to be advantageous because of the re-radiation of the magnetic field at the top or bottom of the shading ring. This fringing lessens the effect of the shading ring by increasing the magnetic field in the plane of maximum radiation (side A of FIGURE 70). The magnetic fields from all six sides of a transformer are predominantly composed of odd harmonics of the power frequency; the even harmonics are generally 20 dB to 40 dB lower in amplitude than the odd ones for each respective face. It also should be noted that the odd harmonic radiation level from each face is not equal because of the direction of current flow in the windings; side A (see FIGURE 70) has radiation levels about 20 dB higher than side C; side B's radiation is much less in value than side C. The shading ring will reduce the larger magnetic fields (sides A and C) by about 6 dB to 9 dB; side B will show little or no effect. On a cost versus performance basis, the use of shading rings is a good method of EMI reduction. However, the designer should orient the transformer within the equipment to obtain lowest all-round magnetic fields external to the equipment. Since the magnetic field decays very rapidly with distance ($1/r^3$ as shown in 6.10), the transformer may be oriented so that its face with the highest emission is towards the greatest distance to the chassis surface.

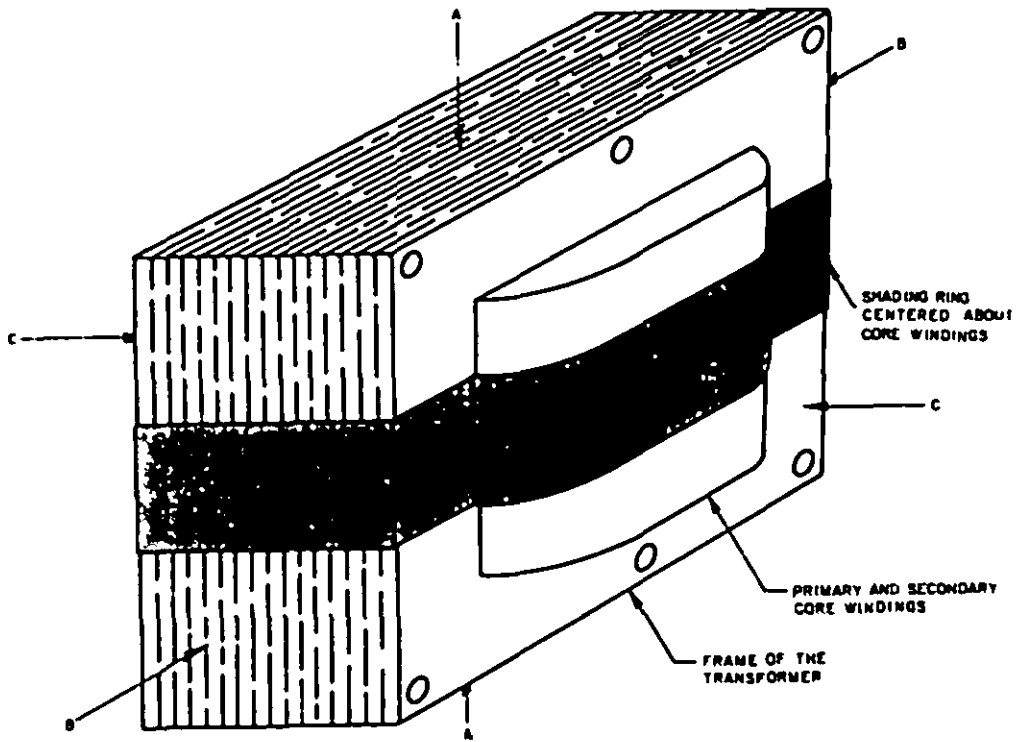


FIGURE 70. Power transformer after adding copper shading ring.

6.5 Ferrites and ferrite beads. Ferrite components are frequently useful for noise suppression. The most commonly used ferrite devices for suppression are shielding beads. Ferrite beads provide an inexpensive and convenient way to add high frequency loss in a circuit without introducing power loss at dc and low frequencies. The beads are small and can be installed simply by slipping them over a component lead or conductor, to produce a single turn inductor/suppressor. Toroids usually supplied for transformer or inductor use can also be used for noise suppression. These cores lend themselves to multi-turn devices. Toroids often have longer magnetic path lengths than comparably inductive beads and can, therefore, tolerate more current.

Ferrite components are useful because of some of their high frequency properties. As the frequency is raised permeability is at first constant, then a critical frequency is reached where permeability starts to fall at about 16 dB per decade. Meanwhile, losses start low, slowly increasing with frequency. As the critical frequency is approached, losses rise dramatically.

FIGURE 71 shows how these properties are reflected in the characteristics of an inductor. An equivalent circuit shows a series inductor and resistor representing the inductance and losses of the core. Using, for example, a single turn through a cylindrical core, we can plot the equivalent series inductance, reactance, resistance, and impedance. At low frequencies the device presents a small inductance whose reactance can usually be neglected. As frequency rises past the critical frequency, the inductance falls; the reactance peaks, then drops off; and the resistance rises. At still higher frequencies, the impedance becomes nearly all resistive, reaching a broad peak before rolling off.

A ferrite core is thus a frequency dependent resistor. FIGURE 72 is a simplified circuit representing the core resistance and inductance at a single frequency and including source and load impedances. Thus this device becomes part of a voltage divider that could attenuate higher frequencies while passing lower ones. Whether this will effectively attenuate the noise depends on the relative magnitudes of the three impedances involved. For example, if Z_s and Z_L were each 1 ohm, and if Z_{core} varies from less than 1.0 ohm at low frequency to 100 ohms at the noise frequency, then there will be substantial attenuation - over 33 dB. On the other hand, if Z_L were one megohm, then the impedance of the core would be insignificant and there would be virtually no attenuation. In such cases, the situation can sometimes be improved by lowering the impedance of the load as with a by-pass capacitor. The insertion loss can be calculated by simply comparing the total impedances around the loop as shown in the formula in FIGURE 72.

Ferrite beads can thus be used to add high frequency loss to a circuit without introducing a dc loss. Shielding beads are available in a wide range of sizes and shapes, and are made in several materials having different critical frequencies (see FIGURE 71). Special variations of beads can also be supplied. They can be ground to tight dimensional tolerances to fit into connectors or filter assemblies. Certain beads can be assembled on wire leads, taped and reeled for automatic insertion. Multihole cores are sometimes used to attenuate noise on wire pairs or to produce multi-turn chokes having low inter-turn capacitance.

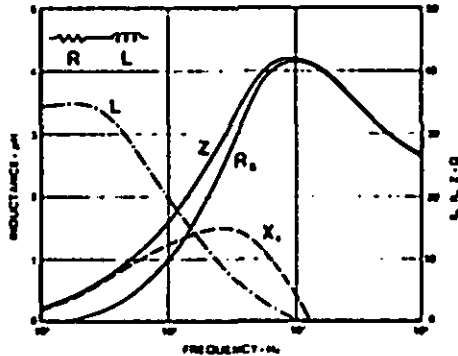
Since the impedance of a single bead is limited to about 100 ohms, beads are most effective in low-impedance circuits such as power supplies, class C power amplifiers, resonant circuits, and SCR switching circuits. If a single bead does not provide sufficient attenuation, multiple beads may be used. However, if two or three beads do not solve the problem, additional beads are not normally effective.

When using ferrite beads in circuits with dc current, care must be taken to guarantee that the current does not cause saturation of the ferrite material.

Since the operation of these products depends only on coupling to the magnetic field surrounding a conductor, contact between the lead and the bead is inconsequential. Nickel-zinc ferrite and magnesium-manganese-zinc ferrite have volume resistivities around 10^6 ohm-cm and act as fairly good insulators. Manganese-zinc ferrite, on the other hand, has volume resistivity around 100 ohm-cm classifying it as a semiconductor. Because of this, it is best to arrange such beads so they will not short two circuits. Usually this can be done by lead dressing. If not, it may be necessary to fix the core in place or insulate it. Manufacturers can supply beads with a variety of insulating coatings such as parylene, varnish, Teflon or enamel.

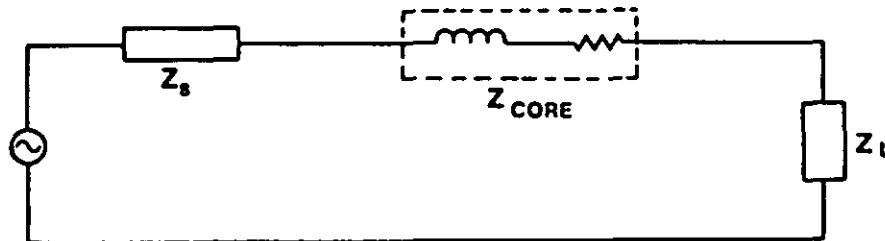
Toroids are useful to suppress common-mode noise. As shown in FIGURE 52, the toroid is wound with two windings, such that the fields resulting from the power currents cancel while the common-mode noise fields add. This approach allows a common-mode choke to carry high power currents without trouble while attenuating common-mode noise. This technique is used quite effectively in power line filters, particularly for lower frequencies where winding self capacitance is not significant. In many cases where noise is normal-mode and large current must be carried, it is necessary to provide a gap to avoid saturation (see 6.3.1).

(For one type of material; other materials will peak at different frequencies and ohms, eg, 150 MHz, 300 MHz instead of 10 MHz)



NOTE: (1) Equivalent resistance increases with frequency due to high frequency core losses
(2) At low frequencies, inductive reactance small

FIGURE 71. Ferrites, inductance, reactance, resistance, impedance vs frequency.



$$\text{INSERTION LOSS} = 20 \log \frac{Z_s + Z_L + Z_{\text{CORE}}}{Z_s + Z_L}$$

NOTES:

1. MOST EFFECTIVE ABOVE 1 MHz
2. Z_{CORE} LIMITED TO ABOUT 100 Ω
3. MOST EFFECTIVE IN LOW IMPEDANCE CIRCUITS (SUCH AS POWER SUPPLIES)

FIGURE 72. Insertion loss of ferrite core (or bead).

Ferrites are brittle ceramics having rather low thermal conductivity and are subject to failure from physical or thermal shock. These conditions become progressively more serious with large parts. Depending on the shock levels, it may become necessary to restrict core movement, protect from bending stresses or to insulate from sharp thermal transients. Like most other ceramics, ferrites are about ten times stronger in compression than tension, so mounting should avoid tensile or bending stresses. Cushioned clamps or adhesives are best for holding parts in place.

Environmentally, ferrites are quite inert being free of any organic or metallic substances. They will not be degraded by solvents, water, weak acids or bases, or temperatures up to about 300 degrees C. In low loss, high frequency materials, moisture or high humidity can increase losses slightly due to eddy currents in the water, but this is inconsequential in suppression applications. Above the Curie temperature, these materials become non-magnetic, so you should expect no suppression. The phenomenon is completely reversible, so temporarily exceeding the Curie temperature has no lasting magnetic effect. Most magnetic properties change with temperature. Foremost of these is permeability which generally rises with increasing temperature, although there are sometimes dips, until it drops sharply at the Curie temperature. Losses change only a little with temperature. Saturation flux density falls with increasing temperature.

6.6 Conductors. Although not usually considered components, conductors do have component characteristics: inductance and resistance. (Much of the discussion in this section are excerpts from reference 42).

The inductance is the sum of the internal plus external inductances. The internal inductance of a straight wire of circular cross-section carrying a uniform low frequency current is independent of wire size, and is negligible compared to the external inductance except for very close conductor spacings. The internal inductance is even less when higher frequency currents are considered since, due to skin effect, the current is concentrated near the surface of the conductor. The external inductance, therefore, is normally the only inductance of significance.

TABLE VII lists values of external inductance and resistance for various gauge conductors. The table shows that raising the conductor higher about the ground plane increases the inductance. This assumes the ground plane is the return circuit. Beyond the height of a few inches, however, the inductance approaches its free-space value, and increasing the spacing has little effect on the inductance. This is because almost all the flux produced by current in the conductor is already contained within the loop.

As is also indicated in TABLE VII the inductance and conductor diameter are inversely related in a logarithmic manner. For this reason, low values of inductance are not easily obtained by increasing the conductor diameter. The spacing between conductors affects the external inductance, whereas the cross-section affects only the internal inductance. The internal inductance can be reduced by using a flat, rectangular conductor instead of a round one. A hollow round tube also has less inductance than the same size solid conductor.

TABLE VII also lists the equations for the external inductance of a straight, round conductor; and for ac resistance as a function of dc resistance, frequency, and conductor diameter (copper).

FIGURE 73 relates some other pertinent characteristics of conductors. The equation is given for inductance of two parallel conductors showing how the inductance increases with center to center spacing and decreases with diameter of the conductors. Also indicated in FIGURE 73 is the lower ac resistance and inductance of rectangular conductors compared to round ones. As a result rectangular conductors are better high frequency conductors. In fact, flat straps or braid are frequently used as ground conductors even in relatively low-frequency circuits.

6.6.1 Planning minimal magnetic loop areas. To prevent radiating magnetic fields, it is important to minimize loop areas particularly where currents are high. One method of planning minimal loop areas is to take a schematic and wiring diagram and color heavily those connecting wires which comprise the main fluctuating current flow. Then, when laying out component location, the loop area should be minimized but care should be taken to not exclude necessary lead length (see FIGURE 49). On PC boards, high current-carrying components should be located nearest the plug-in connector, when possible. Attention should also be given to orienting the terminals of the individual components to minimize loop areas. When attempting to visualize loop area, it is advisable to consider both the vertical and horizontal planes. Also, consider that usually the front-to-back distance for most equipment is greater than the vertical or the lateral distances. Therefore, if a large magnetic field is present, it would be better to have it oriented in the front-to-back direction. This will provide some attenuation of the field before reaching the equipment case due to the greater distance the field has to travel.

TABLE VII. Inductance and resistance of round conductors.

Wire Size (AWG)	d Diameter (In.)	R _{dc} Resistance (mΩ/In.)	L = Inductance (μH per In.)	
			h = 0.25 In. Above Ground Plane	h = 1 In. Above Ground Plane
26	0.016	3.39	0.021	0.028
24	0.020	2.13	0.020	0.027
22	0.025	1.34	0.019	0.026
20	0.032	0.85	0.017	0.024
18	0.040	0.53	0.016	0.023
14	0.064	0.21	0.014	0.021
10	0.102	0.08	0.012	0.019

Inductance if $h > 1.5d$:

$$L = 0.005 \ell \mu (4h/d), \mu\text{H/in.}$$

AC resistance is related to R_{dc} for $d\sqrt{f} > 10$:

$$R_{ac} = (0.096 d\sqrt{f} + 0.26) R_{dc}$$

for copper

- Even at low frequencies a conductor normally has more inductive reactance than resistance
- Two parallel conductors carrying uniform current in opposite directions:
 $L = 0.01 \ell \mu (2D/d), \mu\text{H/in.}$
 where D is center to center spacing & d is conductor diameter
- A flat rectangular conductor has less R_{ac} & L than a round one

FIGURE 73. Conductors.

6.7 Resistors. There are three basic types of fixed resistors:

- a. Wirewound
- b. Film
- c. Composition

In most cases, a satisfactory equivalent circuit for a resistor consists of an inductor in series with the resistor and a capacitor shunted across the resistor (reference 42). The inductance is primarily lead inductance, except for wirewound resistors, where the resistor body is the largest contributor. Except for wirewound resistors, or very low valued resistors of other types, one may normally neglect the inductance during circuit analysis.

The shunt capacitance can be significant when high value resistors are used. For example, consider a 22 megohm resistor with .05 pF of shunt capacitance. At 145 kHz, the capacitive reactance will be 10 percent of the resistance. If this resistor is used above this frequency, the capacitance may affect the circuit performance.

All resistors generate a noise voltage from thermal noise and other noise sources, such as shot and contact noise. These noise voltages, however, will usually be much lower than the other power supply noise sources. In general, they need not be considered in meeting power supply EMI specifications.

6.8 Mechanical contact protection. Electrical breakdown may develop between contacts opening or closing a current-carrying circuit. Breakdown can cause not only physical damage to the contacts; but also high frequency radiation, and voltage and current surges in the wiring.

Two types of breakdown can occur: gas or glow discharge and the metal-vapor or arc discharge. The glow discharge is regenerative, self-supporting, and can occur when the gas between the contacts becomes ionized. To avoid a glow discharge (in air), the voltage across the contacts should be kept below 300 V (only a few milliamperes is usually necessary to sustain the glow). An arc discharge can occur at contact spacings and voltages much below those required for a glow discharge. An arc is formed whenever an energized but unprotected contact is opened or closed, since the voltage gradient usually exceeds the required value when the contact spacing is small. When the arc discharge forms, the electrons emanate from a small area of cathode--where the electric field is strongest. The localized current has a very high density which may be enough to vaporize the contact metal. The appearance of molten metal marks the transition from field emission (electron flow) to a metal-vapor arc. This transition typically takes place in less than a nanosecond. The molten metal, once present, forms a conductive bridge between the contacts, thus maintaining the arc even though the voltage gradient may have decreased below the value necessary to initiate the discharge.

The arc discharge, once formed, must be broken rapidly to minimize damage to the contact material. For that reason, a set of contacts can normally handle a much higher ac than dc voltage. A contact rated at 30 Vdc can, therefore typically handle 115 Vac.

When the contacts are closed, capacitive loads draw much higher inrush currents than their steady-state current. To protect the contact, the initial inrush current must be limited. Soft start circuits are discussed in 6.2.4.

When the contacts are open, inductive loads create a large reverse voltage transient or inductive kick. The energy stored in the magnetic field must be dissipated in the arc or be radiated unless protective circuitry is used. FIGURE 74 shows that there are two requirements for avoiding contact breakdown (reference 42):

- a. Keep the contact voltage below 300 V to prevent a glow discharge.
- b. Keep the initial rate of rise of contact voltage below the value necessary to produce an arc discharge. (A value of 1 volt per microsecond is satisfactory for contacts.)

To determine whether or not breakdown can occur in a specific case, it is necessary to know what voltage is produced across the contacts as they open. This voltage is then compared to the breakdown characteristics in FIGURE 74. FIGURE 75 shows an inductive load connected to a battery through a switch S. The voltage that would be produced across the contacts of the opening switch if no breakdown occurred, is called the available circuit voltage. I_0 is the current flowing through the inductor the instant the switch is opened, and C is the stray capacitance of the wiring. FIGURE 76 compares the available circuit voltage to contact breakdown characteristics (see FIGURE 74). Contact breakdown occurs where the voltage exceeds the breakdown characteristics.

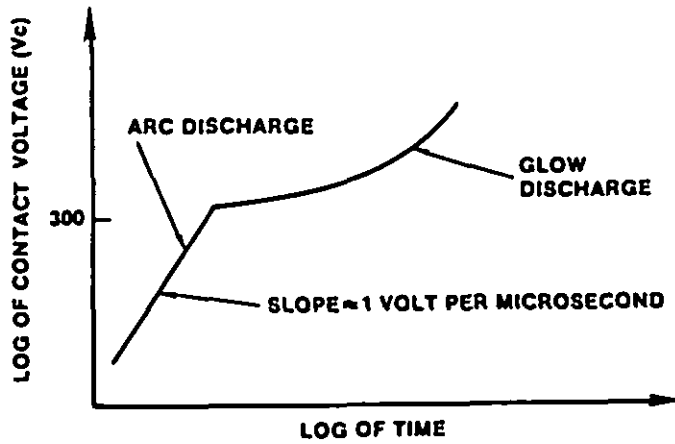


FIGURE 74. Contact breakdown versus time with no protection.

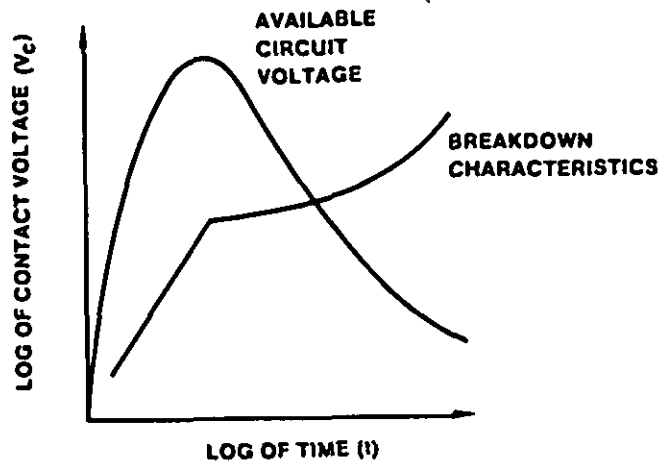


FIGURE 75. Available voltage across opening contact for inductive load.

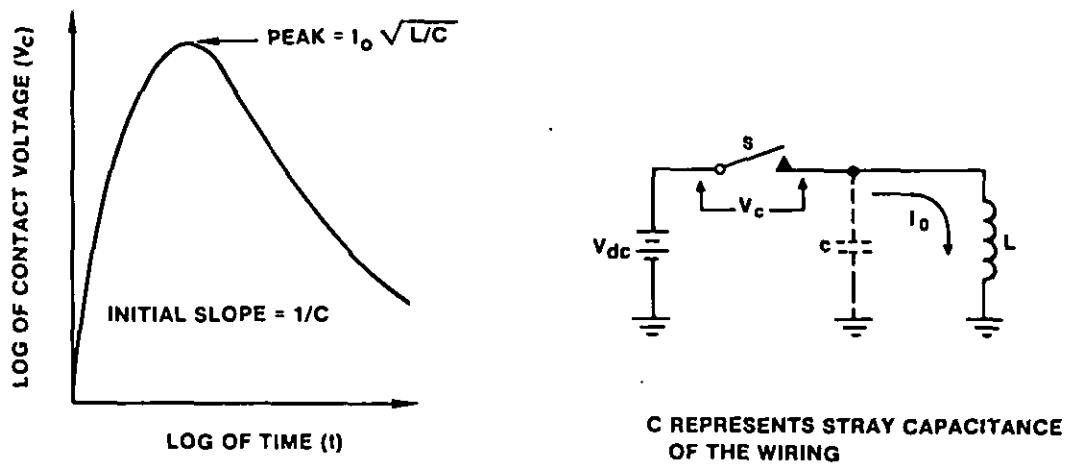


FIGURE 76. Comparison of available voltage and contact breakdown for inductive load.

To protect contacts that control inductive loads, and to minimize radiated and conducted noise, some type of contact protection network must normally be placed across the inductance, the contacts, or both. In some cases the protection network can be connected across either the load or the contacts with equal effectiveness. From a noise reduction point of view it is usually preferable to provide as much transient suppression as possible across the noise source--in this case, the inductor. In most cases, this provides sufficient protection for the contacts. When it is not, additional protection can be used across the contacts.

FIGURE 77 shows six networks commonly placed across a relay coil or other inductance to minimize the transient voltage generated when current is interrupted. In FIGURE 77A a resistor is connected across the inductor. When the switch opens, the inductor drives whatever current was flowing before the opening of the contact through the resistor. This circuit is very wasteful of power since the resistor draws current whenever the load is energized. If R should equal the load resistance, the resistor dissipates as much steady-state power as the load.

Another arrangement is shown in FIGURE 77B, where a varistor (a voltage variable resistor) is connected across the inductor. When the voltage across the varistor is low, its resistance is high, but when the voltage across it is high its resistance is low. This device works the same as the resistor in FIGURE 77A, except that the power dissipated by the varistor while the circuit is energized is reduced.

A better arrangement is shown in FIGURE 77C, where a resistor and capacitor are connected in series and placed across the inductor. This circuit dissipates no power when the inductor is energized. When the contact is opened, the capacitor initially acts as a short circuit, and the inductor drives its current through the resistor. The values for the resistor and the capacitor can be determined by the method described in FIGURE 78.

In FIGURE 77D a semiconductor diode is connected across the inductor. The diode is poled so that when the circuit is energized, no current flows through the diode. However, when the contact opens, the voltage across the inductor is of opposite polarity than that caused by the battery. This voltage forward biases the diode, which then limits the transient voltage across the inductor to a very low value (the forward voltage drop of the diode plus any IR drop in the diode). The voltage across the opening contact is therefore approximately equal to the supply voltage. This circuit is very effective in suppressing the voltage transient. However, the time required for the inductor current to decay is more than for any of the previous circuits and may cause operational problems.

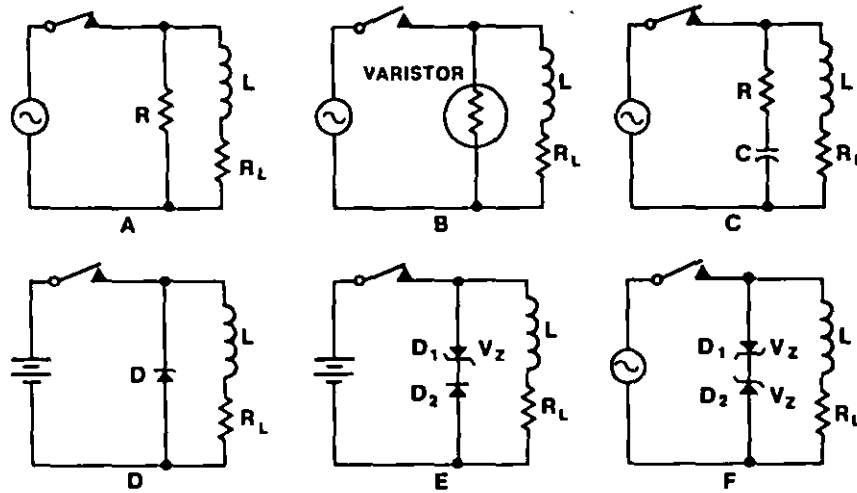
Adding a zener diode in series with a rectifier diode, as shown in FIGURE 77E, allows the inductor current to decay faster. This protection, however, is not as good as that for the diode above and uses an extra component. In this case, the voltage across the opening contact is equal to the zener voltage plus the supply voltage.

Neither of the diode circuits (see FIGURES 77D or E) can be used with ac circuits. Circuits that operate from ac sources or circuits that must operate from two dc polarities can be protected using the networks in FIGURES 77A through C, or by two zener diodes connected back to back, as shown in FIGURE 77F. Each zener must have a voltage breakdown rating greater than the peak value of the ac supply voltage and a current rating equal to the maximum load current.

FIGURE 78 shows two protection networks commonly used across contacts that control inductive loads. The circuit on the left uses an R-C network. If the capacitor is large enough, the load current is momentarily diverted through it as the contact is opened, and arcing does not occur. When the contact is closed, the capacitor voltage (V_{dc}) is discharged through R .

For contact closing, it is desirable to have the resistance as large as possible to limit the discharge current. However, when the contact is opened, it is desirable to have the resistance as small as possible, since the resistor decreases the effectiveness of the capacitor in preventing arcing. The actual value of R must therefore be a compromise between the two conflicting requirements.

Limiting values of R are given in FIGURE 78, and the value of C is also given. The value of C is chosen to meet two requirements: (1) the peak voltage across the contacts should not exceed 300 V (to avoid a glow discharge), and (2) the initial rate of rise contact voltage should not exceed 1 V per microsecond (to avoid an arc discharge). The latter requirement is satisfied if C is at least $1 \mu\text{F}/A$ of load current.



NOTE: CIRCUITS A, B, C, AND F CAN BE USED WITH AC OR DC; CIRCUITS D & E CAN ONLY OPERATE FROM DC

FIGURE 77. Contact protection circuits to minimize "inductive kick" (from inductive load) and minimize radiated and conducted noise.

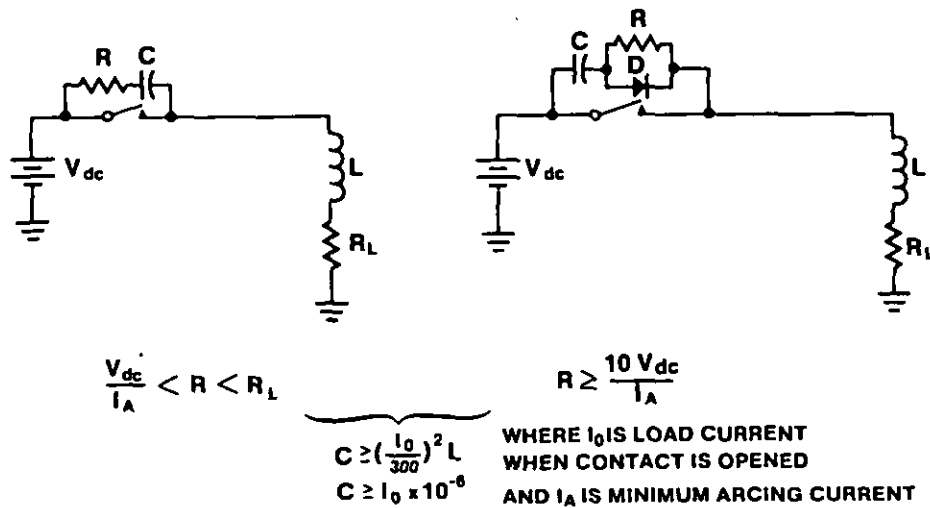


FIGURE 78. Contact protection circuits used across switch contacts.

The right side of FIGURE 78 shows a more expensive circuit that overcomes the disadvantages of the RC circuit on the left. When the contact is open, capacitor C charges up to the supply voltage with the polarity shown in the figure. When the contact closes, the capacitor discharges through resistor R, which limits the current. When the contact opens, however, diode D shorts out the resistor, thus allowing the load current to momentarily flow through the capacitor while the contact opens. The diode must have a breakdown voltage greater than the supply voltage with an adequate surge current rating (greater than the maximum load current). The capacitor value is chosen the same as for the R-C network. Since the diode shorts out the resistor when the contacts open, a compromise resistance value is no longer required. The resistance can now be chosen to limit the current on closure to less than one tenth the arcing current, as shown in FIGURE 78. The R-C-D network provides optimum contact protection, but it is more expensive than other methods and cannot be used in ac circuits.

The information in this section is primarily from reference 42 with some variations.

6.9 Additional filter considerations. This section considers the effect of input and output impedances on filter attenuation and how best to mitigate adverse effects. A related consideration is the precautions to be observed if filter circuits are purchased commercially.

Finally considered are the advantages of filtering on the dc rather than the ac side of the rectifier.

6.9.1 Input and output impedances of filters. As discussed in 5.2.4 and APPENDIX B, the combination of a lightly damped input filter and a lightly damped output filter can turn the switching regulator into an oscillator. A less catastrophic, but nevertheless important consideration is the effect of input and output impedances on the attenuation characteristics of filters in some cases resulting in negative insertion loss or ringing at one or more self-resonant frequencies of the filter.

FIGURE 79 depicts four types of most effective primitive low-pass filters for the four permutations of low and high input and output impedances. For example, the commonly used LC filter in switching power supplies (the third configuration in FIGURE 79) is the most effective primitive low-pass filter for a low input and high output impedance circuits. The four filters on the right side of FIGURE 79 are the corresponding next, less primitive filters. For best results, the high interface impedance should meet a C (shunt) and the low interface impedance should meet an L (series) of the filter.

There would, therefore, be no problem if the interface impedances were known. One could then also accurately calculate and predict the insertion loss. In practical installations, however, one may not know both interfaces. The power supply designer can model the power supply interface (see APPENDICES A and B). However, the power line impedances (generators, cabling and any other system on the generator) is not likely to be known. Also continuous switching with the power system and additions and changes make the interface unavoidably indeterminate.

Schlicke (reference 66) recommends managing this indeterminacy effectively and economically by partitioning and damping. The advantages of partition (multi-section filters) can be attributed to the much steeper cut-off and the much reduced values of the total inductance (sum of L's); smaller and cheaper filters. FIGURES 45 and 44 show this for the LC filter. Partitioning very much reduces the effect of mismatch in the stopband. Stated another way, with partitioning, the stopband performance becomes less dependent on filter configuration (PI, T, or L) and of mismatch conditions.

To reduce negative insertion loss (ringing) damping of the self (eigen) resonances is recommended. See APPENDIX B for filter damping techniques.

Some idea of power line impedances of typical power lines is shown in FIGURE 80 reproduced from a paper by Bull (reference 67). It shows mean values and standard deviations of the magnitude of line impedance, as a function of frequency. It also illustrates the impedance characteristic of a parallel RL circuit, with $R = 50$ ohms and $L = 30$ μ H. The good fit to the mean values of line impedance will be noted. Superimposed onto the original figure are the following impedance curves:

- a. A parallel RL circuit, with $R = 150$ ohms and $L = 50$ μ H.
- b. A parallel RL circuit, with $R = 23$ ohms and $L = 13$ μ H.

These additional curves provide a reasonable fit to the $+ \sigma$ and $- \sigma$ power line impedances values, respectively.

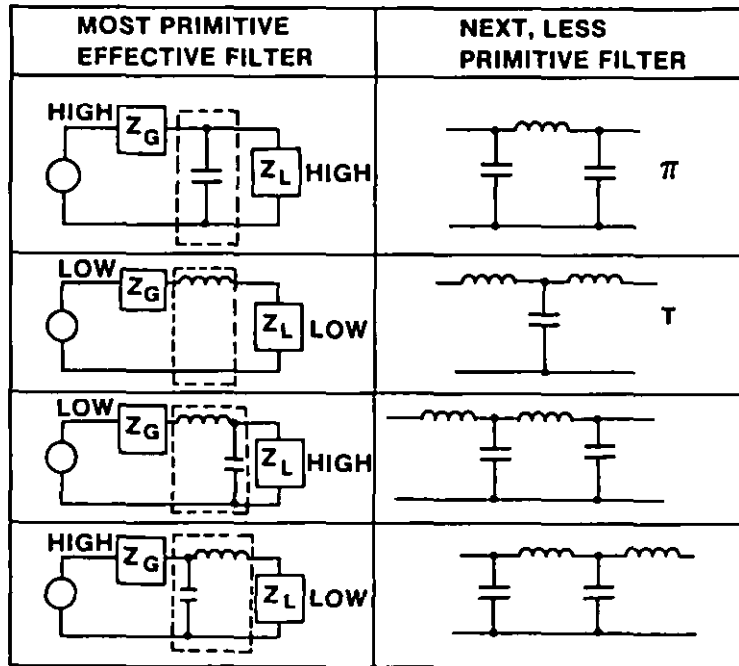


FIGURE 79. Filter input and output impedance.

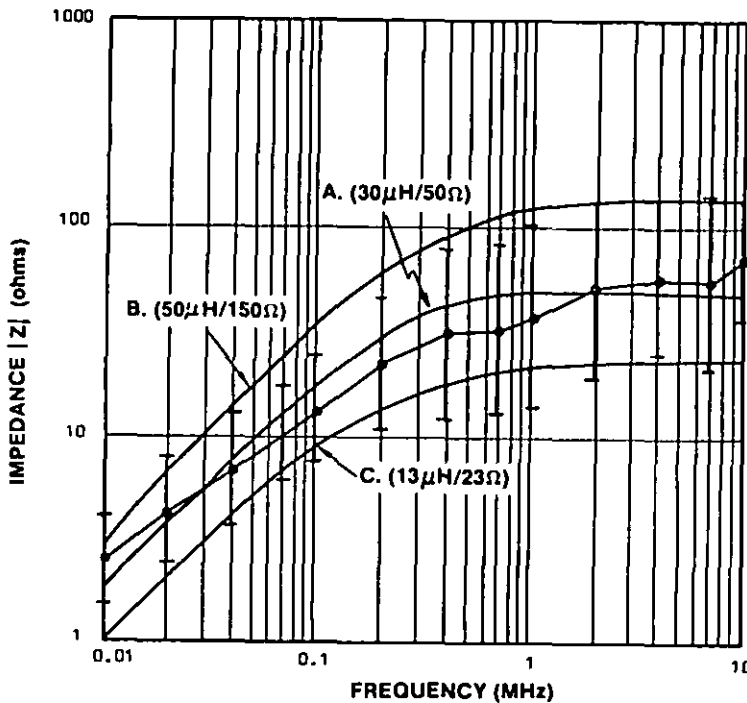


FIGURE 80. Power line impedance data: mean of measured values - good fit to curve A (parallel RL circuit with $R = 50\Omega$ and $L = 30\mu\text{H}$) curves B and C are reasonable fits to standard deviations of measured values.

6.9.2 Off-the-shelf type filters. A number of manufacturers provide low and high current power line filters, some of them specifically designated as being appropriate for switching-mode power supplies. Most of them supply insertion loss data for 50 ohm input and output test conditions. As indicated in 6.9.1 the insertion loss under actual interface conditions may be very different and may even result in insertion gain. As shown in FIGURE 80, the source impedance is more realistically a fraction of an ohm to a few ohms at 10 kHz. The power supply input impedance will depend upon the current and voltage inputs and power supply configuration (see FIGURE 101 in APPENDIX B). Another possible contributor of power line filter problems is the use of marginal or substandard components such as undersized inductor cores which saturate at much less than the rated current. Also as discussed in APPENDIX B, the addition of a filter can cause the entire power supply to become an oscillator. The designer, therefore, should observe the following precautions in selecting an off-the-shelf power line filter:

- a. Obtain circuit diagram and component values and perform insertion loss tests.
- b. Compare filter circuit output impedance to power supply input impedance to predict whether or not instability can occur (see Appendices B and C). Verify by stability tests.
- c. If no filter circuit information is available, insertion loss and stability testing will need to be much more extensive.
- d. Select multi-section filters with damped self resonances wherever possible. Two or three section filters are very effective in minimizing the effects of varying interface impedances.
- e. In general, select filters with high input impedances to match low power line impedances (third filter down in FIGURE 79).
- f. The filter must be built to withstand occasional high voltage transients such as from lightning strokes. For shore use, this peak voltage can be as high as 1500 volts ac(Vac) and aboard ship as high as 2500 Vac (see DoD-STD-1399 spike test).
- g. See 6.9.4 for limits on line-to-ground capacitances.

6.9.2.1 Installation of off-the-shelf power line filters. The most effective location to mount the filters is at the line cord entrance to the chassis. If this is not possible, the line-side wires should be twisted and perhaps shielded. Do not run these leads in the same bundle or parallel to any other leads in the equipment. It is also good practice to twist the load-side leads to the switch.

REO1 magnetic emissions may occur if the line cord entrance to the chassis is not located close to the terminal entrance to the power supply. The internal wiring leading to the power supply carries switching frequency currents which in turn radiate EMI. To decrease these magnetic emissions, a capacitor can be located at the terminal entrance to the power supply. The capacitor then becomes part of the input filter circuit.

6.9.3 DC versus ac filter. In general, as much filtering as possible should be performed on the dc side of the rectifier for the following reasons:

- a. Electrolytics may be used on the dc side-smaller volume capacitors
- b. Less losses in rectifier diodes if there are no switching frequency losses
- c. Inductive filtering on dc side decreases low frequency rectification harmonics
- d. Less radiated EMI since fewer wires carrying the switching frequency
- e. Easier to achieve low line-to-ground capacitances (see 6.9.4).

Some additional filtering may also be needed on the ac side (e.g., common-mode or if rectification harmonics extend to the switching frequency).

6.9.4 EMI filtering and MIL-STD-461B. Paragraph 4.3.1 of MIL-STD-461B, Part 1, states that the use of line-to-ground filters for EMI control shall be minimized. This does not mean that they should not be used nor form a basis for the argument of exceeding the conducted emission requirements on power lines. As explained in the subject paragraph, such filters establish a low impedance path for structure (common-mode) currents through the ground plane and can be a major cause of interference in the systems, platforms or installation because these currents can couple into other equipment using the same ground reference. The dumping of noise currents, as well as leakage currents, into the ground plane, which is often the hull of the ship or the fuselage of an aircraft, makes this ground reference a high noise source. If allowed to continue without any limits to the amount of power line and noise current being dumped into the ground, the bonding of equipment could cause more problems than it would solve. Furthermore, there are limits to the amount of reactive current and maximum capacitance to chassis set forth in Requirement 1, MIL-STD-454 and MIL-E-16400.

Thus, MIL-STD-461B states that the total line-to-ground capacitance shall not exceed 0.1 μF for 60 Hz equipment and 0.02 μF for 400 Hz equipment. This will, in turn, limit the power line current to 5 mA consistent with MIL-STD-454 and MIL-E-16400 requirements. It is important to note that the filtering employed in an equipment must be described fully in the equipment's or subsystem's technical manual, as well as in the EMI Test Report, as specified in MIL-STD-461B. Since many EMI filters are added as a result of EMI tests, the test report is often the first official document showing their use, usually prior to the issuance of an Engineering Change Proposal (ECP).

Procuring activities should be alerted to the fact that many contractors may argue that compliance with the conducted emission or susceptibility requirements of MIL-STD-461B is not possible unless large capacitors are used in the EMI filters. This is believed to be a fallacy since most commercial computing devices now use EMI filters in conformance with Underwriter's Labs (UL) leakage requirements consistent with the MIL-STD-461B requirements. Thus, the technology and commercial filters for conformance to the requirements are available. The only problem which may exist is that the filters are not of military quality or are not on a qualified parts list. This problem can be remedied by either the equipment manufacturer or filter manufacturer pursuing an appropriate component qualification procedure. The important fact is that the filtering requirement must be adhered to, in order to achieve the compatibility of the equipment or subsystem when it is integrated into the overall platform.

To meet these low line-to-ground capacitances, one or more of the following procedures are recommended:

- a. Use of line-to-line capacitors
- b. Use of one or more ferrite beads (see 6.5)
- c. Filtering on the dc side (see 6.9.3)

6.10 Shielding. A shield is a metallic partition between two regions of space. It controls the propagation of electric and magnetic fields from one of the regions to the other. Shields may be used to contain electromagnetic fields if the shield surrounds the noise source or it may also be used to keep electromagnetic radiation out of the region. Circuits, components, cables or complete systems may be shielded. A major reference for this section is the book by Ott (reference 42).

At a point close to the source, the field properties are determined primarily by the source characteristics. Far from the source, the properties of the field depend mainly upon the medium through which the field is propagating. Therefore, the space surrounding a source of radiation can be broken into two regions, as shown in FIGURE 81. Close to the source is the near, or induction, field. At a distance greater than approximately one-sixth of a wavelength, is the far, or radiation, field. The region between the near and far fields is the transition region.

The wave impedance is the ratio of the electric field (E) to the magnetic field (H). In the far field, this ratio E/H equals 377 ohms for air or free space. In the near field, the ratio is determined by the characteristics of the source and the distance from the source to where the field is observed. If the source is high current and low voltage ($E/H < 377$) the near field is predominantly magnetic. As the distance from the source increases, the magnetic field attenuates at a rate $(1/r)^3$ and the electric field attenuates at a rate of $(1/r)^2$. Conversely, if the source has low current and high voltage ($E/H > 377$) the near field is predominately electric, and the electric field attenuates at a rate of $(1/r)^3$ whereas the magnetic field attenuates at a rate of $(1/r)^2$.

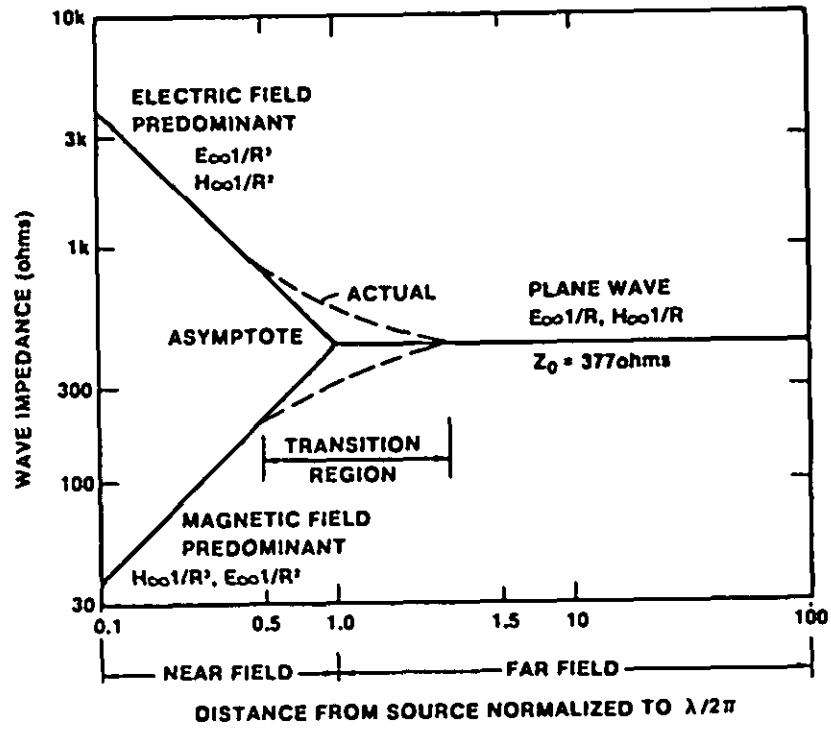


FIGURE 81. Wave impedance for electric and magnetic fields.

In the near field, the electric and magnetic fields must be considered separately, since the ratio of the two is not constant. In the far field, however, they combine to form a plane wave having an impedance of 377 ohms. Therefore, when plane waves are discussed, they are assumed to be in the far field. When individual electric and magnetic fields are discussed they are assumed to be in the near field. At one MHz the near field extends out to about 150 feet (45.7 meters). At lower frequencies, the near field extends even further and, therefore, most coupling is in the near field (see FIGURE 81).

6.10.1 Shielding effectiveness. Shielding can be specified in terms of the reduction in magnetic and electric field or both strength caused by the shield. It is convenient to express this shielding effectiveness in units of dB. Use of dB then permits the shielding produced by various effects or shields to be added to obtain the total shielding. Shielding effectiveness (S) is defined for electric fields and for magnetic fields in FIGURE 82.

Shielding effectiveness is a function of frequency, geometry and material of shield, type of field, and position of shield with respect to field's polarization. It is useful to consider the shielding provided by a plane sheet of conducting material. This simple geometry serves to introduce general shielding concepts but does not include effects due to the geometry of the shield. However, the results of the plane sheet calculations are useful for estimating the relative shielding capability of different materials.

Two types of loss are encountered by an electromagnetic wave striking a metallic surface. The wave is partially reflected from the surface, and the transmitted (nonreflected) portion is attenuated as it passes through the medium. This latter effect, called absorption loss, is the same in either the near or the far field and for electric or magnetic fields. Reflection loss, however, is dependent on the type of field, and the wave impedance. The total shielding effectiveness of a material is equal to the sum of the absorption loss (A) plus the reflection loss (R) plus a correction factor (B) to account for multiple reflections in the shield. Total shielding effectiveness, therefore, can be written as

$$S = (A + R + B) \text{ dB}$$

or

$$S = A + R + B \text{ (dB)}$$

All the terms must be expressed in dB. The multiple reflection factor B can be neglected if the absorption loss A is greater than 10 dB. From a practical point of view, B can also be neglected for electric fields and plane waves (see FIGURE 82).

Absorption loss in a medium occurs because currents induced produce ohmic losses and heating of the material. The electromagnetic wave decreases exponentially through the medium and, therefore, the attenuation is an exponential function of the thickness of the material.

Linearizing the equation by expressing it in dB, the absorption attenuation becomes a linear function of thickness. Doubling the thickness of the shield doubles the loss in dB. The absorption loss (A) also increases with frequency, permeability and conductivity (see FIGURE 83 for the expression for A). In the near field when the magnetic field is predominant, the shielding effectiveness is primarily due to absorption loss.

The reflection loss at the interface between two media is a function of the difference in characteristic impedances of the two media. When an electromagnetic wave passes through a shield, it encounters a second interface between the two media. Both electric and magnetic fields are reflected at each boundary. For electric fields, the largest reflection occurs at the initial interface, and therefore even very thin materials provide good reflection loss (and the multiple reflection correction factors, B, may be ignored). For magnetic fields, however, the largest reflection occurs at the second surface and multiple reflections within the shield reduce the shielding effectiveness. (The near field magnetic reflection loss can be assumed to be negligible at low frequencies. In any case, for absorption loss greater than 10 dB, the correction factor, B, may be ignored.)

In the near field, the reflection loss varies with wave impedance (see FIGURE 81), since reflection loss is a function of the ratio of wave impedance to shield impedance. A high impedance (electric) field has a higher reflection loss than a plane wave. A low impedance (magnetic field) has a lower reflection loss than a plane wave. Thus in the near field when the electric field is predominant, the shielding effectiveness will always be greater than reflection loss for a plane wave. FIGURE 83 gives the expression for this reflection loss which is inversely proportional to frequency and permeability but proportional to conductivity.

$$\begin{array}{l} S \\ \text{for magnetic} \\ \text{fields} \end{array} = 20 \log H_0/H_1 \text{ dB} \qquad \begin{array}{l} S \\ \text{for electric} \\ \text{fields} \end{array} = 20 \log E_0/E_1 \text{ dB}$$

where E_0 (H_0) is incident field strength &
 E_1 (H_1) is field strength emerging from shield

$$\text{Total } S = A + R + B$$

where A is absorption loss which is the same for electric fields, magnetic fields or plane waves

R is reflection loss which is different for electric fields, magnetic fields or plane waves

B is correction factor (ignore for $A > 10\text{dB}$)

FIGURE 82. Shielding effectiveness(s) for metallic sheets in near and far fields.

Where t is thickness in inches

μ_r is relative permeability

σ_r is relative conductivity

f is the frequency

Magnetic field predominant (primarily absorption loss)

$$S \cong A = 3.34 t \sqrt{f \mu_r \sigma_r} \text{ dB}$$

Electric field predominant (primarily reflection loss)

$$S \geq R = 168 - 10 \log (\mu_r t / \sigma_r) \text{ dB}$$

for plane
wave

FIGURE 83. Approximate shielding calculations for metallic sheets in near field ($A > 10 \text{ dB}$).

6.10.2 Magnetic material as a shield. FIGURE 84 lists some of the effects of using a magnetic material as a shield. In addition, it should be noted that the usefulness of magnetic materials as a shield varies with the field strength H . The effect at high field strengths is due to saturation, which varies depending on the type of material and its thickness. At field strengths well above saturation, the permeability falls off rapidly. In general, the higher the permeability the lower the field strength that causes saturation.

To overcome the saturation phenomenon, multilayer magnetic shields can be used (see FIGURE 85). There, the first shield (a low permeability material) saturates at a high level, and the second shield (a high permeability material) saturates at a low level. The first shield reduces the magnitude of the magnetic field to a point that it does not saturate the second; the second shield then provides the majority of the magnetic field shielding. These shields can also be constructed using a conductor, such as copper, for the first shield, and a magnetic material for the second. The low permeability, high saturation material is always placed on the side of the shield closest to the source of the magnetic field. In some difficult cases, additional shield layers may be required to obtain the desired field attenuation. Another advantage of multilayer shields is that there is increased reflection loss due to the additional reflecting surfaces. Even better results seem to be obtained if the layers are separated (see FIGURE 85). Magnetic material manufacturers supply detailed information on these multilayered shields.

When using magnetic materials as shields, it is advisable to consider the orientation of the flux lines. For example, by designing the shield and brackets to follow natural flow of flux lines, better shielding effectiveness can be attained (see FIGURE 86).

6.10.3 Seams, joints, and holes. As indicated in FIGURE 87, the intrinsic shielding effectiveness of the material is frequently of less concern than the leakage through seams, joints and holes. Some considerations to minimize adverse affects of joints and holes are listed in FIGURE 87. FIGURE 88 shows a technique for making a hole into a waveguide below cutoff and thereby obtain a hole magnetically shielded.

A common way to provide ventilation is to use the configuration shown in FIGURE 89. This figure shows a section of shield containing a square array of round holes. The hole diameter is d , the hole center-to-center spacing is c , and the overall dimension of the array is one. The magnetic field shielding effectiveness (reference 42) is given in FIGURE 89. Shielding effectiveness in this case is the increased attenuation provided by the hole pattern over that provided if the total area (1×1) had been removed from the shield.

6.11 Reliability and EMI. Both reliability and EMI are best achieved in an end equipment when they are a serious consideration in the early stages of design. For example, an analytical survey of a circuit prior to chassis layout will identify those portions which by nature are producers of large electromagnetic (EM) emissions. Once identified, the chassis can be so designed that the natural shielding effect of the structure will be employed advantageously or high current-carrying leads can be run through chassis channel numbers.

The techniques and components used to effect EMC, that is, shielding, filtering, and so forth, should be of the same order of reliability as the basic equipment components, and they should not obstruct air flow nor add too much heat to a structural member already operating at a high temperature. MIL-STD-785 provides guidelines for planning and implementing a reliability program.

Other questions which should be considered in the course of the design study are:

- a. Is the nuisance effect of the EMI suppressor such that personnel will discard it? (Human engineering)
- b. Will the EMI device stand the wear and tear of maintenance and operation?
- c. Will it withstand the vibration, humidity, and other environmental requirements of the host equipment?
- d. Does the EMI device ring disproportionately when subjected to power line transients?
- e. Will the EMI device cause the host equipment to exceed its weight or size specifications?

- Increases absorption loss (best for low frequency magnetic fields — very little reflection loss)
- Decreases reflection loss (less shielding for low frequency electric fields)
- Decrease of μ with frequency
- μ depends on field strength
- Machining or working high μ materials may change magnetic properties
- Steel (not stainless) & mumetal are effective up to about 100 kHz
- Somewhere between 100 kHz & 1 MHz nonmagnetic conductors (eg, copper) become better magnetic shields than magnetic material (eg, steel)

FIGURE 84. Magnetic material as a shield.

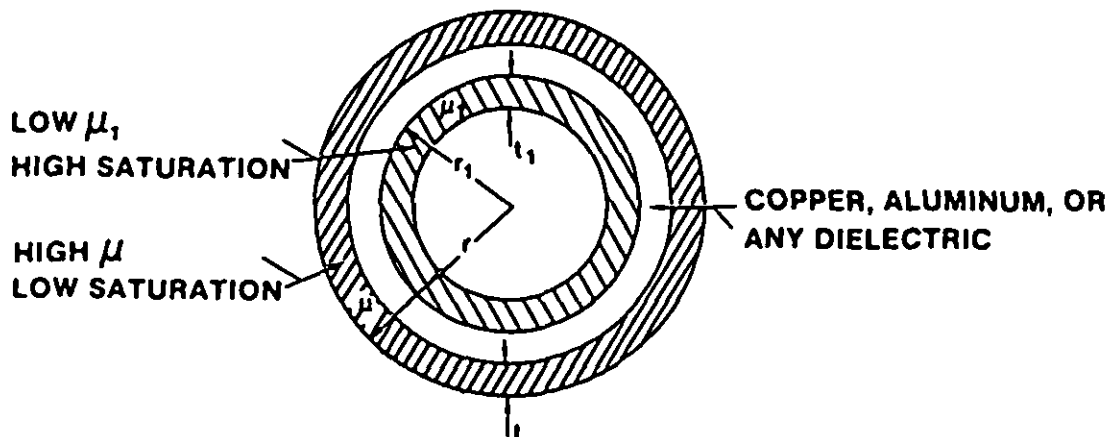


FIGURE 85. Containing magnetic field with multilayer shield.

For Example

- Design bracket ends & chassis to cause flux lines to enter the ends of a U-shaped piece of metal

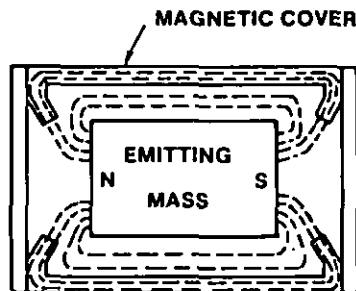
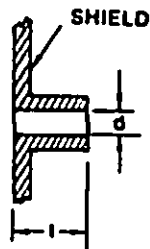


FIGURE 86. Utilizing natural shielding.

- Actual shielding effectiveness obtained in practice is usually determined by the leakage at seams & joints, not by the shielding effectiveness of the material itself
- The maximum dimension (not area) of a hole or discontinuity determines the amount of leakage
- A large number of small holes result in less leakage than a larger hole of the same total area
- EMI gaskets, commonly made of knitted wire mesh, when properly compressed, provide electrical continuity across a joint — can control leakage from low kHz to tens of GHz
- EMI gasket material used should be galvanically compatible with the mating surface to minimize corrosion

FIGURE 87. Seams, joints and holes.



Round Waveguide

Cutoff frequency

$$f_c = (6.9 \times 10^9)/d \text{ Hz}$$

where d is in inches

$$S = 32 t/d \text{ dB}$$

Rectangular Waveguide

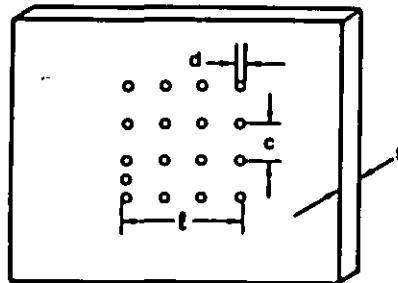
Cutoff frequency

$$f_c = (5.9 \times 10^9)/l \text{ Hz}$$

where l is largest dimension
of cross-section in inches

$$S = 27.2 t/l \text{ dB}$$

FIGURE 88. Hole formed into a waveguide ($d < t$)-magnetic shielding
if operating frequency is \ll cutoff frequency.



$$S = 20 \log c^2 l/d^3 + 32 t/d + 3.8 \text{ dB}$$

where $d < \lambda/2\pi$

For rectangular array l_1 by l_2

$$\text{use } l = \sqrt{l_1 l_2}$$

FIGURE 89. Round holes to provide ventilation.

6.11.1 EMI as a diagnostic tool to increase reliability. When conducting EMI tests on an electric equipment or sub-unit, it is often possible, by making additional use of the EMI test set-up, to identify any weaknesses in the equipment design. Optimizing the design prior to adding filtering and shielding usually increases reliability and performance, and reduces power consumption and cost.

EMI may be only a very small portion, the radiated part, of a much more significant amount of lost energy. It therefore, may signify dissipative losses, an indication of heat, and heat may affect reliability and performance.

6.11.2 Effects from undesired signals. Undesired signals, as well as being undesirable from an interference standpoint, also reduce reliability and operational effectiveness. For example:

a. The circulating current through an L-C resonant circuit depends on the circuit Q. Theoretically, a circuit with infinite Q would have infinite current at resonance. This condition can never be achieved practically; however, any reasonably high Q circuit can have extremely high ac currents in its components. If the capacitor has one percent dissipation factor, the heat build-up is within the capacitor and must find a way out through leads, case, and so forth. This can be the most severe kind of heat build-up. Even some very low dissipation factor capacitors have a problem due to a high ac current, for example, the silver in a silver-mica capacitor migrates through the mica and shorts out the capacitor.

b. Many circuits may appear to be operating properly when the output and input terminals are monitored. There can exist, however, an oscillation completely within some part of the circuit which does not show up in either the input or output terminals. The conception that if it cannot be seen or heard and therefore should be no cause for concern is not valid. The dc voltmeter may be used to determine that each stage is working within its dc dissipation rating. However, the ac dissipation must be added to this, and the engineer is not even aware of its existence. Also, perhaps touching the dc probe to the test point temporarily quenches the oscillation. This type of oscillation is known as parasitic and usually causes degraded or sub-optimum operation since it reduces gain.

c. Sympathetic resonances can occur, for example, when a rectifier smoothing filter or portion of it is resonant at the chopping frequency (or harmonic), of the switching regulator. Reliability and efficiency are reduced by the high circulating current through the filter and regulator.

Custodians:
Navy - EC
Army - CR
Air Force - 11

Preparing activity:
Navy - EC

(Project EMCS-0102)

Review activities:
Army - SC
Navy - SA, SH, AS
Air Force - 13, 17, 89, 99
NASA - NA

User activity:
Navy - YD

MODELING OF SWITCHING-MODE POWER SUPPLIES

10. Introduction. The dc, or static, properties of dc-to-dc converters are well understood. However, their ac, or dynamic, properties are much less well understood. This is because switching converters together with their duty-ratio modulators constitute a nonlinear subsystem whose response is not obvious.

Middlebrook and Cuk (references 2, 37, 49, and 51) have developed a canonical model of a switching-mode dc-to-dc converter, from which not only the large-signal dc but also the small-signal ac dynamic properties can be obtained. Essentially the model is a linearized equivalent circuit. The model is valid if the effective filter cutoff frequency is much lower than the switching frequency (which is always necessary in order to achieve a low output ripple), and for small amplitude ac variations. It is a linearized model to which standard circuit analysis can be applied. It is called a Canonical model because the form of the model is the same for any modulator and power stage. The primary source of the discussion and drawings (with permission) herein is reference 51, a paper presented at Powercon 5.

Although the form of the Canonical model is the same for any converter, the formulas (and of course numerical values) for the elements are different for different converters. Formulas for the model elements are presented for the basic dc-to-dc converters. For some derived converter configurations, the formulas are given for sufficient elements to apply the input filter design criteria of APPENDIX B.

20. Basic dc-to-dc converter models. A model that represents any basic dc-to-dc converter in the continuous conduction mode is shown in FIGURES 90 and 91. FIGURE 90 emphasizes the three essential functions of any dc-to-dc converter: control, basic dc conversion, and low-pass filtering (continuous conduction mode). FIGURE 91 is more detailed relating to the element values in TABLE VIII. Small amplitude ac variations are shown in lower case with a hat over the parameter; for example, \hat{d} represents a small ac variation in duty ratio D.

20.1 Buck, boost, and buck-boost. The formulas for the model elements are given in TABLE VIII for three common converter forms; the buck, boost, and buck-boost (shown in FIGURE 92). The ideal transformer ratio M is a function of the duty ratio, D, and is consistent with the voltage conversion ratios given in 3.3.5.1 on basic topologies. The Canonical model in FIGURE 85 is the same as the one shown in FIGURE 7 except that the voltage and current generators are reflected to the primary side of the transformer. M is the reciprocal of μ in FIGURES 7 and 9.

Within the limits of its restrictions, the Canonical model is both a large-signal dc model and a small-signal ac model of the power stage and contains all the information necessary to determine the dc operating point and the line-to-output and duty ratio-to-output transfer functions.

The Canonical model in FIGURE A2 also includes a simple version of the modulator stage. The modulator is characterized by a voltage V_m such that

$$D = V_c / V_m \quad \text{and} \quad \hat{d} = \hat{V}_c / V_m$$

thereby expressing a linear relationship between control voltage input and duty ratio output, in which V_m is the range of control voltage needed to sweep the duty ratio from 0 to 1. Extension to non-linear dc or a frequency dependent ac characteristic is easily made. Even some linear modulators may require modifying the dc transfer function. For example, since the Silicon General S63524 Regulating Pulse Width Modulator has a ramp offset by a fixed voltage, V_0 , the dc transfer function has to be replaced by

$$D = (V_c - V_0) / V_m.$$

There are two important features in the model. First, the effective inductance L_e is equal to the actual constant filter inductance L only for the buck converter, and is different from L and a function of the duty ratio D (the operating point) for the other two generators. Second, in the buck converter the voltage generator is not frequency dependent, but in the other two converters the voltage generators are frequency dependent expressed by a right half-plane zero. Both of these features make the boost and buck-boost converters more difficult to regulate. In all three basic converters, there is no frequency dependence of the current generator, and C and R_e are the same as those in the actual converter.

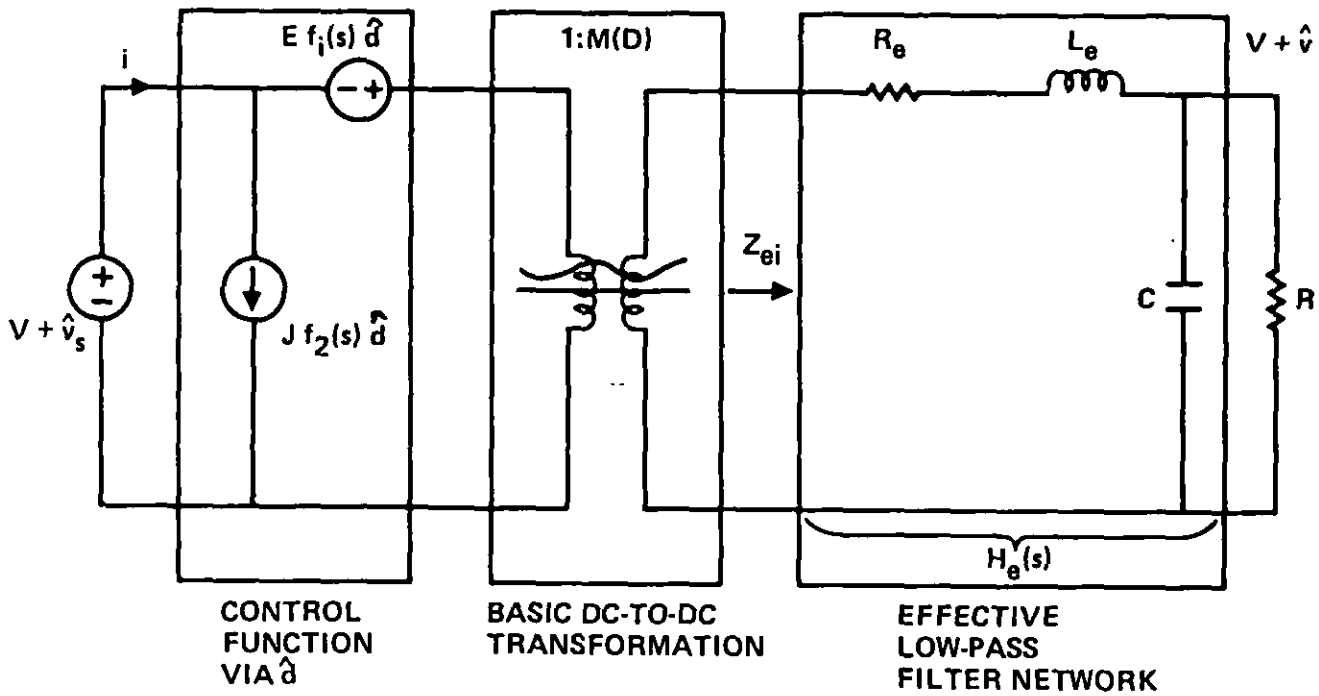


FIGURE 90. Canonical equivalent circuit that models the three essential functions of any dc-to-dc converter: control, basic dc conversion, and low-pass filtering (continuous conduction mode).

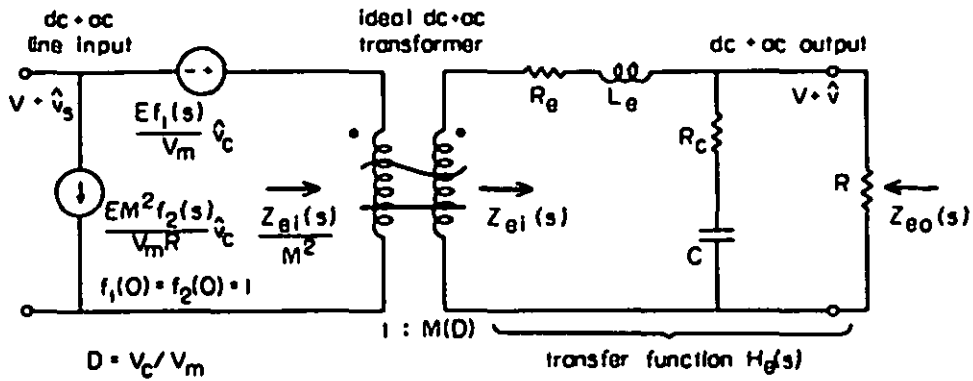


FIGURE 91. Canonical model representing any basic dc-dc converter.

TABLE VIII. Element values in the Canonical model of FIGURE 91 for the buck, boost, and buck-boost converters.

TYPE	M(D)	E	$f_1(s)$	$f_2(s)$	L_e
BUCK	D	$\frac{V}{D^2}$	1	1	L
BOOST	$\frac{1}{1-D}$	V	$1 - s \frac{L_e}{R}$	1	$\frac{L}{(1-D)^2}$
BUCK-BOOST	$\frac{D}{1-D}$	$-\frac{V}{D^2}$	$1 - s \frac{DL_e}{R}$	1	$\frac{L}{(1-D)^2}$

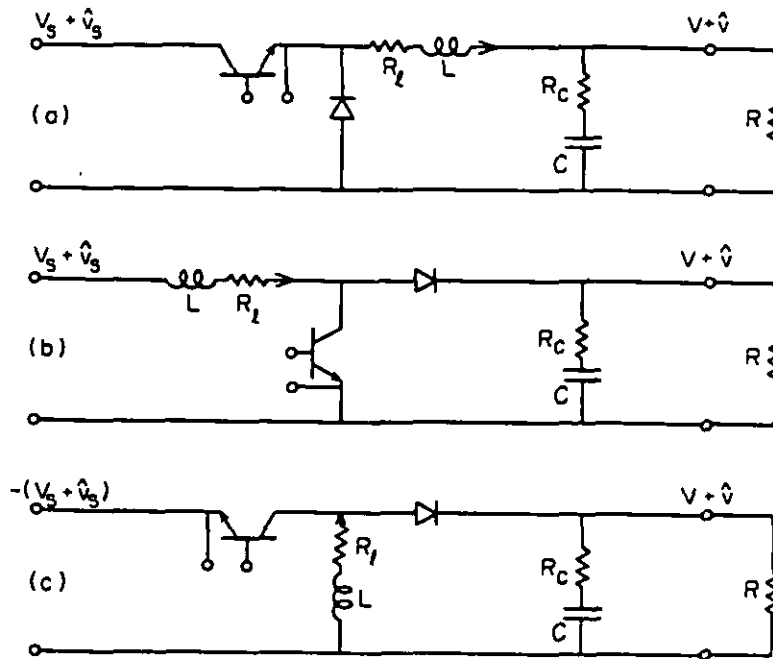


FIGURE 92. The basic dc-to-dc converter circuits for the (a) buck, (b) boost, and (c) buck-boost topologies.

The effective resistance R_e is not, in general, equal to the inductor resistance R_l in the actual converter circuits. R_e is a complex function of the various parasitic ohmic circuit resistances, the duty ratio D , and a resistance due to the transistor storage-time modulation (chapter 8 of reference 2). Since R_e is a parasitic resistance or second-order, in a practical case one merely tries to minimize some of these effects and accepts the resulting value. Those effects that lower the Q in a lossless manner may be advantageous (see APPENDIX B).

20.2 Boost-buck (Cuk). The boost-buck converter is shown in FIGURE 93 and the Canonical circuit model of this new switching converter is shown in FIGURE 94. The model in FIGURE 94 is equivalent to the models in FIGURES 90 and 91 although the low-pass filter network now consists of a two-section filter. Chapter 18 of Reference 2 discusses the origin of this new converter and recommends keeping well separated the resonant frequencies of each L section of the two-section filter. Also to reduce stabilization problems the following condition should be met:

$$L_e / R - R_e C_e D' < 0$$

Chapter 25 of reference 2 points out that this Cuk (boost-buck) converter can be considered as a conventional buck converter preceded by an input filter. Therefore, in a manner similar to the one presented in APPENDIX B, design criteria can be implemented by suitable choice of the relative corner frequencies and the damping of the effective input and output filters inherent in the Cuk converter.

30. Models of extended converter configurations. As stated in Section 20, the Canonical model represents the properties of any dc-to-dc converter, regardless of its detailed configuration. The model is derived for some commonly used extensions of the basic converter. This process requires additions to or redefinitions of the elements in the basic model.

30.1 Push-pull transformer-isolated. The topology for the push-pull converter is discussed in 3.3.5.3. It is basically a buck converter. As far as the Canonical model is concerned, the push-pull duplication is irrelevant; the effect is merely that the input voltage is impressed across the diode for a fraction D of the switching period, just as in the simple buck converter. The only extension to be accounted for is the half-primary to secondary turns ratio $1:n$ shown in FIGURE 95 wherein the circuit and its Canonical model are depicted.

The turns ratio is incorporated into the model's transformer producing a resultant ratio of $1:nD$. The voltage and current generators are thereby transferred to the other side of the $1:n$ transformer. Their values must, therefore, be changed by the respective factors $1/n$ and n , as shown in the Canonical model of FIGURE 95(b). The parasitic properties of the real transformer, such as leakage inductance and stray capacitance, could also be incorporated into the model, if desired.

30.2 Double-output single-ended transformer-isolated forward converter. This forward converter shown in FIGURE 96(a) is basically a buck converter. The transformer has two functions. First, it provided dc isolation achieving core reset by zener-diode clamping of the winding voltage during the switch off-time. Second, the transformer provides multiple outputs at different voltages determined by the respective turns ratios from primary to secondaries. Typically, one output, say V_1 , is the principal output rated at the highest current. V_1 is sensed to provide the feedback signal for closed-loop regulator operation. This output is then the regulated output, and the others are slaved outputs.

The Canonical model is established by referring element values to the secondary winding with n_1 turns. As a first step, a transformer of ratio $1:n_1$ is inserted to the left of the basic Canonical model for a buck converter. Then, this transformer is merged with that in the basic model to give a single transformer of ratio $1:n_1 D$ as shown in FIGURE 96(b). At the same time, the voltage and current generators are modified by the respective factors $1/n_1$ and n_1 . The other output circuit is shown reflected to the n_1 output (the element values are multiplied by the appropriate turns ratio factors). The only other extension required is that the current generator now has the load resistance R term replaced by the total effective load resistance referred to the principal output, namely R_1 in parallel with $(n_1/n_2)^2 R_2$. Additional outputs, of either positive or negative polarity, can obviously be incorporated in a similar manner into the Canonical model.

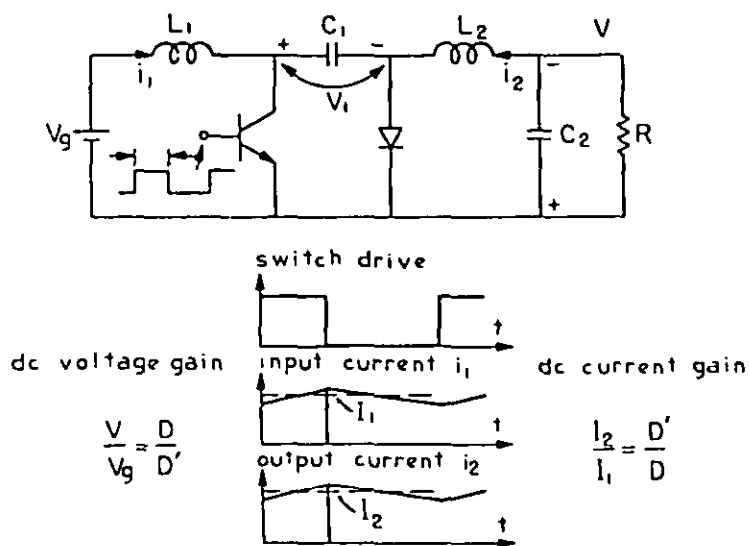
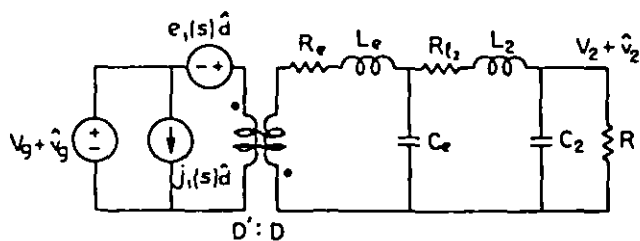


FIGURE 93. Basic Cuk switching-mode power supply configuration.



$$R_e = \left(\frac{D}{D'}\right)^2 R_{t1}, \quad L_e = \left(\frac{D}{D'}\right)^2 L_1, \quad C_e = \left(\frac{C_1}{D^2}\right)$$

FIGURE 94. Canonical circuit model of the Cuk converter for the continuous conduction mode ($D' = 1 - D$ and $M(D) = D/D'$).

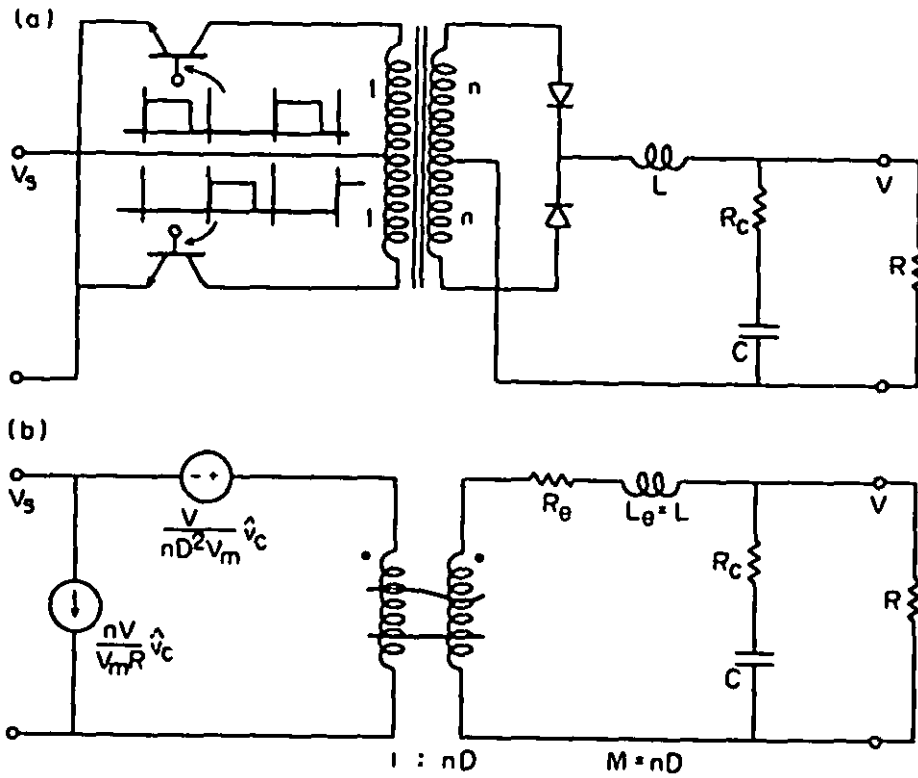


FIGURE 95. Push-pull transformer-coupled ("Quasi-square-wave") converter (buck-derived): (a) circuit; (b) Canonical model.

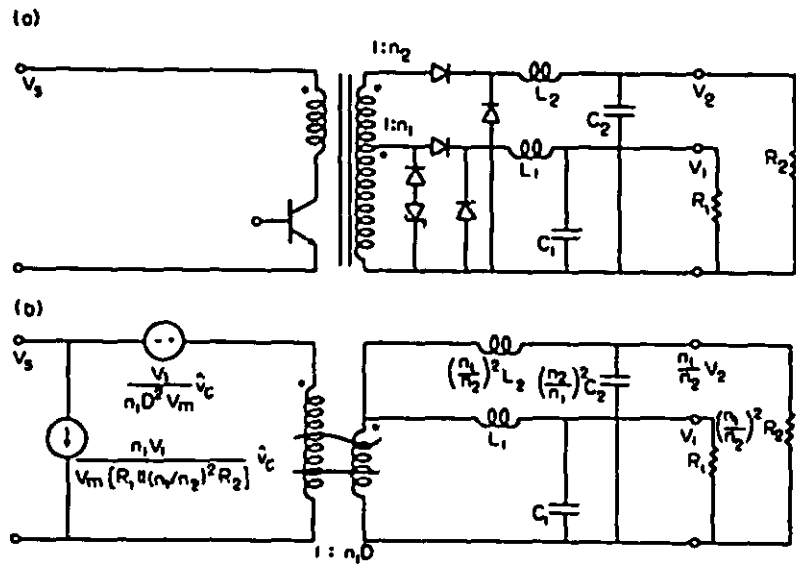


FIGURE 96. Double-output single-ended transformer-coupled ("forward") converter (buck-derived): (a) circuit; (b) Canonical model.

30.3 Single-ended transformer-isolated flyback converter. This flyback converter shown in FIGURE 97(a) is buck-boost derived. Again, V_1 is adopted as the principal output. The model elements are combined with the basic transformer of the basic buck-boost Canonical model to give a single transformer of ratio $(1-D):n_1D$. The voltage and current generators are likewise modified by their respective factors $1/n_1$ and n_1 . These preceding modifications are shown in FIGURE 97(b).

However, the multiple secondary outputs must be incorporated differently than in the buck-derived converters. In this buck-boost derived converter all outputs are served by a common inductor, the isolation transformer's primary inductance L . Therefore, in the extended Canonical model, both outputs are fed from the effective inductance L_e which is the reflected primary inductance $(n_1)^2L$ divided by the $(1-D)^2$ factor from TABLE VIII. It is to be noted that the effective filter in the principal output V_1 involves the total reflected capacitance of all outputs. This is unlike the previous example in which each output retained its individual filter.

Finally, the factor R in the current generator is again replaced by the total effective load at the principal output, namely R_1 in parallel with $(n_1/n_2)^2R_2$; and appropriate substitution for R and L_e is made in the expression from TABLE VIII for the voltage generator right-half-plane zero ω_a .

The appropriately reflected parasitic resistances R_e and R_c for the several outputs could of course be included in the extended Canonical models, but for simplicity have been omitted in FIGURES 96 and 97.

40. Performance properties of the Canonical model. The Canonical model of FIGURE 91 together with the element values of TABLE VIII, or as extended to represent more complicated converters, provides a basis for analysis and design of the converter dynamics. The Canonical model retains identification with the physical origin of its various elements, which is a prerequisite for the recommended design-oriented approach to the system analysis. To help further with the physical understanding of the converter dynamics in the context of the following sections, it is useful to review in graphical form the performance properties of the low-pass filter component of the Canonical model.

The three performance properties of the effective low-pass filter, as identified in the Canonical model of FIGURE 91, are the input impedance $Z_{ei}(s)$, the transfer function $H_e(s)$, and the output impedance $Z_{eo}(s)$. The results are considerably simplified if the (normally good) approximation is made that the load resistance R is much larger than either of the parasitic resistances R_e or R_c .

All three performance properties can be expressed in terms of two normalizing parameters of the filter and of its Q factor. The two normalizing parameters are the corner or resonant frequency $\omega_0 = 1/\sqrt{L_e C}$ and the characteristic resistance $R_0 = \sqrt{L_e/C}$. The Q factor describes the degree of damping, and is determined by the ratios of the three resistances to the characteristic resistance. To a good approximation, the Q factor is given by the parallel combination of the Q 's that would result if each resistance were accounted for alone, namely $Q = (R_0/R_e) \parallel (R_0/R_c) \parallel (R/R_0)$.

Alternatively it can be expressed as $Q = R_0/R_{te}$, where $R_{te} = R_e + R_c + (R_0)^2/R$ is the total effective series damping resistance.

The most useful form in which to express the performance properties is by graphical assembly of the asymptotes that represent their magnitudes as functions of frequency, on the usual dB versus log frequency scales, as shown in FIGURE 98. All of the useful salient features are shown on the graphs, namely the equations for the asymptotes and corner frequencies. The solid lines represent a high- Q , or underdamped case ($Q > 0.5$), and the dashed lines represent a low- Q , or overdamped case ($Q < 0.5$). The value of Q determines the manner in which each function goes through-resonance at ω_0 ; in the low- Q case, an intermediate straight-line asymptote appears that intersects the neighboring asymptotes at corner frequencies given (to a good approximation) by $Q\omega_0$ and ω_0/Q . The input impedance $|Z_{ei}|$ has the minimum characteristics of series resonance, of the total effective series resistance R_{te} ; and the output impedance $|Z_{eo}|$ has the maximum, characteristic of parallel resonance, of $(R_0)^2/R_{te}$ (which is the total effective shunt resistance).

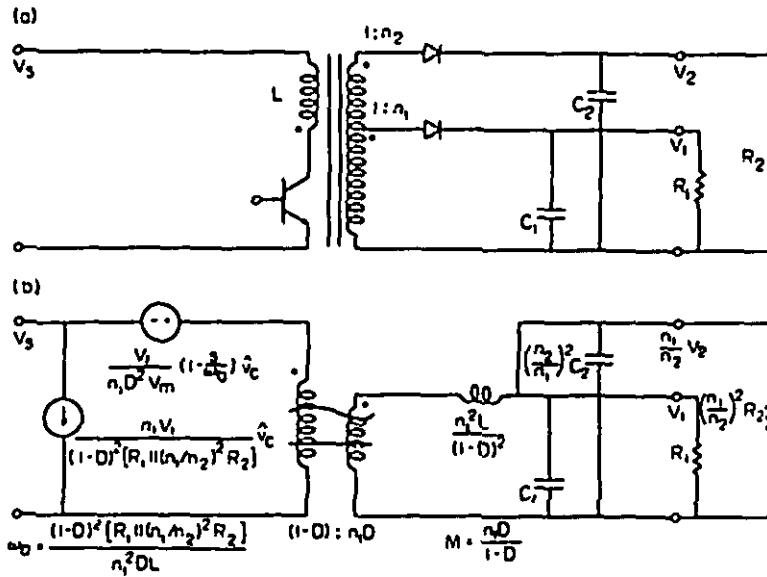


FIGURE 97. Double-output single-ended transformer-coupled ("flyback") converter (buck-boost-derived):
(a) circuit; (b) Canonical model.

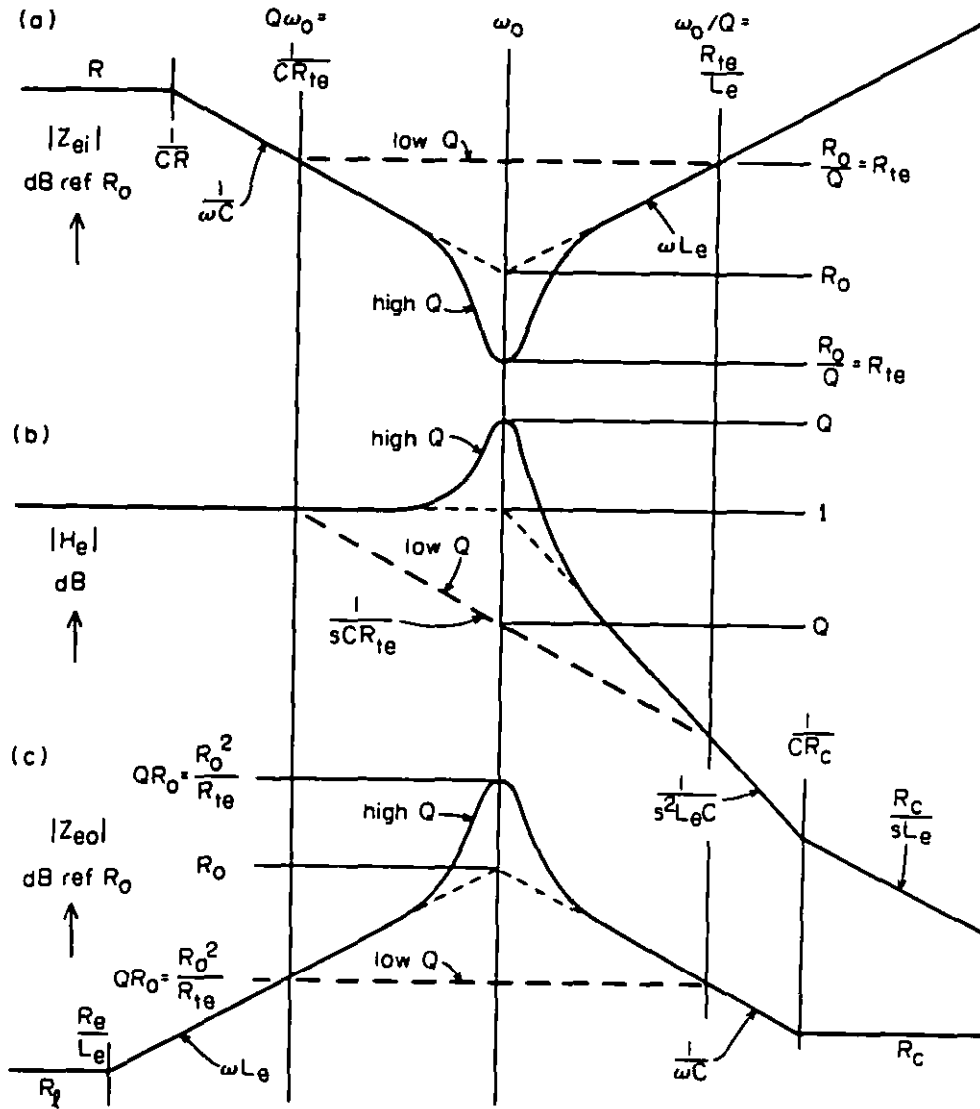


FIGURE 98. Asymptote shapes for the magnitudes of (a) the input impedance $|Z_{ei}|$ (b) the transfer function $|H_e|$, (c) the output impedance $|Z_{eo}|$ of the effective low-pass filter in the Canonical model of FIGURE 91.

PREVENTING INPUT-FILTER OSCILLATIONS IN SWITCHING REGULATORS

10. Introduction. As discussed in 3.3.4.2, switching-mode regulators have a negative input resistance at low frequencies, and can become unstable by addition of input filters. Preferably a suitable input filter or filters should be incorporated into the original regulator design. Knowledge of the design permits criteria developed by Middlebrook to be applied, ensuring not only system stability but also virtually no effect on the important properties of loop gain, output impedance, and line rejection. If, however, a line filter is added to a black box regulator, then one must measure the input impedance as a function of frequency to determine stability; however, the resulting regulator properties can only be incompletely predicted. (The discussion and figures (with permission) in Sections 20, 30, 50 and 70, are taken with some modifications from two papers by R.D. Middlebrook, references 37 and 51, both papers also appearing in the reference 2 volumes.)

20. Design criteria for input filter and converter effective filter. The model shown in FIGURE 99 represents a general switching-mode regulator with addition of a line input filter and incorporation of the Canonical model of APPENDIX A. To prevent instability the magnitude of the output impedance of the input filter (or filters), $|Z_s|$, must be less than the magnitude of the open-loop impedance of the switching-mode power supply. With reference to FIGURE 99, it is seen that $|Z_{e1}/M^2|$ is the value of Z_i that would be observed under open-loop conditions (in which both controlled generators are deactivated), and is thus identified as the regulator open-loop input impedance. Both relevant impedances, $|Z_{e1}/M^2|$ and $|Z_s|$, are shown in FIGURE 100 as a function of frequency.

$|Z_{e1}/M^2|$, shown as the top curve in FIGURE 100, represents the magnitude of the reflected impedance of the series-resonant loaded averaging (output) filter; which is equal to in magnitude to R/M^2 at dc and low frequencies, declines along the asymptote $1/M^2 \omega C$ above the corner frequency $1/RC$, reaches a minimum of R_{te}/M^2 at the resonance (averaging filter cutoff) frequency $\omega_0 = 1/\sqrt{L_e C}$; and then rises along the asymptote $\omega L_e/M^2$ passing through the corner frequency R/L_e . L_e and R_e are the parameters modeled in FIGURE 99 where only for the buck configuration is L_e equivalent to the output filter inductance but also depends on the duty cycle, D , for the boost and buck-boost; and where R_e is the effective resistance. Two cases for $|Z_{e1}/M^2|$ are illustrated in FIGURE 100, the solid line for the high Q , and the dashed line for the low Q ; in each case the minimum impedance is $|R_{te}/M^2|$, but in the low Q case the minimum is spread over a wider frequency range (see APPENDIX A, Sections 20.1 and 40 and FIGURE 98, for determination of R_e , R_{te} , and Q factors).

$|Z_s|$, shown as the lower curve in FIGURE 100 represents the input filter's output impedance, here shown for a single-section filter. However, Z_s may comprise a multiple-section filter; and in addition include the low-pass filter in the ac line (for ac-to-dc power supplies); and also include the impedances of the input power cables and generator if they are significant. The basic single-section input filter illustrated in FIGURE 100 has an output impedance Z_s that represents a damped parallel-resonant circuit, which is equal to R_{1s} at dc and low frequencies, rises along with asymptote ωL_s , and declines along an asymptote $1/\omega C_s$ after reaching a maximum of $|Z_s|_{\max}$ (see figures 102 and 103). A practical input filter, regardless of its complexity, will have an output section and consequently an output impedance Z_s that has similar salient features, so that the general shape of $|Z_s|$ illustrated in FIGURE 100 is adequately characterized by a low-frequency value R_{1s} and a resonant maximum value $|Z_s|_{\max}$ at or about a frequency ω_s .

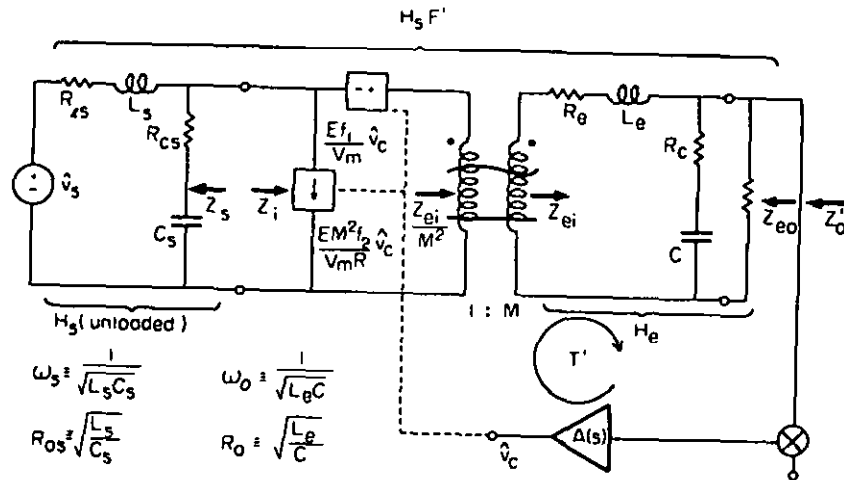


FIGURE 99. Model of the general switching-mode regulator with addition of a line input filter and incorporation of the Canonical model.

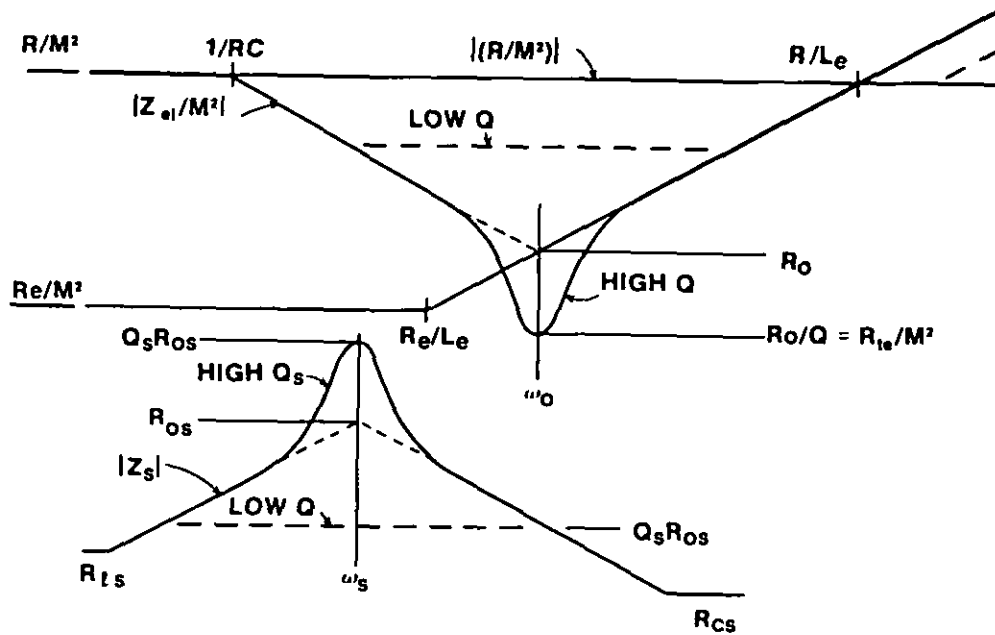


FIGURE 100. Desired relative placement of the magnitude shapes of the input filter output impedance $|Z_s|$ with respect to the open-loop input impedance $|Z_{ei}/M^2|$, and the open-loop short-circuit input impedance $(R_e + sL_e)/M^2$.

20.1 Stability and line rejection criterion. The addition of an input filter will not cause instability if

$$|Z_s| \ll |Z_{ei}/M^2|$$

Stability is assured because the inequality causes the loop gain to be essentially unaffected by the addition of the input filter. The inequality also ensures that the line to output transfer function and, therefore, the line rejection is essentially unaffected. The line to output transfer function determines what frequencies (including noise) are prevented from being transferred from input to output. FIGURE 100 contains all the necessary information for design of the system to satisfy the desirable inequality. It is obviously not desirable to place the input filter cutoff frequency ω_s near the averaging filter cutoff frequency ω_o , since this would impose the lowest limit on the maximum value $|Z_s|_{\max}$. Placing ω_s above ω_o , while relaxing the requirement on $|Z_s|_{\max}$, makes the filtering requirement beyond filter cutoff more stringent since ω_s will then be closer to the regulator switching frequency. The practical solution is usually to place ω_s below rather than above ω_o .

30. Output impedance criterion. If the regulator output impedance is to be essentially unaffected a more stringent condition is required, that

$$|Z_s| \ll |(R_e + sL_e) / M^2|$$

where $(R_e + sL_e) / M^2$ is the regulator open-loop short-circuit impedance, that is, the open-loop value of Z_{ei} that would be measured with the regulator output shorted. As indicated in the center plot of FIGURE 100, $(R_e + sL_e) / M^2$ remains at the dc and low-frequency value R_e/M^2 until the corner frequency R_e/L_e , and then follows the same $\omega L_e/M^2$ asymptote as does Z_{ei}/M^2 .

To meet this inequality in addition to the stability inequality, the design problem is essentially that of placing the typical shape of $|Z_s|$ in both vertical and horizontal positions so that at all frequencies it is below the lowest of both of the other two shapes. Placing ω_s below ω_o relaxes the filtering requirement and also relaxes the maximum $|Z_s|$ requirement as far as comparison with $|Z_{ei}/M^2|$ is concerned, but not as far as comparison with $|(R_e + sL_e)/M^2|$ is concerned. This condition is more difficult to achieve than the condition in 20.1 because R_e is the effective (parasitic) resistance and therefore to be minimized, whereas the load resistance R is almost always much higher. Heavier damping of the input filter resonant peak is required and lossless damping recommendations will be discussed in 50.1.

40. Simplified models for open-loop input impedance. FIGURE 101 shows how to arrive at simple models for the open-loop input impedance Z_{ei}/M^2 , for two different types of switching-mode power supplies. Both examples use transformer isolation but one is buck-derived and the other is buck-boost derived (flyback).

The top figures are circuit schematics for the dc to dc part of two ac to dc power supplies. Both examples are for 155 Vdc inputs and 5 Vdc outputs. 155 Vdc is approximately the dc voltage obtained from rectifying and peak filtering single-phase power at 115 Vac 60 Hz.

The center figures for both examples are the Middlebrook models (see APPENDIX A). In both model-examples a good approximation for M is the ratio of output to input dc voltage ($5/155 = 1/31$).

Since only the open-loop input impedance needs to be modelled a further simplification is shown in the bottom figures with the closed loop feedback generators removed and the transformer ratio M incorporated into the circuit parameters. Note that the inductance in the simplified model is the same as the original circuit inductance only for the buck-derived example. For the flyback the model inductance one must also know the duty ratio D and the transformer ratio n . If, however, M is known, then either D or n is sufficient to determine L_e . For the flyback example, simple algebraic substitution obtains $L_e = L(M/D)^2$ or $L_e = L(n+M)^2$.

Other switching-mode designs may be similarly simplified using the topological circuits in 3.3.5 and the models in APPENDIX A.

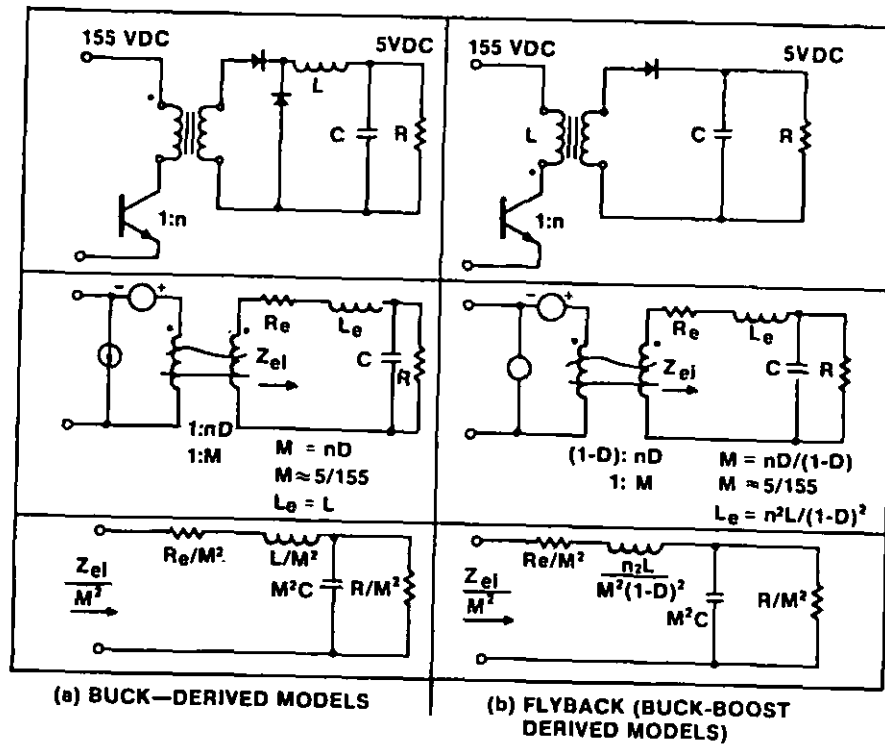


FIGURE 101. Simplified circuit examples of open-loop input impedance.

50. Realization of input filter design requirements. Herein, various filter configurations are discussed with respect to their properties as input filters for switching regulators. The treatment is not quantitatively exact, but is entirely adequate for design purposes and has the merit of permitting easy qualitative comparisons leading to simple design criteria; exact computations can be made if needed for complex circuits or to verify the adequacy of the design when parasitics are included (see APPENDIX C for computer program).

Specifically, the input filter design problem is that of realization of the two functions $H_s(s)$ and Z_s to satisfy the several performance requirements and constraints. The greater the number of elements in the filter, the more degrees of freedom there are available to optimize $H_s(s)$ and Z_s .

The design of $H_s(s)$, the forward voltage transfer function and the reverse current transfer function, is usually imposed by the requirement for a certain attenuation at the regulator switching frequency (see 5.2). For the basic single-section LC filter represented in FIGURE 102, this requirement specifies a filter cutoff frequency $\omega_s = 1/\sqrt{L_s C_s}$ and hence a certain $L_s C_s$ product. The series resistance R_s is always to be minimized in the interest of efficiency, and can be considered fixed; therefore, the only remaining design degree of freedom is through the filter characteristic resistance $R_0 = \sqrt{L_s/C_s}$. This parameter determines the Q-factor and hence the degree of peaking of both the $|H_s(s)|$ and $|Z_s|$ characteristics, as also shown in FIGURE 102. In particular the filter output impedance $|Z_s|$ has a maximum $|Z_s|_{\max} = R_m = (R_0^2/R_s) \sqrt{1 + (R_s/R_0)^2}$ at the filter cutoff frequency ω_s . To keep $|Z_s|_{\max}$ as low as possible the filter characteristic resistance R_0 has to be made low, which in many systems implies an impractically low L_s/C_s ratio. It is because of too high an L_s/C_s ratio and consequent high $|Z_s|_{\max}$ that actual systems with simple input filters of this type are prone to instability.

Given an L_s/C_s ratio that is too high for the required $|Z_s|_{\max}$, an alternative is to lower the Q-factor by addition of extra series damping resistance. Since one does not wish to increase R_s , a resistance R_c may be placed in the series with C_s as shown in FIGURE 103. The $|Z_s|_{\max}$ is now reduced by the factor $R_s \sqrt{1 + (R_c/R_0)^2} / (R_s + R_c)$ from its previous value R_m , but the H_s has been degraded by appearance of a zero at $\omega_s R_0/R_c$ so that the switching frequency attenuation is degraded. Also, since most of the regulator switching frequency input current flow in C_s there may be substantial power loss in R_c .

A more attractive way of lowering the output impedance maximum is to add parallel damping resistance R_p across L_s , as shown in FIGURE 104. The $|Z_s|_{\max}$ is now reduced by the factor $1/(1 + R_0^2/R_s R_p)$ from R_m , but H_s is again degraded by appearance of a zero at $\omega_s R_p/R_0$. Thus, the $|H_s|$ and $|Z_s|$ characteristics are the same in nature as for the series damping resistance R_c , but there is negligible power loss in the parallel damping resistance R_p .

An improvement is to place the parallel damping resistance R_p across C_s instead of across L_s , as shown in FIGURE 105. This has the same desirable effect in lowering $|Z_s|_{\max}$, and does not introduce an unwanted zero in H_s . Since there is also negligible power dissipation in R_p , this arrangement is the best so far discussed, but has the disadvantage that a large blocking capacitor is needed.

A large variety of double-section input filters can be constructed by cascading combinations of the several single-section filters. One possibility is shown in FIGURE 106, in which the series resistances in the dc path are neglected. The $H_s(s)$ of this filter has a zero and four poles, giving a high-frequency asymptote for $H_s(s)$ of -18 dB/octave. It is undesirable to make two resonant frequencies $\omega_1 = 1/\sqrt{L_1 C_1}$ and $\omega_2 = 1/\sqrt{L_2 C_2}$ equal, since it can be shown that this not only causes the output impedance to have a sharp maximum, higher than would otherwise be the case, but also causes the filter input impedance to have a sharp minimum, possibly much less than R_c , which may be undesirable for the source to see. Therefore, the double-section input filter of FIGURE 106 is usually designed with well-separated resonant frequencies such that $\omega_1 \ll \omega_2$.

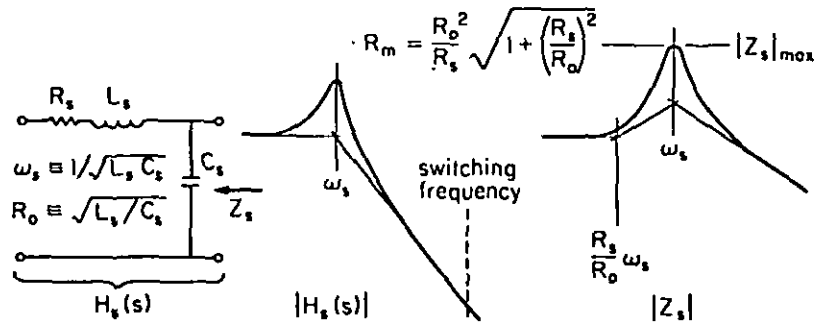


FIGURE 102. The basic single-section input filter, its two pole transfer characteristic $|H_s(s)|$, and output impedance $|Z_s|$ with $|Z_s|_{\max} = R_m$.

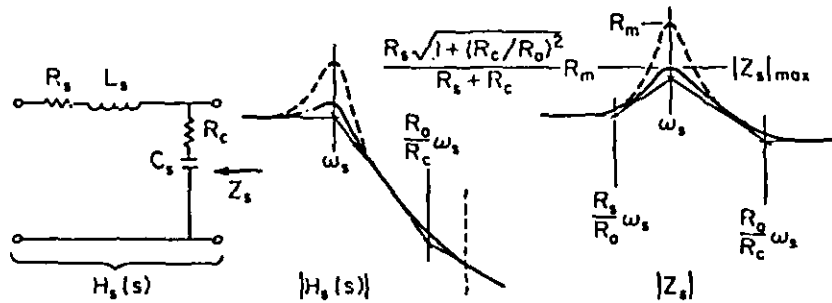


FIGURE 103. Single-section input filter with extra series damping resistance R_c , its two-pole one-zero $|H_s(s)|$, and $|Z_s|$ with $|Z_s|_{\max}$ lower than R_m .

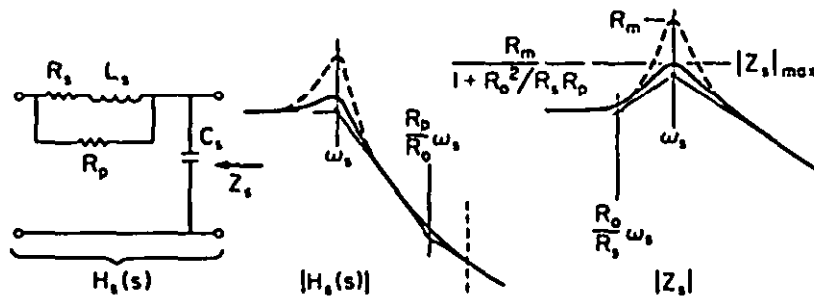


FIGURE 104. Single-section input filter with parallel damping resistance R_p across the inductor, its two-pole one-zero $|H_s(s)|$, and $|Z_s|$ with $|Z_s|_{max}$ lower than R_m .

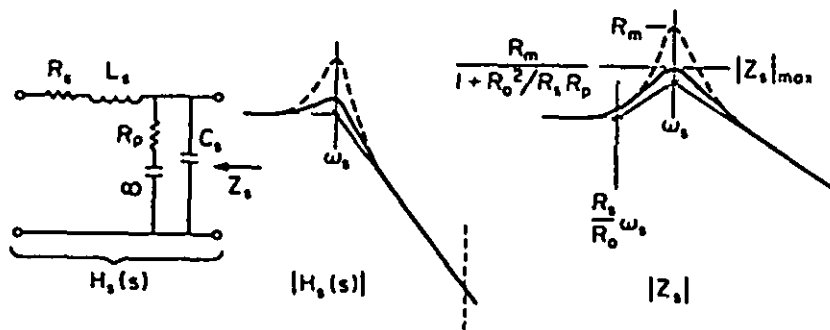


FIGURE 105. Single-section input filter with parallel damping resistance R_p across the capacitor, its two-pole $|H_s(s)|$, and $|Z_s|$ with $|Z_s|_{max}$ lower than R_m .

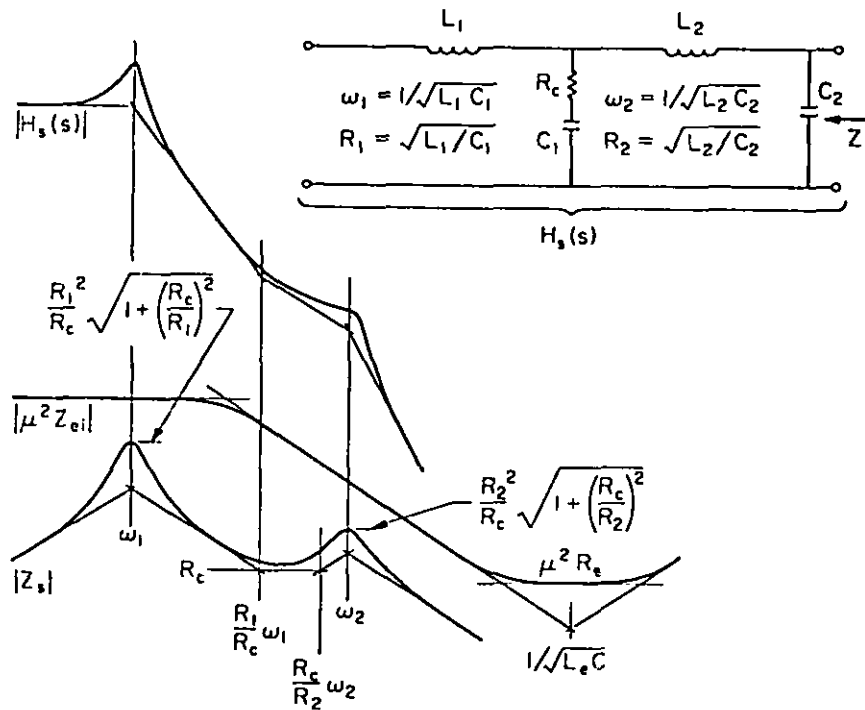


FIGURE 106. Double-section input filter and its four-pole one-zero $|H_s(s)|$ its $|Z_s|$ has two maxima, shown in typical relation to the regulator open-loop input impedance $|\mu^2 Z_{ei}|$

With $\omega_1 \ll \omega_2$, the $|H_s(s)|$ and $|Z_s|$ functions of the double-section input filter can be determined approximately by superposition of those of the two sections separately, as shown in FIGURE 106.

It is seen that the output impedance $|Z_s|$ now has two maxima, both of which must be controlled to satisfy the various inequalities discussed in the previous sections. A practical example, also shown in FIGURE 106, is the case in which the switching regulator open-loop input impedance $|Z_{e1}/M^2|$ is following a -6 dB/octave slope, that is, between the averaging filter corner frequency $1/RC$ and $1/\omega L_e C$: here, the $|Z_s|_{\max}$ at the higher input filter resonance frequency ω_2 must be made smaller than that at the lower input filter resonance frequency ω_1 , in order to maintain equal degrees of inequality $|Z_s| \ll |Z_{e1}/M^2|$ at the two frequencies. This implies that the second section characteristic resistance R_2 should be lower than that of the first section, R_1 .

A paper by T.K. Phelps and W.S. Tate (reference 52) provides design information for nine commonly used one and two-section L-C filters with a goal of optimizing the performance of switching power converters.

50.1 Optimum damping for given blocking capacitance value. The damping of a single-section LC filter (see FIGURE 107) is determined by three resistances: two in series (one with inductance (R_e) and one with capacitance R_c), and one in shunt (R) (across the capacitance and its series resistance). Increasing any of the series resistances is undesirable (resulting in less efficiency or introducing a zero in the transfer function.) As discussed for FIGURE 105, a preferred solution is to parallel the load resistance with a series combination of additional damping shunt resistance and a blocking capacitor (to avoid power loss). This solution is represented in FIGURE 108. The parasitic series resistances and load resistance are omitted since damping is to be controlled by R_d which defines a Q-factor.

$$Q = R_d/R_0$$

where $R_0 = L/C$ is the characteristic resistance of the filter. The blocking capacitor is defined as n times the original filter capacitance C .

An optimum damping resistance R_0 exists for a given blocking capacitance value but the optimum R_0 (to get optimum Q) is different for the three properties of concern; transfer function (H), input impedance (Z_i) and output impedance (Z_o). If damping of one property is optimized, those of the other two will not be optimized. In applications to switching regulators, therefore, compromises are necessary which nevertheless allow a smaller value of blocking capacitance to be employed than otherwise would be the case. Design criteria are given in reference 51.

60. Filter design optimization methodology. A power processing optimization methodology is presented in reference 36 to meet required specifications for a design and concurrently to optimize a given design quantity. Such a quantity can be weight, efficiency, regulator response, or any other physically-realizable entity. Three inductor design examples are given to demonstrate the methodology: (1) A minimum weight inductor with the wire size predetermined; (2) a minimum weight inductor subject to a given loss constraint; and (3) a minimum loss inductor subject to a given weight constraint. Computer programs have been prepared by TRW for these optimum inductor designs as part of the Modelling and Analysis of Power Processing Systems (MAPPS) project (sponsored by NASA Lewis Research Center under Contract #NA3-19690)¹¹¹.

Also given in reference 36 are more complex optimum weight designs, one for a single-stage and a second for a two-stage filter, and they are compared. Theoretical equations and an example are given for each filter. To facilitate a realistic comparison, four requirements were assumed identical for both filters:

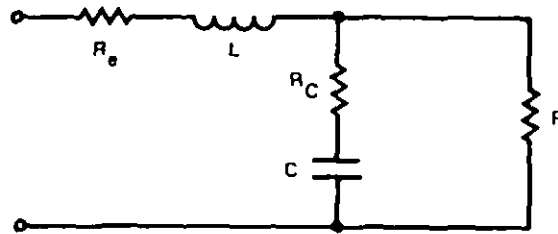
F: frequency of switching current = 20 kHz

G: attenuation required at frequency $F = .002$ (-54 dB)

I_{dc} : dc current in inductors = 3 amps

P: power loss allowed = 0.6 watts

¹¹¹ NOSC has verified the programs' utility by trial applications.



$$Q = \frac{R_o}{R_{te}} \text{ DEGREE OF DAMPING AT } \omega_o$$

$$\text{Where } R_o = \sqrt{\frac{L}{C}}$$

$$\omega_o = \frac{1}{\sqrt{LC}}$$

$$\text{And } R_{te} = R_e + R_c + R_o^2/R$$

= TOTAL EFFECTIVE DAMPING RESISTANCE

FIGURE 107. Q of an LC filter.

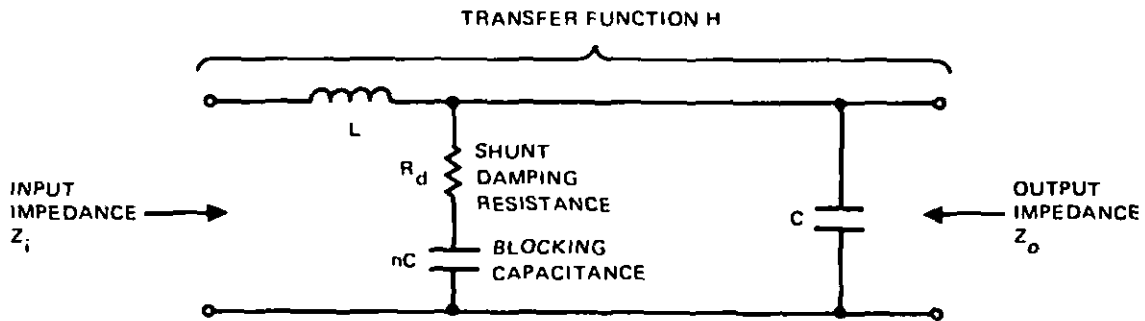


FIGURE 108. Single-section low-pass LC filter with blocked shunt damping resistance.

60.1 Single-section optimum weight filter. FIGURE 45 shows the schematic of the resultant minimum weight one-stage filter (499 grams^{IV}). Using techniques described by Middlebrook in reference 2, a graphical analysis is also shown in FIGURE 45. The graphical analysis enables one to predict the attenuation beyond 20 kHz--the slope is -40 dB per decade (assuming components are frequency invariant). The filter frequency turns out to be

$$f_0 = 1/2\pi\sqrt{LC} = 895 \text{ Hz}$$

and its resonant peaking is

$$20 \log Q = 20 \log(\omega_0 L/R) = 6 \text{ dB}$$

Note that the approximate graphical analysis results in almost exactly -54 dB at 20 kHz (the design requirement).

60.2 Two-section optimum weight filter. FIGURE 44 shows the schematic of the resultant minimum weight two-stage filter (171 grams^V). Here again graphical analysis permits attenuation evaluation at frequencies other than 20 kHz--the slope is -60 dB per decade beyond 20 kHz (assuming constant parameters). The filter transfer function contains four poles and one zero. At the lower resonant frequency,

$$\omega_1^2 = 1/L_1 C_1 = 4.3 \times 10^7$$

$$f_1 = \nu_1/2\pi = 1.05 \text{ kHz}$$

and at a higher resonant frequency

$$\omega_2^2 = 1/L_2 C_2 = 4.85 \times 10^8$$

$$f_2 = \nu_2/2\pi = 3.51 \text{ kHz.}$$

Resonant peaking at the first stage filter (Q₁) (neglecting the small inductor resistance) calculates to be (reference 36)

$$Q_1 = 20 \log_{10} \sqrt{(1 + L_1/C_1 R_c^2) / ((C_2/C_1)^2 + (L_1/C_1 R_c^2)(1 - C_2/C_1 - L_2 C_2/L_1 C_1)^2)}$$

thus

$$Q_1 = 20 \log_{10} \sqrt{(1 + (R_1/R_c)^2) / ((C_2/C_1)^2 + (R_1/R_c)^2 [1 - C_2/C_1 - (\omega_1/\omega_2)^2]^2)}$$

$$Q_1 = 20 \log_{10} 2.05 = 6.3 \text{ dB}$$

and at the second stage,

$$Q_2 = 20 \log_{10} \sqrt{L_2/L_1} = -4.7 \text{ dB}$$

60.3 Optimum filters designed for higher attenuation. Both the one and two-stage filters were designed for -54 dB at 20 kHz. If additional attenuation were required, both filters would need larger components (to resonate at lower frequencies). This would be less costly with the two-stage filter since the slope is -60 dB per decade (for example, another 10.6 dB of attenuation could be obtained by shifting the entire curve in FIGURE 44 to the left so that f₁ is 700 Hz whereas in FIGURE 45, 10.6 dB additional attenuation would require shifting the resonant frequency to 485 Hz.)

Using the same filters, additional attenuation can be achieved by increasing the switching frequency. For example, if the frequency were doubled to 40 kHz the single-section filter (see FIGURE 45) would increase its attenuation 12 dB at the new switching frequency (change in transfer function from -54 dB to -66 dB). The two-section filter (see FIGURE 44) would increase its attenuation even more (18 dB) resulting in a transfer function of -72 dB at the new switching frequency. Higher switching frequencies would result in even higher attenuations.

IV Assumes foil tantalum capacitor, 372 kg/F.

V Assumes foil tantalum capacitor for C₁ (372 kg/F) and polycarbonate capacitor for C₂ (2600 kg/F).

70. "Black-box" direct measurements. If the regulator is a black-box and open-loop input impedance magnitude $|Z_{ei}/M^2|$ is not known then one must resort to measurement. However, direct measurements must be made in the normal closed-loop operation and the impedance magnitude thus obtained is $|Z_i|$. Although measurements taken by Middlebrook indicated that both the low-frequency and high-frequency asymptotes of $|Z_i|$ are essentially the same as of $|Z_{ei}/M^2|$, the dip at the intermediate frequencies is smaller for $|Z_i|$. A filter designed to satisfy $|Z_s| \ll |Z_i|$, which ensures stability, does not necessarily satisfy $|Z_s| \ll |Z_{ei}/M^2|$ or $|Z_s| \ll |(R_{1s} + L_e)/M^2|$ which would ensure negligible disturbance of F (line rejection) or Z_o (output impedance).

FILTER AND LOAD CHARACTERISTICS COMPUTER PROGRAM

10. Introduction. This computer program was prepared as an adjunct to APPENDIX B. The program evaluates the attenuation characteristic of the input low-pass filter and also determines whether or not the Middlebrook stability criterion is being met (so that the addition of this input filter to a switching regulator will not cause the switching regulator to become an oscillator). APPENDIX B, Section 50, determines both the attenuation and stability characteristics by a simplified analysis that is almost always adequate for design purposes. This program, however, will be useful to verify the characteristics of the filter design and include, if significant, the parasitic, source, and load impedances.

The circuit is limited in complexity to the components depicted in FIGURE 109. The multi-section filter represents the input filter configuration, and validly includes the EMI filter in the ac line if the ac current flows continuously. The load components to the right of V_o represents the open-loop input impedance model of the switching regulator (see FIGURE 101 of APPENDIX B).

(NOTE: Although the circuit components are labelled with names useful for this application, this program need not be limited to this application. This program is based on simple circuit analysis equations, and therefore, may also be used for other circuit analysis applications requiring no more circuit complexity than is shown in FIGURE 103.)

Section 20 which follows is an example of the program output and includes a printout of the instructions. The attenuation is obtained by evaluating (and plotting) the voltage gain, voltage out divided by voltage in, V_o/V_s , (see FIGURE 109). In this example the attenuation is first obtained assuming zero source impedance and infinite load impedance (see the first graph of Section 20). When source and load impedance values are inserted a glitch in the attenuation curve occurs at the switching regulator output filter's resonance frequency (see the second graph in Section 20).

Section 20 also evaluates the two impedances needed to determine the stability criterion. They are Z_l , the load input impedance corresponding to the open-loop input impedance of the switching regulator; and Z_s , the output impedance of the input filter configuration (including source impedances if desired). To prevent oscillation the magnitude of Z_s must be very much less than the magnitude of Z_l at any frequency. The program includes a plot of these two impedances superimposed on one graph and the stability criterion can readily be determined thereby. An example was used to demonstrate the violation of the stability criterion and to indicate the necessity of using sufficient frequency points. Initially the two superimposed plots do not cross because too few frequency points were used (see the third graph of Section 20). For high Q circuits such as in this example a greater number of points need to be plotted as shown in the graph of superimposed impedances at the end of the program output.

Section 30 is the program listing. It is written in HP basic for the Hewlett Packard HP-85 desk top Personal Computer. The program listing is stored on a tape cartridge. It is anticipated that cartridges for this program may be made available from the Hewlett Packard library. Until then it may be obtained by supplying a blank tape cartridge either to NAVLEX 832 (W. Jackson, Washington, DC 20363 -tel (202) 692-0599) or to NOSC 5512 (E. Kamm, San Diego, CA 92152 - tel (619) 225-2752).

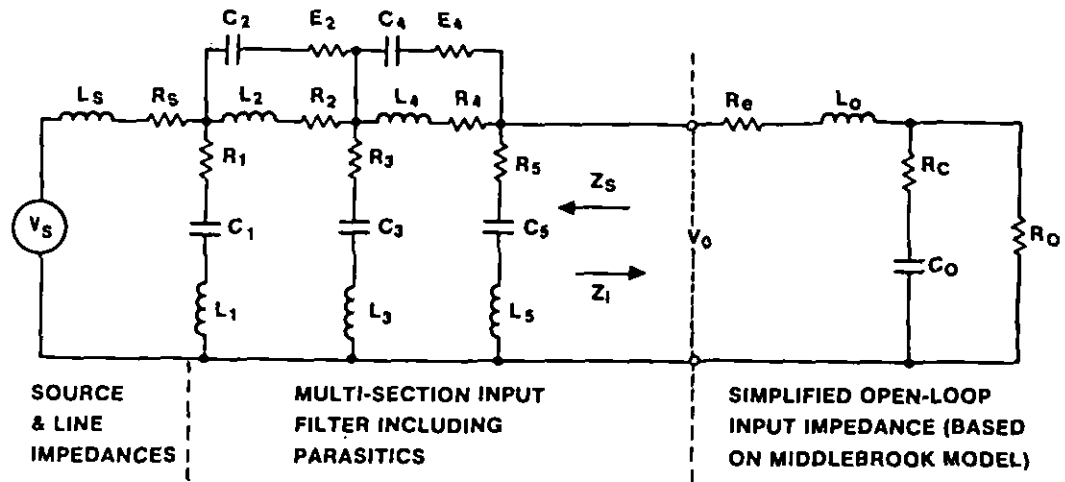


FIGURE 109. Circuit for computer program: evaluation of input filter attenuation and its effect on stability of switching regulator.

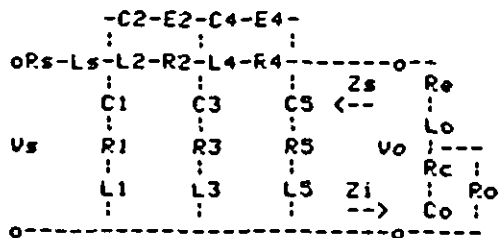
SECTION 20. PROGRAM OUTPUT WITH INSTRUCTIONS

FILTER AND LOAD CHARACTERISTICS PLOTTING PROGRAM

This program evaluates and plots (in dB) the first three filter and load characteristics listed below. In addition the impedances can be plotted superimposed on one graph as listed in item (4) below.

- 1) Filter Voltage Gain (V_{out}/V_s)
- 2) Input Load Impedance (Z_i ref 1 ohm)
- 3) Output Filter Impedance (Z_s ref 1 ohm)
- 4) Superimposed Impedances (Z_i and Z_s)

Impedances are referenced to one ohm. The output impedance, Z_s , is the impedance looking back into the filter with V_s short circuited. The loaded filter will be displayed and you will be asked to enter the value of each component. You will also be asked which characteristic you would like plotted, the frequency range over which the plot is to be made, and if you want the plotted points printed on paper as well.



Do you want a copy of the component values you enter?
 YES

To short circuit an unwanted component, set $R=L=0, C=1E100$.
 To open circuit an unwanted component, set $R=L=1E100, C=1E-100$.

Units of component values:
 $R=Ohms, C=Farads, L=Henries$

Source resistance, R_s
 ?
 0
 Source inductance, L_s
 ?
 0
 Load resistance, R_o
 ?
 1E100

Load shunt capacitance, C_o
 ?
 1E-100
 Load parasitic shunt resistance, R_c
 ?
 1E100
 Load series inductance, L_o
 ?
 1E100
 Load effective parasitic series resistance, R_e
 ?
 1E100
 Shunt capacitance, C_1
 ?
 1E-100
 Equivalent series resistance, R_1 of C_1
 ?
 1E100
 Equivalent series inductance, L_1 of C_1
 ?
 1E100
 Series Inductance, L_2
 ?
 309E-6
 Winding resistance, R_2 of L_2
 ?
 .0237
 Parasitic capacitance, C_2 of L_2
 ?
 1E-100
 Core loss resistance, E_2 of L_2
 ?
 1E100
 Shunt capacitance, C_3
 ?
 75E-6
 Equivalent series resistance, R_3 of C_3
 ?
 2.12
 Equivalent series inductance, L_3 of C_3
 ?
 0
 Series Inductance, L_4
 ?
 103E-6
 Winding resistance, R_4 of L_4
 ?
 .0159
 Parasitic capacitance, C_4 of L_4
 ?
 1E-100
 Core loss resistance, E_4 of L_4
 ?
 1E100
 Shunt capacitance, C_5
 ?
 20E-6
 Equivalent series resistance, R_5 of C_5
 ?
 0
 Equivalent series inductance, L_5 of C_5
 ?
 0

- 1) Filter Voltage Gain (V_{out}/V_s)
- 2) Input Load Impedance (Z_i ref 1 ohm)
- 3) Output Filter Impedance (Z_s ref 1 ohm)
- 4) Superimposed Impedances (Z_i and Z_s)

Enter number of desired Plot?

1

Would you like to Plot:

- 1) Magnitude and Phase
- 2) Magnitude only
- 3) Phase only

?

1

Lower frequency limit?

1E2

Upper frequency limit?

1E6

How many frequency points would you like plotted?

20

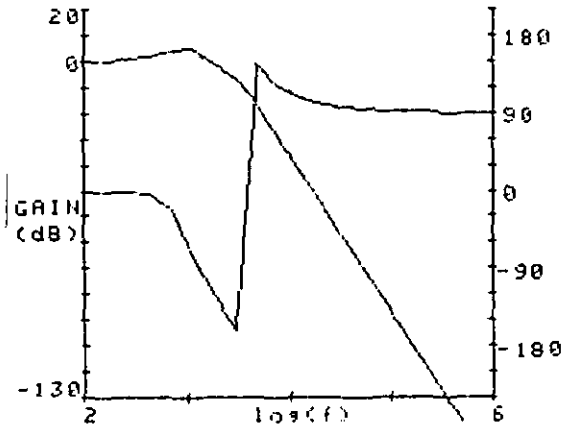
Do you want a Print-out of the plotted values?

YES

FREQ.	MAG.	PHASE
1.00E+002	+1.07E-001	-.15
1.62E+002	+2.80E-001	-.38
2.64E+002	+7.32E-001	-1.22
4.28E+002	+1.88E+000	-4.68
6.95E+002	+4.49E+000	-20.32
1.13E+003	+5.29E+000	-76.20
1.83E+003	-1.03E+000	-122.48
2.98E+003	-6.98E+000	-161.87
4.83E+003	-1.69E+001	+147.00
7.85E+003	-3.02E+001	+118.80
1.27E+004	-4.34E+001	+106.21
2.07E+004	-5.62E+001	+99.63
3.36E+004	-6.90E+001	+95.85
5.46E+004	-8.16E+001	+93.59
8.86E+004	-9.43E+001	+92.20
1.44E+005	-1.07E+002	+91.36
2.34E+005	-1.20E+002	+90.84
3.79E+005	-1.32E+002	+90.51
6.16E+005	-1.45E+002	+90.32
1.00E+006	-1.57E+002	+90.20

Do you want a COPY of the Plot?

YES



Are more plots to be made?

YES

Would you like to change:

- 1) all component values?
- 2) filter component values only?
- 3) source and load values only?
- 4) characteristic to be plotted?
- 5) frequency limits?
- 6) number of points plotted?

?

3

Source resistance, R_s

?

.1

Source inductance, L_s

?

70E-6

Load resistance, R_o

?

10

Load shunt capacitance, C_o

?

5E-6

Load parasitic shunt resistance,

R_c

?

1E-3

Load series inductance, L_o

?

1E-6

Load effective parasitic series resistance, R_e

?

1E-3

- 1) Filter Voltage Gain (V_{out}/V_s)
- 2) Input Load Impedance (Z_i ref 1 ohm)
- 3) Output Filter Impedance (Z_s ref 1 ohm)
- 4) Superimposed Impedances (Z_i and Z_s)

Enter number of desired plot?

1

Would you like to plot?

- 1) Magnitude and Phase
- 2) Magnitude only
- 3) Phase only

?

2

Lower frequency limit?

1E2

Upper frequency limit?

1E6

How many frequency points would you like plotted?

150

Do you want a print-out of the plotted values?

NO

Do you want a copy of the plot?

YES

Are more plots to be made?

YES

Would you like to change?

- 1) all component values?
 - 2) filter component values only?
 - 3) source and load values only?
 - 4) characteristic to be plotted?
 - 5) frequency limits?
 - 6) number of points plotted?
- ?
- 4

- 1) Filter Voltage Gain (V_{out}/V_s)
- 2) Input Load Impedance (Z_i ref 1 ohm)
- 3) Output Filter Impedance (Z_s ref 1 ohm)
- 4) Superimposed Impedances (Z_i and Z_s)

Enter number of desired plot?

4

Lower frequency limit?

1E2

Upper frequency limit?

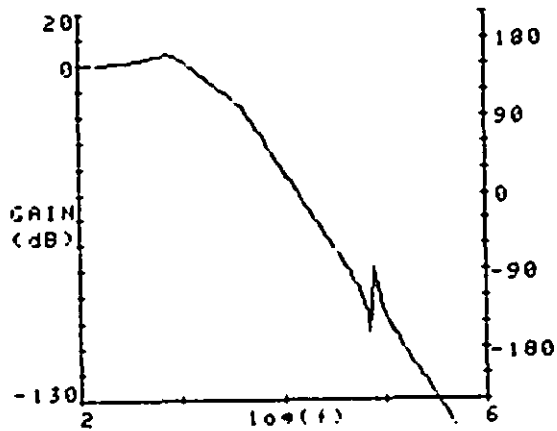
1E6

How many frequency points would you like plotted?

20

Do you want a print-out of the plotted values?

YES



FREQUENCY	IMPEDANCE(Z_i)
1.00E+002	+2.00E+001
1.62E+002	+2.00E+001
2.64E+002	+2.00E+001
4.28E+002	+1.99E+001
6.95E+002	+1.98E+001
1.13E+003	+1.95E+001
1.83E+003	+1.88E+001
2.98E+003	+1.73E+001
4.83E+003	+1.48E+001
7.85E+003	+1.14E+001
1.27E+004	+7.41E+000
2.07E+004	+2.87E+000
3.36E+004	-2.69E+000
5.46E+004	-1.24E+001
8.86E+004	-1.41E+001
1.44E+005	-3.32E+000
2.34E+005	+2.49E+000
3.79E+005	+7.23E+000
6.16E+005	+1.16E+001
1.00E+006	+1.59E+001

FREQUENCY	IMPEDANCE(Zs)
1.00E+002	-9.43E+000
1.62E+002	-5.55E+000
2.64E+002	-1.09E+000
4.28E+002	+4.21E+000
6.95E+002	+1.09E+001
1.13E+003	+1.29E+001
1.83E+003	+1.04E+001
2.98E+003	+1.03E+001
4.83E+003	+7.48E+000
7.85E+003	+1.70E+000
1.27E+004	-3.45E+000
2.07E+004	-8.05E+000
3.36E+004	-1.24E+001
5.46E+004	-1.67E+001
8.86E+004	-2.09E+001
1.44E+005	-2.51E+001
2.34E+005	-2.94E+001
3.79E+005	-3.36E+001
6.16E+005	-3.78E+001
1.00E+006	-4.20E+001

Do you want a copy of the plot?
 YES

Are more plots to be made?

YES

Would you like to change:

- 1) all component values?
- 2) filter component values only?
- 3) source and load values only?
- 4) characteristic to be Plotted?
- 5) frequency limits?
- 6) number of points Plotted?

?

6

How many frequency points would you like Plotted?

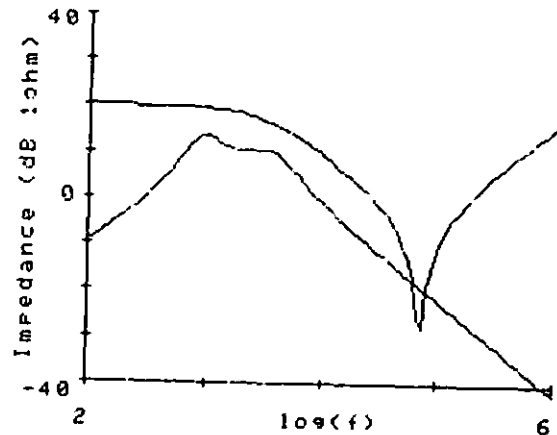
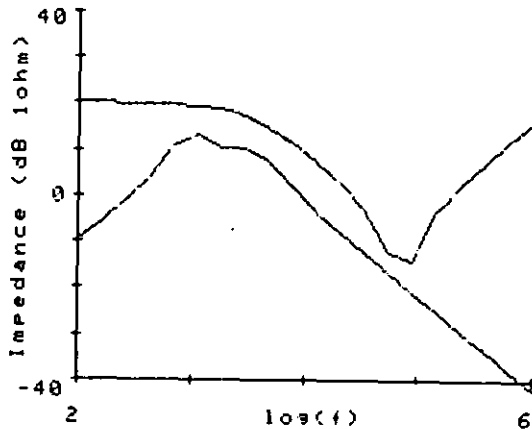
100

Do you want a Print-out of the Plotted values?

NO

Do you want a copy of the plot?

YES



Are more plots to be made?

NO

END OF PROGRAM

MIL-HDBK-2418
APPENDIX C
30 September 1983

```

10 DIM E1(9),E2(9),F1(9),F2(9),
   A1(9),A2(9),B1(9),B2(9)
20 DIM C1(9),C2(9),D1(9),D2(9)
30 A1(9)=0 @ A2(9)=0 @ B1(9)=0
   @ B2(9)=0
40 C1(9)=0 @ C2(9)=0 @ D1(9)=0
   @ D2(9)=0
50 E1(9)=0 @ E2(9)=0 @ F1(9)=0
   @ F2(9)=0
60 DIM R1(6),L(6),C(9),R2(6),G(
   6),B(9),R(6),X(6),T1(9),T2(9
   )
70 DIM P$(10),C$(10)
80 DEFAULT ON
90 REM
100 REM -Call Input Subroutine-
110 GOTO 2360
120 REM
130 REM -Call Graphics Initial-
140 REM -Initialization Subrou-
   tine -
150 GOSUB 1250
160 REM
170 REM ** Calculate filter **
180 REM ** characteristics as**
190 REM ** a function of fre-**
200 REM ** quency, F. **
210 REM
220 REM Process freq. limits
230 O=(J1-1)/(LOG(F2/F1)/LOG(10)
   )
240 REM -- For-next loop eval--
250 REM -- uates filter char --
260 REM -- acteristics in fre--
270 REM -- quency range [F1, --
280 REM -- F2] at 220 points.--
290 FOR J=0 TO J1-1
300 F=F1*10^(J/D)
310 W=2*PI*F
320 REM P1=3.14159265359
330 REM Fill admittance, imped-
340 REM Plot & print F,H(F)
350 GOSUB 3900
360 REM Call subroutine to cal-
370 REM culate characteristic
380 REM at W
390 ON W GOSUB 4210,4640,4690,46
   40
400 H=T1^2+T2^2
410 DEC
420 IF T1>=0 THEN 450
430 IF T2<0 THEN K=ATN(T2/T1)-18
   0 @ GOTO 470
440 IF T2>=0 THEN K=ATN(T2/T1)+1
   80 @ GOTO 470
450 K=ATN(T2/T1)
460 REM Plot & print F,H(F);F,K(
   F)
470 H=10*LOG(H)/LOG(10)
480 K1=K/3-50

```

```

490 IF P$(1,1)@"Y" THEN 660
500 IF J=0 THEN PRINT
510 IF N#1 THEN GOTO 540
520 IF J=0 THEN PRINT "   FREQ.
   MAG.           PHASE"
530 GOTO 590
540 IF J#0 THEN GOTO 600
550 IF N#3 THEN GOTO 580
560 PRINT "FREQUENCY           IM
   PEDANCE(Zs)"
570 GOTO 590
580 PRINT "FREQUENCY           IM
   PEDANCE(Zi)"
590 IF J=0 THEN PRINT
600 IF N#1 THEN GOTO 640
610 PRINT USING 620 ; F,H,K
620 IMAGE D.DDE,3X,SD.DDE,3X,SDO
   D.DD
630 GOTO 660
640 PRINT USING 650 ; F,H
650 IMAGE D.DDE,12X,SD.DDE
660 F=LOG(F)/LOG(10)
670 IF N1=3 THEN PLOT F,K1 @ GOT
   0 770
680 PLOT F,H
690 IF N1=2 THEN GOTO 770
700 IF N#1 THEN GOTO 770
710 IF J=0 THEN X=LOG(F1)/LOG(10
   ) @ Y=-50
720 MOVE X,Y
730 DRAW F,K1
740 X=F @ Y=K1
750 MOVE F,H
760 PLOT F,H
770 NEXT J
780 IF N#4 THEN GOTO 830
790 N5=4
800 N=3
810 PENUP
820 GOTO 290
830 WAIT 3000
840 IF N5=4 THEN N=4
850 REM
860 REM Print out plot
870 BEEP @ ALPHA
880 IF D1$(1,1)@"Y" THEN PRINT
890 DISP "Do you want a copy of
   the plot";
900 INPUT C$
910 IF C$(1,1)@"Y" THEN 970
920 PRINT
930 PRINT
940 GRAPH
950 COPY
960 PRIN
970 REM Ask if more plots are
980 REM are to be made
990 ALPHA
1000 DISP "Are more plots to be
   made";

```

MIL-HDBK-241B
 APPENDIX C
 30 September 1983

```

1010 INPUT C2$
1020 IF C2=C1,1]#*N" THEN 2370
1030 DISP "      END OF PROGR
      AM"
1040 REM --      PROGRAM END      --
1050 NORMAL
1060 STOP
1070 REM
1080 REM *INITIALIZATION ROUTINE
      *
1090 REM
1100 M=0 @ M1=0 @ M5=0
1110 FOR I=0 TO 6
1120 R1(I)=0
1130 L(I)=0
1140 C(I)=0
1150 R2(I)=0
1160 G(I)=0
1170 B(I)=0
1180 R(I)=0
1190 X(I)=0
1200 NEXT I
1210 REM
1220 RETURN
1230 STOP
1240 REM
1250 REM ** GRAPHICS INITIALI-*
1260 REM ** ZATION ROUTINE **
1270 REM
1280 GCLEAR
1290 SCALE 0,255.0,191
1300 SHORT A1,A2
1310 A2=LOG(F1)/LOG(10)
1320 A1=LOG(F2)/LOG(10)
1330 A2=FLOOR(A2)
1340 A1=CEIL(A1)
1350 F1$=VAL$(A2)
1360 F2$=VAL$(A1)
1370 MOVE 32,0
1380 LABEL F1$
1390 B=A2-(A1-A2)/6
1400 IF N#1 THEN GOTO 1710
1410 MOVE 0,84
1420 LABEL "(dB)"
1430 MOVE 0,96
1440 LABEL "GAIN"
1450 MOVE 16,184
1460 LABEL "20"
1470 MOVE 0,12
1480 LABEL "170"
1490 LABEL "170"
1590 MOVE 226,66
1600 LABEL "-90"
1610 MOVE 226,30
1620 LABEL "-180"
1630 MOVE 24,162
1640 LABEL "0"
1650 B1=A1+(A1-A2)/6
1660 SCALE B,B1,-140,20
1670 XAXIS -130,1,A2,A1
1680 YAXIS A2,10,-130,20
1690 YAXIS A1,10,-130,20
1700 RETURN
1710 MOVE 16,184
1720 LABEL "40"
1730 MOVE 11,30
1740 LDIR 90
1750 LABEL "Impedance (dB 1ohm)"
1760 LDIR 0
1770 MOVE 8,12
1780 LABEL "-40"
1790 MOVE 250,0
1800 LABEL F2$
1810 MOVE 128,0
1820 LABEL "log(f)"
1830 MOVE 24,102
1840 LABEL "0"
1850 B1=A1
1860 SCALE B,B1,-50,40
1870 XAXIS -40,1,A2,A1
1880 YAXIS A2,10,-40,40
1890 RETURN
1900 STOP
1910 REM Complex Division:
1920 REM FN D1(A)=Real part
1930 REM FN D2(B)=Imag. part
1940 DEF FND1
1950 A=0
1960 IF ABS(S3)>=1.E-50 OR ABS(S
4)>=1.E-50 THEN 1990
1970 S3=1.E-50
1980 S4=1.E-50
1990 IF ABS(S4)>=1.E-50 THEN 202
0
2000 A=S1/S3
2010 GOTO 2060
2020 IF ABS(S3)>=1.E-50 THEN 205
0
2030 A=S2/S4
2040 GOTO 2060

```

1000 LABEL 50

0

IF ABS(S3)>=1.E-50 THEN 210

```

2130 B=S2/S3
2140 GOTO 2190
2150 IF ABS(S3))=1.E-50 THEN 218
      0
2160 B=-S1/S4
2170 GOTO 2190
2180 B=(S2/S4-S1/S3)/(S3/S4+S4/S
      3)
2190 FND2=B
2200 FN END
2210 RETURN
2220 STOP
2230 REM Complex Multiplication:
2240 REM FN M1(L)=Real Part
2250 REM FN M2(G)=Imag. Part
2260 DEF FNM1
2270 L=0
2280 L=S1*S3-S2*S4
2290 FNM1=L
2300 FN END
2310 DEF FNM2
2320 G=0
2330 G=S1*S4+S2*S3
2340 FNM2=G
2350 FN END
2360 REM
2370 REM ** ROUTINE TO DETER-**
2380 REM ** NINE IF MORE PLOTS**
2390 REM ** ARE WANTED **
2400 REM
2410 DISP "Would you like to cha
      nge:"
2420 DISP
2430 DISP "1)all component value
      s?"
2440 DISP "2)filter component va
      lues only?"
2450 DISP "3)source and load val
      ues only?"
2460 DISP "4)characteristic to b
      e plotted?"
2470 DISP "5)frequency limits?"
2480 DISP "6)number of points pl
      otted?"
2490 INPUT M
2500 IF C3$(1,1)="" THEN 2520
2510 PRINT ALL
2520 ON M GOTO 3150,3300,3150,35
      50,3650,3710
2530 RETURN
2540 STOP
2550 REM
2560 REM ** INPUT ROUTINE **
2570 REM
2580 DISP "Would you like to ski
      p the text and filter diagr
      am";
2590 INPUT D1$
2600 IF D1$(1,1)="" THEN 2970
2610 CLEAR

```

```

2620 PRINT ALL
2630 DISP " FILTER AND L
      OAD"
2640 DISP "CHARACTERISTICS PLOTT
      ING PROGRAM"
2650 DISP
2660 DISP "This program evaluate
      s and plots(in dB) the firs
      t three filter"
2670 DISP "and load characterist
      ics listed"
2680 DISP "below.In addition the
      impedancescan be plotted s
      uperimposed on"
2690 DISP "one graph as listed i
      n item (4) below."
2700 NORMAL
2710 DISP @ DISP @ DISP
2720 DISP "Press (end line) to c
      ontinue";
2730 INPUT C$
2740 PRINT ALL
2750 GOSUB 3790
2760 NORMAL @ DISP
2770 DISP @ DISP @ DISP
2780 DISP "Press (end line) to c
      ontinue";
2790 INPUT C$
2800 PRINT ALL
2810 DISP "Impedances are refere
      nced to oneohm.The output i
      mpedance,Zs,is"
2820 DISP "the impedance looking
      back into the filter with
      Vs short cir-"
2830 DISP "cuted.The loaded fil
      ter will bedisplayed and yo
      u will be asked"
2840 DISP "to enter the value of
      each com-"
2850 DISP "ponent.You will also
      be asked which characteri
      stic you would"
2860 DISP "like plotted, the fre
      quency"
2870 DISP "range over which the
      plot is to"
2880 DISP "be made, and if you w
      ant the"
2890 DISP "plotted points printe
      d on paper as well."
2900 NORMAL
2910 DISP "Press (end line) to c
      ontinue";
2920 INPUT C$
2930 PRINT ALL
2940 DISP
2950 GOSUB 4970
2960 DISP
2970 DISP "Do you want a copy of
      the"

```

```

2980 DISP "component values you
enter";
2990 INPUT C3$
3000 IF C3$[1,1]="Y" THEN 3020
3010 NORMAL @ GOTO 3030
3020 PRINT ALL
3030 DISP
3040 DISP
3050 CLEAR
3060 REM -Call Initialization-
3070 REM - Subroutine -
3080 GOSUB 1080
3090 DISP "To short circuit an un-
wanted component, set R=
L=0,C=1E100 "
3100 DISP "To open circuit an un-
wanted com-ponent, set R=L=1
E100,C=1E-100 "
3110 DISP
3120 DISP "Units of component va-
lues."
3130 DISP "R=Ohms,C=Farads,L=Hen-
ries"
3140 DISP
3150 DISP "Source resistance, Rs
"
3160 INPUT R1(0)
3170 DISP "Source inductance, Ls
"
3180 INPUT L(0)
3190 DISP "Load resistance, Ro"
3200 INPUT R1(6)
3210 DISP "Load shunt capacitanc-
e, Co"
3220 INPUT C(6)
3230 DISP "Load parasitic shunt
resistance,Rc"
3240 INPUT R2(5)
3250 DISP "Load series inductanc-
e, Lo"
3260 INPUT L(6)
3270 DISP "Load effective parasi-
tic series resistance, Re"
3280 INPUT R2(6)
3290 IF M=3 THEN GOTO 3550
3300 FOR I=1 TO 5 STEP 2
3310 DISP USING 3320 ; I
3320 IMAGE "Shunt capacitance, C
",0
3330 INPUT C(I)
3340 DISP USING 3350 ; I,I
3350 IMAGE "Equivalent series re-
sistance, R",D,"of C",D
3360 INPUT R1(I)
3370 DISP USING 3380 ; I,I
3380 IMAGE "Equivalent series in-
ductance, L",D,"of C",D
3390 INPUT L(I)
3400 IF I=5 THEN GOTO 3530
3410 DISP USING 3420 ; I+1
3420 IMAGE "Series Inductance, L
",D
3430 INPUT L(I+1)
3440 DISP USING 3450 ; I+1,I+1
3450 IMAGE "Winding resistance,
R",D," of L",D
3460 INPUT R1(I+1)
3470 DISP USING 3480 ; I+1,I+1
3480 IMAGE "Parasitic capacitanc-
e, C",D," of L",D
3490 INPUT C(I+1)
3500 DISP USING 3510 ; I+1,I+1
3510 IMAGE "Core loss resistance
, E",D," of L",D
3520 INPUT R2(I+1)
3530 NEXT I
3540 REM
3550 GOSUB 3790
3560 DISP "Enter number of desir-
ed plot";
3570 INPUT N
3580 IF N#1 THEN GOTO 3650
3590 DISP "Would you like to plo-
t:"
3600 DISP
3610 DISP "1) Magnitude and Phas-
e"
3620 DISP "2) Magnitude only"
3630 DISP "3) Phase only"
3640 INPUT N1
3650 DISP "Lower frequency limit
";
3660 INPUT F1
3670 DISP "Upper frequency limit
";
3680 INPUT F2
3690 DISP
3700 DISP
3710 DISP "How many frequency po-
ints would you like plotted
";
3720 INPUT J1
3730 DISP "Do you want a Print-o-
ut of the"
3740 DISP "plotted values";
3750 INPUT P$
3760 GOTO 150
3770 STOP
3780 REM Display plot options.
3790 DISP
3800 DISP "1) Filter Voltage Gai-
n (Vout/Vs)"
3810 DISP "2) Input Load Impedan-
ce (Zi ref 1 ohm)"
3820 DISP "3) Output Filter Impe-
dance (Zs ref 1 ohm)"
3830 DISP "4) Superimposed Imped-
ances (Zi and Zs)"
3840 DISP
3850 RETURN

```

MIL-HDBK-241B
APPENDIX C
30 September 1983

```

3860 STOP
3870 REM
3880 STOP
3890 REM
3900 REM *CALCULATE IMPEOANCES*
3910 REM
3920 Z1(0)=R1(0)
3930 Z2(0)=M*L(0)
3940 Z1(6)=(R1(6)+W^2*R1(6)*C(6)
~2*R2(5)*(R1(6)+R2(5)))/(1+
(W*C(6)*(R1(6)+R2(5)))^2)+R
2(6)
3950 Z2(6)=-W*R1(6)^2*C(6)/(1+(W
*C(6)*(R1(6)+R2(5)))^2)+W*L
(6)
3960 S1=1
3970 S2=0
3980 S3=Z1(6)
3990 S4=Z2(6)
4000 Y1(6)=FND1
4010 Y2(6)=FND2
4020 FOR I=1 TO 5 STEP 2
4030 Z1(I)=R1(I)
4040 Z2(I)=(W^2*L(I)*C(I)-1)/(W*
C(I))
4050 S1=1
4060 S2=0
4070 S3=Z1(I)
4080 S4=Z2(I)
4090 Y1(I)=FND1
4100 Y2(I)=FND2
4110 NEXT I
4120 FOR I=2 TO 4 STEP 2
4130 S1=R1(I)-W^2*L(I)*C(I)*R2(I
)
4140 S2=W*(L(I)+R1(I)*C(I)*R2(I
)
4150 S3=1-W^2*C(I)*L(I)
4160 S4=W*C(I)*(R2(I)+R1(I))
4170 Z1(I)=FND1
4180 Z2(I)=FND2
4190 NEXT I
4200 RETURN
4210 REM Calculate V(out)/V(sour
ce)/
4220 T1=0
4230 T2=0
4240 A1(9)=Y1(5)+Y1(6)
4250 A2(9)=Y2(5)+Y2(6)
4260 S1=A1(9)
4270 S2=A2(9)
4280 S3=Z1(4)
4290 S4=Z2(4)
4300 B1(9)=FNM1+1
4310 B2(9)=FNM2
4320 S1=Y1(3)
4330 S2=Y2(3)
4340 S3=B1(9)
4350 S4=B2(9)
4360 C1(9)=FNM1+A1(9)
4370 C2(9)=FNM2+A2(9)
4380 S1=Z1(2)
4390 S2=Z2(2)
4400 S3=C1(9)
4410 S4=C2(9)
4420 D1(9)=FNM1+B1(9)
4430 D2(9)=FNM2+B2(9)
4440 S1=Y1(1)
4450 S2=Y2(1)
4460 S3=O1(9)
4470 S4=D2(9)
4480 E1(9)=FNM1+C1(9)
4490 E2(9)=FNM2+C2(9)
4500 S1=Z1(0)
4510 S2=Z2(0)
4520 S3=E1(9)
4530 S4=E2(9)
4540 F1(9)=FNM1+D1(9)
4550 F2(9)=FNM2+D2(9)
4560 S1=1
4570 S2=0
4580 S3=F1(9)
4590 S4=F2(9)
4600 T1=FND1
4610 T2=FND2
4620 REM Vo/Vs=T1+JT2
4630 RETURN
4640 REM Calculate Load Impedanc
e
4650 REM
4660 T1=Z1(6)
4670 T2=Z2(6)
4680 RETURN
4690 REM Calculate Output Impeda
nce
4700 REM
4710 I1(0)=Z1(0)
4720 I2(0)=Z2(0)
4730 I1(1)=Y1(1)
4740 I2(1)=Y2(1)
4750 I1(2)=Z1(2)
4760 I2(2)=Z2(2)
4770 I1(3)=Y1(3)
4780 I2(3)=Y2(3)
4790 I1(4)=Z1(4)
4800 I2(4)=Z2(4)
4810 I1(5)=Y1(5)
4820 I2(5)=Y2(5)
4830 I1(6)=Z1(6)
4840 I2(6)=Z2(6)
4850 T1=0
4860 T2=0
4870 FOR K=0 TO 5 STEP 1
4880 S1=1
4890 S2=0
4900 S3=I1(K)+T1
4910 S4=I2(K)+T2
4920 T1=FND1
4930 T2=FND2
4940 NEXT K

```

```

4950 RETURN
4960 END
4970 REM
4980 REM *** Filter Diagram ***
4990 REM
5000 DISP "          -C2-E2-C4-E4-"
5010 DISP "          ;          ;"
5020 DISP "oRs-Ls-L2-R2-L4-R4---
-----o-----"
5030 DISP "          |          |          |
      Zs  Re"
5040 DISP "          C1          C3          C5
      <--  |"
5050 DISP "          |          |          |
      Lo"
5060 DISP "Us          R1          R3          R5
      Vo |-----"
5070 DISP "          |          |          |
      Rc |"
5080 DISP "          L1          L3          L5
      Zi  |  Ro"
5090 DISP "          |          |          |
      --> Co |"
5100 DISP "o-----"
-----o-----"
5110 RETURN
5120 STOP

```

APPENDIX D
30 September 1983
FOURIER TRANSFORMS

10. Fourier transform for trapezoidal waveforms.

10.1 Periodic waveform. By Fourier analysis the amplitude at the frequency of the n^{th} harmonic, C_N , of the symmetrical trapezoidal periodic pulse is given FIGURE 110.

For $t_o + t_r = T/2$, C_N is plotted in FIGURE 111 for lower-order harmonics (assuming $[\sin(nt_r/T)]/(nt_r/T) = 1$ which is true for small values of nt_r/T). This is the same result that would be obtained for a square wave where only odd harmonics are obtained.

10.2 Modified three phase waveform. For three phase rectification with no transformer or with a delta-delta transformer, the line current waveform can be represented by FIGURE 112.

A Fourier analysis of this waveform (assuming $t_r = 0$) is shown by Schaefer (reference 6) to result in all odd harmonics except for $n = 3, 9$, and so forth (all odd multiples of 3) with the same amplitudes as for the square wave (see FIGURE 113(a) and (b)). Since the low frequency harmonic spectrum is the same for both the rectangular and trapezoidal pulses, the harmonic relationship shown in FIGURE 113(a) and (b) also apply to (c) and (d).

10.3 Broadband versus narrowband. For $t_o + t_r = T/2$, C_N is plotted in FIGURE 114 for lower order harmonics. This is the same result that would be obtained for a rectangular pulse. FIGURE 115 depicts the spectrum obtained for a single pulse ($T \rightarrow \infty$) and, therefore, amplitudes are per megahertz bandwidth (broadband classification). If coherent ^{VI} broadband amplitudes exist then a definite relationship exists between narrowband and coherent broadband amplitudes. By dividing equation (a) by the pulse repetition rate (P.R.R.) an amplitude per P.R.R. is obtained, as shown in FIGURE 115 (since P.R.R. = $1/T$).

10.4 Envelope approximation of harmonics. The envelope of the low ordered harmonics is actually a $\sin x/x$ function (see FIGURES 114 and 115). A linear envelope, however, can be obtained by using a logarithmic frequency scale as shown in FIGURE 116. The negative amplitudes of the sine function are inverted since only magnitudes are considered.

The linear envelope approximation for a rectangular pulse varies inversely with frequency resulting in a 20 dB per decade decreasing slope (see FIGURE 116).

FIGURE 117 shows the linear approximation for a trapezoidal pulse in three linear sections. Note that for higher frequencies the pulse rise time is more significant and results in a 40 dB per decade decreasing slope. Slower rise times produce less high frequency interference. For periodic pulses the lowest frequency to appear would be $1/T$ or the pulse repetition rate.

The interface levels for any trapezoidal pulse are given on FIGURES 117 and 118. The area under the pulse, maximum amplitude of the pulse, and rate of rise of the pulse define the envelopes of interference in the three frequency regions. The average pulse duration and the pulse rise time determine the corner frequencies.

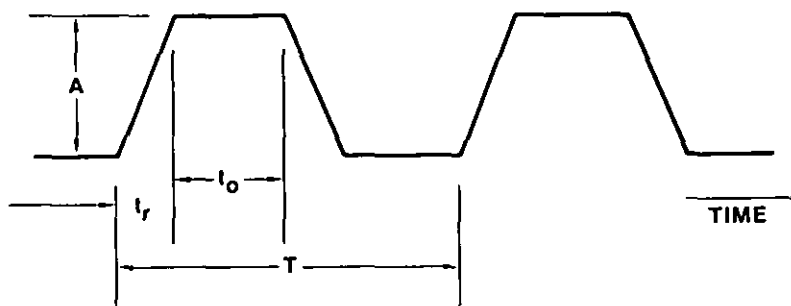
20.0 Envelope approximations for common pulse shapes. The loci of maximum amplitudes for eight common pulse shapes are shown on FIGURE 119. All have a one volt peak amplitude and an average pulse duration of 1μ second. Because all of the pulses have the same area, the interference levels at low frequencies are identical. At frequencies less than $1/d$, the interference level equals 2Ad or 126 dB above μV per MHz. Above a frequency of approximately $1/d$, the interference level drops at a rate determined by the shape of the rise and fall time of the pulse.

For a rectangular pulse or a clipped sawtooth pulse (both of which have step functions) the spectrum extends to higher frequencies; it decreases as the first power of frequency, or at a 20-dB-per-decade-rate.

For a trapezoidal pulse, a critically damped exponential pulse, a triangular pulse, and a cosine pulse (all of which have sharp corners); interference decreases as the second power of frequency or at a 40-dB-per-decade-rate.

For a cosine-squared pulse which has small corners, the interference decreases as the third power of frequency or at a 60-dB-per-decade-rate.

^{VI} "A signal or emission is said to be coherent when neighboring frequency increments are related or well defined in both amplitude and phase" from reference 14.



By Fourier analysis the amplitude at the frequency of the n th harmonic,

$$C_N = 2A \frac{(t_o + t_r)}{T} \cdot \frac{\sin[\pi n(t_o + t_r)/T]}{\pi n(t_o + t_r)/T} \cdot \frac{\sin(\pi n t_r/T)}{\pi n t_r/T}$$

FIGURE 110. Symmetrical trapezoidal periodic pulse.

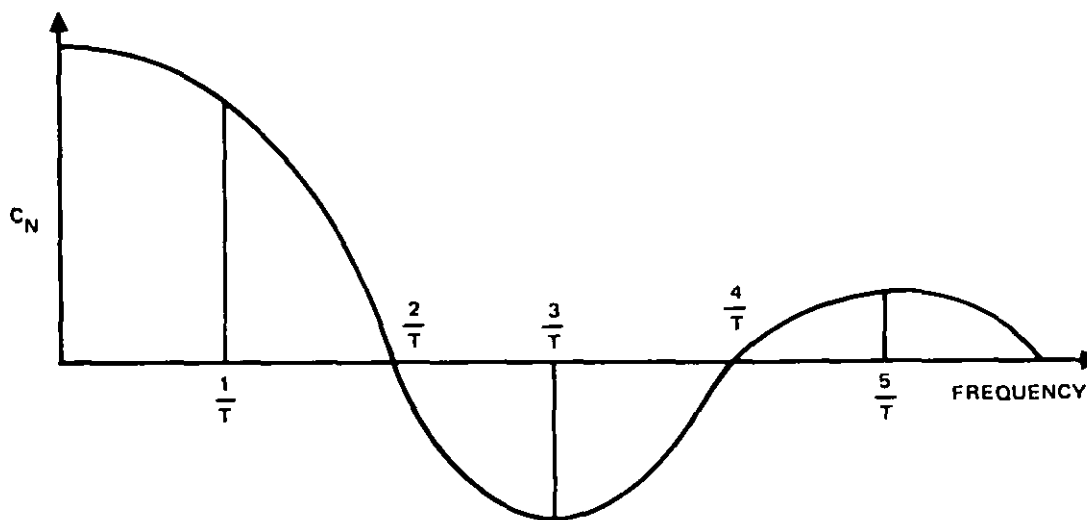


FIGURE 111. Low frequency harmonic spectrum for $t_r + t_o = T/2$ trapezoidal pulse.

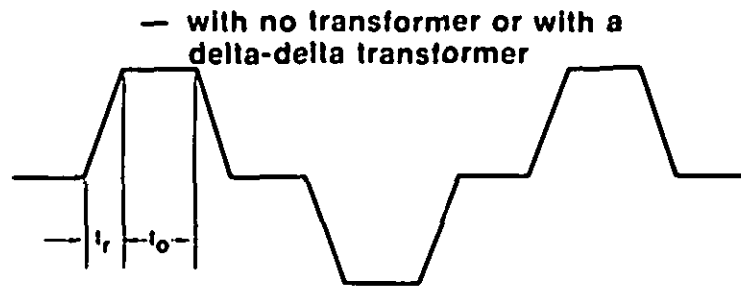


FIGURE 112. Line current waveform for three-phase rectification.

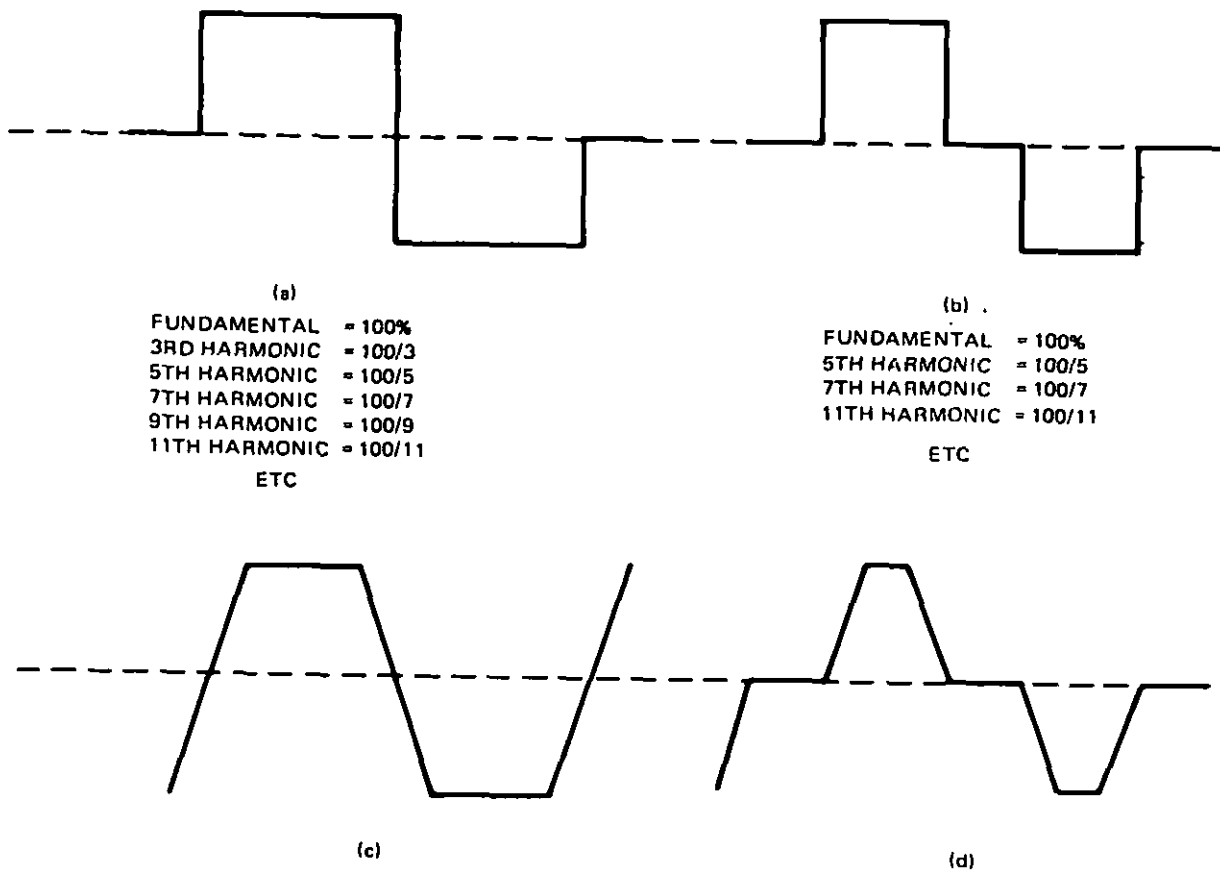
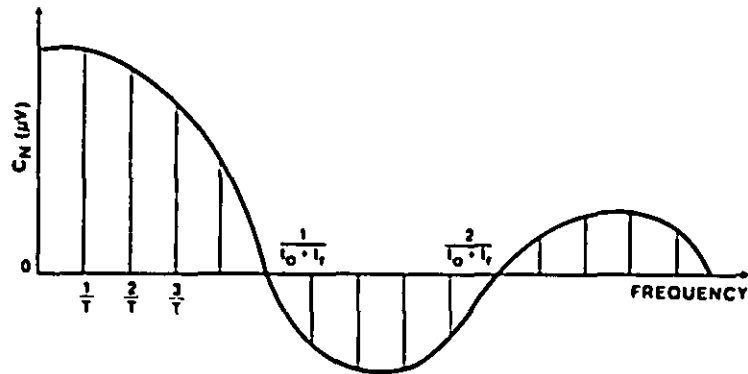
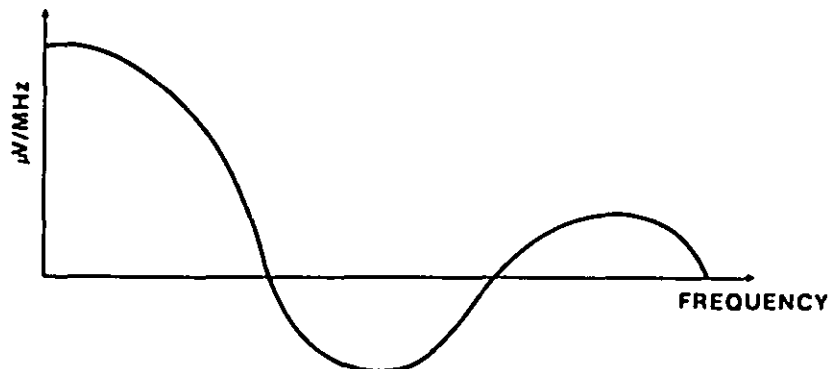


FIGURE 113. Low frequency harmonic comparison for rectangular and trapezoidal waveshapes.



where pulse repetition rate (PRR) = $\frac{1}{T}$

FIGURE 114. Low frequency harmonic spectrum for trapezoidal periodic pulse (narrowband).



To convert to coherent broadband:

$$\text{Let } i_o + i_r = d$$

$$l = \frac{n}{T}$$

$$\frac{\text{narrowband } C_N}{\text{PRR}} = 2Ad \frac{\sin \pi ld}{\pi ld} \text{ broadband}$$

or in dB and MHz:

$$\text{dB}\mu\text{V (narrowband)} - 20 \log (\text{PRR in MHz}) = \text{dB}\mu\text{V/MHz (broadband)}$$

FIGURE 115. Low frequency harmonic envelope for single pulse (broadband).

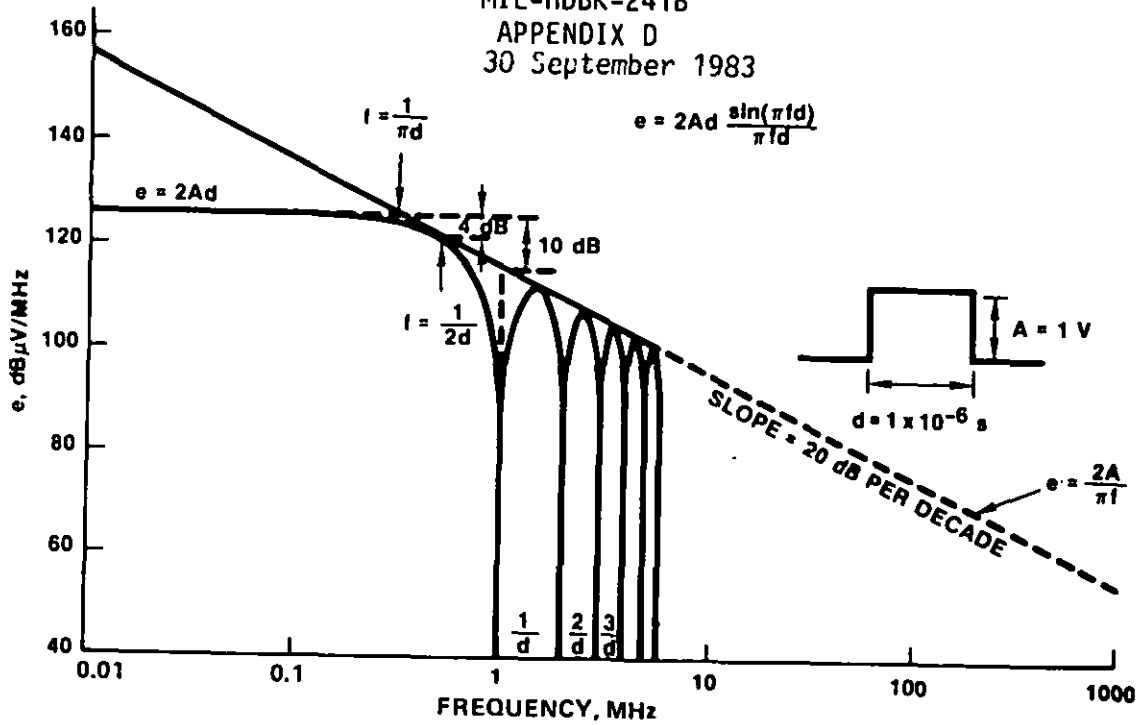


FIGURE 116. Interference level for a 1-V, 1- μs rectangular pulse.

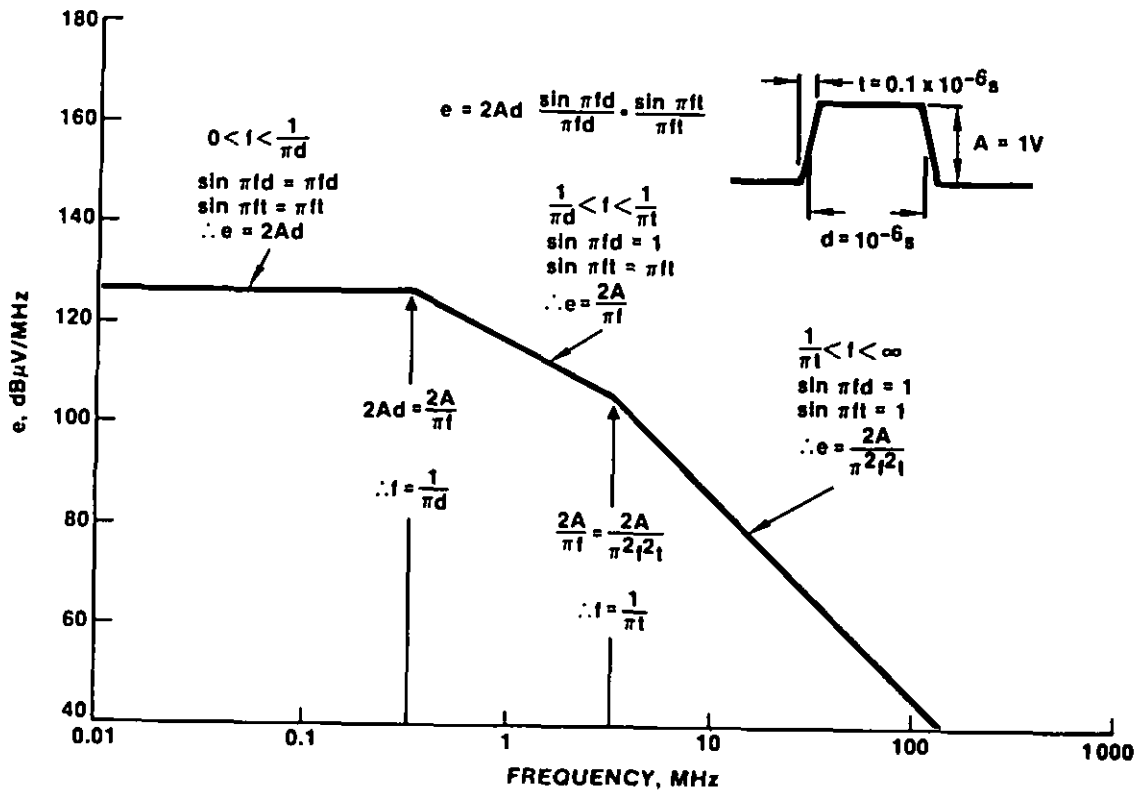


FIGURE 117. Interference level for a 1-V, 1- μs trapezoidal pulse.

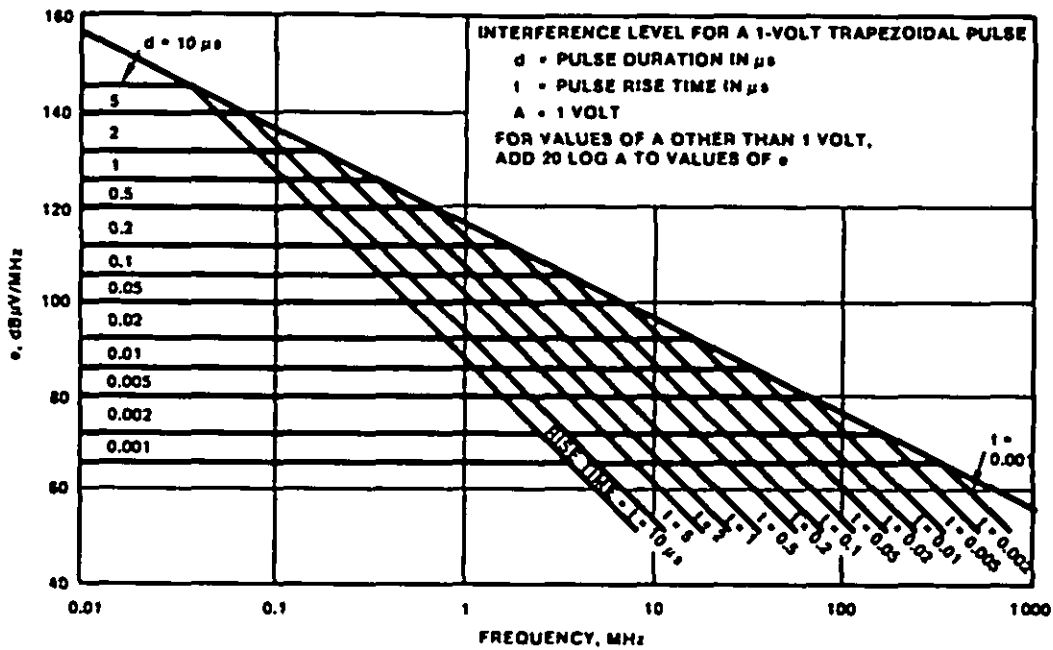


FIGURE 118. Trapezoidal pulse interference.

NOTE: INTERFERENCE LEVEL FOR 1-VOLT.

1-μs PULSE A = 1, d = 10⁻⁶
 2Ad = 126 dBμV/MHz

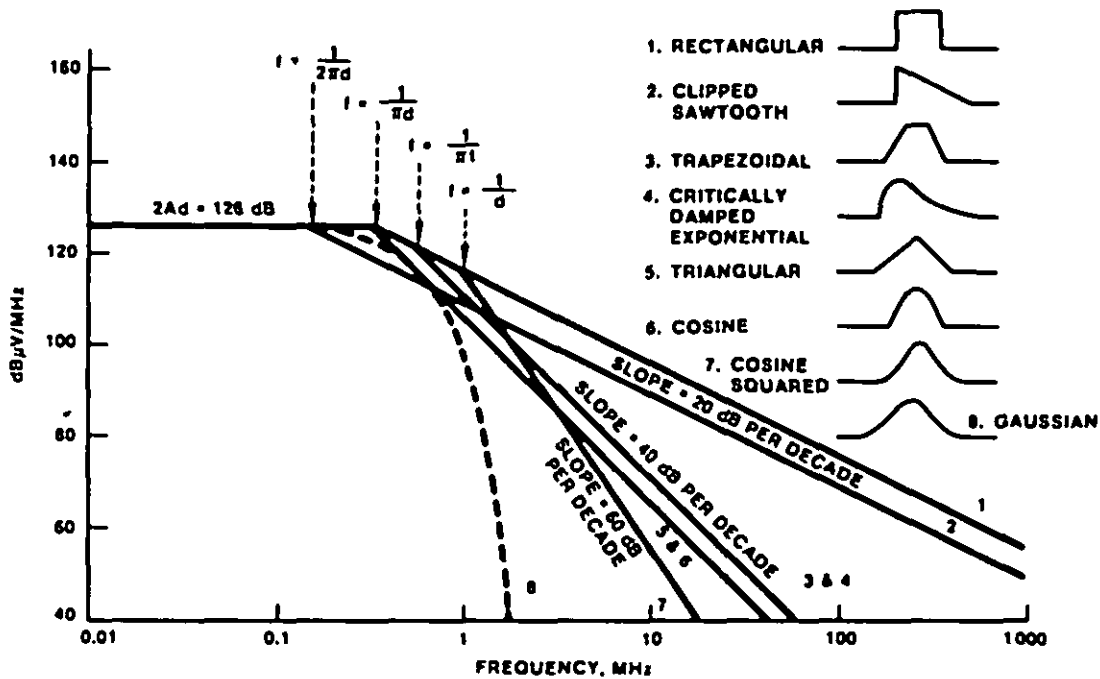


FIGURE 119. Interference levels for eight common pulses.

For a Gaussian pulse, the smoothest pulse considered, the interference drops at a rate that increases with frequency.

The curves on FIGURE 120 are identical to those in FIGURE 119, but the ordinate and abscissa scales have been changed so that the curves can be applied to a pulse of any voltage amplitude and any pulse duration. The ordinate gives the number of decibels below $2Ad$, and the abscissa is plotted in frequency terms of $1/d$. To find the interference level of any pulse, calculate $2Ad$ from the peak pulse amplitude and the average pulse duration and select the curve which most nearly resembles the given pulse shape. This curve will give the number of decibels below $2Ad$ for any frequency.

Although the pulse shapes analyzed here are ideal, the same methods may be used for other waveshapes by considering the waveshape to be made up of a number of rectangular and triangular pulses. For any pulse shape, the interference level at low frequencies depends only on the area under the pulse, at higher frequencies the level depends on the number and steepness of the slopes. The curves on FIGURE 120 are the envelopes of the frequency lobes, each lobe being an envelope of the harmonic lines that make up the frequency spectrum. Although the true curves have numerous sharp nulls, the envelope is less than 3 dB from the average interference level and represents the worst case of maximum interference level.

30.0 Fourier transform of "ringing". A damped sinusoid ringing waveform is described by the equation in FIGURE 121:

The plot in FIGURE 121 is an example of the loci of maximum frequency amplitudes for a damped sinusoid. Note that it peaks at a slightly higher frequency than the ringing frequency and then drops off at 40 dB per decade. Here again, if this waveform were periodic, the lowest frequency that would appear would be $1/T$ or the P.R.R.

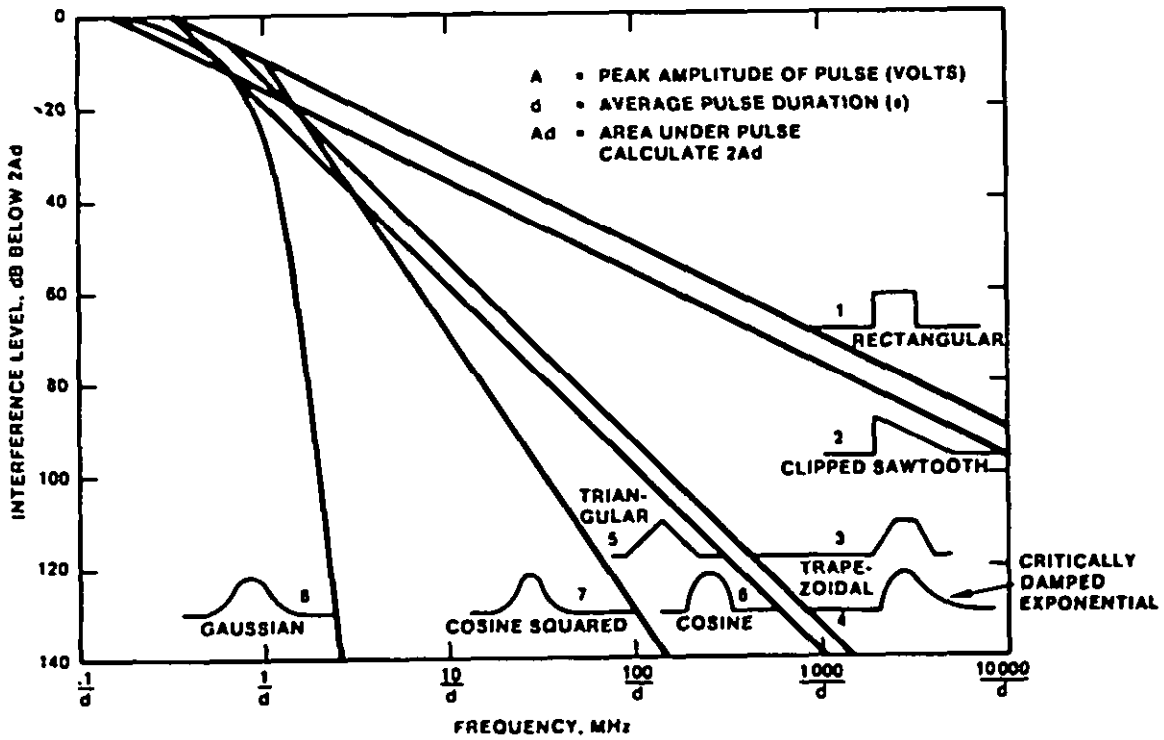


FIGURE 120. Interference levels for various pulse shapes.

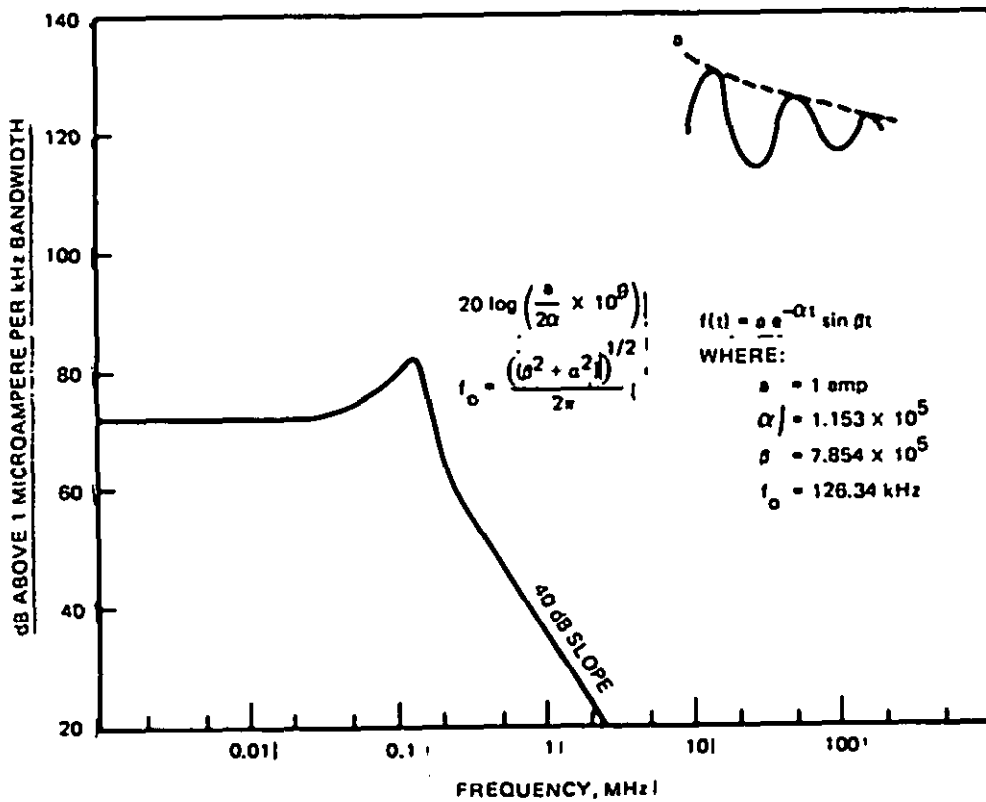


FIGURE 121. Normalized frequency spectrum of damped sinewave pulse.

REFERENCES AND BIBLIOGRAPHY

1. Foutz, J., Switching-Mode Power Supply Technology, paper presented at the Symposium for A Rational Approach to the powering Shipboard Electronics, White Oak, Maryland, 5 December 1978, sponsored by NAVSEA.
2. Middlebrook, R. D. and Cuk, S., Advances in Switched-Mode Power Conversion; Volume I - Modelling, Analysis, and Measurement; and Volume II - Switched-Mode Topologies; Teslaco, 490 S. Rosemead Blvd., Suite 6, Pasadena, CA 91107, 1981.
3. NASACR-135072 (TRW 26629.000)(NTIS Accession Number N77-32398), Development of a Standardized Control Module for DC-to-DC Converters, Y. Yu, R. I. Iwen, F. C. Lee, L. Y. Inouy, 30 August 1977.
4. Venable, H. D. and Foster, S. R., Practical Techniques for Analyzing, Measuring, and Stabilizing Feedback Control Loops in Switching Regulators and Converters, paper presented at Powercon 7, March 1980, San Diego, CA.
5. Bloom, G. and Severns, R., Unusual DC-DC Power Conversion Systems, paper #3 presented at the IEEE MIDCON Professional Program Session 24, 1980 Record, pp. 1-12.
6. Schaefer, J., Rectifier Circuits: Theory and Design, John Wiley & Sons, 1965.
7. Motto, J. M., Introduction to Solid State Power Electronics, Westinghouse, 1977.
8. Distler, R. J., and Munshi, S. G., Critical Inductance and Controlled Rectifiers, IEEE Transactions on Industrial Electronics and Control Instrumentation, vol IECI-12, p 34-37, March 1965.
9. Kamm, E., Design Techniques to Limit EMI from Switching-Mode Converters, Proceedings of Powercon 6, Sixth International Power Electronics Conference (Power Concepts Inc., Ventura, CA), 1979.
10. Yu, Y. and Bless, J. J., Some Design Aspects Concerning Input Filters for DC-DC Converters, paper presented at the IEEE Power Conditioning Specialists Conference, Pasadena, CA, April 1971.
11. Shepherd, W., and Elssawi, K. M. A., Some Properties of a Rectifier Circuit with Sinusoidal Supply Voltage and Resistive Load, IEEE Transactions on Industrial Electronics and Control Instrumentation, vol IECI-24, May 1977.
12. Kamm, E., New Military EMI Specifications Affecting the Input Circuit Architecture of AC to DC Converters Proceedings of Powercon 8, Eighth International Power Electronics Conference (Power Concepts, Inc., Ventura, CA), 1981.
13. IEEE Std 519-1981, IEEE Guide for Harmonic Control and Reactive Compensation of Static Power Converters, Published by the Institute of Electronics Engineers, Inc., 345 East 47th Street, New York, NY 10017, April 17, 1981.
14. Kendall, C. M., Final Report on the Design and Use of EMI Powerline Filters with Transient Protection for Navy Multiplatform Power Systems, September 1977. (Final report of contract for the Naval Ocean Systems Center, Code 9257, San Diego, California 92152, by Chris M. Kendall, P. O. Box 753, Running Springs, California 92382.)
15. David W. Taylor, Naval Ship Research and Development Center Report 76-0049, Investigation of Shipboard 400-Hz Power System Interface Problems, Lawrence F. Rogers and James P. Goodman, December 1976.
16. NOSC TD 107, Reduction of Shipboard 400-Hz Power Requirements -- Cost and Technological Feasibility, E. Kamm, J. Foutz, Naval Ocean Systems Center, San Diego, CA 92152, 16 May 1977.
17. Foutz Engineering Technical Report 81-001, Three Percent Harmonic Current Limit on Shipboard Power System Loads: Requirements and Solutions, J. Foutz, Foutz Engineering, 5921 Walnut Creek Road, Yorba Linda, CA 92686, 31 August 1981.

18. Peterson, Robert L., The Six Phase Center-Tapped Ring Connected Transformer, paper presented at the West Coast Electronic Transformat Subcommittee and Magnetic Group, Los Angeles District, February 4, 1965. Litton Systems Division, Woodland Hills, CA.
19. Williams, Michael L., Reduction of Line Current Harmonics in 3-Phase Off-Line Rectifier Systems by Use of an Efficient 3-Phase to 9-Phase Auto-Transformer Conversion Technique, Investigation performed for NAVSEA 660F under contract No. N00024-79-C-6376 by EG&G Washington Analytical Services Center, Inc., 12 April 1979.
20. Delco Electronics R78-38, 15 kW General Purpose Power Conditioner, final report AC-DC Section, prepared for US Army Mobility Equipment RD Development Command, Fort Belvoir, Virginia, April 1978.
21. Chambers, D., and Wang, D., Dynamic Power Factor Correction In Capacitor Input Off Line Converters, Proceedings of Powercon 6, Sixth International Power Electronics Conference (Power Concepts, Inc., Ventura, CA), 1979.
22. Kataoka, T., Mizumachi, K., and Miyairi, S., A Pulse-Width Controlled AC to DC Converter to Improve Power Factor and Waveform of AC Line Current, paper presented at the IEEE International Semiconductor Power Converter Conference, Orlando, FL, March 1977.
23. Rippel, W. E., Optimizing Boost Chopper Charger Design, Proceedings of Powercon 6, Sixth International Power Electronics Conference (Power Concepts, Inc., Ventura, CA), 1979.
24. Venturini, M., A New Sine Wave In, Sine Wave Out Conversion Technique Eliminates Reactive Elements, Proceedings of Powercon 7, Seventh International Power Electronics Conference (Power Concepts, Inc., Ventura, CA) 1980.
25. Venturini, Marco, Alesina, Alberto, The Generalized Transformer: A New Bidirectional Sinusoidal Waveform Frequency Converter with Continuously Adjustable Input Power Factor, PESC '80 Record, IEEE Power Electronics Specialists Conference - 1980, held in Atlanta, Georgia, June 16-20, 1980.
26. Gjugyl, L., Pelly, B., Static Power Frequency Changers, Wiley, New York, 1976.
27. Kataoka, T., Mizumachi, D., and Miyairi S., A Pulse-Width Controlled AC to DC Converter to Improve Power Factor and Waveform of AC Line Current, paper presented at the IEEE International Semiconductor Power Converter Conference, Orlando, FL, March 1977.
28. Mazzucchelli, M., and Sciutto, G., Improving AC Line Current and Power Factor Using Converters Controlled by a Generalized PWM Method, Proceedings of Powercon 8, Eighth International Power Electronics Conference (Power Concepts, Inc, Ventura, CA) 1981.
29. Kataoka, T., Mizumachi, K., and Miyairi, S., A Pulse-Width Controlled AC to DC Converter to Improve Power Factor and Waveform of AC Line Current, paper presented at the IEEE-IAS International Semiconductor Power Converter Conference, 1977.
30. Schwarz, F. C., and Klaassens, J. B., A Controllable Secondary Multikilowatt DC Current Source with Constant Maximum Power Factor in its Three-Phase Supply Line, paper presented at IEEE Power Specialists Conference, Los Angeles, CA, June 1975.
31. Harashima, F., Hiroshi, I., and Tsuboi, K., A Closed-Loop Control System for the Reduction of Reactive Power Required by Electronic Converters, IEEE Transactions on Industrial Electronics and Control Instrumentation, vol. IECI-23, No. 2, May 1976.
32. Knoll, H., 3 kW-Switch-Mode Power Supply Providing Sinusoidal Mains Current and Large Range of DC-Output, paper presented at International Powerconversion '80 September 1980, Munich, West Germany.
33. Kull, H., Mains Rectifier Providing Nearly Sinusoidal Mains Current and Constant Output Voltage, paper presented at International Powerconversion '80, September 1980, Munich, West Germany.
34. Nijhof, E. B. G., A Single Transformer SMPS Power Supply Operating from the Mains, paper presented at International Powerconversion '80, September 1980, Munich, West Germany.

MIL-HDBK-241B
APPENDIX E
30 September 1983

35. Burgum, F. J., Mains Pollution by Rectifier Systems and the Significance of EN 50 006, paper presented at International Powerconversion '80, September 1980, Munich, West Germany.
36. Yu, Y., et al (TRW Defense & Space Systems), Formulation of a Methodology for Power Circuit Design Optimization, paper presented at IEEE Power Electronics Specialists Conference, Cleveland, Ohio, June 1976.
37. Middlebrook, R. D., Input Filter Considerations in Design and Application of Switching Regulators, paper presented at the IEEE Industry Applications Society Annual Meeting, Chicago, Illinois, October 1976.
38. Macomber, L. L., Switching Regulator Capacitor Technology: Optimizing Ripple and EMI Suppression Performance, Proceedings of POWERCON 5 International Power Electronics Conference (Power Concepts, Inc, Ventura, CA) 1978.
39. Cowdell, R. B., Bypass Filters Extend to the GHz Range when Solid-Tantalum Capacitors are Used, Electronic Design 15, 19 July 1977.
40. Silber, D., Simplifying the Switching Regulator Input Filter, Solid State Power Conversion, May/June 1975.
41. Gottlieb, I., Switching Regulators and Power Supplies, Tab Books, 1976.
42. Ott, H. W., Noise Reduction Techniques in Electronic Systems, John Wiley & Sons, 1976.
43. Blatt, F. M., Pick the Right "Fast" Rectifiers to Design Switchers Effectively, EDN, 20 January 1978.
44. Roehr, B., Transient Response Measurements of High Speed Rectifier Diodes, a Motorola Semiconductor Group paper.
45. Bloom, S. D., and Massey, R. P., (Bell Laboratories), Emission Standards and Design Techniques for EMI Control of Multiple DC-DC Converter Systems, paper presented at IEEE Power Electronics Specialists Conference, Cleveland, Ohio, 10 June 1976.
46. Skanadore, W. R., Methods for Utilizing High Speed Switching Transistors in High Energy Switching Environments, publication from General Semiconductor Industries, Inc., P.O Box 3078, Tempe, Arizona 85281, December 1977.
47. Calkin, E. T. and Hamilton, B. H., Circuit Techniques for Improving the Switching Loci of Transistor Switches in Switching Regulators, IEEE Transactions on Industry Applications, Vol IA-12, July-August 1976.
48. Calkin, E. T. and Hamilton, B. H., A Conceptually New Approach for Regulated DC to DC Converters Employing Transistor Switches and Pulsewidth Control, IEEE Transactions on Industry Applications, Vol IA-12, July-August 1976.
49. Cuk, S. and Middlebrook, R. D., A New Optimum Topology Switching DC-to-DC Converter, paper presented at the IEEE Power Electronics Specialists Conference, Palo Alto, California, June 1977.
50. Shaeffer, L. (Siliconix, Inc.) Improving Converter Performance and Operating Frequency with a New Power FET, Proceedings of POWERCON 4, Fourth International Power Electronics Conference (Power Concepts, Inc., Ventura, CA) 1977.
51. Middlebrook, R. D., Design Techniques for Preventing Input-Filter Oscillations in Switched-Mode Regulators, Proceedings of Powercon 5, Fifth International Power Electronics Conference (Power Concepts, Inc., Ventura, CA) 1978.
52. Phelps, T. K., and Tate, W. S., Optimizing Passive and Input Filter Design, Proceedings of Powercon 6, Sixth International Power Electronics Conference (Power Concepts Inc., Ventura CA) 1979.
53. Hnatek, E. R., Design of Solid-State Power Supplies, Van Nostrand Reinhold Co., 1979.

54. Rippel, W. and Edwards, D., A New High Efficiency Polyphase SCR Inverter Topology Using FET Commutation, proceedings of Powercon 8, Eighth International Power Electronics Conference (Power Concepts, Inc., Ventura, CA) 1981.
55. Foutz Engineering Technical Report TR81-003, Survey of Power Electronics Technology Applicable to Very Low Frequency (VLF) Transmitters, October, 1981 prepared for Naval Electronics Systems Command, PME 110-241B.
56. Texas Tech University Report NP30/78, A Critical Analysis and Assessment of High Power Switches, September, 1978.
57. Blatt, F. M., Pick the Right 'Fast' Rectifiers to Design Switchers Effectively, EDN January 10, 1978.
58. Severns, R., The Design of Switchmode Converters Above 100 kHz, Intersil, Inc., Application Bulletin A034, 1980.
59. Watson, J. K., Applications of Magnetism, John Wiley and Sons, 1980.
60. Aldridge, T. V., and Haas, R. M., Designing the Soft Inductor, A New Component for Use in Switching Converters, Proceedings of Powercon 5, Fifth International Power Electronics Conference (Power Concepts, Inc., Ventura, CA) 1978.
61. TRW Defense and Space Systems, Redondo Beach, CA, Modeling and Analysis of Power Processing Systems (MAPPS), presentation at NASA Lewis Research Center, Cleveland, OH, 3 February 1977.
62. NASA CR 134686, Modeling and Analysis of Power Processing Systems, by J. J. Biess, Yu, Y., Middlebrook, R. D. and Schoenfeld, A. D., (TRW Systems), 21 July 1974.
63. Ninomiya, T., Kakiyama, H., and Harada, K., On the Cross-Noise in Multi-Output DC-to-DC Converters, paper presented at IEEE Power Electronics Specialists Conference, Atlanta, GA, June 1980.
64. Patel, R., Predicting Leakage Inductance of the Transformer, Powerconversion International, Vol. 7, No. 9, Nov/Dec 1981.
65. White, D., Electromagnetic Interference and Compatibility, Vol 2, pg. 235, Don White Consultants, 1976.
66. Schlicke, H., Electromagnetic Compossibility, Interference Control Co., Milwaukee, WI, 1979.
67. Bull, J. H., Impedance of the Supply Mains at Radio Frequencies, 1st Symposium and Technical Exhibition on EMC, Montreux, May 1975.

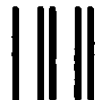
INSTRUCTIONS: In a continuing effort to make our standardization documents better, the DoD provides this form for use in submitting comments and suggestions for improvements. All users of military standardization documents are invited to provide suggestions. This form may be detached, folded along the lines indicated, taped along the loose edge (*DO NOT STAPLE*), and mailed. In block 5, be as specific as possible about particular problem areas such as wording which required interpretation, was too rigid, restrictive, loose, ambiguous, or was incompatible, and give proposed wording changes which would alleviate the problems. Enter in block 6 any remarks not related to a specific paragraph of the document. If block 7 is filled out, an acknowledgement will be mailed to you within 30 days to let you know that your comments were received and are being considered.

NOTE: This form may not be used to request copies of documents, nor to request waivers, deviations, or clarification of specification requirements on current contracts. Comments submitted on this form do not constitute or imply authorization to waive any portion of the referenced document(s) or to amend contractual requirements.

(Fold along this line)

(Fold along this line)

DEPARTMENT OF THE NAVY

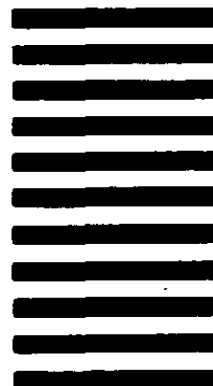


NO POSTAGE
NECESSARY
IF MAILED
IN THE
UNITED STATES

OFFICIAL BUSINESS
PENALTY FOR PRIVATE USE \$300

BUSINESS REPLY MAIL
FIRST CLASS PERMIT NO. 12503 WASHINGTON D. C.
POSTAGE WILL BE PAID BY THE DEPARTMENT OF THE NAVY

Commander
Naval Electronic Systems Command (ELEX 8111)
Washington, DC 20360



STANDARDIZATION DOCUMENT IMPROVEMENT PROPOSAL

(See Instructions - Reverse Side)

1. DOCUMENT NUMBER		2. DOCUMENT TITLE	
3a. NAME OF SUBMITTING ORGANIZATION		4. TYPE OF ORGANIZATION (Mark one)	
b. ADDRESS (Street, City, State, ZIP Code)		<input type="checkbox"/> VENDOR	
		<input type="checkbox"/> USER	
		<input type="checkbox"/> MANUFACTURER	
		<input type="checkbox"/> OTHER (Specify): _____	
5. PROBLEM AREAS			
a. Paragraph Number and Wording:			
b. Recommended Wording:			
c. Reason/Rationale for Recommendation:			
6. REMARKS			
7a. NAME OF SUBMITTER (Last, First, MI) - Optional		b. WORK TELEPHONE NUMBER (Include Area Code) - Optional	
c. MAILING ADDRESS (Street, City, State, ZIP Code) - Optional		8. DATE OF SUBMISSION (YYMMDD)	